

LI

LABORATORY INVESTIGATION

THE BASIC AND TRANSLATIONAL PATHOLOGY RESEARCH JOURNAL

VOLUME 98 | SUPPLEMENT 1 | MARCH 2018

 **USCAP 2018**

ABSTRACTS

HEMATOPATHOLOGY

(1387-1604)

107TH ANNUAL MEETING

**GEARED
TO
LEARN**



MARCH 17-23, 2018

Vancouver Convention Centre
Vancouver, BC, Canada

Published by

SPRINGER NATURE

www.ModernPathology.org

 **USCAP**
Creating a Better Pathologist

AN OFFICIAL JOURNAL OF THE
UNITED STATES AND CANADIAN
ACADEMY OF PATHOLOGY

EDUCATION COMMITTEE

Jason L. Hornick, Chair
 Rhonda Yantiss, Chair, Abstract Review Board
 and Assignment Committee
 Laura W. Lamps, Chair, CME Subcommittee
 Steven D. Billings, Chair, Interactive Microscopy
 Shree G. Sharma, Chair, Informatics Subcommittee
 Raja R. Seethala, Short Course Coordinator
 Ilan Weinreb, Chair, Subcommittee for
 Unique Live Course Offerings
 David B. Kaminsky, Executive Vice President
 (Ex-Officio)
 Aleodor (Doru) Andea
 Zubair Baloch
 Olca Basturk
 Gregory R. Bean, Pathologist-in-Training
 Daniel J. Brat

Amy Chadburn
 Ashley M. Cimino-Mathews
 James R. Cook
 Carol F. Farver
 Meera R. Hameed
 Michelle S. Hirsch
 Anna Marie Mulligan
 Rish Pai
 Vinita Parkash
 Anil Parwani
 Deepa Patil
 Lakshmi Priya Kunju
 John D. Reith
 Raja R. Seethala
 Kwun Wah Wen, Pathologist-in-Training

ABSTRACT REVIEW BOARD

Narasimhan Agaram
 Christina Arnold
 Dan Berney
 Ritu Bhalla
 Parul Bhargava
 Justin Bishop
 Jennifer Black
 Thomas Brenn
 Fadi Brimo
 Natalia Buza
 Yingbei Chen
 Benjamin Chen
 Rebecca Chernock
 Andres Chiesa-Vottero
 James Conner
 Claudiu Cotta
 Tim D'Alfonso
 Leona Doyle
 Daniel Dye
 Andrew Evans
 Alton Farris
 Dennis Firchau
 Ann Folkins
 Karen Fritchie
 Karuna Garg
 James Gill
 Anthony Gill
 Ryan Gill
 Tamara Giorgadze
 Raul Gonzalez
 Anuradha Gopalan
 Jennifer Gordetsky
 Ilyssa Gordon
 Alejandro Gru

Mamta Gupta
 Omar Habeeb
 Marc Halushka
 Krisztina Hanley
 Douglas Hartman
 Yael Heher
 Walter Henricks
 John Higgins
 Jason Hornick
 Mojgan Hosseini
 David Hwang
 Michael Idowu
 Peter Illei
 Kristin Jensen
 Vickie Jo
 Kirk Jones
 Chia-Sui Kao
 Ashraf Khan
 Michael Kluk
 Kristine Konopka
 Gregor Krings
 Asangi Kumarapeli
 Frank Kuo
 Alvaro Laga
 Robin LeGallo
 Melinda Lerwill
 Rebecca Levy
 Zaibo Li
 Yen-Chun Liu
 Tamara Lotan
 Joe Maleszewski
 Adrian Marino-Enriquez
 Jonathan Marotti
 Jerri McLemore

David Meredith
 Dylan Miller
 Roberto Miranda
 Elizabeth Morgan
 Juan-Miguel Mosquera
 Atis Muehlenbachs
 Raouf Nakhleh
 Ericka Olgaard
 Horatiu Olteanu
 Kay Park
 Rajiv Patel
 Yan Peng
 David Pisapia
 Jenny Pogoriler
 Alexi Polydorides
 Sonam Prakash
 Manju Prasad
 Bobbi Pritt
 Peter Pytel
 Charles Quick
 Joseph Rabban
 Raga Ramachandran
 Preetha Ramalingam
 Priya Rao
 Vijaya Reddy
 Robyn Reed
 Michelle Reid
 Natasha Rekhman
 Michael Rivera
 Mike Roh
 Marianna Ruzinova
 Peter Sadow
 Safia Salaria
 Steven Salvatore

Souzan Sanati
 Sandro Santagata
 Anjali Saqi
 Frank Schneider
 Michael Seidman
 Shree Sharma
 Jeanne Shen
 Steven Shen
 Jiaqi Shi
 Wun-Ju Shieh
 Konstantin Shilo
 Steven Smith
 Lauren Smith
 Aliyah Sohani
 Heather Stevenson-Lerner
 Khin Thway
 Evi Vakiani
 Sonal Varma
 Marina Vivero
 Yihong Wang
 Christopher Weber
 Olga Weinberg
 Astrid Weins
 Maria Westerhoff
 Sean Williamson
 Laura Wood
 Wei Xin
 Mina Xu
 Rhonda Yantiss
 Akihiko Yoshida
 Xuefeng Zhang
 Debra Zynger

To cite abstracts in this publication, please use the following format: **Author A, Author B, Author C, et al. Abstract title (abs#). *Laboratory Investigation* 2018; 98 (suppl 1): page#**

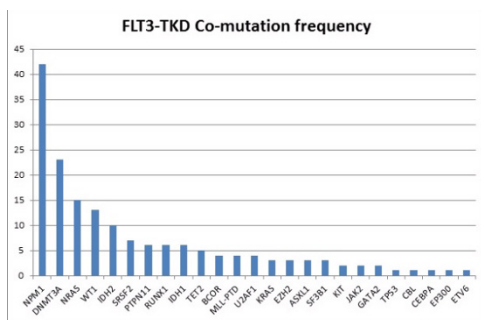
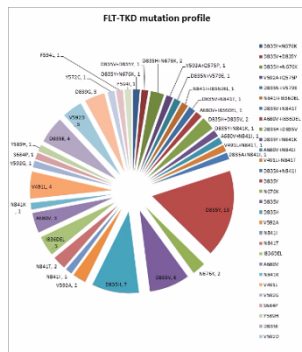
1387 FLT3-Tyrosine Kinase Domain (TKD) Mutation Profile Analysis in Adult Acute Myeloid Leukemia (AML) by Next Generation Sequencing (NGS)

Sharif Adwan¹, Richard Press², Jennifer Dunlap³, Philipp Raess², Xiaohua Wang³, Zhenzhen Zhang⁴, Allison Froman⁴, Guang Fan⁵.
¹Oregon Health & Science University, Portland, OR, ²Oregon Health & Science University, Portland, OR, ³Portland, OR, ⁴OHSU, ⁵Lake Oswego, OR

Background: FLT3-ITD is well known to be associated with inferior prognosis in AML. A recently FDA approved FLT3 inhibitor (Midostaurin) was shown to be effective for both FLT3-ITD & FLT3-TKD mutation positive AML in combination with standard chemotherapy. However, less is known about FLT3-TKD & other coexisting mutations. Therefore it is essential to identify patients with both FLT3-TKD & ITD mutations who may benefit from this newly approved therapy. We herein characterize FLT3-TKD mutations, including missense & deletion mutations, & co-mutations with FLT3-ITD & other gene mutations.

Design: The study included 74 AML patients who harbored FLT3-TKD mutations from the Pathology department/Knight diagnostic laboratory/Oregon Health & Science University (OHSU) from 3/2013 to 9/2017. The targeted-NGS-panel covered genes relevant to hematopoietic malignancies using Ion-Torrent-PGM. Bioinformatics-analysis was performed by Torrent-Suite-v.3.2. Open-source programs & lab-developed algorithms were used for annotation and amino acid prediction.

Results: Among the 74 adult AML patients (age 22-83), 37 were male & 37 female. The FLT3-TKD mutation profile is shown in Figure A. FLT3-TKD mutations were detected on **codon 835(41), 841(10), 836 del(5), 676(5), 680(5), 839(3), & 684(1)**. Point mutations in the juxta membrane domain (JMD) were also seen in our cohort, including codons **592(8), 572(1), 575(1), 579(1), 594(2)**. In addition, **V491L** mutation in extracellular domain (ECD) was detected in 5 AML patients. Interestingly, 2 different FLT3-TKD mutations were often seen together (15). Furthermore, concurrent FLT3-ITD & FLT3-TKD mutations were detected in 14 patients. The majority of FLT3-TKD AML patients had co-mutations with other genes (87%, 64/74 patients), including 11 patients with 1 co-mutation and 53 patients with 2 or more coexisting mutations. Co-mutation frequency of FLT3-TKD with other genes is shown in Figure B. The most common co-mutation was NPM1 (42) followed by DNMT3A (23), NRAS (15), & IDH2 (10).



Conclusions: We describe the spectrum of mutations in FLT3-TKD & patterns of co-mutations. While the majority of FLT3-TKD mutations occur at codon 835, many were seen at other codons & within the JMD and ECD. Moreover, co-mutation of at least 1 additional gene was seen in the vast majority of cases with most showing additional mutations in 2 or more genes. Further studies are warranted to investigate the significance of these coexisting mutations & their effects on prognosis & response to treatment.

1389 SOX9 Is Overexpressed in Follicular Lymphoma and Diffuse Large B Cell Lymphoma with IGH-BCL2

Mustafa Al-Kawaaz¹, Angela A Fache², Ghaith Abu Zeinah¹, Ashlesha S Muley², Yanwen Jiang³, Susan Mathew⁴, Yifang Liu¹, Kristy Richards¹, Wayne Tam⁵.
¹NewYork-Presbyterian Hospital/ Weill Cornell, New York, NY, ²Weill Cornell Medicine, New York, NY, ³Genentech, New York, NY, ⁴Weill Cornell Medical College, New York, NY

Background: SOX9 is a member of the SOX transcription factor family containing Sry-related HMG BOX. It is a downstream regulator of the WNT signaling pathway, and has an important role in stem cell self-renewal and cell differentiation regulation during development. Its expression correlates with prognosis and survival in some solid tumors. Recent RNA sequencing, bioinformatics and CHIP-seq data implicates SOX9 as a candidate master enhancer regulator of the germinal center B-cell (GCB) transcriptome. We plan to further elucidate the role of SOX9 in GCB-related lymphomas by analyzing its expression and identifying its target genes in follicular lymphoma (FL) and diffuse large B cell lymphoma (DLBCL).

Design: SOX9 expression was examined in multiple DLBCL cell lines using Western blotting (WB) and immunohistochemistry (IHC). SOX9 expression was also examined by IHC using DLBCL TMA (114 cases) and FL TMA (242 cases). Of the evaluable DLBCL cases, 54 and 53 were classified as GCB and non-GCB subtype, respectively, by Hans' algorithm. 20 were positive for IGH-BCL2 and 73 were negative. CHIP-seq was performed on GCB-type DLBCL cell lines to identify SOX9 target genes.

Results: By IHC, SOX9 appeared negative or very weakly positive in a small subset of normal GCB cells but was strongly positive in follicular dendritic cells. SOX9 was exclusively expressed in GCB DLBCL cell lines. 11/114 (10%) of DLBCL cases were positive for SOX9. Of the SOX9 positive cases, 10/11 (91%, p=0.008, Fisher's exact test) were GCB-type, 7/9 (78%, p=0.0002) harbored IGH-BCL2 translocation and 3/11 (27%) had prior documented history of FL. SOX9 88/242 (36.4%) of FL cases were positive for SOX9; its expression was independent of histologic grade. SOX9 expression was associated with a lower risk of relapse in the subset of GCB DLBCL cases with IGH-BCL2 translocation (p<0.05). CHIP-seq showed binding of SOX9 to 1,668 upstream distal enhancer regions associated with 963 genes. These target genes were significantly enriched in cell cycle regulation, transcription regulation, epigenetic regulation, MAPK signaling, B cell activation and BCL6 repressed pathways (p<0.001).

Conclusions: SOX9 is over-expressed in a subset of DLBCL, predominantly GCB-type with IGH-BCL2 translocation, and FL, suggesting a role in their pathogenesis. SOX9 may contribute to pathogenesis of these lymphomas by deregulating normal GCB functions. Our data suggests that SOX9 may serve as a prognostic marker and therapeutic target in DLBCL and FL.

1390 pSTAT3 is Superior to c-Myc in Predicting Prognosis in Post-Transplant Diffuse Large B Cell Lymphoma

Mohga Ali¹, Hongjie GU², Charles W Goss², Vikas R Dharnidharka¹, Marianna Ruzinova¹.
¹Washington University School of Medicine, St. Louis, MO, ²Washington University, St. Louis, MO

Background: Post-Transplant Lymphoproliferative Disorder (PTLD) is a life-threatening complication of transplantation. Diffuse Large B Cell Lymphoma (DLBCL) is the most common type of monomorphic PTLD, fulfilling the same diagnostic criteria as DLBCL in immunocompetent hosts. Increased expression of c-Myc in non-transplant DLBCLs is a proxy for presence of MYC translocation and unfavorable prognosis. It also identifies a subset of patients without MYC translocation but with similar poor prognosis. Expression of phosphorylated signal transducer and activator of transcription 3 (pSTAT3) has been linked to poor outcome in non-transplant DLBCL. The prognostic significance of these markers is not established in post-transplant DLBCLs. In this study, we investigated the expression and prognostic significance of c-Myc and pSTAT3 in transplant-associated DLBCLs.

Design: We identified 28 cases of PTLD presenting as DLBCL, seen in our institution between 1991 and 2015. Medical records were reviewed for pertinent clinicopathological data. Immunohistochemistry (IHC) for c-Myc (Y69, Ventana), pSTAT3 (D3A7, Cell Signalling) was scored by 2 hematopathologists. Nuclear expression of any intensity with a cutoff of ≥10% for pSTAT3, and a cutoff of ≥70% for c-Myc were considered positive. Averaged IHC results were correlated with overall survival using Kaplan-Meier method and Log rank test.

Results: In our cohort, 9/28 (32%) patients showed elevated pSTAT3 expression, while 4/28 (14%) patients had c-Myc expression ≥70%. Patients with increased pSTAT3 expression showed worse overall survival (22%) compared to patients without increased pSTAT3 levels (58%) (p=0.001). Cases with c-Myc ≥70% did not show statistically significant association with worse survival (p=0.127). Lower cut off values for c-Myc expression also did not show statistically significant

association with overall survival.

Conclusions: In our cohort, only expression of pSTAT3 was correlated with poor clinical outcome, suggesting that it is a more important prognostic marker than c-Myc in post-transplant DLBCL. Evaluation of larger cohorts is needed to confirm this finding. Elevated expression of STAT3 in 32% of our cases also suggests that transplant-associated DLBCLs may benefit from therapeutic agents targeting the JAK-STAT pathway.

1391 BCOR Mutations in the Myeloid Malignancies: A One-Year Experience at a Comprehensive Cancer Center

Saba Ali¹, Patricia Aoun¹, Milhan Telatar¹, Dennis D Weisenburger¹, Iryo Nakamura¹, Anthony Stein¹, Joo Song¹, Karl Gaal¹, Young Kim¹, Ibrahim Aldoss¹, Amandeep Salhotra¹, Hooi Yew¹, Raju K Pillai¹, Michelle Afkhami¹. ¹City of Hope National Medical Center, Duarte, CA

Background: The advent of whole exome sequencing has revealed novel genes, such as the BCL6 corepressor (BCOR), an X-linked component of the Polycomb group repressive complex 1 (PGRC1). BCOR protein functions as a transcriptional suppressor of BCL-6, and when mutated plays a major role in neoplastic transformation of hematopoietic stem cells through upregulation of HOXA genes. Although the relevance of BCOR somatic mutations in embryogenesis, solid tumors, and hematopoietic malignancies, including acute myeloid leukemia (AML), myelodysplastic syndrome (MDS), and myeloproliferative neoplasms (MPN) has been reported in a few studies the prevalence, associated gene mutations, and prognostic implications remain to be defined.

Design: 238 cases with myeloid malignancies from September 2016 to September 2017 were retrospectively reviewed. Next-generation sequencing (NGS) using a custom-designed hematologic malignancy assay consisting of 73 mutations and 23 fusion genes was performed on isolated DNA and RNA from aspirate smear/peripheral blood samples at the clinical molecular diagnostic laboratories.

Results: Of 120 AML, 54 MDS, 14 MDS/MPN, and 50 MPN cases, BCOR mutations were found in 13 cases (9.1% of AML and 3.7% of MDS cases) with a M:F ratio of 1:1 and a mean age of 63 years. No clinically significant BCOR mutations were found in the MPN and MDS/MPN cases. DNMT3A (38%), STAG2 (38%), TET2 (31%), IDH2 (15.3%), and IDH1 (7.7%) were the genes most frequently mutated in association with BCOR. No NPM1 mutations were found concurrent with BCOR mutations. Cytogenetics was performed on 12 of the 13 cases, and 6 had a normal karyotype whereas 6 had a complex karyotype. Three of the 13 patients with BCOR mutation died within 6 months of molecular testing, two of whom harbored a concurrent DNMT3A mutation.

Conclusions: In our cohort, BCOR mutations were seen mainly in adults (mean age of 63 years) without gender predilection. BCOR mutations were frequently seen in AML followed by MDS cases. Cytogenetic abnormalities were independent of BCOR status in all 12 cases. DNMT3A and STAG2 were the most common mutations associated with BCOR. Concurrent DNMT3A and BCOR mutations appear to confer a poor prognosis; however, a larger cohort is needed to confirm these findings.

1392 Acute Myeloid Leukemia with Myelodysplasia-related Changes with or without Prior Myelodysplastic Syndrome Show Distinct Gene Mutation Profile

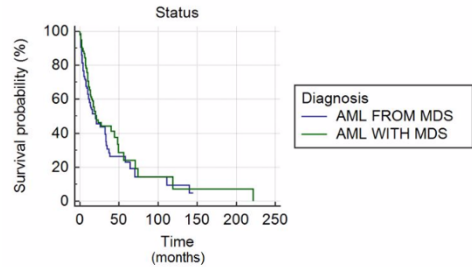
Mary-Margaret Allen¹, Mohammad Hussaini¹, Eric Padron¹, Hailing Zhang¹, Xiaohui Zhang¹, Lynn Moscinski¹, Ling Zhang¹, Jinming Song¹. H. Lee Moffitt Cancer Center, Tampa, FL

Background: Acute myeloid leukemia with myelodysplastic related changes (AML-MRC) usually has a dismal clinical outcome. Within this WHO classification, there are two groups, patients with prior myelodysplastic syndrome (MDS) or myelodysplastic/myeloproliferative neoplasm (MDS/MPN) that progress to AML (hxAML-MRC) and patients that present with *de novo* AML-MRC (dnAML-MRC). Coleman et al. (2015) identified gene mutations highly specific to secondary AML, including *SRSF2*, *SF3B1*, *U2AF1*, *ZRSR2*, *ASXL1*, *EZH2*, *BCOR* or *STAG2*. However, study of the differences in gene profiles and clinical outcomes between the two subgroups of AML-MRC is limited.

Design: Retrospectively, 398 patients with AML-MRC from 2012-2017 and their Next-Generation Sequencing data were reviewed. We compared mutation profiles and overall survival (OS) of patients with hxAML-MRC to those patients with dnAML-MRC. Patients with a prior history of MDS/MPN were excluded.

Results: 180 patients had hxAML-MRC (median age 71 years, male to female ratio (M:F) of 2.28) and 218 patients presented with dnAML-MRC (median age 66 years, M:F of 1.38). Patients with prior MDS had a higher average number of mutations (2.62 vs 1.98, *p*-value = 0.0002). They also had significantly more mutations in *ASXL1* (25.56% vs 16.13%, *p*=0.0242), *RUNX1* (22.67% vs 10.00%, *p*=0.001), *SETBP1*

(8.93% vs 2.59%, *p*=0.0105), *SRSF2* (20.83% vs 7.77%, *p*=0.0004), *TET2* (23.30% vs 14.08%, *p*=0.0246), and *U2AF1* (13.10% vs 5.18%, *p*=0.0094) than dnAML-MRC. There was no significant difference between the two groups in frequencies of mutations in *ABL1*, *CBL*, *CEBPA*, *CSF3R*, *CUX1*, *DNMT3A*, *ETV6*, *EZH2*, *FLT3*, *IDH1*, *IDH2*, *JAK2*, *KIT*, *KMT2A*, *KRAS*, *MPL*, *MYD88*, *NPM1*, *NRAS*, *PHF6*, *SF3B1*, *SH2B3*, *TP53*, or *ZRSR2*. The dnAML-MRC appeared to show more mutations in the *WT1* gene (6.79% vs 1.94%, *p*=0.0528), although statistically insignificant. Despite the distinct mutation profile, the median OS between the two groups was similar (10 months hxAML-MRC vs 12 months dnAML-MRC, *p*= >0.05).



Conclusions: Similar to the Coleman et al. report, we showed the patients with hxAML-MRC have a greater number of mutated genes, and significantly more mutations in *SRSF2*, *U2AF1*, *TET2*, *ASXL1*, *RUNX1* and *SETBP1*. These findings suggest that patients with and without prior MDS are distinct subsets of AML-MRC, which may require different targeted therapy in the era of personalized medicine.

1393 A Combined Biomarker of MYC and Bright CD38 Improves Predictive Power for Identifying Double/Triple Hit High Grade B-Cell Lymphomas

Abdullah Alsuwaidan¹, Mingyi Chen¹, Jesse Jaso¹, Hung Luu¹, Nathan T Sweed¹, Rolando Garcia¹, Franklin Fuda¹, Weina Chen¹. ¹University of Texas Southwestern Medical Center, Dallas, TX

Background: High-grade B-cell lymphomas (HGBLs) with *MYC* and *BCL2* and/or *BCL6* rearrangements (R), so-called "double/triple-hit lymphoma" (DTHL) recognized as a provisional entity in the 2016 WHO revision are present in 5-10% of HGBCLs, and generally aggressive lymphomas that require intensive treatment. While extensively studied, the question remains as to when to FISH (Fluorescence in situ hybridization) these abnormalities. Recent studies have suggested that immunohistochemical (IHC) markers [such as *MYC*, double expressor (DE), and germinal center B-cell-like phenotype (GC)] and flow cytometric (FC) marker (bright CD38) may predict DTHL. However, a comprehensive analysis on the predictive power of combined these markers is largely absent, which became the focus of our study.

Design: Search of an institutional database from 2000 to 2017 yielded 38 cases of DTHL (32 DHL, 6 THL; 89% as DLBCL), and 34 cases of DLBCL lack of *MYC* R. FC immunophenotyping for CD38, IHC, morphology and cytogenetics/FISH analyses (for *MYC*, *BCL2*, and *BCL6*) and clinical presentation were assessed and compared. Bright CD38 was defined as the expression at or above the level of GC B cells. The optimal cut-off for *MYC* IHC (50%) to predict DTHL was determined by receiver operating characteristic curve.

Results: Compared to DLBCL without *MYC* R, DTHL were more likely to have greater expression of CD38 (bright), *MYC*, and Ki-67, and with GC and DE phenotype (Table 1). We thus evaluated the predictive power of each and combined markers for predicting DTHL. While single marker of bright CD38 or *MYC* was a moderately sensitive/specific, a combined of these two markers improved sensitivity (87%) while maintaining specificity (Table 2). The combination of 3 or 4 markers was inferior due to reduced specificity. Notably, none of isolated *MYC* R HGBCL (n=8) was missed using the *MYC*/CD38 markers.

Table 1 – Clinicopathological features of DTHL and DLBCL without *MYC* R

	Age/Sex	Bright CD38+	MYC	Ki-67	GC (Hans')	DE
DTHL	44-90 (61)	16/32	20-90%	40-100%	27/33	25/28 (89%)
(n=38)	(23M, 15F)	(50%)	(70%)	(90%)	(77%)	
DLBCL (MYC R-)	22-78 (56)	4/28	5-75%	30-100%	19/29	8/28
(n=34)	(23M, 11F)	(14%)	(35%)	(85%)	(65%)	(28%)
P values		0.0055	<0.0001	0.3407	0.1603	<0.0001

GC: germinal center B-cell-like phenotype by Hans' algorithm; **DE:** double expressor by BCL2 (>50%) and MYC expression (>40%) by IHC; **MYC R-:** DLBCL without MYC rearrangement. **DTHL:** double / triple hit lymphoma. Age, years (range,median); Other values presented as range (median)

Table 2 – The sensitivity and specificity of single and combined makers for predicting DTHL.

Predictors for DTHL	Sensitivity	Specificity
Bright CD38	50%	87%
MYC IHC (cut-off: 50%)	76%	70%
GC phenotype (Hans')	82%	34%
DE (MYC/BCL2)	89%	71%
Combined	Bright CD38/MYC (2 markers)	87%
	Bright CD38/MYC/DE (3 markers)	93%
	Bright CD38/MYC/DE/GC (4 markers)	100%

Conclusions: Our study for first time demonstrated that the combined approach using both IHC and FC biomarkers is superior to single marker. Specifically, the combination of MYC (>50%) and bright CD38 is highly sensitive and moderately specific for detecting DTHL. Restricting FISH analysis to this subset of HGBCL may decrease the cost by ~ 70% compared to testing all HGBCL while capable of identifying ~ 90% of DTHL. We recommend applying this strategy in correlation with clinical status, i.e. FISH testing all cases with aggressive presentation regardless of marker status in order to further improve diagnosis of DTHL.

1394 Shade of Gray Between Double/Triple-Hit High-Grade Large B Cell Neoplasm (DTH-HGBCL) and CD34 Negative Lymphoblastic Leukemia (B-LL): a subset of DTH-HGBCL Bridging These Entities and Biological Implication

Abdullah Alsuwaidan¹, Prasad Koduru¹, Mingyi Chen¹, Jesse Jaso¹, Hung Luu¹, Nathan T Sweed¹, Rolando Garcia¹, Franklin Fuda¹, Weina Chen¹. ¹University of Texas Southwestern Medical Center, Dallas, TX

Background: High-grade B-cell lymphomas (HGBLs) with MYC and BCL2 and/or BCL6 rearrangements, so-called "double/triple-hit lymphoma" (DTHL) recognized as a provisional entity in the 2016 WHO revision, are generally mature aggressive lymphomas. We encountered rare cases of DTH B-cell lymphoid neoplasm (referred to as "gray zone B-lymphoid neoplasm, GZBLN" in this study) with features intermediate between mature lymphoma and immature B lymphoblastic leukemia/lymphoma (B-LL), which was particularly difficult to be distinguished from CD34 negative (CD34-neg) B-LL or B-LL with DH. This prompted us to further study this subset of neoplasm by comparing them to CD34-neg B-LL and B-LL with DH and by exploring the biological significance of this GZBLN.

Design: Search of an institutional database from 1998 to 2016 in adult identified 38 cases of DTHL, 13 cases of 34-neg B-LL, and 3 cases of DH B-LL (search for all ages). Four- or 10-color flow cytometry (FC) immunophenotyping (IP), immunohistochemistry (IHC), cytogenetics/FISH (for MYC, BCL2, and BCL6, only in DTHL and DH B-LL), and clinical outcomes were assessed and compared.

Results: Most DTHL were DHL (84%) that harbored a BCL2 R (59% in DHL), and were classified as DLBCL (34/38, 89%) with germinal center B-cell-like phenotype (GC, 27/33, 82%) and double expressor (DE, 25/28, 89%) by 2008 WHO criteria (Table 1). The overall survival (OS, a median of 18 months in DTHL) in patients treated with an intense regimen seems better than those reported. Of interest, the IP profile of 3 DHL (~ 8% of DTHL) appears to be better characterized as GZBLN by virtue of the lack of CD20 or slg expression and the minimal Tdt expression. Remarkably, this IP was very similar to CD34-negative B-LL and DH B-LL with exception of Tdt expression in the latter 2 entities (Table 2).

Table 1. Clinicopathological features of DTHL (n=38)

	Age/sex	BCL2 R	BCL6 R	CD10	GC (Hans')	DE	Overall survival (Alive/Dead)**
DHL*	23-90 (59)	19	13	23/32 (72%)	21/27 (78%)	20/23 (87%)	18 (16/13)
(n=32, 84%)	(19M, 13F)	(59%)	(41%)				
DTHL*	51-82 (54)	NA	NA	6/6 (100%)	6/6 (100%)	5/5 (100%)	Undefined (4/2)
(n=6, 16%)	(4M, 2F)						

GC: Germinal center B-cell-like phenotype by Hans' algorithm; DE: double expressor by BCL2 (>50%) and MYC expression (>40%) by IHC; Overall survival as month; A, Alive; D, Dead; R, rearrangement; age, range year (median).

*: Of DHL, 3/5 and 2/5 of DHL harbored a BCL2 R and BCL6 R, respectively. Most of DTHL was classified as DLBCL [34/38, remaining as BCLU (Large B-cell lymphoma with feature intermediate between DLBCL and Burkitt lymphoma)].

** : Majority patients (80%) treated with intense regimen (EPOCH-R)

Table 2. Immunophenotypic (IP) features of gray zone lymphoid malignancy (GZBLN), CD34-neg B-LL, and DH B-LL

	Age/sex	CD10	CD20	CD34	slg	Tdt +
GZ-BLN (n=3)	65-70 (67)	1/3 (33%)	0/3 (0%)	0/2 (0%)	0/3 (0%)	1/2 (50%, but ptd)
(1M, 2F)						
CD34-neg B-LL (n=13)	20-71 (42)	10/13 (77%)	4/13 (31%)	0/13 (0%)	0/11(0%)	13/13 (100%)
(6M, 7F)						
DH B-LL (n=3)	13-69 (40)	3/3 (100%)	2/3 (67%, pt+)	0/3 (0%)	0/3 (0%)	3/3 (100%, one pt)
(2M, 1F)						

GZLM, gray zone lymphoid malignancy; pt, partial expression; ptd, partial dim expression; neg, negative expression.

Conclusions: Our study confirmed the reported characteristics of DTHL, such as a predominance of DLBCL with GC and DE phenotype and an apparently improved clinical outcome under intense chemotherapy. Furthermore, we described a small subset of DTHL with features intermediate between lymphoma and acute leukemia, likely biologically closer to DH B-LL. In fact, all reported cases of DH B-LL including ours are CD34-neg, which suggests a need for evaluation for DTH in CD34-neg B-LL. Intriguingly, GZBLN may lie on a biologic continuum in a spectrum of B-lymphoid neoplasia; therefore, we propose this emerging entity to raise the awareness and call for future molecular characterization of clinical significance.

1395 An Immunohistochemistry Algorithm Subclassifies PTCL-NOS into Gene Expression Profiling Defined Molecular Subgroups with High Accuracy

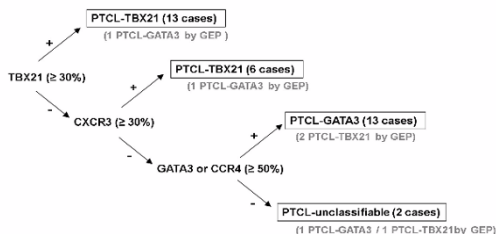
Catalina Amador¹, Timothy Greiner¹, Tayla Hevican¹, Waseem Lone¹, Lynette M Smith¹, Bouska Alyssa¹, Jiayu Yu¹, Anja Mottok², Andreas Rosenwald³, German Ott⁴, Sarah Ondrejka⁵, Lisa Rimsza⁶, Dennis D Weisenburger⁷, Wing Chung Chan⁷, Javeed Iqbal¹. ¹University of Nebraska Medical Center, Omaha, NE, ²Wuerzburg, Bayern, Germany, ³Wuerzburg, Germany, ⁴Robert-Bosch-Krankenhaus, ⁵Cleveland Clinic, Cleveland, OH, ⁶Mayo Clinic, Scottsdale, AZ, ⁷City of Hope National Medical Center, Duarte, CA

Background: Peripheral T-cell lymphoma (PTCL) encompasses a heterogeneous group of aggressive entities. Currently, more than a third cannot be subclassified into distinct entities and are designated as PTCL-not otherwise specified (PTCL-NOS). Using gene expression profiling (GEP), we delineated two major molecular subgroups: 1) PTCL-GATA3, characterized by high expression of GATA3 and its target genes and 2) PTCL-TBX21 with high expression of TBX21 and its target genes. The PTCL-GATA3 subgroup has significantly worse overall survival (OS). The objective of this study was to develop an immunohistochemical (IHC) algorithm that would adequately match the molecular subclassification of PTCL-NOS.

Design: Tissue microarray (TMA) blocks were created from 44 PTCL-NOS cases which had been successfully evaluated by HG-U133plus 2 arrays (14 PTCL-GATA3, 20 PTCL-TBX21, 10 PTCL-unclassifiable). The GATA3 and TBX21subgroups showed a significant difference in OS (p=0.01). TMAs were stained with antibodies to CD3, GATA3 and its target gene (CCR4) and TBX21 and its target (CXCR3). Prior to TMA staining, antibodies were optimized in tonsil and whole tumor

sections. The immunostained slides were evaluated independently by two pathologists and tumor cell percentage recorded in 10% increments. Statistical analyses determined that the optimal tumor positivity thresholds were $\geq 50\%$ for GATA3/CCR4 and $\geq 30\%$ for TBX21/CXCR3.

Results: A high correlation in assessing tumor positivity was found between pathologist (intra-class correlations = 0.77-0.86). GATA3 was positive in 65% of cases, CCR4 in 55%, TBX21 in 35% and CXCR3 in 65%. There was a significant correlation ($p < 0.01$; $r = 0.5$) between the IHC percent positivity with the corresponding mRNA expression levels. An inverse correlation ($p < 0.05$, $r = -0.4$) was seen between the IHC expression of GATA3/CCR4 and TBX21/CXCR3, consistent with GEP analysis. We derived an accurate subclassification algorithm with the four immunostains as shown in Figure 1. Using the IHC algorithm, we accurately classified 28 of 34 cases (error rate of 12%) compared to GEP classification, and 2 of 34 cases were unclassifiable. The IHC algorithm classification was able to predict OS, with GATA3 subgroup associated with inferior OS ($p = 0.04$).



Conclusions: We found that this four antibody IHC algorithm correlates well with the GEP defined molecular classification and is able to predict survival. However, these findings need to be confirmed in independent cohorts and validation studies are being performed.

1396 Molecular Landscape of RAS-Associated Autoimmune Leukoproliferative Disorder (RALD)

Vollter Anastas¹, Weixin Wang², Stephenie Drolf³, Susan Price³, Zhen Zhao³, V. K Rao³, Katherine Calvo⁴. ¹NIH, Bethesda, MD, ²Clinical Center, NIH, ³NIH, ⁴NIH, Bethesda, MD

Background: RAS-Associated Autoimmune Leukoproliferative Disorder (RALD) is a chronic condition presenting in childhood with gain-of-function somatic mutations in RAS leading to monocytosis, lymphocytosis, autoimmunity, and splenomegaly. Despite an indolent course, RALD shares overlapping features with Juvenile Myelomonocytic Leukemia (JMML). The diagnostic distinction between these two diseases needs better clarification as prognosis and optimal treatment differs. In this study we investigated the transcriptome, hematopoietic lineages harboring RAS mutations, and the mutational landscape of RALD for comparison to mutation profiles previously reported in JMML.

Design: RNAseq, targeted myeloid panel, whole exome sequencing (WES), and ddPCR were performed on PBMCs from 7-11 RALD patients. Diffuse large B-cell lymphoma (DLBCL) from one RALD patient was analyzed by WES with Sanger confirmation of mutations. PBMCs were sorted into T, B, and myelomonocytic cells and sequenced for RAS mutations. Plasma cytokine levels were assayed by multiplex ELISA.

Results: Targeted and WES detected previously identified NRAS or KRAS mutations with variant allele frequencies ranging between 32.3%-50.8%. No other pathogenic variants reported in JMML were identified in RALD. Subclonal SETBP1 mutations reported in JMML were not detected by ddPCR. Clonal NRAS and KRAS mutations involved B-cells, T-cells, and myelomonocytic cells. The oldest RALD patient developed two separate B-cell lymphomas, cutaneous MZL and DLBCL after 30 yrs; the DLBCL was analyzed by WES revealing the longstanding NRAS mutation with an additional PTEN mutation not previously detected in PBMCs. RNAseq revealed multiple differentially expressed genes in RALD, a large portion of which were overexpressed and related to immune function and activation. Multiplex cytokine assay showed increased expression of IL-2, IL-6, and IL-10 in plasma in comparison to healthy controls.

Conclusions: RALD represents an indolent disease presenting in childhood characterized by a single somatic NRAS or KRAS mutation leading to autoimmunity and myelomonocytic and lymphoid proliferation. Cytogenetic abnormalities and cooperating mutations found in JMML are not detected in RALD. To date, no RALD patient in our cohort followed for over 10 years, has developed overt myeloid malignancy. Our oldest patient developed two separate B-cell lymphomas suggesting that RALD patients may have an increased risk of lymphoid malignancy with the acquisition of additional somatic mutations.

1397 Lack of Typical Clinicomorphologic Features Associated with Acute Myeloid Leukemia with Variant (Non-Type A) CBFB-MYH11 Fusion Transcript Presents Diagnostic Challenges

Evgeniya Angelova¹, Rajyalakshmi Luthra¹, Keyur Patel², Andres E Quesada¹, Joseph Khoury¹, Zhuang Zuo¹, C. Cameron Yin¹, L. Jeffrey Medeiros¹, Carlos Bueso-Ramos¹, Rashmi Kanagal-Shamanna⁴. ¹The University of Texas MD Anderson Cancer Center, Houston, TX, ²The University of Texas MD Anderson Cancer Center, Sugar Land, TX, ³The University of Texas MD Anderson Cancer Center, Bellaire, TX

Background: AML with CBFB-MYH11 is characterized by monocytic differentiation, eosinophils with abnormal granules and Auer rods. Identification of CBFB-MYH11 is important as these patients respond favorably to high-dose cytarabine. CBFB-MYH11 rearrangement can be difficult to identify by karyotype. Hence, FISH/PCR studies, often triggered based on these morphologic findings, are essential for detection. Depending on the breakpoint location, different variant types of CBFB-MYH11 are recognized [type A (85%), followed by types E and D]. Other studies suggest that non-type A (NTA) patients have atypical clinical or morphologic findings, although data are limited. In such cases, CBFB-MYH11 can be missed unless FISH/PCR assays specifically designed for these transcripts are performed. Hence, it is important to understand the clinicopathologic features of NTA AML.

Design: We searched for AML cases (2008 to 2017) with CBFB-MYH11 detected by a multiplex PCR assay designed for transcripts types A, D and E. At our institution, all AML patients are screened by this assay. We assessed the clinicopathologic and genetic features.

Results: Of 74 AML with CBFB-MYH11, 6 (8%) patients showed NTA [5 type D; 1 E]. These included 3 men, 3 women [median age 56 years (range, 23-78)]. Four patients presented as *de novo*, 1 as therapy-related and 1 as myeloid blast phase of CML. NTA patients had a lower median WBC (6.5 vs. 20.9) and PB blast% (9% vs. 22.5%) compared with type A. Morphologically, NTA patients showed diffuse BM involvement (median 40% blasts). Abnormal eosinophils were noted in only 2 NTA patients compared to 39 in type A (33% vs. 50%). Only 1 NTA patient showed rare Auer rods. NTA group showed TdT expression (40% vs. 0%) by flow. All NTA cases had inv(16) by karyotype/FISH. Additional aberrations noted more than once included +8, +21 and del(7q). Notably, NTA cases lacked trisomy 22 (30% in type A). KRAS, NRAS and FLT3 D835 mutations were present in both groups while KIT mutation was absent in NTA (25% in type A). Over a median follow-up of 34 months (range, 9-78), 1 patient died; rest are in complete remission.

Conclusions: NTA AML with CBFB-MYH11 is rare, commonly presents with non-proliferative features (low WBC and PB blast%, no KIT mutation) and frequently lacks typical cytomorphologic findings (abnormal eosinophils, Auer rods) essential to trigger FISH/PCR studies. Awareness of NTA variants is important as routine PCR assays, unless specifically designed to detect variant transcripts, may miss CBFB-MYH11.

1398 PD-L1 Expression in Nodular Lymphocyte Predominant Hodgkin Lymphoma (NLPHL) and Its Immunoarchitectural Variants

Anand Annan¹, Lisa Durkin², Yan Xie³, Eric Hsi⁴. ¹Decatur, GA, ²Cleveland Clinic, ³Galveston, TX, ⁴Cleveland Clinic, Cleveland, OH

Background: Programmed Death – ligand 1 (PD-L1) expression in epithelial neoplasms is associated with poor prognosis and is a target for anti-cancer therapy. In lymphoid neoplasms, PD-L1 expression has been reported in classical Hodgkin lymphoma (cHL) and some aggressive non-Hodgkin lymphomas; however, its expression pattern in Nodular Lymphocyte Predominant Hodgkin Lymphoma (NLPHL) is not widely reported. In this study, we evaluated PD-L1 expression in NLPHL and its various immunoarchitectural variants, as defined by Fan and colleagues (*Am J Surg Pathol*, 2003).

Design: All cases of NLPHL with available material seen at our institution between January 1, 2000 – June 30, 2017 were reviewed. To assess the immunoarchitectural variants of NLPHL, CD3 (Clone 2GV6, Ventana Medical Systems, Tucson, AZ), CD20 (Clone L26, Agilent Technologies, Santa Clara, CA) and CD21 (Clone 1F8, Abcam, Cambridge, MA) immunostains were utilized. Immunoarchitectural variant was assigned according to the dominant pattern. PD-L1 expression was also assessed by immunohistochemistry (Clone 22C3, Agilent Technologies, Santa Clara, CA) with appropriate controls. PD-L1 expression was defined as $\geq 10\%$ immunoreactivity in lymphocyte predominant (LP) cells, irrespective of staining intensity. Statistical analysis was performed (Fisher exact test), with a p value < 0.05 considered significant.

Results: 38 of 47 cases of NLPHL expressed PD-L1 (81%). The distribution of PD-L1 expression with according to immunoarchitectural pattern is shown in **Table 1**. Briefly, 80% of "classic" nodular pattern – B-cell rich, 93% of nodular with prominent extranodular LP cells, 75% of T-cell rich nodular pattern and 50% of diffuse pattern (T-cell/histiocyte rich B-cell lymphoma like) expressed PD-L1. No difference in PD-L1 expression frequency was seen between patterns.

Table 1: PD-L1 Expression in NPLHL by Immunoarchitectural Pattern[†]

NPLHL Immuno-architecture variants	PD-L1 Expression		
	Positive	Negative	% Positive
Pattern A: "Classic" nodular pattern, B-cell rich*	20	5	80%
Pattern C: Nodular with Prominent Extranodal LP cells*	13	1	93%
Pattern D: Nodular with T-Cell rich background	3	1	75%
Pattern E: Diffuse pattern (T-cell/histiocyte rich B-Cell lymphoma like)	3	3	50%
Pattern F: Diffuse, "moth-eaten" pattern with B-cell rich background	---	---	

[†]Pattern as defined by Fan Z et al. Am J Surg Pathol 2003, 27(10):1346-56.

*Two cases had a mixed A and C patterns, and each of these patterns were individually evaluated for PD-L1 expression

Conclusions: The majority of cases of NPLHL (81%) express PD-L1, comparable to the reported frequency of PD-L1 expression in cHL. There was no significant difference in the PD-L1 expression based on the immunoarchitectural pattern of NPLHL. Further investigation of PD-L1 as a therapeutic target for NPLHL is warranted. Correlations between PD-L1 expression, immunoarchitectural variants, and outcome are ongoing.

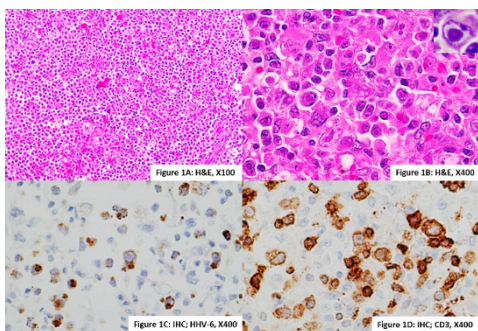
1399 Human Herpes Virus 6 (HHV-6) Associated Lymphadenitis – Pitfalls in Diagnosis

Jayalakshmi Balakrishna¹, Mark Raffeld², Elaine Jaffe³, Stefania Pittaluga⁴. ¹Bethesda, MD, ²NCI/NIH, Bethesda, MD, ³National Cancer Institute/NIH, Bethesda, MD, ⁴National Cancer Institute, Bethesda, MD

Background: HHV-6 is a member of the *Betaherpesvirinae* subfamily. Most people acquire HHV-6 primary infection early in life and reactivation may occur later, most often in immunocompromised individuals, leading to various clinical manifestations. HHV-6 infected cells may be identified in lymph nodes in both reactive and neoplastic conditions.

Design: Cases were retrieved from the archives of hematopathology consultation service at National Institutes of Health from 2003 to 2017 in which infection by HHV-6 had been documented by immunohistochemical stains to HHV-6gp60/110 envelope glycoprotein, which identifies both HHV-6 A and B subtypes (Biodesign Inter, Saco ME, USA). In addition, immunohistochemical stains and PCR for T cell receptor gamma gene rearrangement were performed to rule out a lymphoproliferative disorder. EBER-ISH and immunohistochemical stains and/or molecular analysis for other viruses (CMV, HSV, EBV and HTLV-1) were also performed in cases with clinical suspicion.

Results: Five cases of reactive lymphadenitis positive for HHV-6 were identified. All the patients were adults (Median age 53 years; range 28 – 64 years), including 3 males and 2 females; who presented with generalized lymphadenopathy and fever. None of the patients had known immunocompromise. The lymph node biopsies showed marked paracortical hyperplasia (Figure 1A) and contained admixed large atypical lymphoid cells exhibiting pleomorphic nuclei, vesicular chromatin, and prominent eosinophilic intranuclear inclusions (Figure 1B). Vascular proliferation was seen in 4/5 cases and necrosis in 2/5, raising suspicion of peripheral T-cell lymphoma. Staining for HHV-6 was positive with a membranous and Golgi pattern (Figure 1C) and was restricted to cells with evident inclusions on H&E. HHV-6 infected cells were positive for CD3 (Figure 1D) and CD4. Tests for other viruses were negative. PCR showed a polyclonal pattern of T cell receptor gene rearrangement in 3 out of 4 cases tested; 1 case did not show amplification products.



Conclusions: HHV-6 lymphadenitis can present with morphologic atypia creating a diagnostic pitfall for lymphoma. Careful attention to the characteristic viral inclusions can lead to immunohistochemical

analysis highlighting the replicating virus.

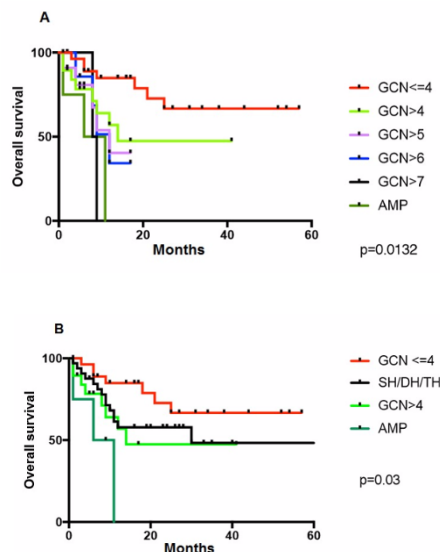
1400 MYC Increased Copy Number (ICN) Has an Unfavorable Prognostic Impact in Patients with Diffuse Large B-Cell (DLBCL) and High Grade Lymphoma Treated with Immuno-Chemotherapy – A Single Center Experience

Piera Balzarini¹, Francesca Schieppati², Simona Fisogni³, Lorenzo Michel⁴, Alessandro Re⁵, Luisa Lorenz⁶, Giuseppe Rossi², alessandra Tucci⁶, Fabio Facchetti⁷. ¹University of Brescia, Brescia, Lombardy, ²ASST Spedali Civili di Brescia, ³Spedali Civili di Brescia, ⁴University of Brescia, Bergamo, ⁵University of Brescia, Brescia, Lombardia, ⁶ASST Spedali Civili di Brescia, Brescia, ⁷University of Brescia

Background: MYC rearrangements occur in 8-14% of DLBCL, and correlate with inferior survival. The prognostic impact of MYC numerical aberrations, however, is debated and a consensus on their correct identification is still lacking. Herein we report a single center experience on MYC ICN identification and describe its clinical impact in the setting of aggressive B cell lymphomas.

Design: Lymphoma samples from 408 patients, diagnosed from 2011 to 2016 with DLBCL (*de novo*, transformed) or B-cell lymphoma, unclassifiable (BCLU), were studied by FISH using break apart probes for MYC, BCL2, and BCL6. Sixty evaluable nuclei with clear signals were scored in each case. MYC ICN was defined by the observation of ≥3 gene copies; "MYC amplification" defined cases with countless copies and a "cloud-like" pattern. FISH results were compared with c-myc expression by immunohistochemistry (IHC) considering cases with expression in ≥40% of lymphoma cells as positive.

Results: MYC abnormalities were detected in 93 cases (22.8%): 36.6% had translocation (MYC-T), 59.1% ICN (MYC-ICN), and 4.3% amplification (MYC-AMP). The MYC-T group included 9 single (SH), 18 double (DH) and 7 triple hit (TH) cases; the overall survival (OS) of the three subgroups did not show significant difference (p=.9). Within the MYC-ICN group, the progressive increase of gene copy number (GCN) correlated with worsening of OS; GCN>7 and AMP showed the most aggressive behavior (p=.01) (Fig. A). The presence of ≤4 copies was set as cut-off to categorize these pts in two subgroups that showed a significantly different OS (p=.04) as illustrated in Fig B. Patients with diagnosis of BCLU clustered in the MYC-T group (p=.03). 82% of those with MYC-ICN were *de novo* DLBCL (p=.06). C-myc positivity, by IHC, was reported in 96% of MYC-T and in 85% of cases with GCN>4, while it was low in the one and single case of the MYC-AMP group with a favorable outcome. An intensified therapeutic regimen was given to 44% of patients (62% of MYC-T and 33% of MYC-ICN) but it did not lead to a significant advantage in their outcome.



Conclusions: MYC numerical aberrations are commonly observed in aggressive B cell lymphomas and have a significant impact on patients' prognosis. In our cohort, cases with GCN>4 or amplification were associated with a significantly worse clinical outcome. Our data are in line with recent observations and suggest to urgently define a consensus on this high-risk category and to consider more effective therapeutic approaches.

1401 Mutational and Immunophenotypic Landscape of Primary Cutaneous Follicle Center Lymphoma

Nicholas Barasch¹, Yen-Chun Liu², Nathanael Bailey², Jonhan Ho¹, Steven H Swerdlow². ¹University of Pittsburgh Medical Center, Pittsburgh, PA, ²University of Pittsburgh School of Medicine, Pittsburgh, PA

Background: Primary cutaneous follicle center lymphoma (PCFCL) is well-known to be distinct from nodal follicular lymphomas (FL) largely based on its infrequent *BCL2* rearrangements (R), diminished CD10 in a greater proportion of cases and clinical behavior. Whether they have a distinct mutational profile, however, is unknown. It is known that pediatric-type FL (PTFL) which uniformly lack *BCL2-R* have a mutational landscape distinct from nodal FL. Therefore, to compare PCFCL to FL and PTFL, mutational analysis of 9 PCFCL was performed together with assessment of germinal center (GC) B cell markers MEF2B and HGAL.

Design: Histologic sections as well as CD20, CD3, BCL2, BCL6, CD10, and IRF4/MUM1 immunostains were reviewed from 9 PCFCL with an available paraffin block (M:F 4:5, 39-82 yrs old). All patients had a documented negative PET/CT (8) or CT (1) scan and bone marrow biopsy. Next generation sequencing using a targeted hybrid-capture procedure on genomic DNA extracted from formalin-fixed paraffin-embedded tissue was performed. A custom probe panel comprising 4099 targets in the coding regions of 220 genes recurrently mutated in B cell lymphoma was used. Non-synonymous variants (NSVs) and insertions/deletions were recorded except those that may represent germline variants with allele frequencies between 40-60%. Results were compared to published data for FL and PTFL. Immunostains for HGAL and MEF2B and FISH studies using a *BCL2* break-apart probe were also performed.

Results: The neoplastic B cells demonstrated strong CD10 expression in 6/9 cases and possible BCL2 expression in only 2/9 cases. MEF2B and HGAL were strongly expressed by the neoplastic cells in all cases including the 3 cases with weak (2) or absent (1) CD10 expression. FISH studies did not demonstrate any *BCL2-R*. Analysis of 7 cases with DNA of sufficient quality showed a total of 23 NSVs within 19 genes (1-5 mutations/sample)(table 1). Two genes were mutated in 2 cases (*CREBBP* and *TNFRSF14*) and none of the cases had *KMT2D* or *MAP2K1* mutations. Possible copy number (CN) losses were identified in regions including 1p, 5p, 6q and 15q. Possible CN gains were identified in regions including 1q, 6p and 11p.

Table 1. Comparison of reported non-synonymous mutation frequencies in pediatric-type follicular lymphoma (PTFL) and follicular lymphoma (FL) to our cohort of primary cutaneous follicle center lymphoma (PCFCL).

Case	Genes	PCF-CL		Pediatric-type Follicular Lymphoma *		Follicular Lymphoma **		PTFL vs. FL	
		%	%*** (Range)	no.	P-value	%*** (Range)	no.	P-value	P-value
1 & 2	CREBBP	29%	3% (0-5%)	64	0.0047	62% (45-83%)	539	NS	<0.0001
3 & 4	TNFRSF14	29%	45% (33-54%)	75	NS	32% (17-41%)	553	NS	NS
1	EP300	14%	5%	58	NS	16% (11-20%)	498	NS	0.0259
1	XPO1	14%	ND			ND			
2	FAS	14%	ND			5% (2-8%)	247	NS	
2	PIK3C3	14%	0%	21	NS	1%	105	0.0129	NS
3	HIST1H1B	14%	2% (0-3%)	58	NS	5% (5-7%)	330	NS	NS
4	FOXO1	14%	3% (0-5%)	58	NS	6% (4-27%)	409	NS	NS
4	SOCS1	14%	14%	21	NS	7% (2-17%)	240	NS	NS
5	STAT6	14%	0%	21	NS	12% (3-16%)	498	NS	NS
6	EZH2	14%	2% (0-5%)	64	NS	19% (8-46%)	901	NS	0.0006
6	FOXO1	14%	ND			ND			
6	ROBO2	14%	5%	21	NS	4%	105	NS	NS
7	CSMD3	14%	5%	21	NS	6%	105	NS	NS
7	FAT2	14%	0%	21	NS	5% (3-6%)	256	NS	NS
7	MEF2B	14%	0%	58	0.0044	14% (8-21%)	498	NS	0.0023
7	NR3C1	14%	ND			1% (0-3%)	363	0.0022	
7	IKZF1	14%	0%	21	NS	5% (3-6%)	293	NS	NS
NA	KMT2D	0%	9% (0-16%)	64	NS	73% (36-82%)	509	<0.0001	<0.0001
NA	MAP2K1	0%	44% (17-49%)	68	0.0245	3 (3-3%)	35	NS	<0.0001
NA	ARID1A	0%	5%	21	NS	11% (6-15%)	512	NS	NS
NA	CARD11	0%	ND			12% (10-17%)	498	NS	
NA	GNA13	0%	7% (0-11%)	58	NS	9% (6-11%)	398	NS	NS
NA	IRF8	0%	17% (10-50%)	66	NS	11% (6-21%)	530	NS	NS
NA	POU2F2	0%	0%	21	NS	7% (6-8%)	219	NS	NS
NA	RRAGC	0%	ND			7% (6-16%)	117	NS	

PTFL* Composite of Mod Path 29, 1-9 (2016); Blood 128, 1093-1100 (2016); Blood 130, 323-377 (2017); Blood 128, 1101-1111 (2016); Hematologica 98, 1237-1242 (2013).

FL** Composite of Lancet 16, 1111-1122 (2015); Leukemia 31, 83-91 (2017); Nat Gen 46 176-181 (2013); Blood 122, 3165-3168 (2013); Blood 123 1487-1498 (2014); Blood 129 473-483 (2017); Blood 128, 1093-1100 (2016); Blood 130, 323-377 (2017); Blood 128, 1101-1111 (2016).

***= Aggregated percentage of reported positive cases.
(Range)= Range of mutation results based on individual reviewed studies.
no.= Aggregate of number of total cases assayed by Sanger, next generation sequencing, whole exome or whole genome sequencing.
NA= Not Applicable, NS = No Significant Difference, ND= No Data.

Conclusions: These results further support the GC origin of PCFCL. However, comparison with published data suggests that, while sharing some genotypic and CN similarities with FL and PTFL, its mutational profile appears distinct from both other entities.

1402 Application of the 2016 World Health Organization (WHO) Criteria to the Diagnosis of Peripheral T-cell Lymphomas with T-follicular Helper Phenotype Using a 5 Marker Panel

Basma Basha¹, Karen Rech¹, Andrew Feldman¹, Julie Vrana¹, Min Shi¹, Rebecca L King¹. ¹Mayo Clinic, Rochester, MN

Background: The 2016 revision of the WHO classification of lymphoid neoplasms introduces a new umbrella category of nodal peripheral T-cell lymphomas (PTCL) with T-follicular helper (TFH) phenotype, which includes angioimmunoblastic T cell lymphoma (AITL), follicular T-cell lymphoma and lymphomas previously classified as PTCL, not otherwise specified (NOS) with a TFH phenotype (PTCL-TFH). TFH phenotype is defined by expression of ≥ 2 TFH markers, which include CD10, BCL6, CXCL13, PD1, ICOS, SAP & CCR5. Our study assesses the function of 5 immunohistochemical (IHC) stains for identification of TFH phenotype on PTCL previously diagnosed using the 2008 WHO classification. We also specifically validate the utility of the addition of ICOS, a marker not previously tested at our institution.

Design: 22 cases of AITL & 29 cases of PTCL-NOS diagnosed per 2008 WHO criteria were identified through a search of tissue archives from 2008 to 2017. IHC was done on formalin-fixed paraffin-embedded tissue with commercially available antibodies to CXCL13, PD1, BCL6,

CD10 & ICOS (D1K2T, Cell Signaling Technology, Inc., Danvers, MA). Appropriate staining in normal control tissue was verified. Positive expression was set at $\geq 20\%$ staining of tumor cells.

Results: ICOS was positive in 20/22 (91%) AITL cases & 15/29 (52%) PTCL-NOS cases. Rates of positivity for other markers for AITL were: CD10 (64%), BCL6 (45%), PD1 (95%), CXCL13 (68%). Rates of positivity in PTCL-NOS were: CD10 (3%), BCL6 (0%), PD1 (59%), CXCL13 (0%). With inclusion of ICOS in the panel, all AITL cases showed expression of ≥ 2 TFH markers. Without ICOS, 3 AITL cases (14%) had < 2 TFH markers. Inclusion of ICOS in the TFH panel would result in reclassification of 12 (41%) PTCL-NOS to PTCL-TFH, compared to only 1 reclassification without it. Applying the 2016 WHO criteria, sensitivity for TFH phenotype is 97% for PD1, 94% for ICOS, 44% for CD10 & CXCL13 and 29% for BCL6. Specificity for TFH phenotype is 100% for CD10, BCL6 & CXCL13, 82% for ICOS and 71% for PD1.

Conclusions: Inclusion of ICOS in a 5 stain panel results in reclassification of a substantial number of PTCL-NOS cases to PTCL-TFH and may aid in confirming AITL in cases lacking expression of other TFH markers as defined by the 2016 WHO criteria. ICOS & PD1 have the highest sensitivity for PTCL-TFH, but lack specificity compared to other markers. Additional work is needed to further define the correlation of these phenotypic categories with clinical behavior, genetic findings, and response to therapy.

1403 p53 Immunohistochemistry Discriminates Reactive Erythroid Proliferations from Pure Erythroid Leukemia in Bone Marrow

Basma Basha¹, Kaaren K Reichard¹. ¹Mayo Clinic, Rochester, MN

Background: Distinguishing non-neoplastic erythroid proliferations from pure erythroid leukemia (PEL) is often a morphologic challenge and is clinically very significant. As findings from key clinical, laboratory and cytogenetic studies may take several days to be resulted, we hypothesized that, since many cases of PEL harbor *TP53* mutations, that p53 immunohistochemistry (IHC) may play a useful surrogate role in this crucial distinction.

Design: Our bone marrow pathology archive was searched from 2012 to 2017 for cases with erythroid "hyperplasia" or "predominance" in the final diagnosis section of the reports. We identified 19 cases with a clinically documented & marked reactive erythroid hyperplasia (EH) (due to vitamin B12 deficiency, hemolytic anemia, hemoglobinopathy, etc.), 5 normal staging bone marrows, and 6 PEL cases for p53 IHC (Ventana, clone DO-7). Each case was scored independently in a blinded fashion by two hematopathologists. Scoring included intensity (1+, weak; 2+, moderate - mixture of weak and strong; 3+, strong) and approximate proportion of staining erythroid precursors. 16 of 19 EH cases & all PEL cases had available karyotypes.

Results: p53 nuclear staining was mainly confined to the pronormoblastic stage. The normal controls exhibited 5-20% staining with 1+ intensity. The EH group showed variable staining - ranging from 1-90% of all erythrocytes with 1-2+ intensity. None of the EH or normal bone marrow cases showed 3+ intensity. All 6 PEL cases had $> 90\%$ staining with 3+ intensity. None of the EH cases had an acquired cytogenetic abnormality. All PEL cases had complex karyotypes, with 3 (50%) showing monosomy 17, and one of the remaining cases had next generation sequencing which showed two mutations in the *TP53* gene.

Conclusions: Strong, diffuse and uniform p53 expression in pronormoblasts supports a diagnosis of pure erythroid leukemia when non-neoplastic erythroid proliferations are in the differential diagnosis. Given that IHC can usually be performed within 24 hours, this may serve as a useful ancillary test in clinically critical cases. Additional future studies are needed to further corroborate the diagnostic utility of these findings.

1404 Bone marrow findings in idiopathic multicentric Castleman disease (iMCD)

Elizaveta Belyaeva¹, David Fajgenbaum¹, Dustin Shilling¹, John Astle², Megan Lim¹, Dale Frank³. ¹Hospital of the University of Pennsylvania, Philadelphia, PA, ²Medical College of Wisconsin, Milwaukee, WI, ³Philadelphia, PA

Background: Multicentric Castleman disease (MCD) is a lymphoproliferative disorder driven by cytokines, especially interleukin 6, produced by human herpes virus-8 (HHV8). Drivers of HHV8-negative or idiopathic MCD (iMCD) are less well understood. Consensus diagnostic criteria for iMCD were only recently established. Many iMCD patients have complex clinical presentations and undergo bone marrow (BM) studies as part of an initial work up. However, BM findings in iMCD have not been formally characterized. We examined 9 BM specimens from 6 patients who met diagnostic criteria for iMCD to determine whether characteristic histologic findings are associated with this diagnosis.

Design: 9 BM specimens from 6 patients with iMCD were identified over a 12 year period. All were male, with an average age at diagnosis

of 39 years (range: 25-65 years). 6 specimens were pre-treatment, 2 post-treatment (2 and 5 years after diagnosis), and 1 from a patient undergoing treatment. We compared our findings to 70 published descriptions of BM from patients with the TAFRO subtype of iMCD.

Results: 8 of 9 specimens were hypercellular (60-90%). 7 of 9 specimens showed megakaryocytic hyperplasia (6-20/HPF), megakaryocytic atypia (11-29% of megakaryocytes), and reticulin fibrosis (grade 1 in 4 specimens, grade 2 in 3 specimens). 7 of 9 specimens lacked lymphoid aggregates. 2 of 9 contained only small ($< 10\%$ of cellularity) lymphoid aggregates. 8 of 9 specimens lacked significant ($> 10\%$ of cellularity) plasma cell infiltrates. Plasma cells were polytypic in all specimens (5 of 9) evaluated. Hypercellularity, megakaryocyte hyperplasia and atypia persisted (2-5 years) in the 2 patients with pre- and post-therapy specimens. In 1 a decrease in reticulin fibrosis was noted. Hypercellularity, megakaryocyte hyperplasia and atypia, and reticulin fibrosis were also the most common findings in our review of 70 published descriptions of BM from patients with the TAFRO subtype of iMCD.

Conclusions: BM findings in iMCD include hypercellularity, reactive megakaryocyte hyperplasia and atypia, and mild to moderate reticulin fibrosis. These changes are non-specific but characteristic, and can persist for years. By contrast, plasmacytosis and regressed germinal centers, typical of lymph nodes from iMCD patients, are not often seen in BM from these patients.

1405 Comparison of Flow Cytometry and Cytogenetic Analysis of Concurrent Peripheral Blood and Bone Marrow at Initial Presentation of Pediatric Acute Leukemia; Institutional Experience

Shane Betman¹, Lenore Omes², Michael Weiner², Govind Bhagat³, Bachir Alobeid¹. ¹New York, NY, ²NYPH Columbia University Medical Center, ³Columbia University Medical Center, New York, NY

Background: At our institution, concurrent peripheral blood (PB) and bone marrow (BM) samples are routinely analyzed by flow cytometry (FC) and cytogenetic (CGC) analysis at initial presentation of acute leukemia in pediatric patients. Despite the two samples representing the same neoplastic process, occasional differences in phenotype/genotype have been observed between PB and BM. We sought to investigate the frequency and diagnostic relevance of these differences.

Design: Pathology records from 2005 to 2017 were queried for all new acute leukemia diagnoses in patients aged 18 or less. Patients were excluded if PB and BM samples were not analyzed concurrently or either sample contained less than 10% blasts. Archived FC data were converted to a numeric percent of blasts expressing each tested marker based on gating previously defined for clinical diagnosis. Each difference of at least 30% in positivity of any marker was reviewed visually and sorted into 1 of 3 categories based on differences in fluorescence intensity and degree of separation of cell populations: artifact (no difference), small, and large phenotypic difference.

Results: A total of 101 leukemia patients were included (69 B-ALL, 20 AML, 11 T-ALL and 1 mixed lineage). Mean sample viability was 97.5% (83-100%) and mean blast count was 60.4% (10-97%). In total, 159 phenotypic differences were noted and categorized: 118 no difference, 26 small, and 15 large. Small or large differences were identified in 27 cases (26.7%) including 20 B-ALL, 4 AML, 2 T-ALL, and 1 mixed lineage case. Of these, 14 had 1 difference, 12 had 2, and 1 case had 3 differences. The most common markers to show differences between PB and BM were TdT (7 cases), CD20 (6), and cIgM (3). Concurrent PB and BM samples were analyzed by CGC in 29 cases. In 20/29, findings were identical. Karyotype failed in 3 PB cases and 1 BM case. Two PB cases had nonspecific clonal alterations not seen in BM, while 2 BM cases had nonspecific findings not seen in PB. One case showed separate subclones in PB and BM that were not present in the other.

Conclusions: Phenotypic/genotypic differences between PB and BM blasts were a common finding; however, diagnoses were ultimately concordant in all cases with no diagnostic impact. Our findings suggest that when a PB sample is diagnostic, FC and CGC analysis of a concurrent BM is less likely in most cases to add value to the diagnostic workup of acute leukemia in children.

1406 The Complexities of P53 Expression in Large B-cell Lymphomas

Shweta Bhavsar¹, Erika M Moore², William E Coyne³, Steven H Swerdlow⁴. ¹UPMC Pittsburgh, Pittsburgh, PA, ²University Hospitals Cleveland Medical Center, Cleveland, OH, ³University of Pittsburgh Medical Center, Pittsburgh, PA, ⁴University of Pittsburgh School of Medicine, Pittsburgh, PA

Background: *TP53* abnormalities are of great importance in many hematopoietic/lymphoid neoplasms with P53 immunohistochemistry (IHC) sometimes, but not always, a useful surrogate. With large B-cell lymphomas (LBL), P53 expression has been associated with an adverse prognosis in many but not all studies, & it has been suggested that LBL with *TP53* & *MYC* abnormalities are like another type of

"double-hit" lymphoma. To further explore the implications of P53 immunostaining, LBL were stained for P53 & the results correlated with other clinicopathologic parameters.

Design: 240 LBL with *BCL2*, *BCL6* & *MYC* FISH studies, had IHC stains at least for CD20, CD3, CD10, BCL6, IRF4/MUM1, BCL2, MYC, Ki-67 & P53 (M:F 145:95, 20-98 yrs.). Evaluable cases were classified as DLBCL, blastoid, or DLBCL/Burkitt-like. Clinical parameters including IPI, treatment, & follow-up were recorded. The frequency & prognostic implications of P53 expression were correlated with the other parameters tested, based on initial grouping of P53 stains into 4 categories [Fig. 1]. After preliminary analyses, cases were grouped into P53 low/intermediate (1-3) & high (4, uniform strong positivity). Cases studied at relapse were not included in the survival data.

Results: Overall only a very weak trend for an adverse prognosis was identified for LBL with high P53 (36/204 [18%] cases, $p=0.16$); however, it did have a significant adverse impact among DLBCL/BL (14/43, $p=0.018$) with a trend ($p<0.1$) for those with IPI 0-2 (10/52) & those ≥ 65 years old (23/136) [Fig. 2]. Treatment strategies, other than no treatment, had similar outcomes. High P53 was more often found in DLBCL/BL than in the other histologic categories ($p=0.010$) & with $\geq 40\%$ MYC+ ($p=0.014$). [Table 1] Significant prognostic implications were not found in subsets defined by MYC or MYC & BCL2 IHC; *MYC*, *BCL2* & *BCL6* FISH studies; or cell of origin. Nevertheless high P53 cases with *MYC* & *BCL2/BCL6* rearrangements had a median survival of only 4.5 mo. (vs 18 mo. for P53 low).

	P53 Cat. 4	P values
Histopathologic groups		
DLBCL (140)	18%	0.01
DLBCL/BL (43)	33%	
Blastoid (26)	4%	
Cytogenetic groups		
MYC & BCL2 &/or BCL6 R (32)	13%	NS
MYC-R only (15)	20%	
No MYC-R (157)	19%	
Phenotypic features		
MYC <40% (67)	7%	0.01
MYC $\geq 40\%$ (127)	21%	
Ki67 <75% (45)	16%	NS
Ki67 $\geq 75\%$ (157)	19%	
GCB – Hans algorithm (129)	16%	NS
non-GCB – Hans algorithm (70)	21%	
Double expressor (80)	19%	NS
Non-double expressor (111)	15%	
Clinical features		
IPI 0/1/2 (52)	19%	NS
IPI 3/4/5 (73)	22%	
Age <65 (68)	19%	NS
Age ≥ 65 (134)	17%	

Cat.= category, R=rearrangement, NS = not significant

Conclusions: Except at the extremes, P53 IHC staining is not easy to interpret due to variation in intensity & common weak staining in many cells. The clinicopathologic correlates of P53 expression based on the easy-to-apply cutoffs used here are complex & limited. Although this retrospective study of a heterogeneous group of cases has limitations, it may be that assessment of *TP53* mutation/deletion in LBL will be of greater practical importance with more uniformly identified & reproducible results.

1407 Development and Clinical Application of a Next Generation Sequencing-Based Anchored Multiplexed PCR assay to Identify Kinase Fusions in Hematological Malignancies

Leonardo Boiocchi¹, Max Jan¹, Long Le¹, Amelia Raymond², John lafrate¹, Valentina Nardi¹. ¹Massachusetts General Hospital, Boston, MA, ²Massachusetts General Hospital, Charlestown, MA

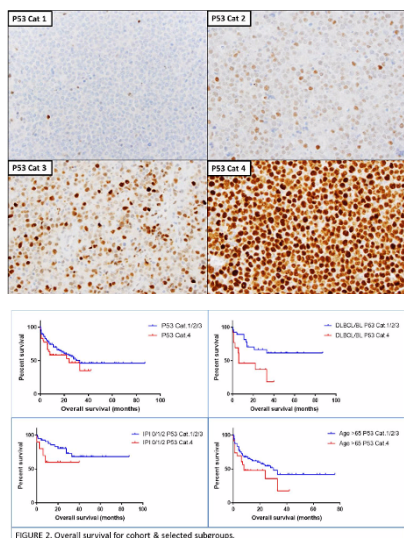
Disclosures: Long Le: Stock, ArcherDX, Consultant, ArcherDX
John lafrate: Ownership Interest, ArcherDX

Background: Detection of gene rearrangements and gene fusions is critical for diagnosis and risk stratification of patients with myeloid and lymphoid leukemias. Translocations and fusions are commonly investigated by conventional karyotyping and FISH but these techniques are not completely sensitive and may not be able to provide detailed information about the specific genes involved. Some rearrangements remain cryptic, particularly actionable rearrangements involving kinases. To increase the rate of detection of these clinically relevant targeted fusion transcripts in hematologic malignancies, we developed a next generation sequencing (NGS)-based anchored multiplex PCR assay (Heme Fusion assay) and routinely perform it on all cases of acute leukemias.

Design: Total nucleic acid was extracted from blood or bone marrow, cDNA was obtained and utilized in 2 hemi-nested PCR reactions with primers (Archer) for 52 genes, sequenced as previously described (Zheng et al., Nat Med 2014) and analyzed with a laboratory-developed algorithm. We analyzed 135 cases (67 validation cases, 68 clinical cases) and compared results of the Heme Fusion assay with conventional cytogenetics and FISH.

Results: A total of 42 cases showed rearrangements (30 in the validation group, 12 in the clinical cohort). Thirty-three of the positive cases (78%) showed concordance with results of cytogenetics and FISH analysis; in the remaining 9 cases (22%) our assay revealed additional information, including cryptic rearrangements (n=7), some of which potentially targetable with tyrosine-kinase inhibitors (n=3; cases 1-3) and others (n=3, cases 7-9) still affecting patient management. Details of these case are summarized in Figure 1.

Case #	Age (y)	Sex	Diagnosis	Key findings	Other tests	Relevant Multiplex PCR	Clinical management
1	27	M	B-ALL	IGHV1-18/IGHJ4 fusion; IGHV1-18/IGHJ4 fusion	FISH: IGHV1-18/IGHJ4 fusion	IGHV1-18/IGHJ4 fusion	Identified cryptic IGHV1-18/IGHJ4 fusion
2	15	M	B-ALL	IGHV1-18/IGHJ4 fusion; IGHV1-18/IGHJ4 fusion	FISH: IGHV1-18/IGHJ4 fusion	IGHV1-18/IGHJ4 fusion	Identified cryptic IGHV1-18/IGHJ4 fusion
3	35	M	B-ALL	IGHV1-18/IGHJ4 fusion; IGHV1-18/IGHJ4 fusion	FISH: IGHV1-18/IGHJ4 fusion	IGHV1-18/IGHJ4 fusion	Identified cryptic IGHV1-18/IGHJ4 fusion
4	50	M	AML	IGHV1-18/IGHJ4 fusion; IGHV1-18/IGHJ4 fusion	FISH: IGHV1-18/IGHJ4 fusion	IGHV1-18/IGHJ4 fusion	Identified cryptic IGHV1-18/IGHJ4 fusion
5	14	F	B-ALL	IGHV1-18/IGHJ4 fusion; IGHV1-18/IGHJ4 fusion	FISH: IGHV1-18/IGHJ4 fusion	IGHV1-18/IGHJ4 fusion	Identified cryptic IGHV1-18/IGHJ4 fusion
6	11	F	B-ALL	IGHV1-18/IGHJ4 fusion; IGHV1-18/IGHJ4 fusion	FISH: IGHV1-18/IGHJ4 fusion	IGHV1-18/IGHJ4 fusion	Identified cryptic IGHV1-18/IGHJ4 fusion
7	22	M	AML	IGHV1-18/IGHJ4 fusion; IGHV1-18/IGHJ4 fusion	FISH: IGHV1-18/IGHJ4 fusion	IGHV1-18/IGHJ4 fusion	Identified cryptic IGHV1-18/IGHJ4 fusion
8	31	M	AML	IGHV1-18/IGHJ4 fusion; IGHV1-18/IGHJ4 fusion	FISH: IGHV1-18/IGHJ4 fusion	IGHV1-18/IGHJ4 fusion	Identified cryptic IGHV1-18/IGHJ4 fusion
9	31	M	AML	IGHV1-18/IGHJ4 fusion; IGHV1-18/IGHJ4 fusion	FISH: IGHV1-18/IGHJ4 fusion	IGHV1-18/IGHJ4 fusion	Identified cryptic IGHV1-18/IGHJ4 fusion



Conclusions: We have developed and implemented a targeted RNA sequencing-based assay for hematological malignancies that has shown to complement conventional techniques providing additional and occasionally critical information that may impact disease diagnosis, prognosis and clinical management in patients with acute leukemias.

1408 Molecular and Clinico-Pathological Features of SF3B1-Mutated Myeloproliferative Neoplasms

Leonardo Boiocchi¹, Olga Pozdnyakova², Waihay J Wong³, Aliyah Sohani¹, Robert Hasserjian¹, Gabriela Hobbs¹, Valentina Nardi¹. ¹Massachusetts General Hospital, Boston, MA, ²Brigham and Women's Hospital, Southborough, MA, ³Brigham and Women's Hospital, Boston, MA

Background: Next-generation sequencing (NGS) assays have broadened the genetic landscape of myeloproliferative neoplasms (MPNs) well beyond *JAK2*, *MPL*, and *CALR*, revealing occasionally unexpected co-occurring mutations. Mutations in *SF3B1* are seen in $\geq 80\%$ of myelodysplastic syndromes with ring sideroblasts (MDS-RS) and of MDS/MPN with RS and thrombocytosis (MDS/MPN-RS-T) but have been only occasionally described in MPNs. Their significance in this context is uncertain. We analyzed in detail the clinico-pathological features associated with *SF3B1* mutations in a large series of BCR-ABL1-negative MPNs.

Design: The study included 151 consecutive cases of BCR-ABL1-negative MPNs for which NGS-based panel testing was performed (Rapid Heme, 94 genes, n=115; Trusight Myeloid panel, 54 genes, n=36) from two Partners Institutions. All cases were classified according to the 2016 WHO classification: 29 cases were Polycythemia Vera (PV) cases, 39 Essential Thrombocythemia (ET), 17 MPN-unclassifiable, 54 Primary Myelofibrosis (PMF) and 12 secondary MF (7 post-PV MF, 5 post-ET MF) were included. An iron stain was performed in all SF3B1-mutated cases with an available marrow aspirate slide as well as in a subset of SF3B1-wild type (WT) cases.

Results: SF3B1 hot-spot mutations were found in 15 cases (10%) (Table 1). JAK2 was co-mutated in 13 cases (80%). Fourteen cases (93%) were MF (9 PMF; 5 secondary MF) and 1 was a PV (7%). Among SF3B1-mutated cases, MF were more frequent than among controls (93% vs 38%; p=0.002). The marrows of all SF3B1-mutated cases showed classical MPN features, with no dysplasia and < 5 % blasts. Iron stain was performed in 10 SF3B1-mutated cases: RS were seen in 4 cases, but only in 2 accounted for >15% of erythroid precursors. MDS/MPN-RS-T was carefully excluded based on prior history of MPN and absence of anemia or thrombocytosis. No RS were present in any WT case. Due to the high proportion of MF among SF3B1-mutated cases, only WT MF cases (n=60) were considered when comparing hematologic parameters: white blood cell count, hemoglobin, or platelet count showed no significant difference (mutated vs. WT: p>0.85 for all).

FOR TABLE DATA, SEE PAGE 570, FIG. 1408

Conclusions: SF3B1 mutations were seen in 10% of MPNs in our cohort, mostly MF cases. SF3B1-mutated cases were morphologically and clinically indistinguishable from SF3B1-WT MPNs except for the presence of RS in a subset of cases. It is important to recognize that a subset of classic MPNs may carry SF3B1 mutations and RS to avoid clinically significant diagnostic pitfalls.

1409 Patterns of CD24 and CD180 expression by flow cytometry can distinguish Mantle Cell Lymphoma (MCL) from other non-Hodgkin B-cell lymphoproliferative disorders (B-LPD)

Kelly A Bowers¹, Cory Johnson¹, Kruthi Murthy¹, Katsiaryna Laziuk², Richard Hammer¹. ¹University of Missouri, Columbia, MO, ²Columbia, MO

Background: Flow cytometric immunophenotyping continues to be an integral component of diagnosis for all hematopoietic neoplasms. This is particularly critical for non-Hodgkin mature B-cell lymphoproliferative disorders (B-LPD), many which have similar morphologic features. CD24 is a pan-B-cell marker, found in progenitor and activated B-cells. CD180 is a TLR-related marker, important for B-cell proliferation and survival. Limited studies have independently investigated CD24, and more recently CD180, but no study has examined the expression of both CD24 and CD180 in B-LPDs.

Design: Flow cytometry results performed from 2016-2017 at University Hospital were examined retrospectively for inclusion of specimens tested with CD24 and CD180 as well as a diagnosis of mature B-LPD by 2008 WHO classification guidelines. The final sample size of 41 patients, included diagnoses of CLL, LPL, MCL, MZL, DLBCL and B-cell neoplasm, NOS. Flow cytometry data was collected and gated via FACSCanto II and FACSDiva (BD Biosciences), then analyzed using Dedoose mixed-method software. Specimens were qualitatively coded negative or positive (dim, moderate, bright, or heterogenous) then frequency of coded patterns compared using Fisher exact tests. Separate dual coding verified inter-relater reliability.

Results: A phenotypic pattern of bright CD24+ and any CD180+ was significant (p=0.0135) with 27% sensitivity, 100% specificity, 100% PPV, and 70% NPV for mantle cell lymphoma (MCL) compared to other B-cell LPDs. Additionally, a phenotypic pattern of any CD24+ with dim CD180+ was significant (p=0.0063) with 85% sensitivity, 64% specificity, 52% PPV, and 90% NPV for 19+20+5+ B-cell neoplasms. Data supports previous findings associated with CD180 expression, including dim CD180+ in CLL and strong CD180+ in normal lymphoid tissues.

Conclusions: Unique phenotypic profiles are the backbone of clinical flow cytometry. This preliminary study shows bright CD24+ and dim 180+ can distinguish between MCL and CLL, respectively. This distinction is vital for treatment decisions and patient outcomes since MCL has a more aggressive clinical course compared to CLL and low-grade B-LPDs. CD24 is a known prognostic marker in many solid tumors thus patterns of CD24+ may be a prognostic in B-LPDs as well. CD24 and CD180 show promising utility for the immunophenotypic classification of mature B-LPDs.

1410 LMO2 is a useful marker in distinguishing between indolent T-lymphoblastic proliferations and T-lymphoblastic leukemia/lymphoma

Nivaz Brar¹, Raheem Peeran², Maciej Tatarczuch³, Beena Kumar⁴, George Grigoriadis⁵, Robert Ohgami⁶. ¹California Northstate University, ²Stanford University School of Medicine, Stanford, CA, ³Monash Health, ⁴Monash Medical Center, Melbourne, VIC, ⁵Stanford University, Stanford, CA

Background: Indolent T-lymphoblastic proliferations (iT-LBP) are reactive expansions of TdT+ T-cells outside of thymic tissue which may be erroneously misdiagnosed as T-lymphoblastic lymphoma (T-LBL). This is in part due to the complex morphologic, immunophenotypic and clinical overlap that can occur between these entities. A singular definitive method for addressing the diagnostic quandary of iT-LBP versus T-LBL is lacking. However, in recent years, LMO2 has been described as a positive marker of T-LBL but consistently negative in reactive immature thymocytes.

Design: We searched our pathology archives for cases of indolent T-lymphoblastic proliferations and identified 7 with adequate material for further immunohistochemical studies. 3 new cases that have not been described in the literature to date were also identified. We performed immunohistochemical staining for LMO2 on these cases with comparison to LMO2 staining patterns on 12 cases of T-LBL.

Results: All cases of iT-LBP were negative for LMO2 (0/7) whereas all cases of T-LBL showed expression of LMO2 (12/12) (p-value < 0.001; Fisher exact test). We additionally describe 3 new cases of iT-LBP which show typical features of iT-LBP in expression of CD4 and CD8, and TdT, absence of CD34, as well as non-clonal TCR studies and clinical indolence without mediastinal adenopathy. One case was seen in a patient with lymphoid architecture showing Castleman-like features.

Conclusions: LMO2 is a diagnostically useful marker for differentiating between iT-LBP and T-LBL. As previously described, iT-LBP typically express CD4 and CD8 and lack CD34. The absence of mediastinal enlargement is also a characteristic feature of this entity which has not been focused on previously.

1411 Statistical Analysis of Monocyte Morphology in Chronic Myelomonocytic Leukemia versus Reactive Monocytosis

Devin R Broadwater¹, LaShanta N Smart², David Lynch³, Jordan Half⁴. ¹Brooke Army Medical Center, Fort Sam Houston, TX, ²Brooke Army Medical Center, San Antonio, TX, ³Brooke Army Medical Center

Background: Monocytosis is a common but non-specific finding that requires careful clinicopathologic correlation to determine the cause or need for more extensive workup. One of the first and most challenging steps in distinguishing reactive monocytosis (RM) from a neoplastic process, such as chronic myelomonocytic leukemia (CMML), is the assessment of peripheral blood monocyte morphology. Currently, little research exists investigating the morphologic characteristics useful in this distinction.

Design: Patients diagnosed with CMML at Brooke Army Medical Center between 2007 and 2017 were identified. Routine blood smears prepared between 1 July and 1 August 2017 and showing monocytosis ($\geq 2 \times 10^9/L$) were also collected. Ten unremarkable blood smears were used as controls. Blood smears from each group were blinded and randomized for review by a hematopathologist. Monocytes not identified as mature, promonocytic, or monoblastic were deemed "abnormal or immature" per criteria established by the 2009 International Working Group on Morphology of Myelodysplastic Syndrome (IWGMDS). Thirty-two morphologic characteristics were assessed for each abnormal monocyte, up to 20 cells per case. Data was statistically analyzed for morphologic characteristics that might predict CMML.

Results: There were 7 CMML and 31 RM patients. The mean age for CMML and RM patients is 68.0 years (range 58-81) and 50.8 years (range 19-96) with a male:female ratio of 4:1 and 2.1:1, respectively. The most common cause likely contributing to reactive monocytosis was trauma (N=9, 29%) followed by burns (N=4, 12%). Features suggestive of CMML over RM were a higher mean relative percentage of mature monocytes (17.5% vs. 5.75%, p=0.048), a higher mean occurrence of abnormal monocytes with "deeply indented" nuclei (7.4 cells vs. 3.7 cells, p=0.005) and presence of more than 1 nucleolus (10.2 cells vs. 7.8 cells, p=0.042). The feature suggesting RM over CMML was a higher mean occurrence of abnormal monocytes with "convoluted" nuclei (7.3 cells vs. 3.4 cells, p=0.039). See **Table 1** and **Figure 1** for additional morphologic characteristics and statistics.

Characteristics Assessed		Mean CMML	Mean Reactive Monocytosis	Mean Control	ANOVA p-value	Two-tailed t-test p-value
Mature Monocytes, % Total WBC		17.5	5.8	2.5	0.000	0.048
Abnormal Monocytes, % Total WBC		12.4	4.3	2.9	0.000	0.132
Promonocytes, % Total WBC		2.0	6.5	0.5	0.786	n/a
Granularity	None	4.0	1.5	0.4	0.105	n/a
	Few	6.8	3.0	5.0	0.006	0.119
	Many	9.0	15.6	14.6	0.006	0.100
Granularity Color	Azurophilic	7.0	2.9	3.4	0.063	n/a
	Pink	9.6	17.2	18.5	0.001	0.089
Cytoplasmic Color	Pale	0.0	0.0	0.0	n/a	n/a
	Light Blue	2.8	2.3	2.2	0.876	n/a
	Basophilic	17.2	17.6	17.8	0.884	n/a
	Other	0.0	0.0	0.0	n/a	n/a
Vacuoles	None	10.0	11.5	11.0	0.793	n/a
	Few	9.0	7.1	7.4	0.649	n/a
	Many	1.0	1.3	1.4	0.915	n/a
Vacuole Size	Small	9.0	6.8	8.1	0.537	n/a
	Large	2.0	2.0	2.1	0.993	n/a
Membrane Scalloping		9.2	2.7	3.1	0.001	0.128
Membrane Blebbing	Small	2.4	1.2	2.9	0.045	0.386
	Large	0.6	0.1	0.0	0.019	0.255
Basophilic Edge		14.2	9.2	10.5	0.136	n/a
Smooth Cell Membrane		18.6	18.5	17.9	0.874	n/a
Nuclear Folding	None	1.0	1.2	1.4	0.842	n/a
	Lightly Indented	7.6	7.7	5.4	0.101	n/a
	Deeply Indented	7.4	3.7	4.2	0.002	0.006
	Convoluted	3.4	7.3	9.1	0.033	0.039
Number of Nucleoli		27.4	24.1	14.5	0.002	0.222
Nucleolus Size	Large	3.0	2.0	1.2	0.461	n/a
	Small	9.4	9.8	7.6	0.139	n/a
N:C Ratio	<50%	1.2	0.3	0.4	0.100	n/a
	50-75%	16.4	14.2	14.0	0.348	n/a
	>75%	2.2	5.6	5.6	0.102	n/a
Chromatin	Condensed	11.0	15.2	18.4	0.002	0.124
	Partially Condensed	8.4	4.8	1.6	0.005	0.212
	Fine	0.0	0.0	0.0	n/a	n/a
Number of Nucleoli	6	0.0	0.1	0.0	0.629	n/a
	5	0.0	0.0	0.0	0.798	n/a
	4	1.0	0.9	0.2	0.095	n/a
	3	3.2	2.6	1.0	0.003	0.221
	2	6.0	4.1	3.0	0.077	n/a
	1	1.8	3.3	4.3	0.130	n/a
0	8.0	8.8	11.0	0.098	n/a	
<i>> 1 Nucleolus Present</i>		10.2	7.8	4.5	0.003	0.042
<i>Deeply Indented Nucleus + >1 Nucleolus</i>		4.0	1.7	0.7	0.0002	0.013
Convoluted Nucleus + >1 Nucleolus		1.8	2.2	2.0	0.796	n/a
Condensed Chromatin + >1 Nucleolus		4.2	4.7	3.3	0.257	n/a
Partially Condensed Chromatin + >1 Nucleolus		5.8	3.1	1.0	0.004	0.124

Table 1. Statistical outcomes: Italicized boxes represent statistically significant characteristics. ANOVA compares CMML, reactive monocytosis and control. If a statistical difference was found, a two tailed t-test was performed between CMML and reactive monocytosis. Values represent number of cells with corresponding morphologic features unless otherwise specified.

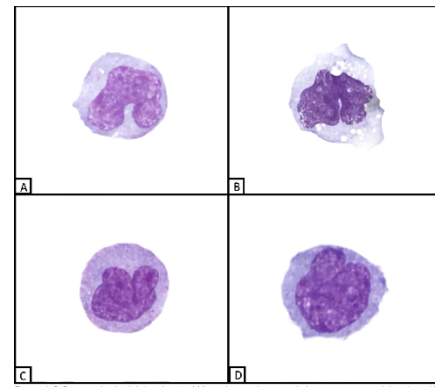


Figure 1. A, B) Demonstrating deeply indented nuclei (folding and deeper than one nucleolus seen more commonly in patients with CMML. C, D) Demonstrating convoluted nuclear folding seen more commonly in patients with reactive monocytosis.

Conclusions: Multiple abnormal monocytes with deep indentation of the nucleus or more than one nucleolus suggest features of monocytic dysplasia. Conversely, multiple abnormal monocytes with nuclear convolution are more suggestive of reactive monocytosis. This suggests the novel idea that morphologic features can distinguish reactive monocytosis from CMML.

1412 Clinicopathologic Analysis of Clonal Composition of Multiple PTLDs Occurring in Individual Solid Organ (SOT) and Bone Marrow Transplant (BMT) Recipients

Miguel D Cantu¹, Wayne Tam², Mustafa Al-Kawaaz¹, Amy Chadburn².
¹New York Presbyterian Weill Cornell, New York, NY, ²Weill Cornell Medical College, New York, NY

Background: Non-Hodgkin lymphomas in an immunocompetent individual occurring in diverse sites or at separate times, if morphologically and phenotypically similar, are usually genetically similar. Thus, a single biopsy may be sufficient to determine diagnosis and treatment. In contrast, we and others have noted separate lesions in immunosuppressed patients, such as transplant (Tpx) recipients, may have different clonal composition even if morphologically similar, a finding that could impact treatment decisions. However, the incidence of clonal diversity in a given PTLD patient and whether it is related to Epstein Barr virus (EBV) status, type of organ transplanted or clinical outcome is not known.

Design: 56 concurrent anatomically separate and non-concurrent PTLDs from 6 bone marrow (BMT) and 7 solid organ (SOT) Tpx recipients (10M:3F; 16-73 years; 2-25 lesions per patient) were studied. PTLDs were considered concurrent if biopsied within 0.5 mo. PTLDs were examined for B cell clonality by Southern blot hybridization (35 PTLDs) or PCR analysis (BIOMED-2 IGH and IGK assays, InvivoScribe; 21 PTLDs). EBV status (31 PTLDs) was determined by EBER ISH (Leica) and LMP1 (DAKO) and EBNA2 (Abcam) IHC. PTLDs were classified as polymorphic (poly) or monomorphic (mono) per the Updated WHO criteria; non-clonal, non-destructive PTLDs were excluded.

Results: There were 4 mono and 52 poly PTLDs; all PTLDs from a single patient had similar morphology.

Clinicopathologic Features Based on Clonal Composition

Clonality	#Poly (Pt)	#Mono (Pt)	EBV Neg/Lat1	EBV Lat 2/3	BMT Pts (Tpx to PTLD)	SOT Pts (Tpx to PTLD)	Dead
Same	23 (7)	4 (2)	4	18	5 (3-11 mo)	4 (45-162 mo)	5/9 (1-32 mo)
Diverse	33 (4)	0	0	9	1 (8.5 mo)	3 (5-36 mo)	4/4 (2-7 mo)

The multiple BMT PTLDs occurred within 1 yr of Tpx (p=0.01). Mono PTLDs were EBV latency 1 or negative; polys were latency 2/3. Clonally diverse PTLDs were more frequent in SOT patients. All patients with clonally diverse lesions died of PTLD compared to 5/9 with clonally identical PTLDs (p=0.2).

Conclusions: Clonal analysis of separate PTLDs in 13 SOT and BMT recipients showed: 1. BMT patients with multiple PTLDs usually have concurrent PTLDs that arise early after transplant (<1 yr); 2. SOT patients with multiple PTLDs tend to have multiclonal disease; and 3. SOT/BMT PTLD patients with clonally diverse lesions tend to have more aggressive disease with short survival.

1413 Deep Learning Based Grading of Follicular Lymphomas

Jun Cao¹, Daniel R Fu², Qinglong Hu³, Baoxin Li¹, Kai Fu⁴. ¹Arizona State University, ²Millard High School, Omaha, NE, ³Carondelet St Joseph Hospital, Tucson, AZ, ⁴University of Nebraska Medical Center, Omaha, NE

Background: Follicular lymphoma (FL) is the second most common non-Hodgkin lymphoma diagnosed in the United States. The grading of FL is essential for the proper treatment of patients; grade 3A and 3B require more aggressive chemotherapy while grade 1 and 2 are considered as indolent and normally only require conservative treatment. Traditionally FL is graded based on the WHO histological procedure, which classifies the FL by counting the number of larger lymphoma cells called centroblasts (CB) in ten high power fields (HPF, defined as 0.159 mm²). However, this procedure is a tedious manual task for pathologists, and is prone to sampling bias.

Design: We use TensorFlow deep learning framework from Google to build our convolutional neural network (CNN) based classifier for four FL grades, grade 1, grade 2, grade 3A and grade 3B. Three convolutional layers with max pooling are used, first two with 32 filter banks and the 3rd one with 64 filter banks, to extract features, and followed by two fully connected layers for classification. In order to train the CNN with limited samples, we divided each training sample into twelve 320x320 samples, and augmenting each image by rotating 90 and 180 degrees as well as mirror imaging each rotated image, to obtain 288 training samples of each original sample. To speed up the training, each image is down-sampled to 128x128 before fed into the CNN.

Results: We have nine images of FL grade 1, nine images of grade 2, 15 images of grade 3A, and 14 images of grade 3B. We used cross validation to training the CNN, with 80/20 split between training and validation. We first train the CNN as a binary classifier for low risk (Grades 1 and 2) and then multi class classifier for grade 1, 2, 3A/B. In all cases, we have reached 100% classification accuracy, comparing to the original grading by the pathologists.

Conclusions: We have developed a fast and highly reproducible software framework to classify the microscopic images of FL into 2 grades (high/low risk) or 4 grades, with near 100% accuracy. It can be used for arbitrary size microscopic FL images and not limited by the HPF sizes. It gives instant grading results and smaller tissue samples can also be used. In additional, if the sample images are grouped into more classes, this framework can be trained to classify the images into more granularity for better quantitative measure of the severity of the disease.

1414 IgG4+ primary cutaneous marginal zone lymphomas (PCMZL) are common and similar to other class-switched PCMZL, but not IgM+ cases

Eric Carlsen¹, Steven H Swerdlow¹, Sarah E Gibson¹. ¹University of Pittsburgh School of Medicine, Pittsburgh, PA

Background: PCMZL are known to include a predominant heavy chain (HC)-switched type and a much less common, distinctive IgM+ type. More recently one study found 39% of cases to be IgG4+ with 2 others reporting only 13-25% IgG4+ cases. In order to further investigate the frequency and characteristics of IgG4+ PCMZL and to explore other potential differences between the HC-switched and IgM+ cases, the clinicopathologic and phenotypic features of 25 biopsies from 18 patients with PCMZL with plasmacytic differentiation were studied.

Design: All biopsies were stained for CD20, HCs including IgG4, light chains (LC), CD3, CD4, CD8, CD279/PD1, GATA3, and FOXP3. 6 patients had >1 biopsy showing PCMZL with different LC and/or HC restriction, which were considered separate lymphomas for analysis. IgG4 was considered positive if present in ≥40% of monotypic plasma cells (PC).

Results: The first biopsy from each of the 18 patients in the study included 7 (39%) IgG4+, 7 IgG+/IgG4-, 2 IgM+, 1 IgM+/IgA+, and 1 IgG4- case with unclear HC restriction. There were no differences in age or gender between IgG4+ and IgG4- cases. All IgG4+ cases were primarily dermal-based and no IgG4+ subcutaneous-based cases were identified. There were no other distinct pathologic features that discriminated IgG4+ from IgG4- cases, and the T-cell microenvironment as assessed by CD279, GATA3, and FOXP3 did not differ significantly. However, IgM+/IgG4- cases were more commonly subcutaneous (p=0.007), showed scattered rather than peripherally clustered PC (p=0.0001), and were more likely to have a B-cell-predominant infiltrate (p=0.003) compared to IgM- cases.

Clinicopathologic Features from the 1 st Biopsy of 18 Patients with PCMZL						
	No.	Median Age (Range)	Male: Female	Primarily Dermal	Primarily Subcutaneous	Sites of Involvement
IgG4+	7	49 (29-62)	2:5	100%	0%	Back (3) Leg (2) Arm (1) Face (1)
IgG+/IgG4-	7	50 (25-80)	4:3	86%	14%	Arm (5) Shoulder (2)
IgM+	2	73.5 (69-78)	0:2	50%	50%	Face (2)
IgM+/IgA+	1	64	0:1	0%	100%	Arm (1)
Unclear HC/ IgG4-	1	49	0:1	0%	100%	Arm/leg (1)

Pathologic Features of 24 Biopsies with HC Restriction from 18 Patients with PCMZL						
	No.	Primarily Dermal	Primarily Subcutaneous	PC Clustered at Edge of B-cell Nodules	CD3:CD20 >50%	CD4:CD8 >3:1
IgG4+	7	100%	0%	100%	86%	100%
IgG+ or IgA+/ IgG4-	12	83%	17%	92%	75%	92%
IgM+	4	25%	75%	0%	0%	50%
IgM+/IgA+	1	0%	100%	0%	0%	0%

Conclusions: IgG4 expression is seen in approximately 50% of dermal-based PCMZL, and was not identified in any primarily subcutaneous-based PCMZL in our cohort. Although IgG4+ PCMZL are not otherwise distinguishable from non-IgG4 class-switched cases, IgM+ PCMZL have distinctive pathologic features including a newly described apparent predilection for the subcutis and scattered, rather than peripherally clustered, PC. Differences in the reported proportion of IgG4+ and HC-switched PCMZL will therefore be impacted by whether or not subcutaneous PCMZL are included, as well as if secondary marginal zone lymphomas involving the skin, which are more likely to be IgM+, have not been excluded.

1415 Evaluation of Extranodal Marginal Zone B Cell Lymphoma by Flow Cytometry

Luis F Carrillo¹, Alexandra Harrington¹, Horatiu Olteanu¹, Steven Kroff¹. ¹Medical College of Wisconsin, Milwaukee, WI

Background: MALT lymphomas have been well characterized using immunohistochemistry, but little data exists regarding their flow cytometry (FC) immunophenotypes, or even how applicable flow cytometry is to the evaluation of these lesions.

Design: Archives were searched over 10 years for cases of MALT lymphoma, and those for which FC analyses were performed were included (65 cases). All were evaluated by either 4- (19 cases) or 8-color (46 cases) flow cytometry using antibodies to CD5, CD10, CD19, CD20, CD23, FMC7, CD38, and surface immunoglobulin Ig in most cases. Intensity of CD19, CD20, and Sig was assessed relative to internal polyclonal B cells. Intensity of CD23, FMC7, and CD38 was compared to an isotype control using the following thresholds: negative <20%; dim(+) 20-49%; positive 50-79%, and bright positive 80-100%.

Results: There were 18 men and 47 women (ages 40-102 yrs, median 67). A clonal B-cell population was detectable in 63/65 cases. One case appeared technically satisfactory but contained no detectable B-cell clone, and another lacked viable B cells. Clonal B cells constituted 0.34-75% of events (median 14%), reactive B cells 0.04-47% of events (median 3.1%), and reactive T cells 0.7-76% of events (median 23%). The ratio of neoplastic to polyclonal B cells ranged from 0.1-1300 (median 44.2); clonal B cells were outnumbered by reactive B cells in 4 cases. CD19 was expressed at normal intensity in 50 cases (76.9%), over-expressed in 11 (16.9%), and under-expressed in 4 (6.2%); CD20 was normal intensity in 46 cases (70.8%), over-expressed in 10 cases (15.4%), and under-expressed in 9 (13.8%); Sig was normal intensity in 51 (78.5%) over-expressed in 4 (6.2%), and under-expressed in 10 (15.4%). CD38 was bright in 11/62 cases (16.9%), positive in 17 (26.2%), dim in 18 (27.7%), and negative in 16 (24.6%). CD23 was bright in 3/59 cases (4.6%), positive in 9 (13.8%), dim in 31 (47.7%), and negative in 15 (24.6%). FMC-7 was bright in 12/60 cases (18.5%), positive in 12

(18.5%), dim in 16 (24.6%), and negative in 20 (30.8%). The median plasma cell percentage was 0.095% (range, 0.01-7.5). In 6 cases the plasma cells showed surface light chain restriction; in the remainder the plasma cells were Sg(-).

Conclusions: FC detects clonal B-cell populations in the large majority of MALT lymphomas. In a minority of cases, the clonal B cells are outnumbered by polyclonal B cells, but can be discriminated by aberrant antigen expression. B-cell antigens show varying intensities of expression across cases.

1416 CD4 T-Cell Predominance and B-Cell Depletion in T-cell/Histiocyte Rich Large B-cell Lymphoma: Flow Cytometric Analysis of Diagnostic Specimens and Staging Bone Marrow Biopsies

Alisa Caudell¹, Tuan Tran², Michael Stump³, John Krause⁴, Kathryn G Lindsey⁵. ¹Mount Pleasant, SC, ²Baylor University Medical Center, ³Charleston, SC, ⁴Baylor University Medical Center, Dallas, TX, ⁵Medical University of South Carolina, Charleston, SC

Background: Contrary to established literature, recent evidence suggests that in many cases CD4+ (rather than CD8+) T-cells may predominate the background T-cell population of T-cell/Histiocyte Rich Large B-cell Lymphomas (THRLBCL). This has potentially important diagnostic implications as predominance of CD4+ versus CD8+ background T-cells has been reported in Nodular Lymphocyte Predominant Hodgkin Lymphoma (NLPHL) versus THRLBCL while mounting evidence suggests a biologic relationship between both. Hypogammaglobulinemia and lymphopenia are also reported with THRLBCL. The incidence and mechanism remains unknown, but the finding suggests a systemic effect.

Design: We accrued cases of THRLBCL and NLPHL from 2 institutions. We hypothesized that the CD4+ T-cell predominance and the B-cell depletion may additionally be present in the flow cytometric analyses of the staging bone marrow biopsies. Twenty-five specimens were identified bearing the diagnosis of THRLBCL and 23 specimens of NLPHL. We analyzed flow cytometric data from the diagnostic specimen, the staging bone marrow biopsy, and peripheral blood if performed and chronicled the clinically available data including history, immunoglobulin level, and CBC (complete blood count) data.

Results: CD4+ T-cells predominated in both sets of diagnostic (or disease recurrence) specimens. CD4:CD8: THRLBCL (n=20) mean=4.6; NLPHL (n=21) mean=6.9. Relative B-cell depletion was also noted as a trend for these specimens. T:B cell ratio: THRLBCL mean=37.3, NLPHL mean=14.2. For the staging marrow specimens, the same trends were observed. In the THRLBCL group, four patients had absolute B-cell lymphopenia (defined as <100 cells/uL), one had hypogammaglobulinemia, and one showed a discrete population of CD4 and CD8 dual positive T-cells. This dual positive population was also observed in 2 cases in the NLPHL group. Preceding the diagnosis of THRLBCL, two patients bore diagnoses of small mature B-cell lymphomas that were not subsequently identified.

FOR TABLE DATA, SEE PAGE 571, FIG. 1416

Conclusions: These data corroborate a recent report suggesting that CD4+ T-cells exist in greater numbers in THRLBCL than originally thought and highlights a similarity to NLPHL. These data also suggest that the mechanism that leads to CD4+ T-cell increases and B-cell depletion in affected nodes may be systemic, changing the milieu of the peripheral blood and bone marrow, a phenomenon not yet reported.

1417 Epstein-Barr virus upregulates autophagy in Hodgkin lymphoma: A potential targeting therapy by autophagy inhibition

Kung-Chao Chang¹, Hui-Wen Chen², Jung-Ting Chiang². ¹Tainan, Taiwan, ²National Cheng Kung University and Hospital

Background: Hodgkin lymphoma (HL) is derived from germinal center B cells with defective surface B-cell receptors, crippled immunoglobulin transcripts, and lost B-cell programs due to epigenetic silencing. Epstein-Barr virus (EBV) may play a role in the tumorigenesis of HL. Accumulation of viral proteins in endoplasmic reticulum (ER) may cause ER stress responses and lead to either apoptosis or survival depending on the driving signals. We have previously found that survival signals of ER stress response were dominantly expressed over the ER death signals. Given that HL cells dominantly express survival signals of ER stress response and autophagy occurs in response to ER stress and ER protein aggregates, we hypothesize that autophagy pathways are upregulated in HL cells that may be associated with EBV status.

Design: Using HL cell lines, L-428 transfected with EBV latent membrane protein 1 (LMP1), and KM-H2 infected with EBV, we studied the altered protein expression of autophagy pathway. Immunostaining on clinical HL samples (n=127) was also performed to test the expression of autophagy (LC3) and the association with EBV positivity, LMP1 expression and prognoses. In addition, autophagy inhibitors and cytotoxic agents were added to study the changes of autophagy signals on HL cells.

Results: *In vitro* EBV-LMP1 transfection induced a modest increase in autophagy signals by LC3-II Western blotting. Treatment of chloroquine (CQ), an autophagy inhibitor, enhanced cell death of LMP1-positive (LMP1+) HL cells compared with LMP1-negative (EGFP) HL cells through caspase activation pathway. Clinically, LC3-II was expressed in 15% of HL samples (19/127) and interestingly positive in all three cases of lymphocyte-depleted (LD, 3/3) subtype and none in lymphocyte-predominant (LP, 0/4) and lymphocyte-rich classical (LRC, 0/10) types. Expression of EBV by EBER in situ hybridization was found in 53.6% (67/125) of all HL cases tested. The expression of autophagy marker LC3-II was not significantly associated with EBV status or clinical outcome. Doxorubicin treatment induced cell death through a similar mechanism.

Conclusions: It indicates that autophagy signaling promotes cell survival and growth in HL cells and EBV upregulated the expression of autophagy signaling. Treatment of autophagy inhibitor and/or cytotoxic agents induced HL cell death, suggesting the potential strategy targeting autophagy inhibition on HL therapy.

1418 Expression of CXCL12 in Bone Marrow Is Different Between Myelodysplastic Syndrome and Aplastic Anemia by Immunohistochemical Stain

Chen Chang¹, Hui-Wen Chen¹, Jung-Ting Chiang¹. ¹National Cheng Kung University Hospital, Tainan, Taiwan

Background: Myelodysplastic syndrome (MDS) and aplastic anemia (AA) are diseases both revealing ineffective hematopoiesis and present cytopenia clinically despite the former generally regarded as "dysplastic" or "neoplastic" in nature while the latter with "immune-mediated" characters. They may cause diagnostic difficulties in some cases, especially those with mild cellular dysplasia and without abnormal cytogenetic changes. Increased bone marrow (BM) stromal stem cells has been reported in MDS. Here, we tested associated markers-CXCL12 and Nestin in BM of MDS and AA. We also compared them to nearly normal marrow as control group.

Design: Formalin-fixed-paraffin-embedded BM tissue blocks with diagnosis of MDS (n=24), AA (n=27) and nearly normal cases (n=16) were collected. BM stromal stem cell markers- CXCL12 and Nestin were tested in these three groups of BM tissue via immunohistochemical (IHC) stains. For measuring of CXCL12 and nestin, semiquantitative score was given from 0-4 as higher scores meaning stronger staining. The staining was further separated into 2 patterns: the first pattern shows linear staining surrounding hematopoietic cells, which is usually strong and continuous (Fig1); the second pattern is interstitial staining along the contour of fat cells, which usually presented as weak and broken-linear staining(Fig 2).

Results: Expression of CXCL12 and nestin is stronger in MDS than in AA ($p=0.014$, $p=0.001$, respectively), but not significantly when compared with control group. The expression patterns 1 and 2 are significantly different between MDS and control group ($p<0.001$), but not in AA and control group. For hypocellular MDS (<35% cellularity, n=7), CXCL12 expression pattern 2 is different from AA ($p=0.007$). In addition, expression of CXCL12 is an unfavorable factor in MDS patients ($p=0.005$).

Table 1 Summary of clinicopathological features

Parameters	MDS (n=24)	AA (n=27)	Control (n=16)	P-value			
				3 groups	MDS/AA	MDS/control	AA/control
Age	57.6	34.3	44.9	0.005	0.001	0.101	0.216
Gender M:F	15:9	18:9	11:5	1.000	1.000	1.000	0.446
WBC (/ μ L)	4609	2363	6543	<0.001	0.038	0.010	<0.001
Neu (%)	35	35	68	<0.001	0.844	<0.001	<0.001
ANC (/ μ L)	2290	894	4483	<0.001	0.380	<0.001	<0.001
Hb (g/dL)	8.4	8.4	10.7	0.016	0.952	0.007	0.011
Platelet (/ μ L)	84760	52333	215714	<0.001	0.025	<0.001	<0.001
PB blast (%)	3.3	0	0	<0.001	<0.001	0.014	1.000
BM cellularity	52	8	40	<0.001	<0.001	0.162	<0.001
BM blast (%)	6.5	0.3	-	-	<0.001	-	-
BM fibrosis (MF score 2)	2/24 (8%)	0/27 (0%)	0/16 (0%)	0.179	0.216	0.508	-
Clonal change of cytogenetics	8/22 (36%)	1/16 (6.3%)	0/11 (0%)	0.013	0.052	0.031	0.593
Follow-up duration (month)	19.6	40	-	-	0.171	-	-
Death	9/24 (37.5%)	5/27 (18.5%)	-	-	0.209	-	-
CXCL12	2	1	1.6	0.036	0.014	0.886	0.074
Pattern 1	20/24 (83.3%)	8/27 (29.6%)	2/16 (12.5%)	<0.001	<0.001	<0.001	0.276
Pattern 2	1/24 (4.1%)	20/27 (74.1%)	12/16 (75.0%)	<0.001	<0.001	<0.001	0.621
Nestin	0.5	0.3	0.4	0.003	0.001	0.354	0.040

Statistical method: for numerical factors, Kruskal Wallis Test for 3 groups and Mann-whitney U test between groups; for categorical factors, chi-square test

Table 2 IHC markers in hypocellular MDS (hMDS), AA and control group

Parameters	hMDS (n=7)	AA (n=27)	Control (n=16)	P-value		
				3 group	hMDS/AA	hMDS/control
CXCL12	0.9	1	1.6	0.156	0.650	0.201
Pattern1	3/7 (42.9%)	8/27 (29.6%)	2/16 (12.5%)	0.264	0.656	0.142
Pattern2	1/7 (14.3%)	20/27 (74.1%)	12/16 (75.0%)	0.013	0.007	0.019
Nestin	0.4	0.3	0.4	0.082	0.143	0.883

Abbreviation: hMDS-hypocellular MDS (<35% cellularity)

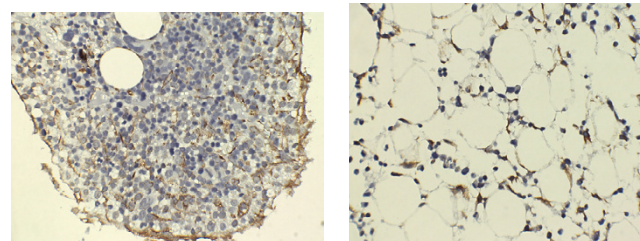
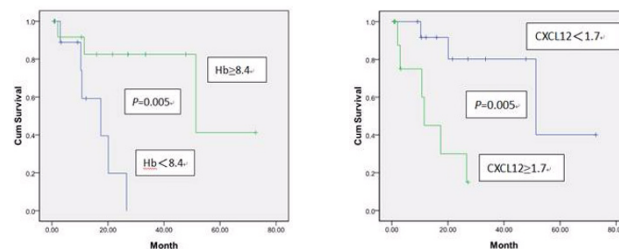
Statistical method: for numerical factors, Kruskal Wallis Test for 3 groups and Mann-whitney U test between groups; for categorical factors, Fisher's exact test

Table3 Unfavorable factors in MDS

Parameters	Prognostic factor	Univariate	Multivariate
		P-value	P-value
Age	59 (50%)	0.939	-
Gender M:F	F (33%)	0.182	0.402
WBC (/ μ L)	3150 (50%)	0.990	-
Neu (%)	29.5 (50%)	0.538	-
ANC (/ μ L)	926 (46%)	0.592	-
Hb (g/dL)	<8.4 (46%)	0.005	-
Platelet (/ μ L)	68000 (50%)	0.542	-
PB blast	Yes (38%)	0.187	0.462
BM cellularity	47.5 (50%)	0.125	0.384
BM fibrosis (MF score 2)	Yes (8%)	0.568	-
Clonal change of cytogenetics	Yes (33%)	0.260	0.799
Excess of BM Blast	5 (58%)	0.679	-
IPSS-R	4.3 (50%)	0.245	0.693
CXCL12	1.7 (46%)	0.005	0.090
Pattern1	Yes (83%)	0.187	0.976
Pattern2	No (96%)	0.749	-
Nestin	0.48 (50%)	0.787	-

Univariate survival analysis: Kaplan-Meier method by log rank test; *if p-value<0.05

Multivariate survival analysis: Cox regression model, variates including p-value <0.3 in univariate model: gender, PB blast, Bone marrow cellularity, clonal change of cytogenetics, IPSS-R score, CXCL12, and pattern 1



Conclusions: CXCL12 IHC expression score and pattern are helpful for differentiating MDS from AA patient. Although more stromal stem cells contributes higher cellularity in MDS theoretically, which practically does not cause diagnostic problem in hypercellular marrow, for hypocellular MDS, the CXCL12 expression pattern is also different from AA in this study. Indeed, this study is limited by small case number and subjective scoring. More further validations are needed. However, we observed that CXCL12 surrounding fat cells is more frequently present in AA. A compensation mechanism after stem cell apoptosis in AA is presumed. In addition, CXCL12 is an unfavorable factor for MDS patients.

1419 Rapid Progression of Myelodysplastic Syndrome to Acute Myeloid Leukemia is Associated with Acquired Genetic Mutations in KRAS

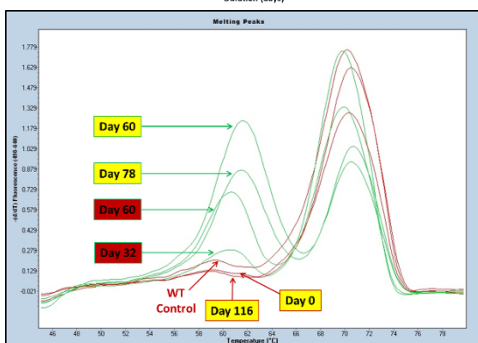
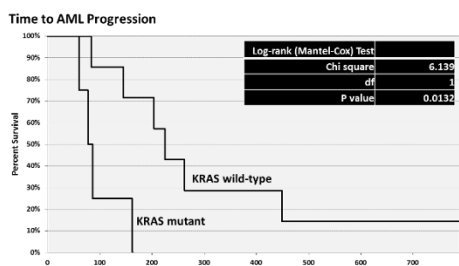
Nathan Charles¹, Molly Accola², Shannon McClintock³, James Varan², David Yang⁴, William Rehauer⁴. ¹Ypsilanti, MI, ²The University of Wisconsin Hospital, Madison, WI, ³The University of Michigan, ⁴University of Wisconsin, Madison, WI

Background: Myelodysplastic syndrome (MDS) is a clonal and genetically heterogeneous primary bone marrow disorder characterized by ineffective hematopoiesis and progression to acute myeloid leukemia (AML) in up to one third of patients. Recent

studies have shown temporally acquired genetic mutations in MDS increase the risk for leukemic transformation. Therefore, our goal was to identify and characterize dynamically acquired driver mutations from paired MDS and AML bone marrow samples that may be responsible for more rapid disease progression and worse patient outcome.

Design: Using an unbiased cancer hot spot next generation sequencing panel, paired bone marrow samples from AML patients with antecedent MDS were analyzed and compared for genetic mutation acquisition. High resolution melting curve analysis and pyrosequencing were used as rapid methods of mutation confirmation. Phospho-kinase array screening was implemented to identify potential downstream effectors for further investigation in transgenic MDS cell lines.

Results: Activating point mutations in *KRAS* were temporally acquired in 4 of 11 patients who also progressed to AML at significantly faster rates than those who remained *KRAS* wild-type ($p \leq 0.05$) (Fig. 1). *KRAS* mutational burden within bone marrow and peripheral blood samples was directly proportional to disease progression as measured by high resolution melting curve analysis (Fig. 2). Analyzing the activation status of 43 distinct kinases showed increased CREB phosphorylation, a downstream effector of *KRAS* signaling. Furthermore, immunohistochemistry revealed significantly increased expression of the CREB transcriptional target and pro-survival factor BCL-2 ($p \leq 0.05$). Subsequently established transgenic MDS cell lines possessing inducible mutant *KRAS* (G12V) preliminarily demonstrate increased survival as compared to wild-type control.



Conclusions: Using next generation sequencing and high resolution melting curve analysis, we have established a paradigm for identifying dynamically acquired and patient specific driver mutations followed by rapid monitoring of mutational burden. Specifically, acquired gain of function *KRAS* mutations are associated with significantly faster AML progression rates potentially mediated via CREB activated transcriptional control of *BCL-2*. Therefore, early detection and targeted disruption of the *KRAS*-CREB-BCL-2 pathway may lengthen or altogether prevent leukemic transformation in MDS patients who acquire *KRAS* mutations during the course of their disease.

1420 Objective Quantification of BCL2 Protein and Transcript in Routine Biopsy Samples Demonstrates Associations with BCL2 Translocation, BCL2 Copy Number Increase, and Response to R-CHOP in Patients with Diffuse Large B-cell Lymphoma

Lina Chen¹, Yi (Daniel) L², Kathrin Tyrtyshkin¹, Lan Deng¹, David Scott³, Michael Rauh¹, Susan Crocker¹, Tara Baetz¹, David LeBrun¹. ¹Queen's University, Kingston, ON, ²Kingston, ON, ³BC Cancer Agency and University of British Columbia, Vancouver, BC, Canada

Background: Biomarkers are needed to better inform clinical management of patients with diffuse large B-cell lymphoma (DLBCL). We quantified BCL2 protein and transcript objectively in routine biopsy samples and investigated associations with *BCL2* cytogenetic status, MYC expression and MYC cytogenetic status, and clinicopathological parameters.

Design: We identified 63 cases of *de novo* DLBCL diagnosed at Kingston General Hospital and treated first-line with R-CHOP. We quantified BCL2 and MYC protein by IHC and BCL2 by multi-channel immunofluorescence (IF) microscopy coupled with computer-assisted image analysis. We enumerated *BCL2* and *MYC* transcripts with the NanoString nCounter® system. We performed fluorescence *in situ* hybridization (FISH) using an *IGH-BCL2* dual color dual fusion probe and a *MYC* dual color break apart probe.

Results: BCL2-positive cases by IHC had higher BCL2 expression by IF (KW* $p < 0.001$) or NanoString (KW $p < 0.001$). BCL2 expression by IF and NanoString were highly correlated (Rho=0.65, $p < 0.001$). *IGH-BCL2* fusion or *BCL2* copy number increase (CNI) was associated with up-regulated BCL2 expression (IF, KW $p = 0.004$ and 0.04, respectively; NanoString, KW $p = 0.0002$ and 0.003, respectively). Lower BCL2 expression by any method was associated with complete response to R-CHOP (IHC, $\chi^2 p = 0.03$; IF, KW $p = 0.03$; NanoString, KW $p = 0.01$) but not other clinical outcome (overall survival or relapse). MYC-positive cases by IHC had higher MYC expression by NanoString (KW $p = 0.004$). MYC translocation, but not CNI, was associated with elevated MYC expression (IHC, $\chi^2 p = 0.007$; NanoString, KW $p = 0.004$). MYC expression, MYC/BCL2 dual expression, *BCL2* cytogenetic status, or MYC cytogenetic status was not associated with clinical outcome. Double hit status results were non-informative due to limited sample size.

*KW: Kruskal-Wallis test

Conclusions: BCL2 and MYC expression can be quantified objectively in routine biopsy samples. Both *BCL2* gene translocation and CNI were associated with elevated BCL2 expression. Lower BCL2 expression, ascertained by either IHC, IF or NanoString, was associated with complete response to R-CHOP therapy. MYC translocation, but not CNI, was associated with elevated MYC expression. MYC expression, MYC/BCL2 dual expression, or *BCL2* or MYC cytogenetic status was not associated with clinical outcome.

1421 Whole Slide Imaging (WSI) Of Peripheral Blood (PB) Smears Shows Improved Detection of Rare Cells Compared to Static Imaging

Rong Chen¹, Katsiaryna Laziuk², Mikhail L Kovalenko³, Richard Hammer². ¹University of Missouri School of Medicine, Columbia, MO, ²Columbia, MO, ³University of Missouri, Columbia, MO

Background: Digital imaging technologies have been employed widely in pathology for the purpose of diagnosis and have in some instances been used for remote diagnosis. Our recent study showed that static high-resolution jpg images of PB films is able to detect clinically urgent events such as acute leukemia (AL), increased blasts and numerous schistocytes/spherocytes, and able to distinguish small-cell lymphoid neoplasms (SCLN) from AL; although is poor at detecting rare cells and few schistocytes. WSI, which scans the entire glass slide, has provided a novel technology in clinical applications. This study evaluates the use of WSI in remote diagnosis of (PB) films requiring review by a pathologist.

Design: One hundred PB films were scanned for WSI by an IT professional with no training in pathology or hematology. Diagnoses were performed independently by two hematopathologists with the images provided remotely using an in-house developed system. Remote image evaluation was compared to the final reports issued by standard microscopic evaluation. Diagnoses of each PB film based on WSI and static high-resolution jpg images from the prior study were also compared.

Results: Pathologist showed an inter-observer agreement of 91% with WSI compared to 89% with static images that was not significant. Overall agreement with the final diagnosis improved from 76% (discrepant if both reviewers didn't agree) to 91% ($P = 0.0044$). Acute leukemia (AL) and blasts were reliably identified in 100% of cases. WSI showed improvement in identifying rare blasts (55% compared to 12%, $P < 0.0001$). One case of APL with pancytopenia not diagnosed due to paucity of cells on static images was recognized on WSI. A significant discrepancy in schistocytes with jpgs (95% and 58%, overall 76%) was improved to 91% with WSI. Both WSI and static imaging showed 100% concordance in detecting sickle cells and SCLN and chronic myelogenous leukemia or leukemoid reactions. There was no misdiagnosis of SCLN as AL.

Conclusions: Both WSI and static high-resolution jpg images of PB films are adequate to detect clinically significant urgent events such as AL, increased blasts, and numerous schistocytes/spherocytes. In addition both techniques are adequate to distinguish SCLN from AL. However static imaging is poor at detecting rare cells, few schistocytes, and infrequent cells. Accurate detection of these cells can be improved with WSI techniques.

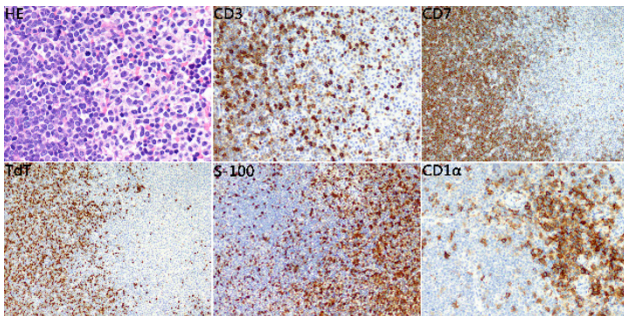
1422 Clinicopathological analysis of composite T-lymphoblastic leukaemia/lymphoma and histiocytic/dendritic cell neoplasms: A study of 7 cases

Yanping Chen¹, Jianping Lu¹, Jianchao Wang¹, Chunwei Xu¹, Gang Chen¹. ¹Fujian Cancer Hospital, Fuzhou, China/Fujian

Background: Composite lymphomas (CLs) have been reported in 1-4.7% of all lymphomas, however, CLs containing both T-lymphoblastic leukaemia/lymphoma (T-ALL/LBL) and histiocytic/dendritic cell (H/DC) neoplasms are very rare and can pose a substantial diagnostic challenge

Design: Here, we studied the clinical and pathological features of 7 patients with both T-ALL/LBL and H/DC neoplasms occurring in lymph nodes, using immunohistochemistry, in situ hybridization for EBV-encoded nuclear RNA (EBER) and polymerase chain reaction (PCR) analysis for TCR rearrangement.

Results: The patients included 5 men and 2 women ranging in age from 7 to 83 years (median age, 47.0 years). The H/DC neoplasms included 1 histiocytic sarcoma, 3 langerhans cell histiocytosis, and 3 interdigitating dendritic cell tumors. One H/DC neoplasm was metachronous, following T-LBL by 5 months; tumors were synchronous in 6. These six cases showed near total effacement of the lymph node architecture by T- LBL (CD3+ and TdT+) with scattering distribution dendritic cell neoplasm component (CD3- and TdT-). The diagnosis of dendritic cell neoplasm was confirmed by detecting S-100, CD1a, CD207. The presence of some degree of nuclear atypia, some mitotic figures and CyclinD1 positive suggest that this is a neoplastic rather than hyperplastic dendritic cell proliferation. All cases were negative for EBER. PCR analysis identified identical TCR rearrangements in only 1 of 7 cases, but interestingly another 2 cases showed identical polyclonal peaks in microdissected neoplastic cells from T-LBL and DC neoplasm components.



Conclusions: Our results suggested that CyclinD1 positive was useful in diagnosing H/DC neoplasms component and the T-ALL/LBL and H/DC cells were derived from a common precursor when occurring in the same patient.

1423 Myeloid Differentiation Associated MicroRNA Set Is Deregulated in Acute Myeloid Leukemia

Jinjun Cheng¹, Meiyun Fan², Yongdong Wang³, James Downing⁴, Jinghui Zhang⁵, Xiang Chen³. ¹Memphis, TN, ²Center of Cancer Research, The University of Tennessee Health Science Center, ³St Jude Children's Research Hospital, ⁴St. Jude Children's Research Hospital, Memphis, TN

During normal hematopoiesis, multiple microRNAs are involved in hematopoietic stem cell self-renewal, progenitor lineage commitment and differentiation by coordination of multiple target genes. Some of these miRs have been associated with the pathogenesis of acute leukemia. Herein, we monitored the granulocytic differentiation from normal bone marrow CD34 positive progenitor cells and explored the miRNAs regulatory networks during normal myeloid differentiation and their potential deregulation in acute myeloid leukemogenesis.

By using Human miRNA v19 Microarray (Agilent Technologies, 046064), we screened expression levels of human miRNAs during in vitro myeloid differentiation and identified a cohort of miRNAs associated with myeloid differentiation. Meanwhile, we extracted the clinical outcome data, mRNA expression and miRNA expression data for AML patients from The Cancer Genome Atlas (TCGA) Data Portal1 (Cancer Genome Atlas Research Network, 2013). By integrating analysis of TCGA and our differentiation data, we are looking for a myeloid differentiation associated microRNA set which is also deregulated in TCGA AML patient cohort. An independent patient cohort will be collected to validate significance of our analysis results.

Our integrated analysis shows that miR-181 family members are likely plays a role in maintaining CD34+ cells in the undifferentiated state, and high expression of these miRs in TCGA AML is associated with early onset of tumor and short survival. Moreover, miR-29b gradually

increased its expression as terminal granulocytic differentiation and may play a role in promoting differentiation, and repression of this miR in TCGA AML is associated with early onset of leukemia. We further explored the potential targeted mRNAs of these identified miRNAs involving in granulocytic differentiation which also are dysregulated in AML pathogenesis and predictive of survival in AML patients. Through step-wise integrated analysis, two miR-mRNA pairs including miR-181 family - PRKCD and miR-29b - DNMT3A are identified to be significantly associated with poor prognosis in AML patients.

In this study, we identified a myeloid differentiation associated microRNA set which is also deregulated in acute myeloid leukemia. An independent patient cohort is necessary to further validate the significance of our analysis results.

1424 Distinct Clinical, Laboratory, Molecular and Pathologic Features of Systemic Mastocytosis Involving the Gastrointestinal Tract

April Chiu¹, Thanai Pongdee¹, Michael Keeney¹, Hee Eun Lee¹, Rong He¹, William R Macon¹, Dong Chen¹. ¹Mayo Clinic, Rochester, MN

Background: Systemic mastocytosis (SM) has a broad spectrum of mast cell (MC)-mediated symptoms and involves extracutaneous organ such as bone marrow (BM) and gastrointestinal tract (GI). However, the latter (SM-GI) is not well-characterized with regards to clinical symptoms, laboratory findings, KIT D816V mutation status, and histopathologic features. The aim of this study is to examine the clinicopathological features of SM-GI.

Design: We searched the Mayo Clinic database for GI biopsies (bx) with a diagnosis of SM in 1995-2017. Patients' age, gender, GI-related symptoms, serum tryptase levels, urine BPGF2, and endoscopic findings were recorded. Both GI and BM bx of the same patients were examined. Available immunohistochemical stains (IHC) of both GI and BM bx included KIT, tryptase, and CD25. Additional IHC including CD30, CD123, PD-1 and PD-L1 were also performed on the GI bx. KIT D816V mutational analyses were performed on BM aspirate or peripheral blood.

Results: A total of 11 patients (4 males and 7 females; median age 65, range 57-83 years) were identified, whose symptoms included diarrhea (n=11) which was the major indication of their GI bx, weight loss (n=9), abdominal pain (n=7), nausea (n=3), vomiting (n=3) and constipation (n=2). Their serum tryptase (median=128 ng/dL) and urine BPGF2 (median=12690 ng/24 hours) levels were markedly elevated. The GI bx were randomly taken from the stomach, duodenum, ileum, and/or colon; and were all involved by SM. The round and spindle-shaped MCs had a band-like subepithelial distribution in the lamina propria. The neoplastic MCs expressed KIT and CD25. Interestingly, in contrast to background normal MCs, the neoplastic MCs in 9 cases had weakly positive or negative staining for tryptase, and in 7 cases partially expressed CD123 and PD-L1 with variable intensity. MCs in all 11 cases were negative for CD30 and PD-1. All patients had BM involvement by SM with disease burden ranging 5-95%. In contrast to their corresponding GI bx, MCs in BM all had strong tryptase expression. All 6 cases with KIT D816V tested were positive for this mutation.

Conclusions: Patients with SM-GI have significant GI symptoms. The neoplastic MCs have distinct band-like subepithelial distribution and immunophenotype such as weak/negative tryptase and variable CD123 and PD-L1 expression. These findings underscore the importance of a further pathologic study of SM-GI and its potential impact on these patients' morbidity, prognosis, and novel immunotherapeutic options.

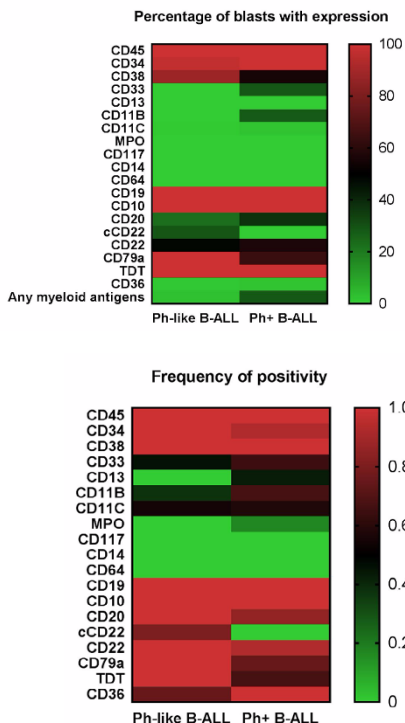
1425 Immunophenotypic Comparison of Philadelphia Chromosome-Like to Philadelphia Chromosome-Positive (Ph+) B-Lymphoblastic Leukemia

Sarah M Choi¹, Lina Shao¹, Daniel Boyer¹. ¹University of Michigan, Ann Arbor, MI

Background: Philadelphia chromosome (Ph)-like (*BCR-ABL1*-like) B-lymphoblastic leukemia (B-ALL) is a newly recognized provisional entity in the WHO classification which was originally identified as a subset of B-ALL with similar gene expression profile to Ph+ B-ALLs and which have recurrent rearrangement of targetable kinase genes, such as *CRLF2*, *PDGFR*, *EPOR*, *JAK2*, and *ABL* family kinases. Immunophenotypically, while Ph+ B-ALLs are known to demonstrate relatively frequent expression of myeloid antigens, the flow cytometric phenotype of Ph-like B-ALL has not yet been described.

Design: We retrospectively analyzed the immunophenotype of 13 cases of B-ALL and one case of mixed phenotype acute leukemia with Ph-like genetic signature in comparison with a control cohort of 14 cases of Ph+ B-ALL. Percentage of positive blasts (Figure 1) and frequency of positivity (Figure 2) was recorded for the following antigens: CD45, CD34, CD38, CD33, CD13, CD11B, CD11C, CD15, MPO, CD117, CD14, CD64, CD123, CD19, CD10, CD20, CD22, CD79A, HLDA, TDT, CD36 and CD71.

Results: Ph-like B-ALLs showed similar overall immunophenotypic profile to Ph+ B-ALLs (Figures 1 and 2). Ph-like B-ALLs showed uniformly consistent CD10 expression and frequent coexpression of myeloid antigens, in particular CD33 (n=5, 45%). In contrast to Ph+ B-ALL (n=6, 43%), CD13 expression was not observed in any of the Ph-like B-ALL cases. While CD20 expression was seen all Ph-like cases, Ph+ B-ALLs also showed frequent CD20 expression (n=12, 86%) and also demonstrated a tendency towards stronger and more uniform CD34 expression.



Conclusions: As might be expected based on the similar gene expression profile to Ph+ B-ALL, Ph-like B-ALL also demonstrates a similar immunophenotypic profile. Some of the phenotypic differences described here warrant further characterization on a larger cohort of samples. Both Ph-like B-ALLs and Ph+ B-ALLs showed frequent expression of CD20. This finding may indicate particular potential in combining rituximab therapy in addition to other targeted kinase inhibition in these poor prognostic B-ALL subgroups.

1426 Double Hit Ph-Negative B-ALL with MYC and BCL2 Rearrangements and CDKN2A Genetic Abnormalities: Report of Three Cases

Betty M Chung¹, Tara Miller¹, Suyang Hao¹, Arthur Zieske¹, April Ewton¹, Youli Zu¹, Sai Ravi K Pingali¹, Swaminathan Iyer¹. ¹Houston Methodist Hospital, Houston, TX

Background: While much research has focused on the features and poorer prognosis of double/triple hit diffuse large B cell lymphoma patients, little is known about the impact of concomitant MYC and BCL2 rearrangements on the outcomes of B-acute lymphoblastic leukemia patients.

Design: Three rare cases of MYC+/BCL2+ double hit B-ALL were identified and clinical characteristics, lab findings, and outcomes were analyzed along with tissue evaluation. Bone marrows were subjected to next-generation sequencing to identify gene mutations which may modify prognosis in these double hit acute leukemia patients.

Results: Patient 1 had a history of treated low grade follicular lymphoma (FL) with complex karyotype with del(17p) prior to presentation with B-acute lymphoblastic leukemia (B-ALL) bone marrow involvement. Patient 2 at initial presentation showed high grade FL and bone marrow involvement by B-ALL and FL. Patient 3 was initially diagnosed with B-ALL in both the bone marrow and a perirenal mass. Patient 1 and 2 FISH showed MYC+/BCL2+ double hit in bone marrow while biopsied lymph nodes only had t(14;18). Patient 3 had t(2;8) and biallelic additional chromatin on chromosome 14 noted as presumptive t(14;18). Patients 1 and 3 achieved short-lived remission while patient 2 had negative post-induction marrow but imaging suggestive of extensive residual disease. Patient 1 had CDKN2A deletion while patients 2 and 3 both had missense mutations in this gene at different exon 2 loci. Patient 2 was noted to have CDKN2A deletion and KIT, ATRX, and STAG2 missense mutations post-induction and expired nine months post-diagnosis. All of these

patients were Philadelphia chromosome negative. Patients 1 and 3 are less than one year from diagnosis and have progressive disease. Patient 1 will go into hospice and patient 3 into a clinical trial with calicheamicin-conjugated anti-CD22 monoclonal antibody.

Conclusions: Double hit B-ALL are thought to be rare, especially those which may have transformed from a clonally related follicular lymphoma. Characterization of the distinct features and outcomes of these patients is limited because fluorescent in situ hybridization for MYC, BCL2, and/or BCL6 translocations are not generally performed for acute leukemia. CDKN2A copy number alterations have been associated with adverse prognosis in B-ALL, independent of age. In this era of precision medicine, it is imperative that we identify additional prognostic and/or predictive biomarkers which may impact disease outcome.

1427 Novel Fusion of TCF3-MEF2B in BCR-ABL Negative B-Lymphoblastic Leukemia

Adam Cloe¹, Raju Pillai¹, Milhan Telatar¹, Hooi Yew¹, Dennis D Weisenburger¹, Vinod Pullarkat¹, Ibrahim Aldoss¹, Ching-Ying Kuo¹, Patricia Aoun¹, Michelle Afkhami¹. ¹City of Hope National Medical Center, Duarte, CA

Background: B-lymphoblastic leukemia (B-ALL) is characterized by a proliferation of immature precursor B-cells. Although the t(9;22) BCR-ABL1 fusion is the most common reported genetic abnormality in adult cases of B-ALL, other fusions have been reported including the Ph-like alterations. These Ph-like patients are typically younger and have poor prognosis. Compared to children with B-ALL, adults and adolescents with B-ALL have inferior outcomes. This is in part due to the lower prevalence of favorable genetic features such as hyperdiploidy and ETV6-RUNX1. In this study we examined the spectrum of Ph-like fusions detected by molecular profiling using a custom next generation sequencing panel.

Design: The laboratory information system was searched to identify patients with B-ALL diagnosed in the last 12 months. 33 cases of B-ALL were found. Next-generation sequencing (NGS) using a custom designed assay targeting 23 gene fusions was performed on RNA isolated from bone marrow aspirates, peripheral blood, or formalin fixed paraffin embedded tissue. The custom assay targets a known gene and identifies any fusion partner.

Results: The mean age of the patients was 39 (range 6-76) with a male to female ratio of 2:1. Four of 33 cases (12%) were positive for BCR-ABL1. The P2RY8-CRLF2, KMT2A-AFF1, TCF3-PBX1, TERF2-JAX2, and NUP214-ABL1 fusions were detected in 12%, 9%, 6%, 3% and 3% of cases, respectively. In one case, the panel identified a novel gene fusion, TCF3-MEF2B. For the remaining cases, no gene fusions were detected.

ID	Gender	Age	BCR-ABL Positive?	Fusion detected
B-ALL-1	M	25	No	TCF3-MEF2B
B-ALL-2	F	49	No	KMT2A-AFF1
B-ALL-3	M	76	No	KMT2A-AFF1
B-ALL-4	M	45	No	KMT2A-AFF1
B-ALL-5	F	26	No	NUP214-ABL1
B-ALL-6	M	40	No	P2RY8-CRLF2
B-ALL-7	M	22	No	P2RY8-CRLF2
B-ALL-8	M	28	No	P2RY8-CRLF2
B-ALL-9	M	70	No	P2RY8-CRLF2
B-ALL-10	F	27	No	TCF3-PBX1
B-ALL-11	M	61	No	TCF3-PBX1
B-ALL-12	M	32	No	TERF2-JAK2
B-ALL-13	M	21	Yes	BCR-ABL1
B-ALL-14	F	20	Yes	BCR-ABL1
B-ALL-15	F	64	Yes	BCR-ABL1
B-ALL-16	M	55	Yes	BCR-ABL1
B-ALL-17	F	6	No	Negative
B-ALL-18	M	61	No	Negative
B-ALL-19	M	40	No	Negative
B-ALL-20	M	60	No	Negative
B-ALL-21	M	24	No	Negative
B-ALL-22	M	29	No	Negative
B-ALL-23	F	31	No	Negative
B-ALL-24	M	25	No	Negative
B-ALL-25	F	29	No	Negative
B-ALL-26	F	55	No	Negative
B-ALL-27	M	38	No	Negative
B-ALL-28	M	39	No	Negative
B-ALL-29	F	36	No	Negative
B-ALL-30	M	24	No	Negative
B-ALL-31	M	28	No	Negative
B-ALL-32	F	72	No	Negative
B-ALL-33	F	44	No	Negative

Conclusions: Comprehensive genotyping with a NGS based- assays is an efficient way to detect known and novel fusions. In contrast to FISH, NGS assays may be designed to identify any partner. Using this technology, we identified a novel TCF3-MEF2B fusion. Although the effect of this fusion is unknown, a similar fusion involving TCF3 and the PBX1 gene results in a chimeric gene that fuses the activating regions of the TCF3 gene to the DNA binding region of PBX1. The resulting gene encodes a protein that causes constitutive activation of genes that the PBX1 protein binds. Similarly to PBX1, MEF2B encodes a transcription factor that is involved in the maturation of B-cells and can activate genes such as BCL-6. As a result, it is likely that the TCF3-MEF2B fusion results in the constitutive activation of genes activated by MEF2B.

1428 Clonal relationship between Blastic Plasmacytoid Dendritic Cell Neoplasm and myeloid neoplasms

Luis Colomo¹, Concepción Fernández², Xavier Calvo³, Blanca Espinet⁴, Beatriz Bellosillo⁵, Leonor Arenillas³. ¹Hospital del Mar, Barcelona, ²Hospital del Mar, ³IMIM-Hospital del Mar, ⁴IMIM-Hospital del Mar, Barcelona, Catalonia, ⁵Barcelona

Background: Blastic Plasmacytoid Dendritic Cell Neoplasm (BPDCN) is an aggressive tumor derived from the precursors of plasmacytoid dendritic cells. Although the incidence is not well-precised, rare cases of BPDCN associate with another myeloid neoplasm, mainly myelodysplastic syndromes (MDS), acute myeloid leukemia and chronic myelomonocytic leukemia (CMML).

Design: We have studied 5 patients with the concurrence of BPDCN and myeloid neoplasms (3 patients with MDS, and 2 CMML). The tumors were characterized by their cytological features, immunophenotype by flow cytometry and/or immunohistochemistry, cytogenetics and targeted sequencing of genes recurrently mutated in myeloid malignancies.

Results: The patients were 3 males and 2 females with a median age of 74 years (range 61-82 years). BPDCN and MDS were synchronous in 2 cases (both patients diagnosed of refractory cytopenia with multilineage dysplasia-RCwMD), whereas BPDCN followed the myeloid neoplasms in 3 cases (1MDS with isolated del(5q), 2 CMML). All cases had involvement of the skin by BPDCN except for the case of MDS with isolated del(5q), that presented only with bone marrow involvement. In such case, del(5q) was also identified in the tumor cells of BPDCN. In addition, a trisomy 8 was identified in the tumor cells of either BPDCN and CMML in one case. Results of targeted sequencing are showed in the table. In all cases, mutations in *TET2* were observed, whereas mutations in the splicing factors *ZRSR2* or *U2AF1* were identified in 3 out of 5 cases. Interestingly, the majority of mutations observed in the MDS/CMML phase were also observed when BPDCN appeared, with the exception of *TP53*, *IKZF1* and *NRAS* mutations that were only observed in BPDCN.

Case	Mutation	% MUT	% MUT
#1		CMML, BM 2011	BPDCN, BM/skin 2013
Male, 78 years	TET2: c.4468G>T; p.(Glu1490Ter)	40	35/40
	ZRSR2: c.868C>T; p.(Arg290Ter)	86	92/86
	ASXL1: c.1934dup; p.(Gly646TrpfsTer12)	18	31/0
	ASXL1: c.1900_1922del; p.Glu-635ArgfsTer15	0	0/9
	IKZF1: c.610_638del; p.Gly204LysfsTer7	0	34/54
#2		MDS 5q-, BM 2008	BPDCN, BM 2015
Female, 82 years	ASXL1: c.1438G>T; p.Glu480Ter	38	49
	TET2: c.3466_3468del; p.Asn-1156del	39	49
	TP53: c.536A>G; p.His179Arg	0	99
#3		CMML, BM 2013	BPDCN, skin 2015
Female, 82 years	TET2: c.2525C>G; p.Ser842Ter	42	90
	U2AF1: c.101C>T; p.Ser34Phe	43	46
	TET2: c.2428C>T; p.Gln810Ter	18	0
#4		RCMD, BM 2013	BPDCN, skin 2015
Male, 61 years	TET2: c.3263C>A; p.Ser1088Ter	21	42
	TET2: c.4122T>G; p.Cys1374Trp	19	39
	NRAS: c.182A>C; p.Gln61Pro	0	50
	ZRSR2: c.312G>A; p.(=) synonym, splicing site	21	91
#5		RCMD, BM 2016	BPDCN, skin 2016
Male, 70 years	TET2: c.1246_1247insCGAAC; p.(Pro416ArgfsTer13)	39	26
	KRAS: c.34G>T; p.(Gly12Cys)	3	53
	ASXL1: c.1934dup; p.(Gly646TrpfsTer12)	34	34

Conclusions: Our results suggest a clonal relationship between BPDCN and myeloid neoplasms. Notably, both tumors shared mutations involving DNA demethylation pathway and spliceosome machinery. In addition, mutations involving tumor suppressor genes (*IKZF1* and *TP53*) and oncogenes (*NRAS* and *KRAS*) may play a role for the development of BPDCN.

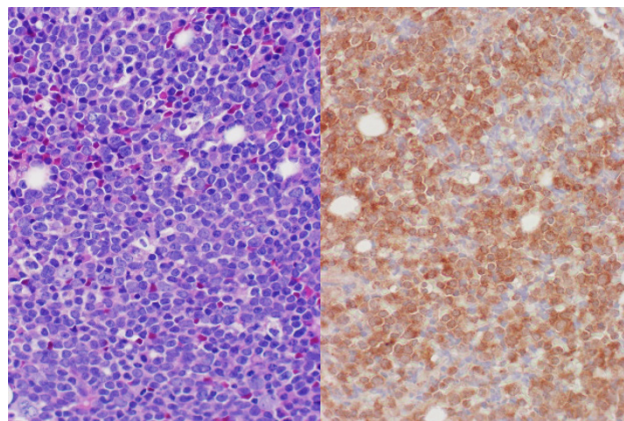
1429 IDH1 Mutation in Myeloid Malignancies: Correlation Between IDH1 Mutation Specific Immunohistochemistry and DNA-Based Sequencing

Joanna Conant¹, Jie Yan², Karen Buehler³, Mohammad Vasef¹. ¹University of New Mexico, Albuquerque, NM, ²University of New Mexico, ³TriCore Reference Laboratory

Background: Isocitrate dehydrogenase (IDH) mutations are identified in a subset of myeloid malignancies including acute myeloid leukemias (AML). In patients with normal karyotype and a *NPM1* mutation, *IDH1* mutations are associated with a favorable prognosis. However, in those with normal karyotype and wild type *NPM1*, *IDH1* mutations have an adverse prognostic impact. Currently, evaluation of *IDH1* mutation in AML is performed by PCR-based sequencing. In this study, we evaluated *IDH1* mutational status using *IDH1* R132H mutation specific immunohistochemistry (IHC) and correlated the results with DNA-based sequencing.

Design: From archival file of the Department of Pathology at the University of New Mexico, four molecularly documented *IDH1*-mutated adult cases of AML and 4 gliomas as determined by either pyrosequencing or next generation sequencing (NGS) and 4 *IDH1*-wild type AML cases were selected for *IDH1* IHC. For *IDH1* molecular testing by pyrosequencing, DNA was extracted from fresh diagnostic samples or recuts of paraffin tissue blocks and was subjected to PCR amplification of the *IDH1* region flanking hotspot mutations followed by pyrosequencing (PyroMark) to determine specific codon 132 base changes. In subset of cases *IDH1* sequencing analysis was performed in a myeloid gene panel by NGS on Illumina platform (NGS). Immunohistochemistry using *IDH1* R132H mutation specific antibody (Dianova, DIA-H09 clone) was performed on formalin-fixed paraffin-embedded tissue sections with appropriately reactive controls.

Results: *IDH1* sequencing analysis confirmed *IDH1* codon 132 mutations in 4 AML cases, including *IDH1* R132H in one and *IDH1* R132C in three. Of these, only the one with the R132H mutation showed strong cytoplasmic positivity for *IDH1* by IHC. Both the decalcified trephine biopsy and clot sections were positive (Figure 1). None of the R132C or *IDH1* mutation negative AMLs were positive by IHC. All four of the *IDH1*-mutated gliomas were positive by IHC.



Conclusions: *IDH1* R132H mutation specific IHC has been demonstrated to be useful and reliable in gliomas. In this proof of concept study, we demonstrate that IHC can also be used in AML to detect the presence of the *IDH1* R132H mutation. Our results suggest that *IDH1* R132H by IHC appears to be a useful, cost-effective alternative to molecular testing. However, since other mutations in *IDH1* exist in this codon and are negative by IHC staining, molecular testing would be indicated if IHC is negative.

1430 Autoimmune Disease and Lymphoma: A Method for Large Scale Search of the Electronic Medical Record Enables Correlation of Clinical Parameters with Type and Risk of Lymphoproliferative Disease

Genevieve M Crane¹, Amy Duffield². ¹Pittsford, NY, ²Johns Hopkins University, Baltimore, MD

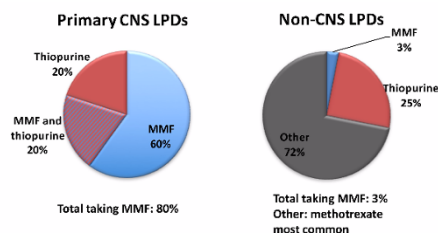
Background: Immunosuppression in solid organ transplantation, HIV and primary immune deficiency is associated with an increased risk of lymphoproliferative disease (LPD). While immunosuppressive therapy (IST) is also used to treat autoimmune disorders, a direct

relationship with LPD risk has been more difficult to establish. This is in part due to the fact that autoimmune disease itself may increase LPD risk, and in contrast to solid organ transplantation, detailed databases to track outcomes are scarce. Nonetheless, treatment does render certain patients with autoimmune disorders vulnerable to unusual lymphomas as demonstrated by the increased risk of hepatosplenic T cell lymphoma in patients with inflammatory bowel disease (IBD) on anti-TNF- α therapy. Here we use a novel method to investigate more broadly how choice of IST may influence LPD risk in these patients.

Design: I2b2 (tranSMART Foundation) was used to query the electronic medical record to identify patients with autoimmune disease including systemic connective tissue disorders, rheumatoid arthritis, myasthenia gravis, IBD and Sjogren syndrome based on diagnostic coding (2012-8/2/17). The total number of patients diagnosed, whether they were taking IST (calcineurin inhibitors, anti-proliferative agents, anti-metabolites and biologic agents) and whether they developed an LPD were evaluated. This was augmented with a traditional pathology database search (1986-2015) at a second institution.

Results: We identified 33,842 patients with autoimmune disease of whom 13-27% were on IST (Table) with an overall LPD incidence of 1.2-2.8%. IST was associated with significantly increased LPD risk only in systemic connective tissue disease. This was more pronounced when aggressive subsets of disease (e.g. CHL and DLBCL) were considered. In myasthenia gravis patients almost all CHL and DLBCL were IST-related (OR 11, $p < 0.05$, Fisher's exact test). Analysis of archived pathology material revealed many of these aggressive lymphomas were isolated to the CNS (7/46), and where the type of IST was known (6/7), all were taking mycophenolate. Methotrexate-associated LPDs had a similar morphologic profile, but none involved the CNS (0/17 vs. 5/13, $p < 0.01$, Fig 1).

	Total patients	% with LPD	% on IST	All LPD			OR	CHL or DLBCL			
				Total cases	on IST	%LPD on IST		Total cases	# on IST	% on IST	
Connective Tissue Disease	11487	1.7%	14%	195	43	22%	1.8**	55	18	33%	3.1**
Rheumatoid Arthritis	11690	1.4%	27%	164	41	25%	0.9	74	19	26%	0.9
Myasthenia Gravis	920	1.2%	27%	11	5	45%	2.3	5	4	80%	10.9*
IBD	7978	1.2%	13%	95	19	20%	1.6	42	8	19%	1.5
Sjogren	1767	2.8%	15%	50	11	22%	1.6	14	5	36%	3.2



Conclusions: LPD risk varies between autoimmune disorders, and IST treatment may shift that risk toward more aggressive LPD morphologies. Drug class also influences LPD type with use of mycophenolate mofetil strikingly more associated with primary CNS LPD as compared to other immunosuppressive agents.

1431 Clinicopathologic Features of Acute Myeloid Leukemia with BCOR/BCORL Mutations

Rory Crotty¹, Valentina Nardi¹, Andrew Brunner¹, Robert Hasserjian¹.
¹Massachusetts General Hospital, Boston, MA

Background: Acute myeloid leukemia (AML) is characterized by molecular heterogeneity, with many putative driver mutations. *BCOR* and *BCORL1* are homologous genes encoding transcriptional corepressors, each mutated in approximately 5% of AML cases. There is limited data on the clinicopathologic features of AML harboring *BCOR/BCORL1* mutations.

Design: We identified patients with AML harboring *BCOR* and/or *BCORL1* mutations diagnosed over a 2-year period at an academic medical center and evaluated the clinical, pathologic, cytogenetic, and molecular genetic features of these cases.

Results: We identified 17 AML cases with *BCOR/BCORL1* mutations (8 *BCOR*, 6 *BCORL1*, and 3 both) with a median variant allele frequency (VAF) of 34%. The majority (68%) were frameshift or nonsense

mutations. The median patient age was 69 years (range 29-81), with a M:F ratio of 13:4. 10/17 cases (59%) arose in *de novo* AML, while seven were a progression of MDS (n=4), MDS/MPN (n=2), or MPN (n=1). One patient had prior aplastic anemia.

Diagnoses by WHO criteria included 9 AML with MDS-related changes, 3 AML with mutated *RUNX1*, 3 AML not otherwise specified, 1 AML with t(3;3), and 1 blast phase MPN. The median bone marrow (BM) cellularity was 35%, with BM cellularity of <50% in seven cases (6/10 *de novo*), and 7/17 (41%) of patients had oligoblastic AML (blasts < 30%).

We compared the ten *de novo BCOR/BCORL1*-mut AML patients to a control group of 100 *de novo* AML lacking *BCOR/BCORL1* mutations. The *BCOR/BCORL1*-mut AML patients presented with lower white blood cell counts ($p=0.008$), BM cellularity ($p=0.005$), and BM blast % ($p=0.05$). *BCOR/BCORL1* mutations co-occurred with other mutations in all but one case, and accounted for the highest VAF in 11/17 cases (65%). The most common co-occurring mutations were *RUNX1* and splicing factor mutations, both in 8/17 cases (47%). Splicing mutations occurred in all seven secondary AML cases, but in only one *de novo* AML case. Of note, no concurrent mutations in *NPM1* or *FLT3* were observed in *BCOR/BCORL1*-mut cases.

Conclusions: *BCOR/BCORL1*-mutated AML frequently exhibits an aleukemic, oligoblastic presentation with BM hypocellularity; it had a male predominance, notable given the location on the X chromosome. In this series, *BCOR/BCORL1* mutations did not co-occur with *NPM1* or *FLT3* mutations, but often co-occurred with *RUNX1* mutations. Our findings suggest that *de novo BCOR/BCORL1*-mut AML exhibits clinicopathologic and genetic features distinct from other *de novo* AML cases.

1432 Immunophenotypic Dysplasia and Frequent T-cell Antigen Expression in Acute Myeloid Leukemia with Complex Karyotype and TP53 Mutations

Katelyn C Dannheim¹, Olga Pozdnyakova², Olga K Weinberg³.
¹Beth Israel Deaconess Medical Center, Boston, MA, ²Brigham and Women's Hospital, Southborough, MA, ³Children's Hospital Boston, Boston, MA

Background: Cytogenetic analysis is a powerful predictor of outcome in acute myeloid leukemia (AML). AML with complex karyotype (AML-CK), defined as three or more unrelated abnormalities, is associated with myelodysplasia, high risk of treatment failure, and frequent disease progression. Limited data is present in the literature on correlation of flow cytometric immunophenotyping (FCI) with karyotype-related cytogenetic abnormalities, including complex karyotype, in AML and mutational analysis.

Design: 25 cases of AML-CK and 83 cases of AML with normal karyotype (AML-NK) were identified from the BWH pathology database with available cytogenetic findings, flow cytometric analysis, and clinical data. FCI was performed on the diagnostic bone marrow aspirates. Mean fluorescence intensity (MFI) for each antigen was recorded in blast, granulocyte, and monocyte populations and results were compared between AML-CK and AML-NK groups using unpaired t-tests. Additional evaluation of AML-CK with TP53 mutations (AML-TP53) was also performed.

Results: 13 of the AML-CK had known mutations or deletions of the TP53 gene. Of the 61 AML-NK with molecular data, none showed abnormalities of TP53. In the 10 other AML-CK cases with molecular data, mutations were found in several different genes, including: *ASXL1*, *BCORL1*, *CSF3R*, *DNMT3A*, *FLT3*, *IDH1*, *JAK2*, *MPL*, *NPM1*, *NRAS*, *PHF6*, *RUNX1*, *SETBP1*, *SF3B1*, *SRSF2*, *TET2*, and *WT1*. When compared to AML-NK, AML-TP53 presented with lower white blood cell count [6.7 vs 46.4 ($\times 10^9/L$), $p=0.0324$] and lower bone marrow cellularity [66.9 vs 80%, $p=0.0404$]. Blasts in AML-TP53 had significantly higher expression of CD5 and CD34, but lower expression of CD33 and CD13. Monocytes showed higher expression of CD7, CD13, and CD11b, and granulocytes showed higher expression of CD3, CD5, and CD7. Similar findings were seen in comparisons of AML-CK to AML-NK (Table 1). No significant differences in antigen expression were seen between AML-TP53 and non-TP53-mutated AML-CK.

	AML-TP53 (n=13)	p Value*	AML-NK (n=83)	p Value†	AML-CK (n=25)
	mean ± SEM		mean ± SEM		mean ± SEM
			BLASTS		
CD5	831.8 ± 576.8	0.0059	185 ± 23.87	0.0091	650.5 ± 312.4
CD10	165.5 ± 12.61	0.0192	203.6 ± 6.005	0.0226	175.4 ± 9.672
CD33	4271 ± 1010	0.1464 (NS)	6767 ± 653.9	0.0111	3490 ± 778
CD34	45533 ± 10194	<0.0001	10185 ± 1868	<0.0001	35393 ± 6702
CD13	14106 ± 3743	0.0111	7052 ± 913.5	0.0707 (NS)	10778 ± 2172
			MONOCYTES		
CD7	1152 ± 462.7	0.0142	594.6 ± 53.07	0.0208	995.1 ± 258.6
CD34	14710 ± 8969	0.0008	1978 ± 492.4	0.0029	10358 ± 4780
CD13	25672 ± 5743	<0.0001	9572 ± 123	<0.0001	25100 ± 5696
CD11b	34863 ± 9311	0.0115	18780 ± 2013	0.0316	29608 ± 6154
			GRANULO-CYTES		
CD14	815.5 ± 59.92	0.0019	587.3 ± 26.64	0.0041	749.2 ± 48.05
CD7	760 ± 82.84	0.001	553.6 ± 20.31	0.0075	683.3 ± 54.85
CD5	390.1 ± 48.44	0.0003	271.5 ± 10.08	0.0008	354.4 ± 28.66
CD3	1055 ± 203	0.0161	735.9 ± 41	0.1033 (NS)	900.8 ± 122.9
CD10	558.6 ± 78.01	0.1084 (NS)	440.7 ± 26.1	0.0273	566.1 ± 54.01
*p Value comparing AML-TP53 and AML-NK			†p Value comparing AML-CK and AML-NK		
Results were significant at p values of <0.05					
Flow cytometric analysis evaluated forward scatter, right-angle side scatter, and expression of the following antigens: CD45, CD14, HLA-DR, CD11b, CD3, CD5, CD7, CD19, CD20, CD10, CD34, CD33, CD64, CD13, CD56, CD15 and CD117					
AML-TP53, acute myeloid leukemia with complex karyotype and TP53 mutation; AML-NK, acute myeloid leukemia with normal karyotype; AML-CK, acute myeloid leukemia with complex karyotype; SEM, standard error of the mean; NS, not significant					

Conclusions: Our study shows distinct immunophenotypic patterns in blasts, monocytes, and granulocytes of AML-CK and AML-TP53 as compared to AML-NK. Higher T-cell antigen expression is seen on blasts in AML-CK, suggesting that more cases could reach criteria for mixed phenotype acute leukemia (MPAL). The WHO classification states that AML-CK is an exclusion criterion for a diagnosis of MPAL and should be considered before making a diagnosis of MPAL. Our results also suggest that FCI could aid in objective evaluation of dysplasia.

1433 Primary Sinonasal Large B-Cell Lymphoma is as Histopathologically Heterogeneous as Systemic Large B-Cell Lymphoma

Megan Desai¹, Tarshen K Seth², David S Morgan², John P Greer², Nishitha M Reddy², Alexandra Kovach¹. ¹Vanderbilt University Medical Center, Nashville, TN, ²Vanderbilt University Medical Center

Background: Sinonasal diffuse large B-cell lymphoma has been shown to harbor a non-germinal center B-cell (non-GCB)-like genetic profile, 1p31 and RGS1 abnormalities, and associated poor prognosis. We reviewed our institutional experience with sinonasal large B-cell lymphoma (snLBCL) in light of these data and the 2016 revised WHO classification to inform diagnostic and management strategies.

Design: Electronic health records and pathology archives were queried for snLBCL (1990-2017) and the clinicopathologic material analyzed.

Results: We identified 34 cases (16 nasopharynx, 9 nasal, 8 maxillary sinus, 1 inferior turbinate) with variably available clinical data [age 14.1-87.5 years (yrs), median age 67.4 yrs; M:F ratio 1.8]. A majority (27/30 evaluable, 90%) had stage IE (9) or IIE (18) disease, and most (23/25 evaluable, 92%) had favorable (0-2) IPI scores. Pathologic review led to 2016 revised WHO classification where possible: DLBCL not otherwise specified (NOS), GCB phenotype (9, 26%), including 2 CD5+ cases; DLBCL, NOS, non-GCB (4, 12%); DLBCL, NOS, unreported cell of origin (3, 9%); high-grade B-cell lymphoma (3, 9%, 2 NOS and 1 with isolated C-MYC rearrangement); and EBV+ DLBCL (2, 6%). Lacking IHC and FISH data, 13 older cases (38%) were termed large B-cell lymphoma consistent with DLBCL (LBCL). Among 10 cases immunostained for C-MYC and BCL2 (8 DLBCL NOS, 2 LBCL), 5 (50%) showed a double-expressor phenotype. Upfront therapy included R-CHOP (20/30 evaluable, 90%), R-EPOCH (2, 6%), hyper-CVAD (1, 3%), CHOP (2, 6%), steroids alone (1, 3%), and no therapy (1, 3%); radiation was incorporated for 14 patients (pts) (47%). Among 28 pts with follow-up information [median 26 months (mos)], median overall survival was 25 mos; 10 pts died of disease, including 2/2 pts with poor (3-4) IPI, 3/3 HGBCL pts, and 1/2 EBV+ DLBCL pts.

Conclusions: This small series highlights similar heterogeneity between snLBCL and systemic LBCL. There were frequent cases of DLBCL NOS with a GCB phenotype among cases with reported Hans classifier, with further IHC and FISH for WHO classification of the complete cohort in process; given published evidence that snDLBCL shows a non-GCB-type genomic profile, our preliminary results raise the possibility that the Hans classifier in snLBCL may have limitations. Our cohort showed at least a 36% disease-related mortality rate, perhaps in part due to HGBCL and EBV+ cases but despite frequent low-stage disease presentation, corroborating evidence of a potentially aggressive site.

1434 EnHANS: A Digital Image Analysis Tool for Automated Scoring of IHC Stains and Classification of Diffuse Large B-cell Lymphoma Sub-types Based on Hans Algorithm

Rajan Dewar¹, Amanda Kitson¹, Srikanth Ragothaman¹, Muhammad N Aslam¹, Daniel Xia². ¹University of Michigan, Ann Arbor, MI, ²University Health Network, Toronto, ON

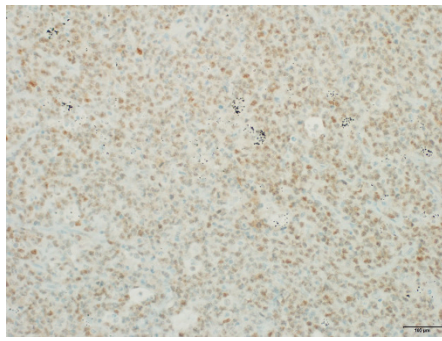
Background: Activated B-cell (ABC) and Germinal Center B-cell (GCB) are the two cell of origin (COO) based sub-types of Diffuse Large B-cell Lymphoma (DLBCL), and are shown to have prognostic value. Subsequent to the original Gene Expression profiling study, a simple immunostain based algorithm (Hans) has been widely used to aid in the sub-typing of DLBCL. The Hans algorithm is based on three immunostains: CD10, BCL6 and MUM1. Despite the simplicity, Hans algorithm suffers from several pitfalls: variability of immunostains, inter-observer variations in stain interpretations and failure to correlate with outcome, in as much as 22% of DLBCL cases. We have developed an automated image analysis based algorithm (EnHANS) which could be useful in classifying DLBCL.

Design: 11 cases of DLBCL from a well-curated cohort were included. H&E stains and immunostains for CD10, BCL6, and MUM1 were performed and scanned. The EnHANS platform was trained on static digital IHC images to recognize positive cells (CD10 – membrane staining; BCL6 and MUM1 – nuclear). Using a 30% threshold, the algorithm automatically subtyped the DLBCLs according to cell-of-origin. Two pathologists scored the whole slide and one pathologist scored digital images used by EnHANS to derive subtypes for all 11 cases, blinded to the EnHANS data. (Note: ABC term is used instead of Non-GCB for simplicity).

Results: The results are shown in Table/Figure 1 (discordances are highlighted). The concordance between EnHANS and pathologists is 82% (9/11 cases) for the DLBCL subtype, 82% (9/11) for CD10 expression, 64% (7/11) for BCL6 expression, and 100% for MUM1 expression. The majority of the discordances occurred where the percentages of positive cells as determined by EnHANS were close to the 30% threshold. In one case (#4), EnHANS failed to recognize staining artifact and misclassified the CD10 stain as positive. In another case (#11), a BCL6 stain was scored as “weak positive” and “negative” by the two pathologists and “positive” by EnHANS.

S. No.	CD10	BCL6	MUM1	EnHANS subtype
1	9.83	47.65	50.91	ABC
2	0.12	42.2	58.79	ABC
3	7.2	46.14	47.4	ABC
4	30.66	43.94	72.96	GCB
5	20.23	43.65	73.59	ABC
6	0.2	23.61	55.95	ABC
7	0.08	51.1	69.88	ABC
8	55.27	43.06	69.23	GCB
9	28.02	58.41	48.36	ABC
10	42.84	58.485	30.34	GCB
11	21.4	41.04	63.9	ABC

S. No.	CD10	BCL6	MUM1	Manual subtype	enHANS subtype
1	NEG	POS	POS	ABC	ABC
2	NEG	POS	POS	ABC	ABC
3	NEG	NEG	POS	ABC	ABC
4	NEG	NEG	POS	ABC	GCB
5	NEG	NEG	POS	ABC	ABC
6	NEG	NEG	POS	ABC	ABC
7	NEG	POS	POS	ABC	ABC
8	POS	POS	POS	GCB	GCB
9	POS	POS	POS	GCB	ABC
10	POS	POS	POS	GCB	GCB
11	NEG	NEG	POS	ABC	ABC



Conclusions: Image analysis tools may have a role in the automated classification of DLBCL subtypes, particularly in cases where the percentages of positive cells by IHC are close to established thresholds. We plan to refine the EnHANS algorithm by using additional cases from our curated cohort with correlation to human pathologist scores.

1435 Implementing a comprehensive 8 marker flow cytometry to enable accurate diagnosis of acute pediatric leukemia in Low-Middle Income Countries

Rajan Dewar¹, Usha Kota¹. ¹University of Michigan, Ann Arbor, MI

Background: Pediatric leukemia, especially B-Acute Lymphoblastic Leukemia (B-ALL) occurring in children is a curable disease with long term survival. However, accurate identification of this leukemia sub-type and timely institution of therapy is important in successful management of this disease. Flow cytometry based immunophenotypic classification, which enables this in western country is not performed routinely in Low and Middle Income Countries (LMICs). In these countries, simple 1-2 laser flow cytometry with 4-5 color capacity is available as a routine tool even in remote locations to monitor HIV treatment. We proposed that a comprehensive (8-marker) panel of immunophenotyping can be developed and implemented this in India and Ethiopia to aid in the accurate sub-classification of pediatric leukemia.

Design: An 8-marker flow cytometry panel was developed and validated for use at the host institution and in two laboratories. The 8-markers consisted of CD45-HLA-DR-CD10-CD19-CD20-CD5-CD3-CD13. In Ethiopia, CD34 was added in place or in addition to CD20. Blasts were identified based on CD45/SSC strategy and a one-three tube flow cytometry was performed based on the instrument capability. After validation, all new suspected pediatric leukemia (age 0-18) blood or bone marrow samples were run with the 8-marker panel. The flow cytometry data was correlated with morphology and clinical features.

Results: A total of 163 specimens were processed by flow cytometry. 3 specimens were rejected based on sub-optimal volume. 53 females and 102 male children were included (rest gender not specified). 70 blood specimens and 60 bone marrow specimens were run (rest unspecified or characterized as hemodiluted / bone marrow). Of the total 160 patient samples, 96 patients were leukemic blasts identified with a B-ALL immunophenotype. 1 Acute promyelocytic leukemia, 11 Thymic (T-ALL) and 12 Acute myeloid leukemia were able to be accurately categorized based on this comprehensive panel. 40 patient samples could not be definitely categorized or showed a mixed phenotype.

Conclusions: Flow cytometry facilities with limited capacity is available in most Low and Middle Income countries, as an HIV monitoring service. These instruments can be validated for accurate immunophenotyping of pediatric leukemia, enabling appropriate treatment which could be potentially life saving. Further refinement of this approach and cost-effectiveness of these markers need to further studied.

Acknowledgements: CIRHT, Jiv Daya Foundation.

1436 Identifying Minimal Residual Disease (MRD) in Chimeric Antigen Receptor T-Cell (CART)-19/CART-22 Treated B-Lymphoblastic Leukemia/Lymphoma (B-LL) by Flow Cytometry (FC): a Role for CD24 and CD9

Meggie E Doucet¹, Weina Chen¹, Crystal Goecker¹, Jesse Jaso¹, Mingyi Chen¹, Franklin Fuda¹. ¹University of Texas Southwestern Medical Center, Dallas, TX

Background: Adoptive cell therapy using genetically modified T-cells expressing CAR specific for CD19 has shown remarkable efficacy against chemo-refractory B-LL. Distinguishing normal B-cells from B-lymphoblasts is critical in identifying MRD in B-LL. This task is often challenging, especially in patients undergoing CART-19 and

more recently CART-22 therapy where residual B-LL may lack the conventional gating marker CD19 as well as CD22. Alternative gating markers are needed to detect MRD in these patients. CD24 and CD9 are candidate markers normally expressed on B-lineage cells. The goal of our study is to identify a pattern of expression of CD24 and CD9 in both normal B-cells and B-LL and determine if these markers can be used for MRD analysis.

Design: 10-color FC identified 15 cases with hematogones (HG) (13 bone marrow, 2 lymph node) and 13 cases with B-LL (9 bone marrow, 3 peripheral blood, 1 solid tissue). Expression of CD24 and CD9 in HG, B-LL, plasma cells (PC), and mature B-cells was evaluated in conjunction with CD10, CD19, CD20, CD34, CD38, CD45, CD81 and CD5.

Results: HG consistently expressed CD24 with a reproducible pattern between three stages of maturation. CD24 expression decreased in mature B-cells and became very dim to (-) in PC. All B-LL expressed CD24, but the intensity and uniformity varied between cases. Two cases showed a subset of CD24(-) B-LL, and one biphenotypic case was largely CD24(-).

HG consistently expressed CD9 with variable intensity at each stage of maturation without a distinct maturation pattern. CD9 expression decreased in mature B-cells and then increased in PC. B-LL was predominantly positive for CD9 with varying intensities of expression. Some cases showed abnormal dim or bright uniformity of CD9 and a few cases showed minute CD9(-) subsets.

Conclusions: Our study identified dual utility for CD24 and CD9 in assessing B-LL. First, the reproducible expression patterns of both markers on maturing B-cells was often lost in B-LL. Such aberrancy is helpful in identifying B-LL. Second, all cases of B-LL showed expression of both markers suggesting their use as surrogates for CD19 and CD22 in CART patients. However, as shown here, subsets of B-LL may lack CD24 and/or CD9 expression. Additionally, CD9 and CD24 are not specific for B-lineage cells within the lymphocyte/lymphoblast gate. Therefore, when assessing MRD in CART treated B-LL these markers must be used in concert with other features identified on the original B-LL.

1437 Bone Marrow Findings in Patients with Acute Promyelocytic Leukemia Treated with Arsenic Trioxide

Amy Duffield¹, Karin P Miller¹. ¹Johns Hopkins University, Baltimore, MD

Background: The treatment of low risk acute promyelocytic leukemia (APL) has recently shifted from a combination of all trans retinoic acid (ATRA) + cytotoxic chemotherapy to ATRA + arsenic trioxide (ATO). Bone marrow biopsies from patients treated with ATO have unusual but characteristic features.

Design: The Pathology Database was searched for APL from 6/2011-8/2017. 17 samples were identified from patients treated with ATRA+ATO induction therapy.

Results: The mean patient age was 49.1 (20-78 years; 7 women, 10 men). Biopsies were performed 13-74 days after initiating ATO; all biopsies except 1 (74 day interval) were performed during ATO treatment. The marrow was hypercellular for age in 11/15 evaluable cases, but was rarely normocellular (3) or hypocellular (1). The myeloid:erythroid (M:E) ratio was $\leq 1:1$ in all but 3 specimens (median 1:2, range 10:1-1:6). The 74 day interval case had a ratio of 2:1, and 2 specimens with normal or high ratios (3:1, 10:1) had extensive residual APL. All cases showed megaloblastoid maturation of erythroid precursors, and 12/17 had dysplastic changes (nuclear membrane irregularities, basophilic stippling, cytoplasmic vacuoles) in $\geq 10\%$ of erythroid precursors (mean 20.7%, range 1-50%). Flow cytometry showed variable expression of CD71 on erythroid precursors in 8/15 evaluable cases. Megakaryocytes were increased in 14/16 evaluable specimens, and 12 cases showed dysplastic changes (small size, abnormal nuclear lobation) in $\geq 10\%$ of cells. Except for 2 cases with extensive residual APL, the myeloid lineage did not show significant dysplasia, though 6 cases showed focal morphologic atypia (cytoplasmic vacuoles, eosinophil precursors with basophilic granules). Flow cytometric evaluation of myeloid maturation was normal in 13/15 cases; the 2 abnormal cases had extensive residual disease. All specimens had no increase ($<5\%$) in blasts, as confirmed by flow cytometry. Cytogenetic and molecular studies were performed on a subset of the cases. All 11 cases that were karyotyped were negative. FISH studies on 13 cases showed 9 negative cases, 3 cases with limited disease (6%, 2%, 1.5%), and one case with extensive disease (78%). Molecular studies were positive in 8 of 11 cases.

Conclusions: The marrow of APL patients treated with ATRA+ATO is often hypercellular with increased megakaryocytes, a decreased M:E ratio, and dysplasia in the erythroid precursors and megakaryocytes. An increased M:E ratio and/or abnormalities of the myeloid lineage may indicate significant residual APL.

1438 BCL-6 Remains Superior to MEF2B To Reach Better Concordance Between Immunohistochemistry Algorithms to Classify DLCL

Siraj El Jamal¹, Zakaria Grada², Hend Abulsayen³, Ali Saad⁴, Shafinaz Hussein¹, Mostafa Fraig⁵, Julie Teruya-Feldstein⁶. ¹Icahn School of Medicine at Mount Sinai, New York, NY, ²Dartmouth Hitchcock Medical Center, Lebanon, NH, ³SUNY Downstate, ⁴University of Mississippi Medical Center, Jackson, MS, ⁵Univ. of Louisville Hosp, Louisville, KY, ⁶Mount Sinai Hospital Icahn School of Medicine, New York, NY

Background: Diffuse large B-cell lymphoma (DLBCL) gene expression profiling shows two major groups: activated B-cell-like (ABC) and germinal center B-cell-like (GCB). In a previous study, we found that MEF2B acts as a member of the transcriptional complex for BCL6 and it's strongly correlated to BCL6 expression. In this study, we investigate the effect of substitution of MEF2B for BCL6 in the concordance rate between three major immunohistochemistry (IHC) algorithms that use BCL6 to classify DLBCL: Hans, Choi, and Visco.

Design: We used tissue microarrays (TMAs) for 94 primary nodal DLBCL cases. All cases were confirmed to be DLBCL according to the WHO criteria. We stained the TMAs for MEF2B, CD10, GCET-1, BCL6, MUM-1, and FOXP1. We classified each case to ABC or GCB according to the three algorithms. Then, we used MEF2B in place of BCL6 in each of the algorithms, and we reclassified each case accordingly. Concordance across the algorithms in their original format and when using MEF2B was measured using κ statistics.

Results: Using the original algorithms, allocation to GCB group ranged from 19.3% by Hans to 21.5% by Visco. Concordance rate varied from κ 0.82 to 0.93. Hans and Visco algorithms show the highest degree of concordance. Replacing BCL6 with MEF2B decreased the concordance among all the three algorithms, ranging from κ 0.51 to 0.57 [Table 1; the number between () is κ when using MEF2B].

κ (+MEF2B)	Hans	Choi	Visco
Hans		0.89; (0.53)	0.93; (0.57)
Choi	0.89; (0.53)		0.82; (0.51)
Visco	0.93; (0.57)	0.82; (0.51)	

Conclusions: The concordance rates among the different IHC algorithms to classify cases of DLBCL that use BCL6 are very similar and show strong agreement ($\kappa > 0.8$). When using MEF2B, the concordance rates do not improve; in fact, the concordance rates decrease substantially. BCL6 remains a robust marker in the DLBCL classification using IHC and it is superior to MEF2B.

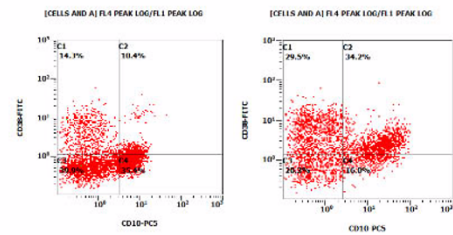
1439 Checkpoint inhibition in Lymphoma therapy: Variable expression of CD38 in bone marrow versus nodal tissue of NHL patients may regulate lymphoma micro-environment and hence predict relapse and responsiveness to therapy

Shohreh Eliaszhadeh¹, Tycel Phillips¹, Rajan Dewar¹. ¹University of Michigan, Ann Arbor, MI

Background: Immune checkpoint inhibition therapy, eg., PD-1/PD-L1 axis blockade is successful in many resistant / relapsed lymphoma. However, a subset of patients show resistance to checkpoint blockade and the mechanism of resistance is unknown. At ASCO 2017 annual meeting, researchers from MDACC showed data from animal models that implied upregulation of CD38 on tumor cells and Tregs that showed immune checkpoint regulation and CD38 is involved in resistance to PD-1/PD-L1 axis blockade. This finding raised the question if CD38 expression is related to tumor micro-environment, and if CD38 expression is different in lymphoma cells involving bone marrow and lymph nodal tissue. PD-1 blockade may be effective in CD38 negative lymphoma cells, but CD38 overexpressing sub-clone, may evade PD-1 inhibition. In this study, we evaluate CD38 expression in bone marrow and lymph node samples of Non-Hodgkin lymphoma patients treated with PD-1 inhibitors.

Design: 73 specimens from 16 patients with advanced B-cell Lymphoma, treated with PD-1 inhibitor were selected for this study. 7 had Follicular lymphoma, 8 had DLBCL and 1 Hodgkin. Both bone marrow and lymph nodal tissue flow cytometry scatter plots from the time of diagnosis, staging and follow-up, through PD-1 therapy were analyzed. CD38 expression was measured by flow cytometry (as CD10/CD38 or CD19/CD38) on a logarithmic scale (Kaluza). Neoplastic clonal B-cells, non-clonal B-cells and T-cells showed CD38 expression in these patients; only clonal B analysis is shown.

Results: 36 specimens had a neoplastic clone. Paired analysis of bone marrow (Figure - left) and tissue biopsies (Figure - right) from patients showed that CD38 expression was variable in lymphoma cells (Illustrated example in Figure). Lymph node expression of CD38 (mean fluorescence =2.73) was significantly ($p=0.011$; two-tailed T-Test) higher than marrow (mean 1.07). Lymphoma type was not associated with CD38 expression.



Conclusions: CD38 expression is significantly higher in nodal tissue neoplastic B-cells than bone marrow B-cells. This may be a significant predictor of disease resistance and relapse in patients treated with PD-1 inhibitor therapy. Identification of CD38 overexpression in lymphoma cells of these patients may identify a subset of patients who may benefit from PD-1 and CD38 inhibition.

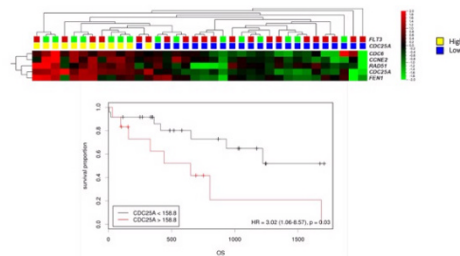
1440 Acute Myeloid Leukemia with Normal Cytogenetics (AML-CN): Poor Prognosis Associated with Overexpression of Cell Division Cycle 25 (CDC25) Phosphatase A is Independent of FLT3 Mutational Status

Ghaleb Elyamany¹, Mohammad O Mansoor², Fahad Farooq², Meer-Shabani Taher-Rad³, Ariz Akhter². ¹Prince Sultan Military Medical City, Riyadh, ²University of Calgary, ³University of Calgary/ Calgary Laboratory Services

Background: AML-CN is associated with intermediate risk and wavering clinical course. Mutational status of FLT3/NPM1/ CEBPA genes has improved risk stratification; however, prognosis remains dismal due to variable response to conventional therapy. Novel targets through enhanced understanding of AML biology are needed. CDC25A regulate cell cycle through activation of cyclin-dependent kinases. Overexpression of CDC25A has been linked with oncogenic transformation, genomic instability and adverse prognosis and anti-CDC25A activity have been reported in AML cell lines. We compared established risk factors in AML-CN patients with expression of CDC25A and a series of cell cycle-related molecules and correlate it with overall survival (OS) in a standardized AML-CN patient cohort .

Design: We investigated the expression of a series of genes (n=102) associated with cell cycle /apoptosis /DNA repair regulation in a cohort (n=36) of AML-CN patients. RNA from diagnostic BM biopsies was hybridized with probes of Pan-Cancer Pathway panel by Nanostring technologies. GEP results were correlated with clinical, laboratory and molecular data.

Results: ROC curve (AUC =65%; 81% specificity/ 53% sensitivity) based dichotomization divided 36 young AML-CN patients (median age 56 yrs., range 18-66 yrs.) into high (12/36;33%) and low (24/36;67%) CDC25A expressers . Distinct CDC25A expression groups revealed no significant differences across age, gender and hematological data (P=0.734). High CDC25A expression was independent of FLT3 mutation (58% vs. 33%P= 0.175) and did not correlate with STAT3 or FLT3 mRNA expression (P>0.05). Over expression of CDC25A correlated with higher expression of AKT3 (>1.5 fold difference; P=0.05). Several cell cycle related genes namely CDK4 /Cyclin E2 /CDC6/CDK7 and Cyclin D3 showed over expression in relation to high CDC25A (P<0.05; FDR <0.1). High CDC25A also related with increased expression of DNA repair gene, Flap endonuclease 1 (FEN1) (>1.5 fold; P=0.0002; FDR <0.1). High mortality {8/12 (67%) vs. 6/24; (25%) P=0.028} and shorter OS {345 D vs 1245 D; HR 3.45 (1.06-8.47; P<0.0001)} was linked with high CDC25A expression.



Conclusions: Overexpression of CDC25A transcripts exerts poor prognosis through its effect on cell cycle regulation which is independent of FLT3 mutational status and can serve as a potential therapeutic target among AML-CN patients.

1441 Identification of Complex Karyotypes in Chronic Lymphocytic Leukemia: Comparison of Chromosome Banding Analysis and Genomic Microarray Techniques

Blanca Espinet¹, Silvia Ramos², Andrea Gómez-Llonín², Sandrine Bougeon³, María José Calasanz⁴, Laura Blanco⁵, Rosa Collado⁶, Rocío Salgado⁷, Margarita Ortega⁸, María José Larrayoz⁹, Ana Batlle¹⁰, Andrea Campeny¹¹, Alberto Valiente¹², Eugenia Abella², Eva Gimeno¹³, Pau Abrisqueta¹⁴, Felix Carbonell¹⁵, Carolina Moreno¹⁶, Francesc Bosch⁸, Ana Ferrer, Marta Salido¹³, Gonzalo Blanco¹, Jacqueline Schoumans³, Anna Puiggros², María Ángeles Piñan¹⁷. ¹IMIM-Hospital del Mar, Barcelona, Catalonia, ²IMIM-Hospital del Mar, ³Lausanne University Hospital, ⁴Universidad de Navarra, Pamplona, Navarra, ⁵Hospital de Sant Pau, ⁶Consorcio Hospital General Universitario, Valencia, ⁷Fundación Jiménez Díaz, Madrid, ⁸Hospital Universitari Vall d'Hebron, Barcelona, ⁹Universidad de Navarra, ¹⁰Hospital Universitario Marqués de Valdecilla, Santander, ¹¹Hospital San Pedro, Logroño, La Rioja, ¹²Complejo Hospitalario de Navarra, ¹³IMIM-Hospital del Mar, Barcelona, ¹⁴Hospital Universitari Vall d'Hebron, Barcelona, ¹⁵Consorcio Hospital General Universitario, Valencia, ¹⁶Hospital de Sant Pau, Barcelona, ¹⁷Hospital de Cruces, Bilbao

Background: Recent publications have highlighted the importance of complex karyotypes (CK; defined as ≥ 3 aberrations) as an independent predictive marker for refractoriness in chronic lymphocytic leukemia (CLL) patients, even treated with new agents (ibrutinib, venetoclax). CK have been defined using chromosome banding analysis (CBA). Genomic (CGH/SNP) microarray techniques are also capable to detect genomic complexity and do not require in vitro cultures. The aims were 1.To assess the complexity by genomic arrays in patients with CK by CBA; 2.To compare both methods regarding the number and type of aberrations detected to categorize patients based on genomic complexity.

Design: 57 CLL patients with CK were included [Median age: 67; 72% males]. Median time from diagnosis to CBA/microarray analysis was 1 month (range, 0-137), and 5 patients (8.8%) had received prior treatment. The cohort was enriched in delATM and delTP53 (23.8% and 47%, respectively). DNA from peripheral blood mononuclear cells or CD19+ lymphocytes was hybridized to CytoGenetics Whole-Genome 2.7M (n=2) or CytoScan HD (n=55) array, results were analyzed with Chromosomal Analysis Suite Software (Affymetrix). Number, size and type of aberrations detected were compared between techniques.

Results: A median of 4 aberrations (range:3-19) were detected by CBA, significantly lower than the copy number abnormalities (CNA) by microarrays (median 6, range:0-29; P=0.009). The median size of CNA was 5.3Mb (range: 0.1-174Mb). Current recommendations for microarray analyses suggest that only CLL known abnormalities (11q-, +12, 13q-, 17p-) and CNA >5Mb should be considered for clinical interpretation (Schoumans et al, 2016). Most CNA between 1 and 5Mb involved those associated to apparently balanced translocations by CBA, and in some cases revealed a higher genomic instability than previously recognized. Six cases showed chromothripsis, associated with impaired outcome. In contrast, genomic microarrays did not detect balanced translocations or subclonal aberrations, probably represented in a minor proportion of the sample but expanded during CBA culture. 22 patients (39%) could only be considered complex by CBA.

Conclusions: 1.The number of abnormalities differs by CBA or genomic microarrays. 2.Current 5Mb cut-off for clinically relevant CNA should be revised, as could underscore genomic instability. 3.More studies should be performed to establish standard criteria for prognostic stratification of CLL patients based on genomic complexity.

1442 Chronic Lymphocytic Leukemia (CLL) with Immunoglobulin Heavy Chain Gene (IGH)-BCL3 Translocation Exhibits a More Aggressive Clinical Course

Hong Fang¹, Kari G Chaffee², Curtis Hanson¹, Daniel L Van Dyke³, Neil E Kay³, Sameer A Parikh³, Kaaren Reichard⁴. ¹Mayo Clinic, Rochester, MN, ²Mayo Clinic Rochester, Rochester, MN, ³Mayo Clinic Rochester, ⁴Rochester, MN

Background: Genetic findings play a key role in the prognostication and clinical management of patients with CLL. Several groups have reported that CLL cases with IGH-BCL2 or IGH-BCL3 translocation may be associated with a more aggressive disease course. We studied a large series of CLL patients with an IGH translocation and reviewed the clinical data and disease course.

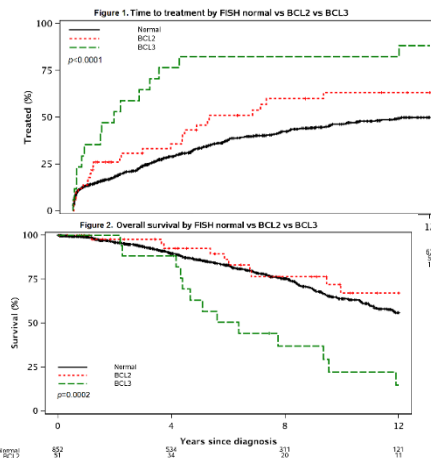
Design: Between 3/08/02 and 3/31/17, peripheral blood samples from patients at Mayo Clinic Rochester with a presumed B-cell lymphoproliferative disorder were analyzed by FISH. FISH for del(13q), del(6q), +12, del(17p13) (TP53) and del(11q22.3) (ATM) (standard FISH panel) and IGH rearrangement were performed. Patients with an IGH rearrangement were identified as having BCL2 or BCL3 partners using dual fusion probe sets. Of the cases with IGH-BCL2 or IGH-BCL3, the diagnosis of CLL was confirmed by reviewing flow cytometric studies in all cases and peripheral blood and bone marrow

morphology in some cases (KKR and CAH). CLL cases lacking any genetic abnormality by Dohner5 risk stratification (i.e. "normal FISH") served as the comparison group. The detailed clinical and laboratory data were retrospectively reviewed and analyzed. Clinical variables were compared across FISH groups using chi-square (qualitative) and Kruskal-Wallis (quantitative) tests. Overall survival was measured as time from diagnosis to last known alive date and was analyzed using the log-rank test. Time to treatment was measured as time from diagnosis to treatment date or last known untreated date and was analyzed using the Gray K-sample test accounting for competing risk of death.

Results: 51 CLL patients with IGH-BCL2 translocation and 18 with IGH-BCL3 translocation were identified. There were significant differences on the status of CD38, IGHV, CD49d, time to treatment, and overall survival between the IGH-BCL3 translocation group and the groups with IGH-BCL2 or normal FISH (Table 1, Figures 1 and 2).

Table 1: Clinicopathologic features of CLL cases with BCL2-IGH, BCL3-IGH or normal FISH

Clinical Parameter	BCL3 (N=18)	BCL2 (N=51)	Normal FISH (N=852)	p-value BCL3 vs Normal	p-value BCL3 vs BCL2	p-value BCL2 vs Normal
Age (median, years)	60.2	64.7	63.4	0.29	0.20	0.72
Gender (%male)	61%	69%	70%	0.41	0.56	0.83
Rai Stage						
* 0	47%	59%	60%	0.19	0.49	0.92
* 1 or 2	35%	33%	33%			
* 3 or 4	18%	8%	7%			
CD38 (%positive)	91%	26%	23%	<0.0001	0.0001	0.75
ZAP70 (%positive)	63%	26%	35%	0.11	0.05	0.29
IGHV (%unmutated)	100%	30%	45%	0.0003	0.0001	0.10
CD49d (%positive)	83%	45%	34%	0.01	0.09	0.20
Time to Treatment (median, years)	1.4	4.6	12.0	<0.0001	0.008	0.07
Overall Survival (median, years)	6.4	Not reached	13.7	0.0001	0.0002	0.25



Conclusions: The presence of an IGH-BCL3 translocation in CLL appears to be associated with the need for early initiation of therapy. This study also shows that the IGH partner gene seems to be important. IGH-BCL3 is associated with a worse prognosis than IGH-BCL2 while IGH-BCL2 appears to have a similar overall survival to CLL normal FISH cases. Further studies on the biological significance of IGH translocations in CLL are warranted.

1443 CD38 expression in Diffuse Large B-cell Lymphoma. A new therapeutic target?

Pedro Farinha¹, Susana Ben-Neriah¹, Anja Mottok², Daisuke Ennish¹, Barbara Meissner¹, Merrill Boyle¹, Diego Villa¹, Kerry Savage¹, Laurie H Sehn¹, Joseph Connors¹, Graham Slack³, Randy Gascoyne⁴, Christian Steidl¹, David Scott¹. ¹British Columbia Cancer Agency, Vancouver, BC, ²University of Würzburg, Würzburg, Bavaria, ³Department of Pathology and Laboratory Medicine, Vancouver, BC, ⁴BC Cancer Research Centre, Vancouver, BC

Background: Diffuse large B-cell lymphoma (DLBCL) is the most common high-grade lymphoma. Despite major therapeutic advances, up to 40% of patients remain incurable with a dismal prognosis. The

ABC cell-of-origin phenotype (COO) and presence of *MYC* and *BCL2/BCL6* rearrangements (double/triple hit disease, DHT) are established poor prognosis markers. CD38 is a transmembrane glycoprotein with roles in cell activation, cell adhesion, signal transduction and Ca^{2+} signaling in plasma cells, B cells, regulatory T cells and NK cells. It is highly expressed in myeloma (MM) cells. Daratumumab (Dmab), an FDA-approved CD38-blocking monoclonal antibody has shown efficacy in MM patients. It also showed marked anti-tumor activity in mouse xenograft models of non-Hodgkin-lymphoma. The frequency of CD38 protein expression in DLBCL and its clinical significance are largely unknown.

Design: We analyzed CD38 protein expression by immunohistochemistry (SPC32) on tissue microarrays comprising diagnostic FFPE biopsies from 348 patients with DLBCL uniformly treated with RCHOP at the BC Cancer Agency. CD38 was semiquantitatively assessed on tumor cells using HistoScore (HS): intensity (1, 2, 3) and % of positive cells. The HS was correlated with clinicopathological variables including COO (Lymph2Cx) and FISH analysis for *MYC/BCL2/BCL6* rearrangements using breakapart (BA) probes.

Results: COO: GCB 195 (56%); ABC 113 (33%). Rearrangements of *MYC*, *BCL6* and *BCL2* were present in 52 (15%), 77 (23%) and 93 (29%) of cases, respectively, with 27 (9%) being DHT cases. CD38 was expressed in 211 (62%) (HS>0) with 20 (6%) showing strong expression in all malignant cells (HS=300). The majority of CD38+ (HS>0) cases were GCB, 65% vs 25% ABC ($p<0.001$). CD38 expression correlated significantly with the presence of DHT ($p<0.001$) with all but one of the DHT cases expressing CD38 (96%). CD38 expression was also significantly associated with the presence of *MYC* BA ($p=0.01$) and *BCL2* BA ($p=0.003$) and absence of *BCL6* BA ($p=0.01$). There was no correlation with IPI factors. Finally, CD38 expression was not associated with significant survival difference in the total cohort or in the COO subtypes.

Conclusions: Using a large cohort of DLBCL patients uniformly treated with RCHOP we show CD38 is expressed in the majority. It is significantly associated with GCB subtype and presence of DHT. These findings suggest anti-CD38 Dmab may represent a new targeted therapy in patients with DLBCL.

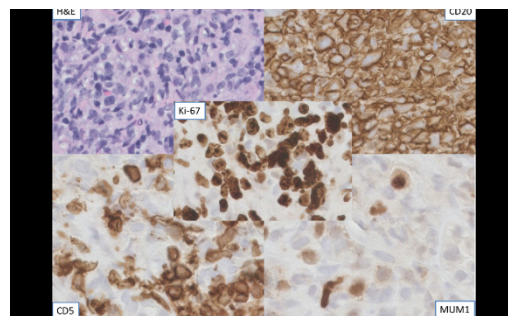
1444 Molecular Landscape of Chronic lymphocytic leukemia transformation to Richter syndrome (RS): a study by targeted next Generation sequencing

Taliya Farooq¹, Christian Salib¹, Payal Keswarpu², Weihua Huang³, Fouzia Shakil⁴, Humayun Islam¹, Nevenka Dimitrova⁵, John T Fallon¹, Minghao Zhong⁶. ¹Westchester Medical Center at New York Medical College, Valhalla, NY, ²Philips, Elmsford, NY, ³Westchester Medical Center at New York Medical College, ⁴Westchester Medical Center, Dobbs Ferry, NY, ⁵Pelham, NY, ⁶Westchester Medical Center/ New York Medical College

Background: Chronic lymphocytic leukemia/small lymphocytic lymphoma (CLL/SLL) is a common and characteristically indolent B-cell lymphoproliferative disorder. CLL/SLL can transform into diffuse large B-cell lymphoma (DLBCL) in a minority of patients (approximately 2% of cases). This transformation is termed Richter syndrome (RS). This study was aimed at elucidating relevant questions regarding RS pathogenesis, including the genetic determinants of the transformation event, and the pathogenetic relationship between RS and non-CLL De novo DLBCL. Therefore, we performed targeted next generation sequencing to comprehensively evaluate DLBCL arising in CLL/SLL for molecular changes.

Design: One of our Surgical Pathology's Databases was searched for all CLL/SLL transforming into DLBCL. Macrodissection was performed in some cases to ensure that at least 20% of the cells were neoplastic. Genomic DNA was extracted from formalin-fixed paraffin-embedded (FFPE) tissues by Qiagen AllPrep DNA/RNA Kit. The isolated genomic DNA was subject to targeted sequencing by the TruSeq Amplicon - Cancer Panel which can detect mutations from 48 cancer related genes. To obtain a comparative assessment of the genetic landscape of RS vs Denovo DLBCL, we compared the frequency of the most prevalent genetic lesions in 6 RS cases, characterized by WES and targeted sequencing data of genes commonly mutated in DLBCL (Pasqualucci et al., 2011).

Results: Six cases of RS were identified at our institution. Microscopic and immunophenotypic findings of prototype case is shown in image. Total 27 mutations were identified from these 6 cases (average 4.5 mutations/ case). The most common mutation was *P53*, which was detected in 4 out of 6 cases. The other less common mutations include *HNFI1A* and *NOTCH1*. Some of the mutation equally represented in both De novo DLBCL and RS DLBCL, with similar frequency (e.g. deletion of *PTE1*).



Conclusions: Firstly, this data underlines the fact that, despite the morphological and phenotypic similarities between RS and De novo DLBCL, the molecular profile of these two conditions is different. Secondly, no mutation with FDA approved targeted therapy was identified in these cases. However, one case carried few mutations that can have associated potential clinical trials. Because of poor prognosis associated with RS DLBCL, novel therapies are needed to be explored for RS patients. Thus, in this context this test can have certain degree of clinical implication especially in refractory RS cases.

1445 Molecular and Immunophenotypic Prognostic Factors of Diffuse Large B-cell Lymphoma in Malawi

Yuri Fedoriv¹, Nathan Montgomery², Sara Selitsky², Tamiwe Tomoka⁴, Bal Dhunge⁵, Maurice L Mulenga⁶, Joel Parker³, Satish Gopal³. ¹University of North Carolina, Pittsboro, NC, ²University of North Carolina, Chapel Hill, NC, ³University of North Carolina, ⁴UNC Project Malawi, ⁵UNC Project Malawi, Lilongwe, Lilongwe, ⁶Kamuzu Central Hospital, Lilongwe, Malawi

Background: Diffuse Large B-cell Lymphoma (DLBCL) is the most common lymphoma worldwide and in sub-Saharan Africa (SSA) and is highly associated with HIV. We have previously shown that patients can be effectively treated for DLBCL in SSA with standard chemotherapy, but prognostic markers to tailor therapeutic interventions are lacking. Here we correlate prognostic markers used in resource-rich settings, including cell-of-origin (COO) classification, cMYC/BCL2 expression, and proliferation index with patient outcomes from the ongoing Kamuzu Central Hospital (KCH) Lymphoma Study in Malawi.

Design: After primary diagnosis at KCH, tissue blocks were submitted to our U.S. institution for additional immunohistochemical assessment (IHC) and genomic classification. To date, 59 DLBCLs have been characterized in this manner, with over half arising in HIV+ patients (32 HIV+/27 HIV-). Lymphoma-related clinical and laboratory data including International Prognostic Index (IPI) and outcomes were documented for all patients. Of the DLBCL samples, 36 (22 HIV+/14 HIV-) have undergone whole transcriptome sequencing with comparison to published expression data and correlation to survival and pathologic features.

Results: Age-adjusted IPI was associated with overall survival (OS) and progression free survival (PFS) ($p<0.0001$), but there were no survival differences related to HIV status. After validating the IHC COO classifier with the gene expression signature, the IHC classifier was applied to the entire cohort. There was no OS difference between the Germinal Center- and Activated B-cell-type DLBCLs ($p=0.9656$) in HIV+ or HIV- subsets. Ki67 IHC proliferation index of $\geq 80\%$ was associated with worse OS in the HIV+ but not HIV- subgroup ($p=0.0336$ vs $p=0.1109$), and expression-based proliferation signatures confirmed this finding. IHC co-expression of cMYC and BCL2 (12 of 41 cases stained), was associated with inferior survival amongst all cases ($p=0.0120$).

Conclusions: Given the challenges of administering chemotherapy in SSA, prognostic markers are essential to improve DLBCL treatment through risk-stratified approaches. Ki67 and cMYC/BCL2 staining can be readily implemented in the KCH Pathology Laboratory and outcome difference investigated prospectively within ongoing clinical trials in Malawi and other cancer centers in SSA. Lack of survival differences related to COO may reflect biological differences in tumor biology or non-biologic factors that significantly impact outcomes in resource-limited settings.

1446 TP53 Aberrations Predict for Worse Outcome in Diffuse Large B-cell Lymphoma - Richter transformation, A Single Institution Series of 76 Cases

Shiraz Fida¹, Madina Sukhanova¹, Y. Lynn Wang¹, Sonali Smith¹, Wendy Stock¹, Elizabeth Hyjek², Girish Venkataraman³. ¹University of Chicago Medicine, Chicago, IL, ²University of Chicago, Chicago, IL, ³The University of Chicago Medical Center, Chicago, IL

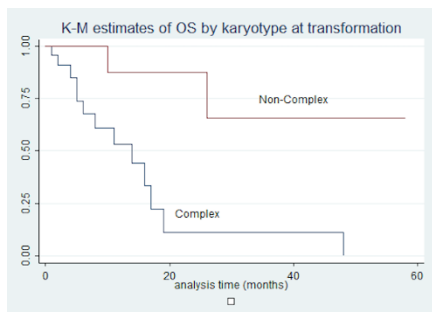
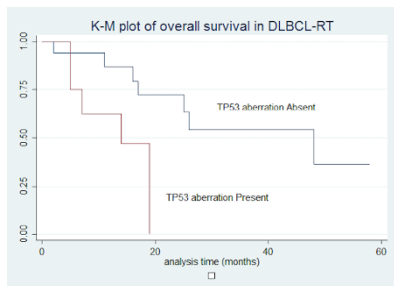
Background: Richter transformation (RT), also known as Richter syndrome, is a rare complication of chronic lymphocytic leukemia (CLL) that has an aggressive clinical course and unfavorable prognosis. Majority of these transformations occur in the form of diffuse large B-cell lymphoma (DLBCL), and less frequently in the form of prolymphocytic leukemia (PLL), or classical Hodgkin lymphoma (cHL).

Design: After searching our pathology archives for RT cases between 2000-2017, we identified a total of 76 cases. All clinical demographic, pathology (cytogenetics, immunohistochemistry, flow cytometry) were collated, and the outcome of interest modeled for survival analysis was overall survival (OS). For analysis purposes, karyotype was dichotomized into complex and non-complex (simple and normal) groups. The data were analyzed in Stata@11 using descriptive statistics. Outcome modeling was performed using Log-rank test for binary variables.

Results: Richter transformation occurred mostly in males (78%), with a median age of 65 years (range: 41-95) at transformation. There were 68 DLBCL-RT (including 7 PLL-RT) and 8 cHL-RT. Among DLBCL-RT, 87% of the preceding CLL had typical phenotype (CD5+, CD23+, FMC7-), 66% with CD38 (by flow; > 20%) and 77% positive for ZAP-70 (by immunohistochemistry). There was no correlation between CD38 expression and ZAP-70 (p=0.68, Fisher's exact test). Fifty percent carried complex CLL karyotype with 41% harboring TP53 aberration by FISH, followed by Trisomy 12 (31%), del13q (31%), and ATM deletion (17%).

Transformation occurred at median of 54 months (0-352 range). DLBCL-RT was non-germinal center phenotype in 81% with expression of CD5 (60%), p53 (52%), MYC (88%) and BCL2 (87%). Among DLBCL-RT, a total of 29 patients died at a median of 5.5 months (0-58 months).

In univariate analysis, age at transformation, type of CLL (typical vs. atypical), site (nodal vs. extranodal), CD38 or ZAP-70 positivity, did not impact outcome. Only TP53 aberrations by FISH in the CLL (p=0.027, log rank test) (Figure 1) and presence of complex karyotype at transformation were predictive of adverse outcome (p=0.006, log rank test) (Figure 2). Survival was worse for those who received cytotoxic therapy before RT (p=0.051, log rank test). MYC or BCL2 genetic alterations at transformation did not impact outcome.



Conclusions: Richter-transformation in CLL has an aggressive outcome and only TP53 alterations in the CLL and complex karyotype at transformation impacted outcome.

1447 No One Sent Flow? LEF1 versus CD200 by Immunohistochemistry

Amelia Fierro-Fine¹, Mohamed Salama², Sheryl R Tripp³, Erica A Hammond⁴, Jessica Kohan², Sandra K White¹, K. David LF⁵. ¹University of Utah, Salt Lake City, UT, ²Salt Lake City, UT, ³ARUP Laboratories, Salt Lake City, UT, ⁴ARUP, Taylorsville, UT, ⁵University of Utah/ARUP Laboratories, Salt Lake City, UT

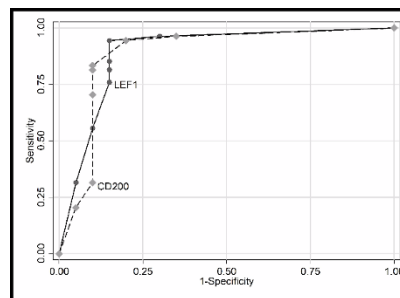
Background: Although the immunophenotype of chronic lymphocytic leukemia/small lymphocytic lymphoma (CLL/SLL) is relatively straightforward by flow cytometry, when flow cytometry is unavailable the diagnosis often requires many immunostains, and can be difficult especially on needle core specimens. Based on published

literature, CD200 and LEF1 by immunohistochemistry (IHC) appear to be highly sensitive and specific markers for CLL/SLL. However, there have been no direct comparisons between these two markers. In prior studies and clinical practice, IHC for CD200 typically demonstrates membranous and cytoplasmic staining while LEF1 shows nuclear staining, in addition to T-cells. By morphology and digital imaging software, we assess for stain agreement between CD200 and LEF1.

Design: We retrospectively analyzed 74 FFPE tissue samples from 66 patients with diagnoses of B-cell lymphomas (54 CLL/SLL, 6 mantle cell lymphoma, 2 follicular lymphoma, 1 marginal zone lymphoma, 10 diffuse large B-cell lymphoma, and 1 composite CLL/SLL with DLBCL and follicular lymphoma) including 21 small biopsy samples submitted to the University of Utah Pathology Department between 2009 and 2017. Percentage of tumor cell staining and intensity for LEF1 and CD200 were manually scored in areas with few CD3 positive T-cells at 20x using predetermined cut-offs for positive staining (25% CD200 and 10% LEF-1) based on literature. Additionally, a subset of both CLL and non-CLL cases (18) was scanned on a Leica (Buffalo Grove, IL) Aperio AT2 scanner at 20X, and staining analyzed using Indica Labs (Corrales, NM) HALO CytoNuclear and Membrane algorithm modified to digitally score positivity for LEF1 and CD200, respectively.

Results: With manual scoring, both LEF1 and CD200 showed high sensitivity and specificity for CLL/SLL as seen in previous studies (Table 1). The level of agreement between the two stains was high (Kappa 0.72, 88% agreement). The computer assisted digital image analysis also showed good agreement between manual and digital scoring for both LEF1 (Kappa 0.68 with 89% agreement) and CD200 (Kappa 0.56 with 83% agreement).

Antibody	Sensitivity	Specificity	AUROC
LEF1	94.4% (95% CI: 84.6-98.8%)	85.0% (95% CI: 62.1-96.8%)	0.90 (95% CI: 0.81-0.98)
CD200	83.3% (95% CI: 70.7-92.1%)	90.0% (95% CI: 68.3-98.8%)	0.80 (95% CI: 0.71-0.89)



Conclusions: LEF1 and CD200 are both useful in the diagnosis of CLL/SLL, especially in settings where flow cytometry is unavailable, and shows good agreement. This holds true when digital image analysis algorithms are applied. However, we found that the nuclear staining pattern and intensity of LEF1 is more easily interpreted compared to a more variable and weaker staining pattern of CD200.

1448 Donor Derived MDS/AML in Patients with Germline GATA2 Mutations

Pallavi Galera¹, Amy Hsu², Weixin Wang³, Jason R Schwartz⁴, Jeffery Klotz⁴, Sally Arafi⁵, Steven M Holland⁶, Dennis Hickstein⁷, Katherine Calvo⁸. ¹Shrewsbury, MA, ²NIAID, NIH, ³Clinical Center, NIH, ⁴St Jude Children's Research Hospital, Memphis, TN, ⁵Stanford University, ⁷NIH, Bethesda, MD, ⁸NCI/NIH

Background: Germline heterozygous mutations in GATA2 are associated with bone marrow failure and immunodeficiency with high risk of transformation to MDS/AML. Penetrance and expressivity is variable. Hematopoietic stem cell transplantation (HSCT) offers the only cure, however, donor selection may result in poor outcome if the GATA2 mutation is not recognized and related donors are not screened. We describe 3 families with GATA2 mutations, in which one member was transplanted using a mutation positive healthy matched related donor (MRD) resulting in post-HSCT MDS/AML.

Design: Families with germline GATA2 mutations and subsequent post-MRD HSCT MDS/AML were reviewed.

Results: 3 families were identified. The 1st patient (pt) presented with fever and pancytopenia at 21 yrs; bone marrow showed AML-MRC with NRAS mutation, monosomy 7 and trisomy 13. He underwent HSCT from his haploidentical mother. 2 years later he developed MDS

with trisomy 8 in donor cells. Germline *GATA2* mutation was identified in both donor and recipient.

The 2nd pt presented with pneumonia, pancytopenia, and warts at age 13 and was later diagnosed with MDS-EB and monosomy 7. He underwent syngeneic HSCT from his healthy identical twin brother with emergence of MDS with monosomy 7 and additional t(6;20) at day +140. 14 yrs later, the donor twin developed pancytopenia at age 27 and was diagnosed with MDS with germline *GATA2* mutation, and he expired prior to HSCT due to sepsis.

The 3rd pt's family has over 110 members with reported "blood dyscrasias" over multiple generations. His father was diagnosed with aplastic anemia and lymphedema at age 30 and died at 41. 5 of 7 children had MDS. 2 adolescent female siblings underwent MRD HSCT for MDS from a 9 yo healthy male sibling donor. Both sisters died post-HSCT, one from AML and the other from CMV. 20 yrs later, the male sibling donor developed MDS and died following MUD HSCT. In 2016 a remaining 51 yo male sibling presented with chronic neutropenia, numerous warts, recurrent infections, bilateral lymphedema, and cellulitis. He was found to have MDS with a novel germline *GATA2* mutation.

Conclusions: Age at presentation, disease manifestations, and progression are highly variable in pts with germline *GATA2* mutations, even within family members with the same mutation. Because phenotype is often unreliable, it is imperative to consider *GATA2* deficiency in patients with MDS/AML, and to molecularly screen patients and potential related donors for *GATA2* mutations prior to HSCT.

1449 Clinicopathologic and Immunophenotypic Features of MYD88 L265P-positive Lymphoplasmacytic Lymphoma/Waldenström Macroglobulinemia (LPL/WM): A Study of 30 Cases

Sofia Garces¹, Wenting Huang¹, Shaoying Li¹, Shimin Hu¹, Wei Wang¹, C. Cameron Yin¹, Jie Xu¹, L. Jeffrey Medeiros¹, Pei Lin¹. ¹The University of Texas MD Anderson Cancer Center, Houston, TX

Background: Discovery of the *MYD88* L265P mutation in >90% of cases of LPL/WM has facilitated classification of neoplasms designated previously as "B-cell lymphoma with plasmacytic differentiation" and affords a more comprehensive characterization of LPL/WM. This study is focused on the morphologic and immunophenotypic spectrum of LPL/WM with *MYD88* L265P in bone marrow (BM).

Design: We reviewed the clinicopathologic features and outcomes of 30 untreated patients with *MYD88* L265P-positive LPL/WM. The diagnosis was established by exclusion of other low-grade B-cell lymphomas according to the revised World Health Organization criteria.

Results: The study includes 18 men and 12 women with a median age of 62 years (range, 46-86). All patients had serum monoclonal IgM (median, 25.40 g/L; range, 4.5-82.7). Morphologic examination of BM showed LPL/WM ranging from 10-95% (median, 50%) involvement. The pattern was non-paratrabeular (interstitial, nodular and/or diffuse) in 22 (73%) and a predominantly paratrabeular in 8 (27%) cases; a sinusoidal pattern was not present. The LPL/WM cells were mostly small lymphocytes, plasmacytoid lymphocytes and plasma cells. In 5 (17%) patients, scattered larger cells were also present. Flow cytometry showed lymphocytes positive for monotypic surface light chain, CD19, CD20, and CD79b. CD22 was positive variably: 22 (73%) dim and 8 (27%) moderate. CD38 was also variable: 23 (82%) heterogeneous and 5 (18%) dim homogenous. CD23 was dim or partial in 7/16 (44%), CD10 was partial in 6 (20%), and CD5 was partial in 3 (10%) cases. Plasma cells expressed CD38, CD138 and monotypic cytoplasmic light chain; 26 (87%) were positive for CD19 (often dim or partial). Plasma cells were positive for CD81 in 29 (97%) and dim/partial CD27 in 13 (43%) cases. CD56 and CD117 were negative. Three (10%) cases had cytogenetic abnormalities (+4, +15 and a complex karyotype) and 27 cases had a normal karyotype. *CXCR4* mutation was identified in 8/21 (38%) patients assessed. The median follow-up from diagnosis was 15 months (range, 1-288) and all patients were alive with disease at last follow-up.

Conclusions: Inclusion of *MYD88* L265P into the diagnostic criteria of LPL/WM is helpful in better defining the spectrum of this disease. Certain features previously considered atypical for LPL/WM, such as paratrabeular pattern and a mixed population of small to large cells, were observed in about 30% and 20% of patients, respectively. In this cohort, *CXCR4* mutation was seen in almost 40% of patients.

1450 Disease Progression in Myeloproliferative Neoplasms: Revisiting the Criteria for "Accelerated Phase"

Julia T Geyer¹, Elizabeth Margolske², Leonardo Boiocchi³, Robert Hasserjian⁴, Umberto Gianelli⁵, Attilio Orazi⁶. ¹Weill Cornell Medical College, New York, NY, ²NYP/Weill Cornell Medical College, New York, NY, ³Massachusetts General Hospital, Boston, MA, ⁴IRCCS Ca' Granda - Maggiore Policlinico Hospital Foundation, Milano, Italy, ⁵Weill Cornell

Medical College/NYP, New York, NY

Background: Bone marrow (BM) fibrosis and accelerated/blast phase are the main forms of disease progression in myeloproliferative neoplasms (MPN). An accelerated phase (AP) is considered when there are $\geq 10\%$ blasts in BM or peripheral blood (PB) or presence of "significant" dysplasia. There are currently no clear criteria for myelodysplastic (MDS) type progression in MPN. In this study, we review the prognostic significance of various forms of disease progression.

Design: Sixty-one patients with the diagnosis of Ph-negative MPN were selected. We assessed features of progression, including: increased PB ($\geq 2\%$) and/or BM ($\geq 5\%$) blasts; dysgranulopoiesis (MDS-like pattern), persistent leukocytosis with atypical chronic myeloid leukemia (aCML)-like features or persistent absolute monocytosis with chronic myelomonocytic leukemia (CMML)-like features. All patients had detailed clinical follow-up. Patients presenting in blast phase were excluded. Controls included 40 consecutive MPNs with no increased blasts, dysplasia or leukocytosis. R software was used for statistical analysis.

Results: Cases included polycythemia vera (PV) (21), essential thrombocythemia (ET) (1), MPN unclassifiable (1), post-PV myelofibrosis (30), primary myelofibrosis (7) and post-ET myelofibrosis (1). 44 (72%) had increased blasts, including 5 (8%) diagnostic of AP. 17 (28%) had other types of progression (4 MDS-like, 10 aCML-like, 3 CMML-like). On follow up, 13 (23%) patients developed AP and 8 (13%) BP. 26 (43%) of patients expired (median 11 months following disease progression), compared to 2/40 (5%) control patients ($p < 0.0001$). Patients with $\geq 2\%$ PB blasts and non-fibrotic BM had median overall survival of 12 years, compared to 30 years for those with $\geq 2\%$ PB blasts and BM fibrosis ($p = 0.0009$). Maximally selected rank statistics determined an optimal PB blast cut-off of 3%. There was no significant survival difference between patients with AP MPN and those with other types of progression.

Conclusions: The blast threshold for AP in MPN is significantly higher than for MDS with excess blasts. Based on our results, the overall survival of MPN patients with $\geq 2\%$ PB blasts / $\geq 5\%$ BM blasts was similar to that of AP MPN and significantly worse than that of MPN controls. Patients with myelodysplasia and/or persistent leukocytosis also had an aggressive disease course. These results suggest that additional morphologic parameters are of value in recognizing early disease progression in MPN, an occurrence with important clinical implications.

1451 New Biomarkers in T-cell Lymphoma: Case Series of CD161 Expression in T-cell Prolymphocytic Lymphoma

Scott R Gilles¹, Bartosz Grzywacz². ¹University of Minnesota, Lauderdale, MN, ²University of Minnesota, Minneapolis, MN

Background: T-cell lymphomas are a troubling area for pathologists due to the limited repertoire of diagnostic tools available for diagnosis and monitoring. CD161 (NKR1) is a C-type lectin-like receptor normally present on NK cells. It can be found on minor T-cell subsets including Th17 cells, mucosal-associated invariant T-cells (MAIT), and CD161^{int} CD8⁺ T-cells. The majority of peripheral blood CD3⁺ T-cells are negative for CD161 (normal range 7.9-30.4% of T cells) (Morice, Br J of Haematol 2003). CD161 has been part of the flow cytometric T/NK panel used at our institution since 2010. We have observed increased CD161 expression in cases of T-cell prolymphocytic leukemia/lymphoma (T-PLL). This immunophenotype has been particularly useful in minimal residual disease detection. To our knowledge there is no published data on expression of CD161 in T-PLL.

Design: The pathology database at the University of Minnesota was searched for T-PLL cases. Once cases were identified, morphology slides, flow cytometric immunophenotyping data, and electronic medical records were reviewed and data including immunophenotype, cytogenetic results, morphologic features, and clinical features were recorded.

Results: Eight cases of T-PLL with CD161 immunophenotypic data were identified. Of the eight cases, 5 cases were positive for CD161 expression (Range: 80-98% of the lymphomatous T cells). Interestingly all of the CD161 positive cases were positive for CD8, whereas the 3 negative cases were all CD4⁺CD8⁻. In one case with two subsets: CD4⁺CD8⁺ and CD4⁺CD8⁻ only the former subset was CD161 positive. CD161 expression was seen in cases with translocation involving both TCL1 and MTCP1 oncogene. The expression of CD161 by CD8 positive T cells has been very useful in minimal residual disease detection in cerebrospinal fluid and other samples, with sensitivity reaching 1 in 10³ cells.

Conclusions: These novel results suggest that CD161 is frequently aberrantly expressed in T-PLL. In addition it appears to be characteristic of the CD8⁺ cases. While more research is needed to evaluate specificity and utility as a tool for differential diagnosis, it has proven to be valuable as a marker for monitoring residual disease in three cases at our institution; including one case of CSF involvement. Additionally these findings may shed light onto the putative cell of

origin of T-PLL, suggesting that they can be derived from MAIT and/or tissue-homing CD8+ T-cell subsets.

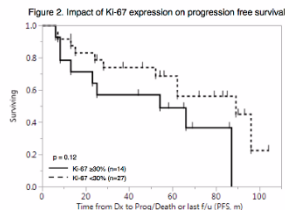
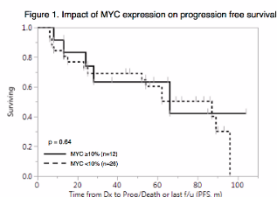
1452 MYC rearrangement and over-expression in non-transformed follicular lymphoma

Emily Glynn¹, Stephen D Smith², Prathima Reddy², Kerstin L Edlefsen³, Jonathan Fromm⁴, Christine Donovan⁴, Ajay Gopal⁴, Lorinda Soma¹.
¹Seattle, WA, ²University of Washington School of Medicine, ³University of Washington Medical Center, Seattle, WA, ⁴University of Washington, Seattle, WA

Background: The coexistence of MYC and BCL2 and/or BCL6 rearrangements and over-expression of MYC and BCL2 by immunohistochemistry (IHC) are features associated with aggressive clinical course in B cell neoplasms with a diffuse large B cell lymphoma (DLBCL) histology. However, data on the frequency and prognostic significance of these findings in non-transformed follicular lymphoma (FL) is limited. The aim of this study was to determine whether the level of MYC expression was predictive of a MYC rearrangement and to investigate the impact of the following on FL clinical course: rearrangement of MYC and IGH-BCL2 and/or BCL6 and MYC over-expression by IHC.

Design: The laboratory information system was queried for lymph node excisions containing non-transformed FL collected between 1/1/2005-12/31/2013. The Ki-67 expression, WHO grade, and available clinical data including stage, treatment, subsequent histologic transformation, relapse, and survival was collected for all cases. MYC IHC was performed on each case and 4 pathologists independently scored the level of expression. Fluorescence in situ hybridization (FISH) for MYC rearrangement was performed on cases with >10% MYC expression and FISH for IGH-BCL2 and BCL6 was performed on cases with a MYC rearrangement.

Results: Fifty cases were included in the study, 38 of which had WHO grade 1-2 histology. Seventeen of the 50 cases had MYC expression >10% and 2 of 17 were positive for rearrangement of MYC and IGH-BCL2 (both grade 1-2 FL). The first patient progressed to DLBCL within 2 years, was treated with R-CHOP, and is currently in remission. The second patient also had a BCL6 rearrangement and presented with advanced disease and was transitioned to hospice 1 year after diagnosis. Only 3 of the 50 cases had MYC expression > 40%; the level of MYC expression in the 2 cases with a MYC rearrangement was 30-50% and 10-20%. There was no association between overexpression of MYC (either >10% or >40%) and Ki-67 expression >30% and WHO grade or progression free survival (figures 1 and 2, respectively).



Conclusions: In conclusion, our findings show that most follicular lymphomas show <10% MYC expression, with only a few cases >40%, and MYC expression level is not predictive of a MYC rearrangement. This limited cohort suggests the presence of a MYC and IGH-BCL2 and/or BCL6 rearrangement in non-transformed follicular lymphoma may be associated with a more aggressive clinical course; however, MYC expression by IHC did not impact progression free survival.

1453 Genomic Analysis in Myeloid Sarcoma and Comparison with Paired Acute Myeloid Leukemia

Nancy Greenland¹, Jessica Van Ziffle², Sonam Prakash², Linlin Wang¹.
¹San Francisco, CA, ²University of California, San Francisco, CA

Background: Myeloid sarcoma (MS) is a rare manifestation of acute myeloid leukemia (AML) characterized by extramedullary proliferation of myeloid blasts. Due to the rarity of MS, the clonal evolution of cell populations giving rise to AML and MS in the same individual is not well understood. In an effort to reveal a genomic signature of clonal progression, we used capture-based next generation sequencing (NGS) to interrogate the genetic variants present in matched MS and AML samples from a small cohort of individuals.

Design: DNA was extracted from normal tissue, MS tissue and AML bone marrow samples from seven individuals. Targeted genomic profiling using a capture-based next generation sequencing assay of about 500 cancer genes was used to evaluate single nucleotide variants, insertions, deletions, copy number variations (CNVs) and structural variations.

Results: The majority of variants identified in the AML sample were also identified in the MS from the same subject. Overall, 84% (range 60-100%) of the gene mutations in AML were present in MS (Table 1). Similarly, the majority of variants identified in the MS sample were found in AML, averaging 80% of variants (range 60-100%). The gene variants identified were typical of those found in AML. MS samples had a tendency for increased CNVs relative to their paired AML (Table 1).

Table 1. Mutations and copy number variations identified in AML and MS tissues.

Subject	1	2	3	4	5	6	7
AML	TP53 LRP1B EPH81 KMT2D BRCA2 MAP3K9	TP53 STAG2 WT1 (p.422_424del) WT1 (p.H441fs) SHH CEBPA POLE	SYNE1 PHOX2B ADAMTS17 UZAF1 ZFXH3	FLT3 NPM1 RAO21	NRAS WT1 (p.S381fs) POLE NCCR1 FLT3	NRAS CEBPA BCORL1 DNMT3A IDH2 BCOR CHD4 GPC3	BRAF TET2 ASXL1 NPM1 SRSF2 KMT2A SMC3 NF1 CUX1 SETBP1 PAX8 IGF1R SPOB TERT
MS	TP53 LRP1B EPH81 KMT2D BRCA2 MAP3K9	TP53 STAG2 WT1 (p.422_424del) WT1 (p.H441fs) SHH CEBPA POLE NKK2-1 FLT3	SYNE1 PHOX2B ADAMTS17 SETD2 ATRX	FLT3 NPM1	NRAS WT1 (p.S381fs) POLE NCCR1 GATA1 NF1	NRAS CEBPA BCORL1 DNMT3A IDH2 BCOR CHD4 EIF1AX	BRAF TET2 ASXL1 NPM1 SRSF2 KMT2A SMC3 NF1 CUX1 SETBP1 PAX8 IGF1R SPOB CHK2 MYH9 ERBB3 CIC ARID1A POLE
Copy number variations							
AML	+5p12-15.3 +8 -9p11.1-24.3 -12p12.1-13.2 +13q12.1-13.3 -13q13.3-34 -15 -17p11.1-13.2 +18 21 (cnLOH*)	none	none	+1q42.1-44 +4p14-15.2 +8	none	none	+8
MS	+5p12-15.3 +8 -12p12.1-13.2 +13q11-13.3 -13q13.3-34 -17p11.1-13.1 +18 -21	-9p13.1-13.2 +10q25.2-28.3 +11q13.3-28 +12p12.1-13.3 +12p11.2-12.1 -15q24.1-28.3 -16p11.2-13.3 -17p11.1-13.3	-2p22.3-24.3	+1q42.1-44 +8	+8 +9q21.1-33.1 +17q21.2-25.3 +22	+19	+8

Mutations or copy number variations unique to one tissue type in an individual are shown in bold.
 *cnLOH = copy number loss of heterozygosity.

Conclusions: Somatic variants frequently seen in AML can be identified in MS using NGS from FFPE tissue, offering a tool for prognosis and potential selection of targeted therapies. The similar variant profiles observed in MS and AML from the same individual support the notion that these tumors are derived from a common precursor, rather than *de novo* tumors in a susceptible host. In addition, the presence of variants that differ between MS and AML in one individual indicate clonal heterogeneity during progression from this common precursor clone.

1454 PD1 and PDL1 Expression in Richter Transformation

Brannan Griffin¹, Yi-Hua Chen², Amir Behdad¹, Shuo Ma¹, Katalin Kelemen³, Qing Chen¹.
¹Northwestern University, Feinberg School of Medicine, Chicago, IL, ²Northwestern University, Chicago, IL, ³Mayo Clinic Arizona, Phoenix, AZ

Background: Richter transformation (RT) is an aggressive progression of chronic lymphocytic leukemia (CLL), often to diffuse large B cell lymphoma (DLBCL), with dismal prognosis and limited therapeutic response. Antibodies targeting programmed cell death 1 (PD1) and its ligand (PDL1) have proven to be effective therapeutic options in certain solid tumors and lymphomas, and response rate appears to correlate with PDL1 expression on tumor or immune cells. This study evaluates PD1 and PDL1 expression in RT cases, and explores the rationale and mechanism for targeting PD1/PDL1 pathway in RT treatment.

Design: We studied 15 patients diagnosed with RT (13 DLBCL and 2 paraimmunoblastic type), 9 cases of CLL (6 with expanded proliferation centers), and 25 cases of de novo DLBCL. All were evaluated by immunohistochemistry using anti PD1 (MRO-22), PDL1 (SP142) or PAX5/PDL1 antibodies.

Results: Median age of RT patients at first diagnosis was 64 years (range 39-85). Of 12 patients with follow-up data, 8 died with median survival since RT 6.3 months (1 week-12 months). TP53 deletion was found in 4/11 cases, and trisomy 12 in 3. PDL1 expression was seen only in scattered lymphoma cells in 2/15 RT cases (13%). Remarkably, 13/15 RT cases (87%) displayed PD1 expression by lymphoma cells: 5 uniformly strong, 2 moderate, 6 weak and/or focal. The two negative cases likely had unrelated large cell clones given the different phenotype. All RT cases contained high numbers of PDL1+ macrophages. Interestingly, PD1+ B cells were frequently seen in proliferation centers (PCs) of CLL cases, especially numerous in expanded PCs, but CLL cells outside of PCs had no PD1 or PDL1 expression. In contrast to RT, only 1/25 de novo DLBCL cases showed focal PD1 expression by tumor cells, and 2 had PDL1 expression.

Conclusions: We found surprisingly high PD1 expression by

lymphoma cells in RT patients, and frequent PD1 expression in expanded proliferation centers. Our data suggest PD1 expression by B-lymphoma cells may promote tumor survival in RT, and may play a role in transformation. This may occur via interaction with PDL1+ macrophages and subsequent production of immune suppressive cytokines such as IL-10, as suggested by recent animal model studies. It is conceivable that PD1 immunotherapy may be particularly effective in RT treatment. Indeed, a few RT patients showed promising response to anti-PD1 therapy in recent small series. We propose that patients with high PD1 expression would benefit most from therapy targeting PD1/PDL1.

1455 Myeloid Cell Nuclear Differentiation Antigen (MNDA) in the Diagnostic Evaluation of B-Cell Lymphomas: A Novel Marker in the Differential Diagnosis of Low Grade Follicular Lymphoma (FL) and Marginal Zone Lymphoma (MZL)

Neha Gupta¹, Mohammad Aldabagh², Judith Brody³, Peihong Hsu⁴, Ayesha Sheikh², Kalpana Reddy⁵, Xinmin Zhang¹, Silvat Sheikh-Fayyaz². ¹Donald and Barbara Zucker School of Medicine at Hofstra/Northwell, Lake Success, NY, ²Northwell Health, ³Northwell Health, New Hyde Park, NY, ⁴North Shore-LIJ Health System, New Hyde Park, NY, ⁵Northwell Health, Mineola, NY, ⁶Donald and Barbara Zucker School of Medicine at Hofstra/Northwell

Background: MNDA is a nuclear protein that is involved in apoptosis and innate immunity as well as in the regulation of protein-protein interaction. It is normally expressed in the myelomonocytic lineage and in a subset of B lymphocytes. Few studies have shown the expression of MNDA in MZL. FL cases are rarely positive for MNDA. We undertook this study to evaluate the expression pattern of MNDA in low grade B-cell lymphomas and its potential as a differential marker for MZL and FL.

Design: We collected 157 cases of small B-cell lymphoma diagnosed in our institution over a 3-year period, including 90 MZL, 20 chronic lymphocytic leukemia /small lymphocytic lymphoma (CLL/SLL), 24 FL, and 23 mantle cell lymphoma (MCL). The biopsy sites included lymph nodes and a variety of extranodal sites. Immunohistochemical study for MNDA was scored positive when >15% of tumor cells were stained. The staining intensity was scored as strong, moderate or dim. CD43 was evaluated as positive or negative.

Results: Of the 90 MZL cases, 34 (38.0%) were positive for MNDA. This included 12 nodal MZL (35.0%), 1 splenic MZL (2.9%) and 21 extranodal MZL (61.8%) cases. MNDA showed strong expression in 10 cases, moderate to strong expression in 2 cases and dim expression in 22 cases. MNDA staining was observed in only 4.0% (1/24) of FL cases. This was grade 3B FL with focal diffuse large B-cell lymphoma features. CLL showed dim MNDA expression in 20.0% (4/20) of cases. In MCL, MNDA expression was observed in 21.7% (5/23) cases. Strong MNDA expression was observed in one MCL case with pleomorphic morphology whereas other 4 cases showed dim staining. CD43 expression was positive in 22% MNDA+ MZL cases and 50% MNDA-negative MZL cases.

Conclusions: MNDA was preferentially expressed in MZL, especially extranodal MZL followed by CLL and MCL, but rarely expressed in FL. Our study shows that MNDA is a useful marker for the diagnosis of CD43 negative MZL and for differentiating MZL and low grade FL.

1456 Identification of Aggressive Variants of Mantle Cell Lymphoma Based on Flow Cytometry

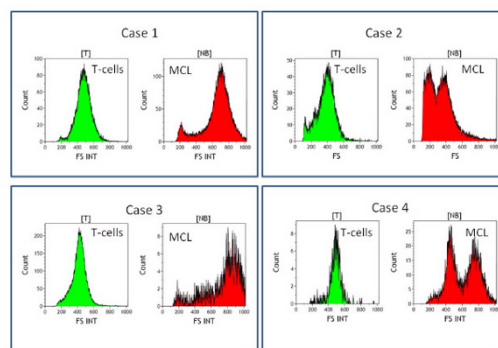
Alia Gupta¹, Marc Smith², James Huang². ¹Troy, MI, ²William Beaumont Hospital

Background: Mantle cell lymphoma (MCL) is clinically and pathologically heterogeneous with highly variable outcome. Some patients have chronic/indolent course while others with pleomorphic or blastic variants have significantly shorter survival. The aim of our study is to explore if flow cytometry analysis can help with identification of aggressive MCL variants.

Design: We retrospectively identified 48 nodal MCL diagnosed at our institution from 2010 to 2017. The original list mode data was reanalyzed. Median (Med), arithmetic mean (AMean), geometric mean (GMean) standard deviation (SD) and coefficient of variation (CV) of forward scatter (FSC) of all neoplastic B-cell and reactive T-cell events were collected. The numerical parameters and histograms of FSC were correlated with the clinical and pathological features. Student T-test and chi-squared test were used.

Results: Out of all 48 cases, the average of FSC Med, AMean, and GMean for neoplastic B-cell events was 444, 440, and 417. The average of FSC Med, AMean, and GMean for reactive T-cell events was 409, 403, and 385. No overt statistical differences were detected in FSC Med, AMean, and GMean between neoplastic B-cell events and reactive T-cells (t-test, p>0.05). However, 15 cases of MCL showed very abnormal FSC histogram patterns: increased events of very low FSC, very high FSC or both (as shown in the figure of representative cases). These patterns are likely caused by lymphogranular bodies (low

FSC) or unusually large lymphocytes (high FSC). Of these 15 cases, 10 (67%) were aggressive variants (5 pleomorphic and 5 blastic). In the remaining 33 cases, only 6 were classified as aggressive variants. Chi-squared test showed the difference was statistically significant (p=0.001) with relative risk of 3.7 and odds ratio of 9.



Conclusions: MCL cases with very abnormal FSC histogram patterns are easily recognizable and likely to be aggressive. Therefore, we recommend evaluation of cytometric FSC parameters and histograms in all MCL cases. We also encourage further study of FSC in regards to clinical outcome (currently in progress at our institution) to determine if FSC may provide additional independent prognostic information that has not been previously reported.

1457 Chronic Myeloid Leukemia with Atypical BCR-ABL1 Fusion Transcripts: Report of Four cases

Cong Han, Tianjin, China

Background: The majority of chronic myeloid leukemia (CML) patients have breakpoints in the M-BCR, which result in either e13a2 or e14a2 fusion mRNAs. Rarely, CML patients with atypical BCR-ABL1 transcripts are occasionally observed. In this study, four patients with atypical fusion transcripts e6a2, e8a2 and e13a2 were reported. We investigated the precise features of the molecular rearrangements and the minimal residual disease follow-up for these patients.

Design: Multiplex reverse transcription-polymerase chain reaction and direct sequencing were performed to detect atypical fusion transcripts. Real-time quantification reverse transcription-polymerase chain reaction was carried out to monitor minimal residual disease.

Results: We identified four atypical fusion transcripts. In patient 1, an e13a2 transcript harboring a deletion of the last 40 nucleotides of BCR exon 13 was identified. At the genomic level, the partial BCR e13 was fused to the 45 nucleotides of ABL1 intron 1b, with 7 nucleotides ACAACA insertion between the two junctions, creating an atypical e13 partial/1b partial novel exon. In patient 2, an unusual e8a2 BCR-ABL transcript was identified. The partial BCR e8 was fused to the ABL1 exon 2, with 7 nucleotides of ABL1 intron 1b insertion between the two junctions. The results showed that BCR-ABL translocation breakpoints can occasionally occur within coding exons and not conform to consensus splice sites. The third patient expressed an e8a2 transcript resulting from a complex rearrangement involving a third partner gene NSC1(exon2) and the fourth patient revealed the presence of e6a2 transcript. All these patients were treated with TKI. Patient 1 showed favorable molecular evolution under TKI therapy and quickly achieved major molecular response. In patient 2(e8a2), the BCR-ABL/ABL ratio was 86.80% at diagnosis, 88.21% after 2 months, 20.71% after 4 months of therapy. In patient 4(e6a2), the BCR-ABL/ABL ratio was 9.51% at diagnosis, 67.61% after 3 months, 31.26% after 5 months of therapy.

Conclusions: Our study showed that BCR-ABL translocation breakpoints can occur within coding exons and create novel intronic pseudo-exons. Patients with e8a2 and e6a2 transcripts were resistant to TKI treatment, suggesting a worse prognosis of CML with e8a2 and e6a2 BCR-ABL.

1458 Evaluation of Molecular Minimal Residual Disease in Multiple Myeloma: An Institutional Experience

Tim Hanley¹, Parker Clement², Laura Dickey³, K. David Li⁴. ¹University of Utah Health Sciences Center, Salt Lake City, UT, ²Salt Lake City, UT, ³University of Utah, Salt Lake City, UT, ⁴University of Utah/ARUP Laboratories, Salt Lake City, UT

Background: Assessment of minimal residual disease (MRD) in multiple myeloma (MM) is used increasingly by clinicians to evaluate treatment efficacy and prognosis. At our institution, clinicians often evaluate and follow MM patients using both molecular (molMRD) and standard five color multiparameter flow cytometry (MPFC) methods. We wished to compare the efficacy of molMRD to our MPFC assay and

to investigate correlations between clinical and laboratory factors and the presence of molMRD.

Design: We evaluated bone marrow biopsies from 121 MM patients at our institution between 2004 and 2017 who had both molMRD and MPFC performed. We acquired clinical, pathology, and cytogenetic data from these patients at diagnosis and at follow-up. molMRD evaluation was performed using clonoSEQ MRD by Adaptive Biotechnologies. Flow cytometric evaluation was performed using a laboratory developed five color multiparameter analysis for plasma cells (PCs) with a minimum of 100,000 events collected.

Results: Of the 121 MM patients, 107 (88%) were positive and 14 (12%) were negative for molMRD at diagnosis. All patients had monoclonal PCs by MPFC at diagnosis. Of the 107 patients who were molMRD+ at diagnosis, 86 (80%) were tested for molMRD at post-transplant or post-therapy follow-up, where 65 (76%) were positive and 21 (24%) were negative. Of the 65 MM patients who were molMRD+ at follow-up (average interval 39.7 months, range 1.4-143 months), 21 (32%) were MPFC-. These patients had lower disease burdens by molMRD testing and were more likely to have normal MM FISH results ($p=0.004$). Of the 21 patients who were molMRD- at follow-up, 3 (14%) were MPFC+. Furthermore, patients with monoclonal PCs demonstrating aberrant immunophenotypes (CD52+ [$p=0.003$], CD56+ [$p=0.0002$], and/or CD117+ [$p=0.03$]) were more likely to be molMRD+ at follow-up. Conversely, patients with CD19 expression ($p=0.0003$) were less likely to be molMRD+ at follow-up. Finally, patients with age < 60 at diagnosis ($p=0.02$) and patients with WBC < 5000/uL at follow-up ($p=0.004$) were more likely to be molMRD+.

Conclusions: Our experience shows that molMRD is more sensitive than conventional MPFC for the detection of MRD in MM; however, a small percentage (14%) of follow-up molMRD- cases had detectable residual disease by MPFC. In addition, a subset of patients (12%) who were molMRD- at diagnosis had monoclonal PC populations by MPFC. The overall findings suggest that molMRD is not useful in a subset of patients for monitoring MRD, and MPFC is still required.

1459 Toll-Like Receptor Expression Is Altered in B-cell Lymphoproliferative Disorders

Tim Hanley¹, Laura Dickey², K. David L³. ¹University of Utah Health Sciences Center, Salt Lake City, UT, ²University of Utah, Salt Lake City, UT, ³University of Utah/ARUP Laboratories, Salt Lake City, UT

Background: Toll-like receptors (TLRs) are innate immune receptors that play a pivotal role in the recognition of microbial pathogens and the initiation of immune responses, in part by mediating B-cell activation and maturation. Studies suggest that TLR expression may be altered in B-cell neoplasms, and that this altered expression may lead to aberrant cellular activation. As such, TLRs may represent important diagnostic or prognostic markers, as well as possible therapeutic targets, for B-cell neoplasms. We therefore wished to evaluate TLR expression patterns on neoplastic B cells and to determine whether TLR signaling alters proliferation or survival of neoplastic B cells.

Design: We examined 24 specimens with B-cell lymphoma diagnoses (8 chronic lymphocytic leukemia/small lymphocytic lymphoma (CLL/SLL), 8 mantle cell lymphoma (MCL), 8 follicular lymphoma (FL)), and four specimens from healthy donors for TLR2, TLR4, TLR5, and TLR9 expression by flow cytometry. To evaluate the effects of TLR ligand treatment on cell survival, we treated neoplastic B cells with ligands for TLR2 (PAM3CSK4, FSL-1), TLR4 (LPS), TLR5 (flagellin), or TLR9 (ODN 2006) ± vincristine, a pro-apoptotic chemotherapeutic drug, and assessed apoptosis by Annexin V staining. To examine the effects of TLR signaling on cell proliferation, we treated neoplastic B cells with TLR ligands and assessed proliferation by CFSE dye dilution.

Results: Overall, we determined that TLR expression patterns were altered in all three B-cell neoplasms compared to B cells isolated from healthy donors. MCL tumor cells exhibited increased TLR2 ($p = 0.0006$) and TLR5 ($p = 0.007$) expression, and decreased TLR9 ($p = 0.0015$) expression. CLL/SLL tumor cells showed increased TLR2 ($p = 0.05$) expression, but decreased TLR9 ($p < 0.0001$) expression. Unlike CLL/SLL and MCL tumor cells, FL tumor cells showed increased TLR9 expression. Furthermore, we observed differences in neoplastic cell survival in response to TLR activation. Activation of TLR2, which is overexpressed on CLL/SLL tumor cells, showed protective effects to vincristine-mediated apoptosis ($p = 0.03$). Finally, TLR signaling did not affect cellular proliferation in the absence of additional stimuli.

Conclusions: In summary, we found that TLR expression patterns are altered in a subset of B-cell neoplasms, and that altered expression may contribute to enhanced survival of neoplastic B cells. Further studies are warranted to assess the role of TLR signaling in neoplastic B-cell survival and proliferation.

1460 National Survey of Pathologists on the Application of Ancillary Testing in the Diagnosis of Acute Myeloid Leukemia

Robert Hasserjian¹, Jessica Altman², Ellen Denzer³, AnneMarie Block⁴, Heidi Klepin⁵, Bruno Medeiros⁶, Amanda Noe⁷, Wendy Scales⁸, Martin Tallman⁹, Kathleen Wiley¹⁰, Linda Burns³. ¹Massachusetts General Hospital, Boston, MA, ²Northwestern University, Feinberg School of Medicine, ³National Marrow Donor Program/Be The Match, ⁴Roswell Park Cancer Institute, ⁵Wake Forest Baptist Health, ⁶Stanford University School of Medicine, ⁷The France Foundation, ⁸The France Foundation, Old Lyme, CT, ⁹Memorial Sloan Kettering Cancer Center, ¹⁰Oncology Nursing Society, Pittsburgh, PA

Background: The correct classification of acute myeloid leukemia (AML) according to the current World Health Organization (WHO) classification system requires the application of multiple testing modalities. However, it is unclear how pathologists are currently applying ancillary testing in diagnosing AML.

Design: A cross-sectional, web-based survey of health professionals from the American Society of Hematology, the American Society of Clinical Pathology, and the Oncology Nursing Society was conducted April 7 – June 1, 2017. The survey consisted of 78 questions, which included practice and provider characteristics, diagnosis and evaluation, and AML-related practice concerns.

Results: A total of 1,246 individuals participated in part or all of the survey; complete survey data were collected from 130 pathologists, who had been in practice for a median of 6 years and saw a median of 10 newly diagnosed AML cases in the past 24 months. The WHO classification system was used by 128 (98%), while 24 (18%) additionally used the French-American-British (FAB) system. For 111 respondents (85%), there was a mechanism for the pathologist to order ancillary testing, while for 14 (11%) all ancillary testing was ordered by clinicians. The usage of ancillary testing according to the pathologist's practice setting is shown in Table 1; 105 pathologists (81%) integrated the results of all testing in a single report. Pathologists based in academic centers and community-based pathologists reported similar usage of genetic testing at diagnosis, while community-based pathologists used cytogenetic testing in followup samples less frequently. The most common clinical care concerns were insufficient clinical information (29%), bone marrow sample adequacy (24%), challenges in selection and interpretation of molecular testing (17%), and suboptimal pathologist experience in classifying AML (8%). Community-based pathologists were more likely to report concerns about AML classification ($p=0.007$) and molecular testing ($P=0.04$) compared to academic center-based pathologists.

Table 1.	Pathologists at Academic Centers (n = 55)	Pathologists in Community Practice (n = 61)
Tests Ordered in the Initial Diagnosis of AML		
Cytochemical staining	37/55 (67%)	33/61 (54%)
Cytogenetics	54/55 (98%)	60/61 (98%)
FLT3, NPM1, and CEBPA mutations	54/55 (98%)	57/61 (93%)
Next generation sequencing panel	40/55 (73%)	41/61 (67%)
Gene expression profiling	23/55 (42%)	24/61 (39%)
Tests Ordered in Post-Treatment/Follow-up		
Cytogenetics	51/55 (93%)**	47/61 (77%)**
Next generation sequencing panel	25/55 (45%)	21/61 (34%)

*Respondents based in industry (n=1), reference labs (n=12), or not specified (n=1) are not included in Table 1.

** $P=0.02$ (Fisher's exact test)

Conclusions: Although the vast majority of responding pathologists applied the WHO classification to the initial diagnosis of AML, some concerns were raised regarding lack of clinical information and sample adequacy, as well as difficulties in AML subtyping and in genetic test selection and interpretation. These findings indicate an opportunity to close existing practice gaps by educating pathologists and clinicians about current standards in AML diagnosis.

1461 NPM1 Mutation is a Distinguishing Feature of Acute Myeloid Leukemia (AML) and a High Risk Marker in Chronic Myeloid Neoplasms (CMN)

Rong He¹, Manli Jiang², David Viswanatha¹, Dong Chen¹, Liuyan Jiang³, Surendra Dasari¹, James Hoyer¹, Mark Hubbard⁴, Kurt B Besson⁴, Simon Althoff⁵, Mechelle Miller⁴, Dana Roh⁴. ¹Mayo Clinic, Rochester, MN, ²Rochester Clinic, ³Mayo Clinic Florida, Jacksonville, FL, ⁴Mayo Clinic

Background: NPM1 mutation is present in about 30% of AML, and

commonly occurs in the last exon resulting in a C-terminal frameshift and aberrant protein cytoplasmic re-localization and oncogenic transformation. Favorable clinical outcome has been documented in *NPM1^{+/FLT3⁻}* normal karyotype (NK) AML. However, the prevalence and clinical features of *NPM1⁺* CMN have not been thoroughly examined.

Design: We retrospectively analyzed 999 cases underwent a myeloid-targeting next generation sequencing (NGS) panel testing (7/2015-5/2017), including 225 AMLs, 181 myelodysplastic syndromes (MDS), 188 myeloproliferative neoplasms (MPN), 69 MDS/MPN, and 336 other cases without definitive pathologic features of myeloid neoplasms (non-Dx). Clinical and other laboratory findings were obtained from medical records.

Results: *NPM1* mutations were detected in 51/999 cases and were highly enriched in AML (90.2%, 46/51) but relatively rare in CMN (9.8%, 5/51). The frequency in various MNs was AML 20.4% (46/225), MDS 1.6% (3/181), MDS/MPN 2.9% (2/69), and MPN/non-Dx 0%. The 5 *NPM1⁺* CMN included CMML-1 (6% blasts), CMML-2 and 3 MDS-RAEB2. Of these 5 patients, 3/5 progressed to AML, 1/5 (RAEB2) received azacitidine (Aza) but died without progression at day 302, and 1/5 (RAEB2) received Aza, allogeneic stem cell transplantation (Tx) and remained stable 75 days post Tx. The 3 cases progressed to AML included CMML-1 (at day 43, transfusion only) and CMML-2 (at day 30, observation only), and a RAEB-2 (at day 425 post Aza/LDE22). All 3 cases were NK with no co-mutations in 2 and DNMT3A/GATA2 co-mutations in 1. The other 2 *NPM1⁺* CMN were trisomy 8/DNMT3A⁻ and NK/IDH2^{+/NRAS⁻, respectively.}

Conclusions: *NPM1* mutations are highly enriched in AML and only rarely seen in CMN, particularly high grade MDS and MDS/MPN. *NPM1* mutation in CMN is associated with high risk of AML progression in the absence of chemotherapy. It is a high risk molecular marker in CMN, which may be of diagnostic value in morphologically challenging high grade MNs, and warrants close clinical monitoring and early clinical intervention.

1462 t(14;16)/IGH-MAF in Multiple Myeloma is Associated with Other High-Risk Genetic Features

Jian He¹, Xinyan Lu², Shaoying Li³, Shimin Hu³, Wei Wang³, C. Cameron Yin³, L. Jeffrey Medeiros³, Pei Lin³, Jie Xu³. ¹Spring, TX, ²Northwestern University Feinberg School of Medicine, Chicago, IL, ³The University of Texas MD Anderson Cancer Center, Houston, TX

Background: Earlier studies have shown that t(14;16)(q32;q23)/IGH-MAF is a high-risk factor in multiple myeloma (MM). However, this translocation is known to be an early event in pathogenesis that can be detected in precursor lesions suggesting that t(14;16), by itself, may not be an adverse prognostic factor. The presence of concurrent genetic abnormalities has not been explored extensively in patients with this subset of MM. In this study, we focus on the clinicopathological and genetic features of MM associated with t(14;16).

Design: Cases of MM associated with t(14;16)/IGH-MAF detected by conventional karyotyping and/or fluorescence in situ hybridization (FISH) diagnosed over a 6-year interval formed the study cohort. Clinicopathologic data, other concurrent genetic abnormalities, treatment regimens, and clinical follow-up data were collected and analyzed.

Results: We identified 19 patients with MM associated with t(14;16)/IGH-MAF, including 7 men and 12 women with a median age of 64 years (range, 47-82) at time of diagnosis. Twelve patients had de novo disease and 7 patients had relapsed MM. Serum M paraprotein levels ranged from 1.0-94 g/L (median, 19 g/L). The bone marrow aspiration and biopsy specimens showed a median of 45% plasma cells (range, 5-95%). The percentage of t(14;16) nuclear fusion signals by FISH ranged from 5.5% to 91% (median, 16.5%). Other coexisting genetic aberrations included: chromosome 13 deletion (n=12, 63.2%), TP53 deletion (n=9, 47.4%), CKS1B amplification (n=5, 26.3%) and a complex karyotype (n=18, 95%). The group with a complex karyotype included 10 cases with a hypodiploid karyotype. All patients received treatment containing proteasome inhibitors and 9 (47.4%) received a stem cell transplant. The median follow-up time was 32.4 months (range 5.2-79.4). At the time of last follow-up, 18 patients died and one was alive. The median overall survival after t(14;16) detection was 17.8 months (range, 0.2 to 40.3 months). Patients with concurrent TP53 deletion had a poorer outcome (median 24.0 vs 4.5 months, P = 0.01).

Conclusions: The t(14;16)(q32;q23)/IGH-MAF in MM is associated frequently with other high-risk genetic abnormalities including deletion of chromosome 13, TP53 deletion, a complex karyotype and CKS1B amplification. These data suggest that the poor prognosis of patients with MM associated with t(14;16)/IGH-MAF may, at least in part, be attributable to concurrent genetic abnormalities.

1463 Indications for Bone Marrow Biopsy at Time of First Assessment in Patients with Chronic Myeloid Leukemia in the Era of Tyrosine Kinase Inhibitor Therapy

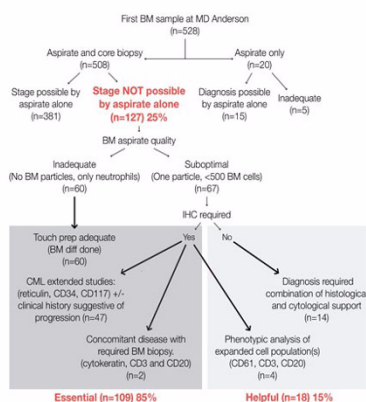
Juliana E Hidalgo-Lopez¹, Andres E Quesada¹, Zimu Gong¹, Wei Wang¹, Rashmi Kanagal-Shamanna¹, Shimin Hu¹, C. Cameron Yin¹, Jorge Cortes¹, Roland L Bassett Jr¹, L. Jeffrey Medeiros¹, Hagop M Kantarjian¹, Carlos Bueso-Ramos¹. ¹The University of Texas MD Anderson Cancer Center, Houston, TX

Background: The National Comprehensive Cancer Network guidelines for the management of chronic myeloid leukemia (CML) emphasize the importance of morphologic review of both the bone marrow (BM) core biopsy specimen and aspirate smears. However, the role of BM biopsy in the workup of CML patients (pts) has been questioned as others suggest that BM aspiration along with cytogenetic and/or molecular studies is sufficient.

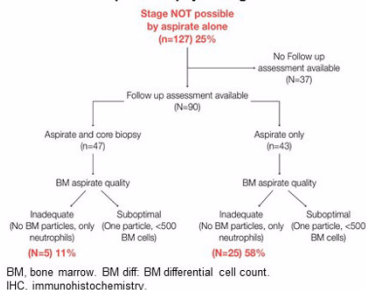
Design: We studied all cases of CML seen at our hospital over 6 years. In all patients who come to our institution, the initial BM assessment is always performed with aspirate and core biopsy. Laboratory and clinical data were collected and BM biopsy and/or aspirate smears were reviewed. The biopsy was considered essential when the diagnosis was based on biopsy alone. The biopsy was considered helpful if required for other non-essential reasons.

Results: 508 pts who underwent core biopsy and aspiration were the study cohort. In 109 (85%) pts the biopsy was essential because the aspirate was either inadequate (n=60) or suboptimal (n=49). The biopsy was helpful in 18 (15%) pts. At initial presentation, among patients with either an essential or helpful biopsy, 103 pts were in chronic phase (CP) and 24 in accelerated (AP) or blast phase (BP). The BM was needed to distinguish AP from BP in 9/12 patients (p=0.0028). Myelofibrosis (MF 2-3) was noted in 40% of pts and was more frequent in pts with AP/BP (n=8) than CP (n=7) (p=0.0039). There was no significant difference in BCR/ABL1 levels in PB or BM or cytogenetic or molecular response rate between pts in whom biopsy was versus was not essential/helpful. In the 127 pts in whom biopsy was essential/helpful at initial diagnosis, 90 pts underwent subsequent BM evaluation: 43 underwent aspiration only and 47 had core biopsy. BM aspirates were more frequently inadequate among pts who did not undergo biopsy (58% vs. 11%; p = 0.001). Fig.1

Flowchart showing the diagnostic criteria used for BM workup



Flowchart showing the follow up quality in pts who required biopsy at diagnosis



Conclusions: Core biopsy is required for diagnosis of CML at first assessment in about 25% of patients. BM core biopsy is indicated in patients who meet any criteria for AP/BP, or who have a dry tap at BM collection. The requirement of core biopsy is mainly related to the presence of myelofibrosis. The pts who require core biopsy at time of first assessment should undergo core biopsy for subsequent BM assessment because this pt subset is more likely to have repeat inadequate BM aspirates.

1464 Comparative Evaluation of Plasmacytoid Dendritic Cell Content in Reactive and Neoplastic Lymphoid Aggregates in Bone Marrow (BM)

Amanda M Hopp¹, Horatiu Olteanu², Alexandra Harrington², Steven Kroff². ¹Medical College of Wisconsin, Wauwatosa, WI, ²Medical College/WI, Milwaukee, WI

Background: Discrimination between reactive and neoplastic lymphoid aggregates in BM is often challenging. We incidentally noted prominent plasmacytoid dendritic cell (PDC) populations in some reactive lymphoid aggregates in BMs. PDCs are interferon-secreting cells, active in viral infections and autoimmune states. We hypothesized that assessment of these cells might be useful in the discrimination of benign and lymphomatous BM lymphoid aggregates.

Design: BM biopsies from 15 non-lymphomatous (i.e. reactive) and 24 small B-cell lymphoma cases were selected based on the presence of discrete lymphoid aggregates, ≥ 1 year of follow-up, and flow cytometric evaluation. Reactive cases were from various clinical settings. Lymphoma cases included CLL/SLL (5), follicular lymphoma (12), lymphoplasmacytic lymphoma (3), mantle cell lymphoma (3) and splenic marginal zone lymphoma (1). Each case was stained for CD3, CD20 and CD123 by IHC. The aggregates were evaluated for T and B-cell proportions and distribution, and the average number per 50x high-power field (hpf) and distribution of CD123(+) PDCs in the aggregates. Number of PDCs/hpf was compared using the Mann-Whitney U test.

Results: The mean PDCs/hpf was higher in reactive than lymphomatous aggregates (109.8 vs 51.3; $p=0.006$), although a wide range was seen in both groups. A cutoff of <45 PDCs/hpf in the aggregates was 75% sensitive and 80% specific for lymphomatous aggregates. Aggregates with T-cell predominance had higher PDC counts compared to those with B-cell predominance for all cases (112 vs. 41; $p=0.001$) and lymphoma cases (104 vs 41; $p=0.045$). There was no difference in PDCs/hpf between lymphoma types. A peripheral distribution pattern of PDCs was observed in 3 of 15 (20.0%) reactive cases, 2 of which consisted of reactive germinal centers. Peripheral PDCs were also seen in 4 of 12 follicular lymphomas (33.3%) and 1 of 3 mantle cell lymphomas (33.3%), but none of the other lymphoma types. Remaining cases showed random admixtures of PDCs in the aggregates.

Conclusions: PDCs were significantly more numerous in reactive than lymphomatous aggregates, with 75% sensitivity and 80% specificity for lymphoma with a cutoff of <45 PDCs/hpf. Additionally, the number of PDCs was higher in aggregates with greater T-cells. Finally, a distinctive peripheral distribution pattern appeared to be associated with follicular proliferations (both reactive and neoplastic), although there were too few cases to draw definitive conclusions.

1465 The Work-up of Patients with Hypereosinophilia at a Tertiary Referral Center

Zhihong Hu¹, Srdan Verstovsek², Roberto Miranda², Sanam Loghavi³, Wayne Tam⁴, Attilio Orazi⁵, Sa Wang⁶. ¹The University of Texas Health Science Center at Houston, Houston, TX, ²The University of Texas MD Anderson Cancer Center, Houston, TX, ³Houston, TX, ⁴Weill Cornell Medical College, New York, NY, ⁵Weill Cornell Medical College/NYP, New York, NY

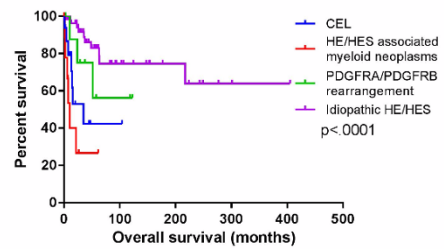
Background: Hypereosinophilia (HE) may be the primary complaint/clinical manifestation for consultations or referral. The work-up of HE can be challenging due to broad and complex causes of HE that can be reactive or neoplastic. In some patients, the causes of HE are unrevealing, being considered as idiopathic hypereosinophilic syndrome (HES) if tissue damage, otherwise, idiopathic HE. In this study, we reviewed a total 126 patients who presented or being referred to us for evaluation and clinical management of HE, and examined the final diagnoses of these patients.

Design: With appropriate work-up that included BM morphology, flow cytometry, cytogenetic and molecular studies, we found 29/126 (25%) patients with reactive HE due to paraneoplastic syndromes ($n=7$); Lymphocyte-variant HES ($n=5$); autoimmune diseases ($n=5$); infection ($n=3$); the etiology for HE remained unknown in 9 patients but HE resolved. 9 patients had *PDGFRA* and 2 had *PDGFRB* rearrangement; and 10 patients had well-defined myeloid neoplasms, including systemic mastocytosis, AML, MPN or MDS/MPN. Chronic eosinophilic leukemia (CEL) as defined by cytogenetic abnormalities and/or increased blasts was diagnosed in 8 (6%) patients. Of the remaining 68 patients, NGS detected mutations in 16/39 (41%) patients, and BM showed abnormal morphology in 10/16 (63%) patients. Moreover, in 3 patients, NGS was not performed but bone marrow showed marked abnormal findings consistent with MPN or MDS/MPN, adding additional 13 patients to the CEL, NOS category. The remaining 55 (44%) patients would be considered to have idiopathic HES/HE.

Results: With a median follow up of 26 (range, 0-405) months, the median OS for CEL was 26 months, better than patients with HE associated with another hematopoietic myeloid neoplasm (median OS: 10 months) but significantly inferior to patients with idiopathic HES (not reached) or patients with *PDGFRA* or *PDGFRB* (not reached)

(Figure 1).

Comparisons of overall survival in HE/HES patients



Conclusions: A proper diagnostic algorithm that excludes reactive causes of HE/HES and combines associated molecular/cytogenetic abnormalities and BM morphology, is essential to reach a correct diagnosis and disease risk stratification. The detection of somatic mutations by NGS helps to identify additional cases of CEL, NOS but the mutation data should be interpreted cautiously in conjunction with BM morphology. After an extensive work-up, the causes of HE are unrevealing in about 40-50% patients, being considered as idiopathic HE/HES. Future study is needed for this group of patients.

1466 Characterization of 3q26.2/EVI1 Rearrangements in Myelodysplastic/myeloproliferative Neoplasms

Zhihong Hu¹, Shimin Hu², Xiaohong Iris Wang³, L. Jeffrey Medeiros², Wei Wang². ¹The University of Texas Health Science Center at Houston, Houston, TX, ²The University of Texas MD Anderson Cancer Center, Houston, TX, ³Bellaire, TX

Background: 3q26.2/*EVI1* rearrangement plays an important role in leukemogenesis and is associated with treatment resistance and poor prognosis in patients with acute myeloid leukemia (AML), myelodysplastic syndrome (MDS), chronic myeloid leukemia (CML) and myeloproliferative neoplasms (MPN). In the risk stratification of cytogenetic changes in cases of AML and MDS, 3q26.2 rearrangements are in the adverse prognostic group. In this cohort, we have studied myelodysplastic/myeloproliferative neoplasms (MDS/MPN) cases with 3q26.2 rearrangements to determine the potential impact of these cytogenetic abnormalities on the clinicopathological features of patients.

Design: Cases of MDS/MPN diagnosed in our institution during over 16 years were reviewed and cases with 3q26.2 rearrangements detected by conventional karyotyping were included. Clinicopathological data, treatment regimens, response and follow-up data were collected and analyzed.

Results: The study is composed of 12 patients with a median age of 66 years (range, 51-79) at time of initial diagnosis, including 10 CMML and 2 MDS/MPN, unclassifiable. Anemia occurred in all 12 (100%) patients, leukocytosis in 7/12 (58%) and thrombocytopenia in 3/12 (25%). 5/12 (42%) patients presented with splenomegaly and 10/11 (91%) with an elevated serum LDH level. Bone marrow biopsy showed multilineage dysplasia in all patients, with dysplastic megakaryocytes most frequent 12/12 (100%). *Inv(3)(q21q26.2)* was the most common 3q26.2 rearrangement, identified in 7 (58%) patients. The remaining 3q26.2 rearrangements included 2 cases of *t(3;21)(q26.2;q22)*, and 1 case each of *t(3;3)(q21;q26.2)*, *t(2;3)(p21;q26)*, and *t(3;6)(q26.2;q26)*. Six (50%) patients had 3q26.2 rearrangements as a sole cytogenetic abnormality and 6 (50%) patients had additional abnormalities, with -7 being most common. Molecular studies revealed *DNMT3A* mutations (3/5, 60%), *RAS* mutations (2/10, 20%), and *IDH2* mutation (1/7, 14%). Most patients received hypomethylating agent-based chemotherapy. The median follow-up was 9.4 months (range, 1.5 to 22.5) and at time of last follow-up 3 patients showed persistent disease and 9 died. The median survival was 13.4 months.

Conclusions: The clinicopathological features of cases of MDS/MPN with 3q26.2/*EVI1* rearrangements resemble AML and MDS, with the exception that more MDS/MPN patients present with thrombocytopenia. Emergence of 3q26.2/*EVI1* rearrangements in MDS/MPN is associated with aggressive clinical behavior, poor response to treatment, and a poor prognosis.

1467 Evaluation of JAK2V617F and CALR Mutational Analysis Using Circulating Cell-Free DNA (ccfDNA)

Steven Huang¹, Ming Ma², Rong He³, David Viswanatha³. ¹Mayo High School, ²Mayo Clinic, ³Mayo Clinic, Rochester, MN

Background: In cancer patients, the circulating cell-free DNA (ccfDNA) in plasma contains circulating tumor DNA (ctDNA) derived from degenerating tumor cells. ctDNA is a potentially useful source for determining tumor somatic mutation composition with particular application to disease monitoring. As a proof-of-concept, we

evaluated the utility of ccfDNA in hematologic malignancies using a highly sensitive quantitative allele-specific PCR *JAK2V617F* assay and a qualitative fragment sizing *CALR* assay, both of which are routinely tested from the leukocyte component of bone marrow (BM) or peripheral blood (PB) samples.

Design: Concurrent peripheral blood samples of cases sent for the routine laboratory *JAK2V617F* or *CALR* testing were retrieved. Plasma was collected and ccfDNA was extracted using the Maxwell RSC and ccfDNA Plasma Kit (Promega, Madison, WI) following manufacturer's instruction. The ccfDNA was then used for *JAK2V617F* and/or *CALR* testing and the results compared with those obtained from the routine laboratory testing.

Results: 16 paired samples were tested for *JAK2V617F*. All 9/16 cases tested negative by the routine laboratory testing were also negative using ccfDNA. All 7/16 positive cases with levels ranging from 0.09%-27.5% were positive using extracted ccfDNA. The quantitative analyte levels were comparable with <0.5 log differences in 5/7 cases while other 2 showed 1.0 and 1.2 log higher levels in the routine testing, which were not clinically significant for disease diagnosis, prognosis or intervention. 15 paired samples were tested for *CALR* mutations and were 100% concordant with cellular DNA results (10/15 negative and 5/15 positive cases the latter showing identical insertion/deletion events of del52bp, ins5bp, and ins2bp).

Conclusions: Molecular testing of *JAK2V617F* and *CALR* using ccfDNA showed highly concordant results with routine testing using the cellular component of BM or PB samples. As a proof of concept, these findings support the feasibility and potential utility of ccfDNA testing in hematologic malignancies, particularly when a BM sample is inadequate, BM/tissue biopsy is contraindicated, hematologic malignancies that are non-circulating/aleukemic, or the primary tumor site is challenging to approach such a lymphoma. The use of ccfDNA is also attractive following therapy when circulating tumor cell burden may be low relative to BM or tissue disease.

1468 AID-Generated Acquired IGH Glycosylation Sites but Not Somatic Hypermutation Rate Differentiate Low-grade versus High-grade Follicular Lymphoma

Chad Hudson¹, Janice Spence¹, Diana G Adlowitz², Richard Burack³. ¹Rochester, NY, ²URMC, Rochester, NY, ³Univ of Rochester, Rochester, NY

Background: B cell development is substantially shaped by the enzyme activation-induced deaminase (AID) which functions include regulating the production of mutations in the immunoglobulin genes (somatic hypermutation (SHM)). AID is induced in germinal center B cells and is highly expressed in follicular lymphoma (FL), a neoplasm of germinal center B cells. FL-derived IGH is more likely to have AID/SHM-generated acquired glycosylation sites (AG sites) in the variable region (IGHV) than IGH from both non-neoplastic B cells and the malignant B cells in non-germinal center-derived B cells neoplasms, making glycosylation site status an intriguing marker for FL. This proclivity for IGHV glycosylation in FL is thought to be related to antigen-independent signaling mediated by glycosylated immunoglobulin. As it is thought that signaling pathways supporting centrocytes and centroblasts differ, we sought to test if IGHV glycosylation is different in centrocyte-rich (low grade, grade 1-2) and centroblast-rich (high grade, grade 3) FL.

Design: The clonally rearranged IGH gene in 41 low-grade FL specimens and 11 high-grade FL specimens was amplified by PCR using IGHV family-specific with junctional IGHJ region primers and sequenced. The resulting sequences were analyzed using V-quest (IMGT.org) to determine percent identity to germline sequences, a measure of SHM. AID/SHM-generated AG sites were determined by analysis of the predicted protein sequence.

Results: Low-grade FL had significantly more AG sites per specimen than high-grade FL (1.38±0.98 vs 0.73±0.47, $p=0.037$). Further, while there was no significant difference between low-grade and high-grade FL in having at least one AG site (36/41 vs 8/11, $p=0.3$), there was a significant difference in having multiple AG sites as 30% of low-grade FL specimens (12/41) had multiple AG sites while none (0/11) of the high-grade FL specimens had multiple AG sites ($p=0.05$). There was no difference in SHM rate between low-grade and high-grade FL (low-grade: median: 87% identity to germline sequence, range: 69-96%; high-grade: median: 86%, range: 83-92%).

Conclusions: While AG sites are a general feature of FL, a low-grade FL specimen is significantly more likely to have multiple AG sites in the IGHV region than a high-grade FL specimen. This suggests that the accumulation of multiple AG sites might be a feature unique to low-grade FL and may be a useful factor in differentiating low-grade FL vs high-grade FL in diagnostically challenging cases.

1469 Increased AID-Generated Acquired Glycosylation Sites in Diffuse Large B-cell Lymphomas with IGH-BCL2 and CD10 Expression

Chad Hudson¹, Janice Spence¹, Diana G Adlowitz², Madalynn Bryant³, Richard Burack⁴. ¹Rochester, NY, ²URMC, Rochester, NY, ³University of Rochester Medical Center, ⁴University of Rochester, Rochester, NY

Background: B cell development is substantially shaped by the enzyme activation-induced deaminase (AID) which regulates two major steps in B-cell development, one of which is somatic hypermutation (SHM), the production of mutations in the variable regions of immunoglobulin genes. AID is induced in germinal center B cells and is highly expressed in germinal center B cell neoplasms. We have previously shown that in follicular lymphoma (FL), a germinal center B-cell-derived lymphoma, the immunoglobulin heavy chain gene contains more AID/SHM-generated acquired glycosylation sites in the variable region (IGHV) than IGH from marginal zone lymphoma. Diffuse large B cell lymphoma, the most common mature B cell neoplasm, is often separated into two groups by cell of origin, germinal center-derived and non-germinal center-derived. Two important markers for germinal center origin are the presence of an IGH-BCL2 translocation and CD10 expression. We hypothesize that like FL, germinal center-derived GCBs will have an increased predilection for harboring acquired IGHV glycosylation sites.

Design: The clonally rearranged IGH gene in 32 DLBCL specimens was amplified by PCR using IGHV family-specific with junctional IGHJ region primers and sequenced. The resulting sequences were analyzed using V-quest (IMGT.org) to determine percent identity to germline sequences, a measure of SHM. AID-generated glycosylation sites were determined by analysis of the predicted protein sequence.

Results: The 32 DLBCL cases were categorized by IGH-BCL2 translocation status (13 positive/17 negative/2 not classified), CD10 expression (25 positive/7 negative), and cell of origin by the Hans' algorithm (27 germinal-center B-cell type (GCB) and 5 activated B-cell type (ABC)). Twelve of thirteen IGH-BCL2-positive DLBCL cases had an acquired glycosylation site vs 8 of 17 IGH-BCL2-negative cases ($p=0.02$). Similarly, CD10-positive cases were more likely to have an acquired glycosylation site than CD10-negative (20/25 vs 1/7, $p=0.003$) as were GCB cases vs ABC (20/27 vs 1/5, $p=0.037$). There were no significant differences in SHM rate between groups regardless of categorization method.

Conclusions: Both the presence of an IGH-BCL2 translocation and CD10-positivity, markers of germinal center origin, are associated with an increased likelihood to have an acquired glycosylation site. These data suggest that acquired glycosylation sites in IGHV may contribute to the distinctive biology of t(14;18)-positive and CD10-positive DLBCL.

1470 Lack of MUM1 Expression Characterizes B-Lymphoblastic Leukemia/Lymphoma

Chad Hudson¹, Roula Katerji², Richard Burack³. ¹Rochester, NY, ²University of Rochester Medical Center, Rochester, NY, ³University of Rochester, Rochester, NY

Background: While the differential diagnosis of B-lymphoblastic leukemia/lymphoma (B-LBL) versus an aggressive mature B-cell neoplasm is usually not challenging, there are cases in which this is a diagnostic dilemma. In such cases, the immunophenotype of the large malignant blast-like cells is often "in between" the normal lymphoblast phenotype (CD10/CD19/CD34/TdT-positive, surface light chain-negative) and a mature B cell phenotype (CD19/surface light chain-positive) and there is a relative lack of additional immunostains that can be used to differentiate between the two entities. MUM1 (IRF4) is a transcription factor that in B cell lymphomas is often used as a marker of post-germinal center cell of origin. As the cell of origin in B-LBL is not a post-germinal B cell, MUM1 is an intriguing candidate as a marker that would favor against B-LBL in these challenging cases.

Design: MUM1 expression was determined by immunohistochemistry in 30 cases of B-LBL and 55 cases of aggressive B-cell neoplasms (48 cases of diffuse large B cell lymphoma, 6 cases of high-grade B cell lymphoma with MYC and BCL2 and/or BCL6 rearrangements).

Results: Twenty-nine of the 30 B-LBL specimens were negative for MUM1 expression with the one positive case showing dim, variable expression. On the other hand, 59% (33/54) of the aggressive mature B cell neoplasm cases were positive for MUM1 expression, indicating that as expected, B-LBL specimens were significantly less likely to be MUM1-positive ($p<0.001$). Further, when only adult cases of B-LBL were considered (the population in which this diagnostic dilemma is most relevant), MUM1 was uniformly negative (0/18).

Conclusions: These data indicate that the evaluation of MUM1 expression is useful when the differential diagnosis includes B-LBL as well as other aggressive B-cell neoplasms.

1471 Molecular Characterization of Primary Effusion Lymphoma

Alicia M Hunt¹, Nidhi Aggarwal². ¹University of Pittsburgh School of Medicine, Pittsburgh, PA, ²Pittsburgh, PA

Background: Primary effusion lymphoma (PEL) is an HHV-8 driven neoplasm that is primarily seen in patients with HIV/AIDS and other immunodeficiencies. HHV8 infection appears to be necessary but not sufficient for development of PEL. While the virus involved with the disease has been characterized by molecular methods, PEL has not been similarly characterized. In general, patients with PEL have a poor prognosis with a short survival. At our institution, we had a patient who survived 6 months without any apparent treatment which led us to investigate the molecular alterations in PEL by NGS that are necessary in addition to the HHV-8 virus that might impact the disease characteristics.

Design: Cases of PEL were identified in our archives from 2001 to present. Slides and blocks were obtained when available. 3 cases underwent NGS sequencing (Illumina NextSeq) for the exonic regions of 220 lymphoma-related genes. Variants were reported after comparison to the ExAC database of population SNPs, dbSNP, and COSMIC, and were run through in silico prediction software.

Results: Eight (8) cases of PEL from six (6) patients were identified in our archives from 2001 to present with cytogenetic characterization available in 1 case. 4/6 patients were positive for HIV. 2/6 patients were elderly (80 and 93 years). Material was available for sequencing in 3 cases. Patients ranged in age from 34 to 93 years old at the time of diagnosis. All cases passed QC parameters and were sequenced. Variants were found in all cases (see **Table**) however no recurrent gene mutation was identified among the 3 cases studies. Two cases had 1 variant each and 1 had 3 variants. 3 of the 5 variants were at 44-48% allelic frequency raising the possibility of germline variants; however, these variants are not present in the ExAC database or dbSNP and have not been previously reported. The other 2 variants (in MTOR and CSMD3) have never been described in the literature. In addition, 2 cases appeared to demonstrate copy number gain in a portion of chromosome 8q and 2 cases showed copy number gain of a portion of chromosome 1q. One case with copy number gain of chromosome 8q had FISH results with extra copies of the MYC gene, located at 8q24.21.

Specimen	Gene	Amino acid change	Allele Frequency	Classification
1	MTOR	p.E740Q	7%	VUS
2	CSMD3	p.E1125G	21%	VUS
	MALT1	p.E812K	44%	VUS
	DSEL	p.L810R	43%	VUS
3	TET2	p.P1617S	48%	VUS

Conclusions: In the small sample set sequenced in this study, no recurrent gene mutations were seen; however, more samples need to be sequenced before a conclusive statement can be made. There do appear to be some consistent copy number changes, consistent with FISH results.

1472 Caution is Required in the Use of Myc Immunohistochemical (IHC) Stain as Surrogate for MYC Gene Translocation or as a Prognostic Marker

Meghan M Hupp¹, Monna Marolt², Elizabeth Courville³, ¹University of Minnesota, Minneapolis, MN, ²Wyoming, MN, ³Minneapolis, MN

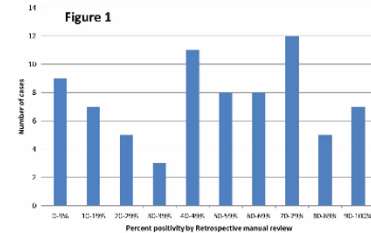
Background: With the 2016 WHO revisions, evaluation of MYC status has been solidified as a part of the workup of large B cell lymphomas. In addition, myc protein overexpression may be a potential prognostic indicator in the context of "double-expressor lymphomas", with both MYC and BCL2 protein overexpression as defined by IHC. The incorporation of myc IHC stain has become common in routine hematopathology practice, including at our institution. After the standard validation process for new IHC stains, we began offering c-myc IHC stain with a recommended cut-off ($\geq 40\%$ as positive).

Design: This retrospective study included all aggressive B cell lymphoma cases with a MYC stain performed as part of routine clinical care from 3/2015 to 12/2016. The original pathologist interpretation (positive, negative, or equivocal) was recorded. In addition, up to 10 areas (1mmx1mm each) on the IHC slide were selected from the most viable, intact, and neoplasm-rich areas on H&E. The average percent positivity from these areas was determined retrospectively by a hematopathologist. The myc IHC stain was not used as a triaging tool for FISH analysis during this time period.

Results: Our cohort consisted of 87 cases [72 (82.8%) diffuse large B cell lymphoma, 12 (13.8%) monomorphic PTL, and 3 (3.4%) Burkitt lymphoma]. Myc IHC was interpreted as positive in 39 (45%), negative in 39, equivocal in 8 (9%), and not given in 1 (1%). 11 cases were deemed insufficient material to evaluate by retrospective method. The distribution of % myc positivity by retrospective review is shown in Fig 1. Of the fourteen cases with a MYC translocation by FISH analysis, the

median positivity by retrospective review was 88% (range 0-100%). Sensitivity and specificities in Table 1.

Table 1	Sensitivity	Specificity
Original IHC interpretation*, all cases	0.93	0.65
Original IHC interpretation*, core biopsies only	0.80	0.69
Original IHC interpretation*, excisional biopsies only	1.0	0.63
Original IHC interpretation*, germinal center subtype only	0.80	0.70
Original IHC interpretation*, non-germinal center subtype only	1.0	0.57
Retrospective review*, all cases	0.86	0.36
Using a cut-off of $\geq 40\%$ as positive		



Conclusions: Nearly 1/3rd of our cohort had a myc positivity surrounding the cut-off of 40% which augments bias in interpretation. Indeed, when interpreted in a more systematic fashion and blinded to the morphology and results of additional IHC in the setting of retrospective manual review, the specificity drastically decreased from the original pathologist's interpretation, suggesting that, in a clinical setting, our pathologists used other clues to predict a MYC gene translocation, thus influencing interpretation of the myc IHC stain. Caution is required in using the myc IHC stain as a triaging tool for the MYC gene translocation or potential prognostic marker, particularly using a 40% cut-off in isolation.

1473 Isolated TP53 Mutations Portend Worse Prognosis in MDS and AML Compared to TP53 Mutations with Concurrent Myeloid-Associated Mutations

Mohammad Hussaini¹, Mohammad Abuel-Haija², Eric Padron³, Sallman David⁴, Jinming Song. ¹Moffitt Cancer Center, Tampa, Florida, ²Lafayette, IN, ³H. Lee Moffitt Cancer Center, ⁴Moffitt Cancer Center

Background: TP53 mutations have established adverse prognostic impact in MDS and AML even after adjusting for other recognized risk factors such as age and cytogenetics. A large prior sequencing study has shown that leukemia-free survival decreases with the number of driver mutations identified. We hypothesize, however, that the dismal prognosis of founder TP53 mutations may abrogate the need for and/or impact of additional myeloid driver mutations.

Design: IRB approval was obtained. Institutional databases were queried for next-generation sequencing cases of MDS and AML with TP53 mutations. Clinical and laboratory data were extracted from chart review and internal data warehouse. Unpaired t-test was performed for statistical analysis.

Results: 150 patients with TP53-mutated MDS or AML were identified. 96 had TP53 with concurrent mutation in myeloid associated genes (conTP53) and 54 had mutations in TP53 only (isoTP53). There were 27 low-grade MDS (19 conTP53, 8 isoTP53), 38 high-grade MDS (21 conTP53, 17 isoTP53), and 85 AML (56 conTP53, 29 isoTP53). Average age in conTP53 was 68 years (41 F, 55 M) and 67 years in isoTP53 (19 F, 35 M). Average number of mutations was 3.2/case (conTP53) vs 1.2/case (isoTP53). Average number of TP53 mutations/case was similar (1.3/case) in both groups as was average TP53 variant allele frequency (VAF) (34.4% and 37.7%).

Overall survival (OS) was 31.6 months for conTP53 vs. 16.8 months for isoTP53 (95% CI= -2.55 to 32.02; p=0.0941). In low grade MDS, OS was 58.5 months for conTP53 vs. 21.3 months for isoTP53 (p= 0.27). In high grade MDS, OS was 29.7 months for conTP53 vs. 23.7 months for isoTP53 (p= 0.71). In AML, OS was 23.1 months for conTP53 vs. 11.5 months for isoTP53 (p= 0.21). Thrombocytopenia and leukopenia were more pronounced in conTP53 (84K/L and 8.1 K/L, respectively) vs. isoTP53 (58K/L and 4.0 K/L, respectively); however the difference was not statistically significant.

Conclusions: TP53 mutations occur more commonly with additional mutations than as isolated TP53 mutations. Number of TP53 mutations per case and VAFs are similar in conTP53 and isoTP53. In both MDS and AML, patients with isoTP53 have shorter OS, although statistical significance was not reached. Thus, isoTP53 may represent

an aggressive subgroup of MDS and AML where the lack of genomic surveillance allows for rapid progression without enough time and/or lack of selective pressure to acquire additional 'genetic' hits. Validation in larger cohort studies is needed.

1474 Immunophenotypic Characteristics Of Malignant Lymphomas in Zaria Nigeria: A Fifteen Year Retrospective Analysis

Yawale Iliyasu¹, Leona Ayers², Abdulmumini H Rafindad³, Abdullah A Abba³. ¹Ahmadu Bello University, Zaria, Kaduna, ²Ohio State University, Columbus, OH, ³Ahmadu Bello University Zaria Nigeria

Background: The immunophenotypic characteristics of malignant lymphomas in Zaria, Nigeria have not been known for decades. AIDS-related lymphomas have not been characterized two decades after the HIV-AIDS pandemic. All these are due to the non-availability of immunohistochemistry. The establishment of the Sub-Saharan Africa Lymphoma Consortium, an AIDS and Cancer Specimen Resource of the NCI provided a unique opportunity to characterize all malignant lymphomas in Zaria diagnosed by morphology alone over a fifteen year period.

Design: Ninety (n=90) paraffin blocks were used to construct a tissue microarray (TMA) and the tissue sections were stained with H & E for morphology. TMA sections were stained using 30 monoclonal antibodies for common lymphoma antigens and 11 antibodies to exclude other disease processes. The tumors were typed using the WHO Classification of Tumors of Hematopoietic and Lymphoid Tissue of 2016.

Results: Ninety cases were analyzed with 74 malignant lymphomas and 16 other disease processes. The youngest patient was 3 years and the oldest 81 years with the mean age of 39 years. The jaw was the commonest anatomical site (20%). Burkitt's (32.2%), DLBCL (17.7%), Hodgkin's (12.2%), and Follicular lymphoma (FL) were the commonest lymphomas seen. 92% of the tumors were EBV positive.

Conclusions: Burkitt's, DLBCL, HL and FL are the commonest lymphomas seen in our environment. AIDS-related lymphomas (apart from Burkitt's which is endemic in Zaria) like plasmablastic lymphomas and HHV8 lymphoproliferative disorders were not found. Metastatic carcinomas, undifferentiated sarcomas and neuroblastoma were difficult to diagnose without immunohistochemistry.

1475 EBV+ Diffuse Large B-Cell Lymphoma, NOS Shows Over-Expression of PD-L1/PD-1

Geetha Jagannathan¹, Jerald Gong², Guldeep Uppa³. ¹Philadelphia, PA, ²Thomas Jefferson Medical College, Philadelphia, PA, ³Glen Mills, PA

Background: The spectrum of EBV+ diffuse large B-cell lymphoma (DLBCL) has broadened with the inclusion of younger patients in WHO 2016 classification. Programmed cell death ligand-1 (PD-L1) and Programmed cell death-1 (PD-1) expression have been well reported in T-cell lymphomas and certain subgroups of DLBCL. Targeted blockade of the PD-1/ PD-L1 pathway has shown promising outcomes in clinical trials for multiple tumor types. However, PD-L1 expression in EBV+ DLBCL has not been well studied.

Design: A retrospective analysis of 12 cases of EBV+ DLBCL and 10 cases of EBV- DLBCL was performed (2011 to 2016). Immunohistochemical staining for PD-1 (clone NAT105, Ventana) and PD-L1 (clone SP142, Ventana) was performed on 10 cases in each group. Two pathologists evaluated PD-1 in tumor cells (TCs) and tumor-infiltrating lymphocytes (TILs), and PD-L1 in TCs, TILs and tumor associated macrophages (TAMs). Staining of $\geq 5\%$ of the TCs was considered positive for PD-L1 and PD-1. A cut-off of $\geq 20\%$ was used for tumor microenvironment. Clinical data were retrieved from the electronic databases.

Results: The median age for EBV+ DLBCL, NOS was 65.5 years (range 19-86) and in the control group was 69.5 years (range 50-84). Both the groups had a slight male predominance. The TCs in 70% (7/10) of the EBV+ DLBCL, NOS cases showed PD-L1 expression with most showing overexpression in $\geq 30\%$ TCs (5/7). All EBV+ cases with PD-L1+ TCs except 1 showed PD-1+ TILs (6/7). PD-L1 expression in TCs was noted only in two cases of EBV- DLBCL. TILs in EBV- DLBCL showed positivity for PD-1 in 70% (7/10) cases. TAMs in EBV- DLBCL showed PD-L1 expression in 80% (8/10). EBV+ DLBCL cases that expressed PD-L1 were frequently non-germinal in origin (60%, 5/7).

	EBV+ DLBCL			EBV- DLBCL		
	Tumor cells	Tumor Infiltrating lymphocytes	Tumor-associated macrophages	Tumor cells	Tumor Infiltrating lymphocytes	Tumor-associated macrophages
PD-L1	7/10	0/10	8/10	2/10	2/10	8/10
PD-1	1/10	8/10	NA*	1/10	7/10	NA*

* Not assessed

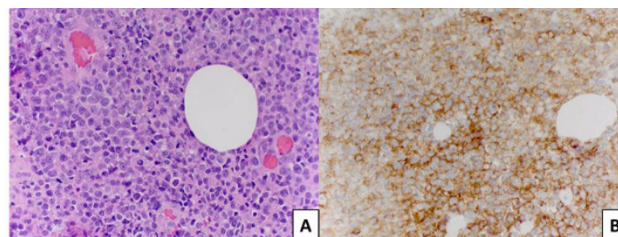


Figure 1: A. H&E of an EBV+DLBCL, NOS; B. Tumor cells staining with PD-L1

Conclusions: Our study shows that PD-L1 and PD-1 are frequently and preferentially expressed in lymphoma cells and TILs, respectively in EBV+ DLBCL, NOS. This finding suggests the presence of T-cell receptor-mediated immune inhibition between lymphoma cells and TILs. Upregulation of PD-1/PD-L1 pathway may serve as the target of therapeutic blockade in the future treatment of these patients.

1476 MHC Class II Transactivator (CIITA) Abnormalities Are Frequent in B-cell Lineage Lymphomas and Are Associated With Loss of MHC Class II (MHCII) Expression

Fatima Zahra Jelloul¹, Janine D Pichardo¹, Pallavi Khattar¹, Anuradha Ananthamurthy², Mamta Rao¹, Ruth Areeyqur¹, Achim Jungbluth¹, Lu Wang¹, Yanming Zhang¹, Ahmet Dogan¹. ¹Memorial Sloan Kettering Cancer Center, New York, NY, ²Bangalore

Background: CIITA is the master regulator of MHCII antigen presenting pathway. CIITA mutations have been reported in primary mediastinal B-cell lymphoma (PMBL) and Classical Hodgkin lymphoma (CHL) and it is believed that this leads to reduction of MHCII surface expression, contributing to immune escape and adverse outcomes. However so far CIITA protein expression has not been studied in normal and neoplastic lymphoid cells. Here we report the frequency of CIITA mutations and expression in B-cell lymphomas and investigate the correlation of CIITA abnormalities with MHCII expression.

Design: CIITA mutations and fusions were investigated in 186 cases of B-cell lymphoma as part of a targeted hybridization capture NGS assay. In addition, tissue samples from 10 normal lymphoid tissues and 264 B-cell lymphoma cases including 88 CHL, 44 diffuse large B cell lymphoma (DLBCL), 22 PMBL, 32 follicular lymphoma (FL), 28 marginal zone lymphoma (MZL), 24 mantle cell lymphoma (MCL) and 26 small lymphocytic lymphoma (SLL) were evaluated for expression of CIITA (Clone 7-1H) and MHCII (Clone LG-II-612.14) by immunohistochemistry (IHC). Expression was scored as positive if $>20\%$ of tumor cells expressed of CIITA and/or MHCII.

Results: NGS assay identified six B-cell lymphomas with deleterious mutation/fusions of CIITA (3 PMBL, 1 DLBCL, 2 MZL). Fusions were confirmed by FISH assay. By IHC, CIITA and MHCII were uniformly expressed by normal B-cell subsets. Expression of CIITA and MHCII in B-cell malignancies is shown in Table 1. Overall, CIITA and MHCII protein expression were concordant in 218/264 cases (82.6%). Among the discordant cases, 27/46 (58.7%) had loss of MHCII expression with retained expression of CIITA and 19/46 (41.3%) had loss of CIITA with retained expression of MHCII. Among different subsets of lymphomas, loss of both CIITA and MHCII expression was more commonly seen in DLBCL (11/44, 25%), MCL (6/24, 25%), CHL (16/88, 18.2%), PMBL (4/22, 18.2%) and MZL (4/28, 14.3%) than in FL (2/32, 6.3%) and CLL/SLL (1/26, 3.8%). Deleterious CIITA mutations correlated with loss of CIITA and MHCII expression.

Table 1: CIITA and MHCII expression by IHC in normal lymphoid tissue and different subsets of B-cell lymphomas

	CIITA+/MHCII+	CIITA-/MHCII-	CIITA+/MHCII-	CIITA-/MHCII+
CHL (88)	54 (61.4%)	16 (18.2%)	6 (6.8%)	12 (13.6%)
DLBCL (44)	25 (56.8%)	11 (25%)	8 (18.2%)	0
PMBL (22)	16 (72.7%)	4 (18.2%)	2 (9.1%)	0
MCL (24)	12 (50%)	6 (25%)	2 (8.3%)	4 (16.7%)
MZL (28)	16 (57.1%)	4 (14.3%)	7 (25%)	1 (3.6%)
FL (32)	29 (90.6%)	2 (6.3%)	1 (3.1%)	0
CLL/SLL (26)	22 (84.6%)	1 (3.8%)	1 (3.8%)	2 (7.7%)
Normal B cell subsets (10)	10/10 (100%)	0	0	0

Conclusions: Our study shows that loss of CIITA expression by mutations and other mechanism is frequent in B-cell lineage lymphomas and is associated with loss MHCII expression. These results contribute to growing evidence implicating immune escape as a dominant oncogenic mechanism across B cell lymphomas, with potential implications for immune mediated therapies.

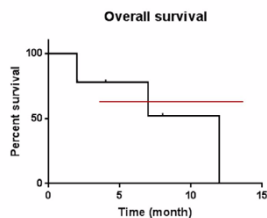
1477 Extramedullary Plasmablastic Transformation of Plasma Cell Myeloma: Clinicopathologic Study of 10 cases

Fatima Zahra Jelloul¹, Tapan Bhavsar², Janine D Pichardo¹, Mariko Yabe¹, Mamta Rao¹, Yanming Zhang¹, Ahmet Dogan¹, Wenbin Xiao¹
¹Memorial Sloan Kettering Cancer Center, New York, NY, ²Wayne State University Detroit Receiving Hospital

Background: Plasmablastic transformation occasionally occurs in patients with plasma cell myeloma (PCM) and is associated with aggressive behavior. Discordance in morphology with typical mature plasma cells in bone marrow and extramedullary plasmablastic transformation has only been rarely reported. Here we summarize the clinicopathologic features of 10 such cases.

Design: We searched pathology archives at MSKCC from 2000 to 2017 and identified 17 cases of PCM with extramedullary plasmablastic transformation. Only 8 cases had concurrent bone marrow biopsy (BMB) for review and therefore were included in this study. 2 additional cases were submitted from Detroit Receiving Hospital. Clinicopathological features were reviewed.

Results: The study group included 7 males and 3 females with a median age of 64 years (range 48-76). All patients presented with single or multiple extramedullary masses. 7 patients had prior history of PCM and the other 3 fulfilled PCM criteria at presentation. Extramedullary tissue biopsies from all cases showed cells with plasmablastic morphology as the predominant cell type, while concurrent BMB showed small mature plasma cells as the only cell type. The neoplastic cells from tissue and BMB shared identical light chain restriction in all cases and in 1 case where IGH gene rearrangement was performed, identical rearrangement pattern. EBER ISH was negative in all cases. In tissue biopsies, CyclinD1 was positive in 4/5 cases, CD56 was positive in 7/8 cases, and CMYC was positive in 5/6 cases. Ki-67 showed high proliferation rate (median: 80%, range: 50%-90%). FISH studies showed no CMYC rearrangements in 3 examined cases and 1 had extra-copies of CMYC. In addition, 2 cases showed similar findings in tissue and BMB including CDKN2C deletion in 1 case and FGFR3-IGH fusion in the other. All patients were treated by combinations of steroids, bortezomib and thalidomide or lenalidomide with addition of EPOCH in 3 patients and PACE in 2 others. After a median follow up of 4 months (range 2-12 months), 3 patients had initial good response and are now evaluated for autologous stem cell transplant, 2 had persistent or recurrent disease and 4 patients died (median overall survival: 12 months).



Conclusions: Plasmablastic transformation of PCM is associated with CMYC upregulation but absence of CMYC rearrangements. Despite overall remarkable improvement in the survival of PCM patients in recent years, this subgroup remains refractory to commonly used therapies and has a very poor prognosis.

1478 Lineage switch in adult acute leukemia heralds refractoriness to treatment and a dismal clinical outcome: report of 4 cases with cytogenetic abnormalities other than MLL rearrangement

Rachel Jug¹, Catherine Luedke², Lianhe Yang³, Xin Liu⁴, Chad McCall⁵, Anand Lagoo², Endi Wang⁵. ¹Duke Health, Durham, NC, ²Duke University Medical Center, Durham, NC, ³Duke Health, ⁴Duke University Medical Center, Cary, NC, ⁵Duke University Medical Center

Background: Lineage switch occurs in rare cases of acute leukemia (AL). The literature is limited to small series of pediatric AL, particularly with MLL abnormalities.

Design: We identified and retrospectively analyzed 4 cases of AL undergoing lineage switch post chemotherapy.

Results: All 4 patients were male with a median age of 50 years (range 23-69) at diagnosis. Cases 2-4 presented with leukocytosis and anemia/thrombocytopenia and case 1 presented with pancytopenia. Cases 1 and 2 presented as B-lymphoblastic leukemia (B-ALL) with complex cytogenetic abnormalities with subclone heterogeneity. A lymph node biopsy in case 3 revealed T-lymphoblastic lymphoma (T-ALL) exhibiting -7, add(9)(q33). Case 4 exhibited a normal karyotype at initial diagnosis of acute myeloid leukemia without maturation (AML-M1). Lineage switch occurred at a median interval of 274 days (range 16-334 days) post chemotherapy initiation. Case 1 underwent lineage switch to acute monocytic leukemia (AML M5b) at the first

relapse, was treated with partial response, and subsequently relapsed as B-ALL. Case 2 converted to a pure erythroid leukemia (AML M6b). Case 3 switched to AML-M5b. Case 4 underwent a switch during induction chemotherapy from AML-M1 to acute megakaryoblastic leukemia (AML-M7). At the time of lineage switch, cases 1 and 2 demonstrated complex cytogenetic abnormalities with persistent stem line changes and additional subclone heterogeneity. Case 3 retained the monosomy 7 and a novel tetraploid clone was identified in case 4, suggesting clonal evolution/subclone emergence. Unfortunately, despite treatments tailored to the switched leukemic lineages, all patients died of disease progression shortly after lineage switch (mean 27 days, range 4-59).

Conclusions: Lineage switch can occur between B-ALL and AML, or within AML subtypes. Conversion occurs during chemotherapeutic induction or at AL relapse. Cytogenetic studies in these adult patients demonstrate complex abnormalities with subclone heterogeneity/evolution, suggestive of genomic instability, rather than MLL rearrangements, as seen in pediatric cases. Neoplastic transformation likely occurs at the level of pluripotent stem cell and genomic instability results in formation of heterogeneous subclones with various differentiation potentials, possibly selected for by chemotherapy. Lineage switch in AL portends a dismal clinical outcome.

1479 In-Situ Protein Expression Analysis of B-Cell Maturation Antigen (BCMA)

Achim Jungbluth¹, Ahmet Dogan¹, Denise Frosina¹, Miriam Fayad¹, Eric Smith¹. ¹Memorial Sloan Kettering Cancer Center, New York, NY

Background: BCMA belongs to the TNF-receptor superfamily, encoded by TNFRSF17 acting as a cell surface receptor for BAFF. BCMA is preferentially expressed in mature B-cells. Based on its expression pattern, BCMA is considered a valuable target for immunotherapy of plasma cell myeloma (PCM), in particular CART-cell based approaches. However, BCMA expression data is based on FACS studies and little is known about the in-situ tissue expression. Due to the lack of expression data and a request for eligibility testing for a CART clinical trial, we developed an IHC protocol for BCMA analysis in archival material.

Design: Commercially available monoclonal antibodies (mAbs) as well as antibody preparations of the hybridoma clones giving rise for the CAR-T cell variable region were tested. Specificity was analyzed in cell lines of BCMA-transfected and un-transfected 3T3 cells, on in-house developed carrier-based multi-tissue blocks of normal and tumor tissues as well as on PCM specimens.

Results: 10 monoclonal antibodies (mAbs) to BCMA were tested including the hybridomas giving rise to the transfected chimeric antigen receptor of the CART-cells employed in the clinical trial. Two commercial mAbs, clone D-6 (Santa Cruz) and G-4 (Santa Cruz) showed excellent IHC staining in initial tests. Eventually, mAb D-6 displayed superior staining and was chosen for further analyses. D-6 produced excellent staining BCMA-positive cell lines and was negative in BCMA-negative cells. There was consistent and robust staining of plasma cells in all 30 PCM specimens including decalcified bone marrow biopsies. In normal tissues, staining was present in lymphoid cells consistent with mature B-cells in various locations such as lymphoid tissues and lamina propria of the GI tract. No other cell or tissue population was positive for mAb D-6 except occasional membranous staining of gastric crypt epithelia. Various solid tumors (5 cases each) were also tested: colorectal ca, renal cell ca., invasive ductal breast ca., melanoma, serous ovarian ca., seminoma, hepatocellular ca. All were D-6 negative

Conclusions: Precision medicine generates a steep increase in therapies resulting in a higher demand for accurate accompanying tests. Based on the request for an anti-BCMA CAR-T cell trial, we developed a robust IHC protocol for the detection of BCMA based on commercially available mAb D-6., which can now be employed in surgical pathology and/or in a clinical trial setting.

1480 Myelodysplastic Syndrome with SRSF2/U2AF1 Mutations Shows Ring Sideroblastic Phenotype Similar To SF3B1 Mutation but has Adverse Clinicopathologic Features

Rashmi Kanagal-Shamanna¹, Juliana E Hidalgo-Lopez², Keyur Pate³, Rajyalakshmi Luthra², Mark Routbort⁴, Andres E Quesada², Chong Zhao², John Lee², L. Jeffrey Medeiros², Carlos Bueso-Ramos². ¹The University of Texas MD Anderson Cancer Center, Bellaire, TX, ²The University of Texas MD Anderson Cancer Center, Houston, TX, ³The University of Texas MD Anderson Cancer Center, Sugar Land, TX, ⁴Bellaire, TX

Background: Frequent splicing factor (SF) genes in MDS include SF3B1, SRSF2 and U2AF1. MDS with SF3B1 (MDS-SF3B1) is a distinct entity associated with ring sideroblast (RS) phenotype and low-risk of AML transformation. Hence, 2016 WHO has incorporated SF3B1 mutation as a criterion for classification of MDS

with 5-15% RS into MDS-RS-SLD/MLD to generate homogeneous cohorts. In contrast to MDS-SF3B1, MDS-SRSF2/U2AF1 has a high-risk of AML transformation, but data on phenotypic correlations pertinent to 2016 WHO are limited. Herein, we compared the clinicopathologic features of MDS with SF3B1, SRSF2 and U2AF1 mutations.

Design: We identified all cases of MDS with SF3B1/SRSF2/U2AF1 mutations from our NGS database. For comparison, we used 62 MDS wild-type for 3 SF genes (MDS-WT). We reviewed BM morphologic findings and retrieved pertinent clinical data.

Results: We identified 108 *de novo* MDS with SF mutations with a median VAF of 42.3% [53 SF3B1, 26 SRSF2; 26 U2AF1]. We excluded 2 cases of MDS-SF3B1 with del(5q). Majority of MDS-SF3B1 presented with <5% blasts (88%), compared with MDS-SRSF2 (61%) and MDS-U2AF1 (65%). Of these, using WHO cytopenia(s) criteria, 44 (90%) MDS-SF3B1 had unicytopenia and 5 had pancytopenia. In contrast, 10 (53%, p=0.002) MDS-SRSF2 and 9 (47%, p=0.004) MDS-U2AF1 had unicytopenia. By IPSS, 43/48 MDS-SF3B1 were low-risk compared with 10/19 MDS-SRSF2 (p=0.002) and 9/19 MDS-U2AF1 (p=0.005). Upon review of initial diagnostic bone marrows, all MDS-SF3B1 showed erythroid dysplasia; granulocytic (17/21) and megakaryocytic (13/21) dysplasia(s) were less common. In contrast, all MDS-SRSF2/U2AF1 showed trilineage dysplasia. 2016 WHO subtypes are shown in table 1; MDS-SF3B1 had a higher frequency of RS-phenotype [MDS-RS-SLD/MLD] compared with MDS-SRSF2 (p=0.0003) or MDS-U2AF1 (p=0.0001). Cases with RS>5% included 42 MDS-SF3B1, 10 MDS-SRSF2, 4 MDS-U2AF1 and 25 MDS-WT. RS>=15% included 36 MDS-SF3B1, 9 SRSF2, 3 U2AF1 and 10 MDS-WT. ASXL1 mutation (median VAF 44%) was less frequent in MDS-SF3B1 compared with MDS-SRSF2 (p=0.004) or U2AF1 (p0.02); none of other genes showed significant differences.

Conclusions: Compared with MDS-SF3B1, MDS-SRSF2/U2AF1 shows frequent adverse features (cytopenias in >1 lineage, intermediate-1 risk IPSS or higher, trilineage dysplasia and concurrent ASXL1 mutation). Identification of RS phenotype in MDS-SRSF2/U2AF1 cases suggests the need for SF3B1 mutation analysis even in MDS cases >=15% RS to further refine 2016 WHO MDS-RS-SLD/MLD categories.

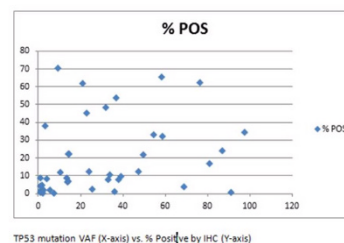
1481 P53 immunohistochemistry does not correlate with mutation status and should not be used as a screening tool for TP53 mutations in myeloid malignancies

Kristin Karner¹, Sheryl R Tripp², Jessica Kohan³, Mohamed Salama³.
¹University of Utah/ARUP, Salt Lake City, UT, ²ARUP Laboratories, Salt Lake City, UT, ³Salt Lake City, UT

Background: TP53 mutations are seen in a subset of myeloid malignancies including MDS and AML and are associated with a worse prognosis. Given the higher cost of NGS in investigating TP53 molecular mutations, some groups have proposed using P53 immunohistochemical staining as a cost-effective screening tool.

Design: Our database was searched for myeloid malignancies including MDS, CMML and AML that had TP53 mutations identified by NGS. Of the 65 cases that were identified, 41 cases had adequate tissue for P53 immunohistochemical evaluation using standard protocol. An additional 7 control cases were identified that were myeloid malignancies that did not have a TP53 mutation. Of these, 4 cases had adequate tissue for P53 IHC. P53 stained core biopsy slides were scanned on the Leica Aperio AT2 scanner at 20X. The whole slide images were analyzed using Indica Labs' HALO CytoNuclear algorithm modified to detect and classify cells/nuclei. The type of TP53 mutation and variant allele frequency were recorded from the NGS mutation report and correlated with percent positivity of P53 immunohistochemical staining.

Results: While none of the negative controls showed positive P53 IHC staining (all had less than 7% moderate to strong positivity), only 7 of the 41 cases with TP53 mutations showed positivity, defined as moderate or strong staining totaling greater than 30%. Of these 7 cases, there was no significant correlation with VAF score and no association of particular mutations with positivity. There was also no association of TP53 mutation with any particular co-mutation that would result in positivity (as some other mutations may also alter P53 expression downstream). VAF scores among all TP53 mutated cases showed no correlation with total, weak, moderate or strong positivity by IHC using Pearson's correlation coefficient (r=0.29, 0.30, 0.30 and 0.25 respectively).



TP53 mutation VAF (X-axis) vs. % Positive by IHC (Y-axis)

Conclusions: The majority of cases of myeloid malignancy with TP53 mutations still show negativity by immunohistochemical staining methods and there was no significant correlation of TP53 mutation with IHC expression, nor correlation of VAF percentage with IHC expression, as some previous literature had suggested. These results indicate that P53 IHC staining should not be used as a screening tool for TP53 mutations as it would miss many cases. In addition, more work needs to be done regarding the "wild type" pattern of P53 expression. While it is possible that positivity might suggest a TP53 mutation, negativity would certainly not exclude it.

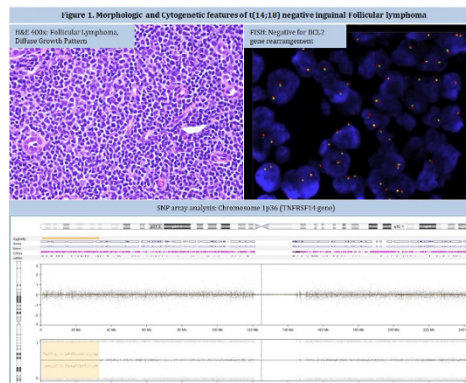
1482 t(14;18) Negative Inguinal Follicular Lymphoma Is Characterized By Genetic Abnormalities of 1p36/TNFRSF14 and 16p/CREBBP Regions

Pallavi Khattar¹, Janine D Pichardo¹, Fatima Zahra Jelloul¹, Cimera Robert¹, Ruth Areeyqur¹, Mamta Rao¹, Yanming Zhang¹, Maria Arcila², Lu Wang³, Ahmet Dogan¹. ¹Memorial Sloan Kettering Cancer Center, New York, NY, ²New York, NY, ³St Jude Children's Research Hospital, Memphis, TN

Background: A distinctive subtype of t(14;18) negative nodal follicular lymphoma (FL) characterized by deletions in the chromosomal region 1p36 has been recently described (Katzenberger Blood 2009). These tumors frequently present as localized large masses, show a predominantly diffuse growth pattern, lack BCL2 protein expression but express CD23 suggesting a unique biology. A high frequency of TNFRSF14 mutations was recently reported in this subtype. In this study, we investigated genetic characteristics of these tumors using comprehensive genomic profiling tools including SNP array and NGS analysis.

Design: We identified cases of stage 1-2 FL presenting as isolated inguinal mass with BCL2 weak to negative expression and positive CD23 expression. The clinical features were identified by the chart review. The histopathological features, immunophenotype and molecular data were reviewed. Formalin fixed paraffin-embedded FL tissue samples were analyzed by BCL2 rearrangement FISH assay (Abbott molecular). Nineteen t(14;18) negative cases with morphologic and immunophenotypic features that are suggestive of FL with 1p36 deletion were analyzed by SNP array (OncoScan Affymetrix) and targeted NGS platform comprising 400 genes.

Results: Abnormalities at 1p36 were observed in 16/19 cases, 12 of which presented as copy-neutral loss of heterozygosity (CN-LOH) and 4 showed deletion of 1p36. TNFRSF14 gene (1p36.32) was always involved. One case showed focal homozygous deletion of TNFRSF14 gene. In addition, the other most common recurrent abnormalities detected were whole arm or large region of CN-LOH of 16p (common affected region: 16p13.1-pter), all including the CREBBP gene in 11/19 cases. (Figure1&2). At the time of submission mutation analysis was available in 2 cases; both showed deleterious mutations in TNFRSF14 (2/2) and CREBBP (1/2) gene



Case #	Sex	Grade	Histologic features	Immunohistochemistry				SNP Chromosome 16p	
				BCL2	CD10	CD23	FISH BCL2	SNP Chromosome 16p	SNP Chromosome 16p
1	M	1-2	Positive	Positive	Positive	Positive	None	CE-1001 (p11.2) 1.0	CE-1001 (p11.2) 1.0
2	F	1-2	Positive	Positive	Positive	Positive	None	CE-1001 (p11.2) 1.0	CE-1001 (p11.2) 1.0
3	M	1-2	Positive	Positive	Positive	Positive	None	CE-1001 (p11.2) 1.0	CE-1001 (p11.2) 1.0
4	M	1-2	Positive	Positive	Positive	Positive	None	CE-1001 (p11.2) 1.0	CE-1001 (p11.2) 1.0
5	M	1-2	Positive	Positive	Positive	Positive	None	CE-1001 (p11.2) 1.0	CE-1001 (p11.2) 1.0
6	M	1-2	Positive	Positive	Positive	Positive	None	CE-1001 (p11.2) 1.0	CE-1001 (p11.2) 1.0
7	M	1-2	Positive	Positive	Positive	Positive	None	CE-1001 (p11.2) 1.0	CE-1001 (p11.2) 1.0
8	M	1-2	Positive	Positive	Positive	Positive	None	CE-1001 (p11.2) 1.0	CE-1001 (p11.2) 1.0
9	M	1-2	Positive	Positive	Positive	Positive	None	CE-1001 (p11.2) 1.0	CE-1001 (p11.2) 1.0
10	M	1-2	Positive	Positive	Positive	Positive	None	CE-1001 (p11.2) 1.0	CE-1001 (p11.2) 1.0
11	M	1-2	Positive	Positive	Positive	Positive	None	CE-1001 (p11.2) 1.0	CE-1001 (p11.2) 1.0
12	M	1-2	Positive	Positive	Positive	Positive	None	CE-1001 (p11.2) 1.0	CE-1001 (p11.2) 1.0
13	M	1-2	Positive	Positive	Positive	Positive	None	CE-1001 (p11.2) 1.0	CE-1001 (p11.2) 1.0
14	M	1-2	Positive	Positive	Positive	Positive	None	CE-1001 (p11.2) 1.0	CE-1001 (p11.2) 1.0
15	M	1-2	Positive	Positive	Positive	Positive	None	CE-1001 (p11.2) 1.0	CE-1001 (p11.2) 1.0
16	M	1-2	Positive	Positive	Positive	Positive	None	CE-1001 (p11.2) 1.0	CE-1001 (p11.2) 1.0
17	M	1-2	Positive	Positive	Positive	Positive	None	CE-1001 (p11.2) 1.0	CE-1001 (p11.2) 1.0
18	M	1-2	Positive	Positive	Positive	Positive	None	CE-1001 (p11.2) 1.0	CE-1001 (p11.2) 1.0
19	M	1-2	Positive	Positive	Positive	Positive	None	CE-1001 (p11.2) 1.0	CE-1001 (p11.2) 1.0
20	M	1-2	Positive	Positive	Positive	Positive	None	CE-1001 (p11.2) 1.0	CE-1001 (p11.2) 1.0
21	M	1-2	Positive	Positive	Positive	Positive	None	CE-1001 (p11.2) 1.0	CE-1001 (p11.2) 1.0
22	M	1-2	Positive	Positive	Positive	Positive	None	CE-1001 (p11.2) 1.0	CE-1001 (p11.2) 1.0
23	M	1-2	Positive	Positive	Positive	Positive	None	CE-1001 (p11.2) 1.0	CE-1001 (p11.2) 1.0
24	M	1-2	Positive	Positive	Positive	Positive	None	CE-1001 (p11.2) 1.0	CE-1001 (p11.2) 1.0
25	M	1-2	Positive	Positive	Positive	Positive	None	CE-1001 (p11.2) 1.0	CE-1001 (p11.2) 1.0
26	M	1-2	Positive	Positive	Positive	Positive	None	CE-1001 (p11.2) 1.0	CE-1001 (p11.2) 1.0
27	M	1-2	Positive	Positive	Positive	Positive	None	CE-1001 (p11.2) 1.0	CE-1001 (p11.2) 1.0
28	M	1-2	Positive	Positive	Positive	Positive	None	CE-1001 (p11.2) 1.0	CE-1001 (p11.2) 1.0
29	M	1-2	Positive	Positive	Positive	Positive	None	CE-1001 (p11.2) 1.0	CE-1001 (p11.2) 1.0
30	M	1-2	Positive	Positive	Positive	Positive	None	CE-1001 (p11.2) 1.0	CE-1001 (p11.2) 1.0
31	M	1-2	Positive	Positive	Positive	Positive	None	CE-1001 (p11.2) 1.0	CE-1001 (p11.2) 1.0
32	M	1-2	Positive	Positive	Positive	Positive	None	CE-1001 (p11.2) 1.0	CE-1001 (p11.2) 1.0
33	M	1-2	Positive	Positive	Positive	Positive	None	CE-1001 (p11.2) 1.0	CE-1001 (p11.2) 1.0
34	M	1-2	Positive	Positive	Positive	Positive	None	CE-1001 (p11.2) 1.0	CE-1001 (p11.2) 1.0
35	M	1-2	Positive	Positive	Positive	Positive	None	CE-1001 (p11.2) 1.0	CE-1001 (p11.2) 1.0
36	M	1-2	Positive	Positive	Positive	Positive	None	CE-1001 (p11.2) 1.0	CE-1001 (p11.2) 1.0
37	M	1-2	Positive	Positive	Positive	Positive	None	CE-1001 (p11.2) 1.0	CE-1001 (p11.2) 1.0
38	M	1-2	Positive	Positive	Positive	Positive	None	CE-1001 (p11.2) 1.0	CE-1001 (p11.2) 1.0
39	M	1-2	Positive	Positive	Positive	Positive	None	CE-1001 (p11.2) 1.0	CE-1001 (p11.2) 1.0
40	M	1-2	Positive	Positive	Positive	Positive	None	CE-1001 (p11.2) 1.0	CE-1001 (p11.2) 1.0
41	M	1-2	Positive	Positive	Positive	Positive	None	CE-1001 (p11.2) 1.0	CE-1001 (p11.2) 1.0
42	M	1-2	Positive	Positive	Positive	Positive	None	CE-1001 (p11.2) 1.0	CE-1001 (p11.2) 1.0
43	M	1-2	Positive	Positive	Positive	Positive	None	CE-1001 (p11.2) 1.0	CE-1001 (p11.2) 1.0
44	M	1-2	Positive	Positive	Positive	Positive	None	CE-1001 (p11.2) 1.0	CE-1001 (p11.2) 1.0
45	M	1-2	Positive	Positive	Positive	Positive	None	CE-1001 (p11.2) 1.0	CE-1001 (p11.2) 1.0
46	M	1-2	Positive	Positive	Positive	Positive	None	CE-1001 (p11.2) 1.0	CE-1001 (p11.2) 1.0
47	M	1-2	Positive	Positive	Positive	Positive	None	CE-1001 (p11.2) 1.0	CE-1001 (p11.2) 1.0
48	M	1-2	Positive	Positive	Positive	Positive	None	CE-1001 (p11.2) 1.0	CE-1001 (p11.2) 1.0
49	M	1-2	Positive	Positive	Positive	Positive	None	CE-1001 (p11.2) 1.0	CE-1001 (p11.2) 1.0
50	M	1-2	Positive	Positive	Positive	Positive	None	CE-1001 (p11.2) 1.0	CE-1001 (p11.2) 1.0

Conclusions: We demonstrated that CN-LOH of 1p36 is more common than 1p36 deletion in the subtype of t(14;18) negative FL associated with 1p36 abnormalities. Our study also showed that CN-LOH of 16p is the most common recurrent abnormality in 1p36 deletion/LOH-associated FL. Preliminary mutation results are indicative of the cooperation of deleterious mutations in TNFRSF14 and CREBBP in lymphomagenesis. Our study suggested that BCL2 negative inguinal FL represents a unique clinicopathological entity distinct from systemic BCL2 positive FL. Therefore, SNP array analysis is superior to locus specific FISH assay in the genetic evaluation of this subtype of lymphoma

1483 The Utility of Phosphohistone-H3 (PHH3) Immunohistochemistry as an Adjunct in Grading Follicular Lymphoma

Michelle Khieu¹, Devin R Broadwater¹, Jean Coviello¹, David Lynch¹, Jordan Hall¹. ¹Brooke Army Medical Center, San Antonio, TX

Background: Routine histologic grading of follicular lymphoma (FL) is currently performed by examining hematoxylin & eosin (H&E) stained sections and estimating the average number of centroblasts per 40x high power field (HPF) over ten representative neoplastic follicles. Whether this is truly the best method for grading FL remains controversial. The 2008 World Health Organization (WHO) classification endorsed the use of Ki67 immunohistochemistry (IHC) as a clinically justified adjunct due to general correlation of proliferation index with histologic grade; however, interpretation of Ki67 has high interobserver variability. In this study, the correlation between histologic grade and mitotic count (MC) was investigated using the mitosis-specific immunohistochemical stain phosphohistone-H3 (PHH3). Interobserver variability in Ki67 and PHH3 interpretation was also examined.

Design: Follicular lymphoma cases available at Brooke Army Medical Center between January 2005 and April 2017 were identified. Cases were blinded, randomized, and reviewed by three staff hematopathologists. The average Ki67 proliferation index, MC per HPF using PHH3, MC per HPF on H&E stain, and number of centroblasts per HPF were recorded. Results were assessed for correlations and interobserver variability.

Results: Thirty cases of FL were studied, including 17 low-grade (LGFL: 5 grade-1 and 12 grade-2) and 13 high-grade (HGFL: 12 grade-3A and 1 grade-3B). PHH3 MC resulted in the strongest correlation to grade ($r = 0.773$) compared to Ki67 ($r = 0.679$) and H&E MC ($r = 0.562$) and the strongest linear relationship to centroblast count ($p = 0.006$, $R^2 = 0.574$) (Figure 1). The mean PHH3 MC for LGFL was 2.4 per HPF compared to a mean H&E MC of 0.7 per HPF (mean difference = 1.7, $p < 0.0001$, 95% CI [1.5 – 1.9]). The mean PHH3 MC for HGFL was 7.3 per HPF compared to a mean H&E MC of 2.4 per HPF (mean difference = 4.9, $p < 0.0001$, 95% CI [4.3 – 5.3]). Agreement amongst pathologists was strongest for PHH3 (intraclass correlation coefficient [ICC] = 0.89, 95% CI [0.81-0.94]) followed by Ki67 (ICC = 0.85, 95% CI [0.75-0.92]) and H&E MC (ICC = 0.79, 95% CI [0.65-0.88]). Examples of staining patterns demonstrated in Figure 2.

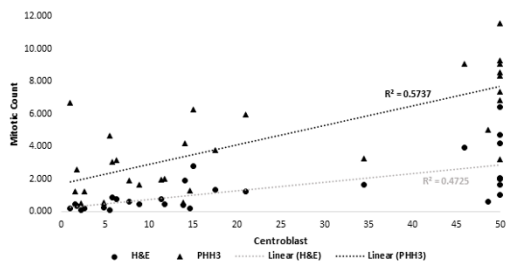


Figure 1. Mitotic count on H&E and PHH3 compared to centroblast count (counts >50 per hpf were recorded as 50).

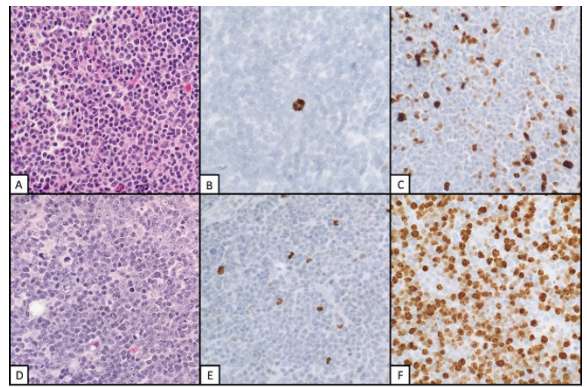


Figure 2. A-C Low-grade (Grade 1) follicular lymphoma. 40x (H&E, PHH3, Ki67). D-F High-grade (grade 3B) follicular lymphoma. 40x (H&E, PHH3, Ki67).

Conclusions: PHH3 MC more strongly correlated with routine histologic grade of FL than Ki67 proliferation index or H&E MC and showed the greatest interobserver agreement. These results support the feasibility of using PHH3 as an adjunct in FL grading.

1484 Ph-like B Acute Lymphoblastic Leukemia (B-ALL) Has Higher CD22 Expression Compared to Other Subtypes of Adults B-ALL

Sergej Konoplev¹, Marian J Kersh², Marina Konopleva², Nitin Jain², Elias J Jabbar², Jeff Jorgensen², Sa Wang². ¹Houston, TX, ²The University of Texas MD Anderson Cancer Center, Houston, TX

Background: The outcome of adult patients with B Lymphoblastic Leukemia (B-ALL) remains dismal, particularly for Ph-like B ALL. Inotuzumab ozogamicin, an antibody-drug conjugate against CD22 has demonstrated a significant activity in patients with B-ALL. We investigated the expression of CD22 in newly diagnosed adult patients with different subtypes of B-ALL.

Design: We retrospectively analyzed CD22 expression in adult patients with untreated de novo B-ALL presented to our institution between January 2015 and September 2017. Patients with a prior history of hematologic malignancies were excluded. CD22 expression was assessed by MFC with APC-conjugated anti-CD22 antibody (BD Bioscience; clone S-HCL-1) for the percentage of neoplastic cells expressing CD22 and median fluorescence intensity (MFI).

Results: The study group included 84 men and 50 women with a median age of 44 (range, 18-82) (44 Ph+44; 24 Ph-like CRLF2+; 7 MLL+, 7 Hyperdiploid; 7 Hypodiploid; 4 Ph-like non-CRLF2; 2 E2A-PBX1+, and 39 NOS). CD22 percentage and MFI are shown in Table 1. CD22 was expressed in all cases except for two MLL+ patients and one Ph+ patient. CD22 expression percentage was the highest in patients with Ph-like CRLF2+, Hyperdiploid and hypodiploid B-ALL and was the lowest in MLL+ patients. CD22 expression intensity as assessed by MFI was significantly higher in Ph-like CRLF2+ compared to Ph+ patients ($p=0.006$) or NOS patients ($p=0.036$).

	Ph-like CRLF2+	Hyper-diploid	Hypo-diploid	NOS	Ph+	Ph-like non-CRLF2	E2A-PBX1+	MLL+
CD22%	93+/-1	83+/-5	81+/-7	91+/-2	78+/-4	90+/-4	92+/-1	33+/-9
MFI	3562 +/-569	3392 +/-1119	2399 +/-742	2259 +/-155	1766 +/-201	1719 +/-336	1100 +/-429	548 +/-88

Mean +/- SD

Conclusions: Ph-like CRLF2+ patients and patients with hyperdiploid and hypodiploid B-ALL show the highest expression of CD22 and might benefit from Inotuzumab ozogamicin therapy. Low expression of CD22 in MLL+ patients could explain the low response rate of this group to Inotuzumab ozogamicin reported previously.

1485 In silico Analysis of anti-leukemia Immune Response and Immune Evasion in Acute Myeloid Leukemia

Rosemarie Krupar¹, Cleopatra Schreiber¹, Anne Offermann¹, Claudia Lengerke³, Christoph Thorns⁴, Andrew G Sikora⁵, Perner Sven¹. ¹University Hospital Schleswig-Holstein, Leibniz Center for Medicine and Biosciences, Luebeck and Borstel, Germany, ³University of Basel and University Hospital Basel, Basel, Switzerland, ⁴Institute of Pathology of the Marienkrankenhaus Hamburg, Germany, ⁵Baylor College of Medicine, Houston, TX

Background: In contrast to the tumor immune microenvironment, little is known about the role of the leukemia immune microenvironment (LIME). We hypothesized that acute myeloid leukemias (AML) with low peripheral blood leukemic blasts (pblasts) have a residual anti-leukemia immune response in the bone marrow (BM), whereas AMLs with high pblasts have overruled BM immune control.

Design: The Cancer Genome Atlas (TCGA) database was used to characterize the LIME of 168 AML patients. AMLs were stratified according to mean pblast percentage in pblasts <40% (pblasts-l) and pblasts >40% (pblasts-h). Gene up- or downregulations (z-Score=0) of immune-relevant genes were compared and correlated to 60-months overall survival (OS). Additionally, mutation frequencies, expression of AML specific antigens and cytogenetic abnormalities were assessed.

Results: Pblasts-l AMLs presented with more frequent up-regulations of *CD8A* (cytotoxic T cells), *NCR1* (natural killer cells), *CD4* (T helper cells) and *FOXP3* (regulatory T cells) in the BM. Genes relevant for cytotoxic immune response, as *B2M* (major histocompatibility complex I/MHCI), *GZMB* (granzyme), *PRF* (perforin), *IFNG* (interferon γ), *FASL* (fas ligand) and *TNFSF10* (TRAIL) were also more frequently up-regulated in pblasts-l AMLs. Up-regulation of the immune checkpoint molecules PD1, Lag3 and CD80 predicted decreased OS. In contrast, increased MHCII expression correlated with survival benefit selectively in pblasts-l, but not pblasts-h AMLs. We hypothesized that functional presentation of leukemia antigens via MHCII might contribute to confine blasts to the BM. While the AML specific antigens *WT1*, *PRTN3*, *PRAME* or *RHAMM* showed no relevant differences, *P53* mutations were more frequently present in pblasts-l AMLs (16% versus 3%). Next, we correlated the presence of gene fusions, which can also serve as leukemia antigens. There was no difference for *CBFB-MYH11*, *RUNX1-RUNX1T1* and *BCR-ABL1*. But *PML-RARA* was significantly more often detected in pblasts-l AMLs (19.2% versus 2.6%). Interestingly, only *PML-RARA* AMLs with up-regulated MHCII had a survival benefit (OS fraction 86%), while *PML-RARA* AMLs without MHCII up-regulation and AMLs without *PML-RARA* translocation showed OS fractions of 33% and 36%.

Conclusions: The study demonstrates the impact of the LIME in AML and supports the integration of immune checkpoint modulators into treatment. Additionally, our results define *PML-RARA* gene fusion as a target of anti-leukemia immune response in the context of functional MHCII expression.

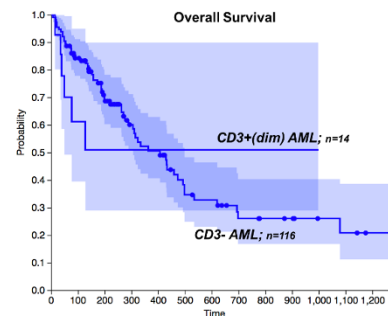
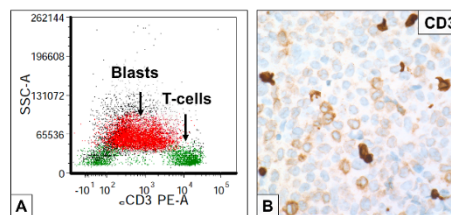
1486 The Significance of Dim Cytoplasmic CD3 Expression in Acute Myeloid Leukemia: A Long-Term Retrospective Study Identifies an Association with Acute Promyelocytic Leukemia with FLT3-ITD Mutations

Jyoti Kumar¹, Alexandra Nagy¹, Norman Lacayo¹, Jason Gotlib¹, James L Zehnder², Robert Ohgami¹. ¹Stanford University, Stanford, CA, ²Stanford University School of Medicine, Stanford, CA

Background: Acute myeloid leukemia (AML) is classified based on morphologic, immunophenotypic, molecular and cytogenetic features. Rarely, dim cytoplasmic CD3 (cCD3) expression has been noted on cases of AML which is not lineage defining according to the 2016 revised WHO criteria. However, the significance of such cCD3 expression in AML is largely uncertain. There has been no previous study to date that systematically analyzed such cases.

Design: We searched our archives from 2008-2017 for cases of AML with an immunophenotype that included dim or partial cCD3 expression by flow cytometry to understand the significance of such atypical expression patterns. Patient clinical data, molecular, cytogenetic and morphologic features were collected and analyzed.

Results: In our initial analysis of 130 cases, 14 cases of AML with dim to partial cCD3 expression on the blast population were identified by flow cytometry (Figure 1A) and correlated with ancillary immunohistochemical (IPOX) staining (Figure 1B). At first, no subtype of AML appeared to have a more statistically significant prevalence of cCD3 expression. There was also no significant difference in overall survival when comparing patients with cCD3+ and cCD3- AML (Figure 2). However, 4 cases of acute promyelocytic leukemia (APL) were identified amongst the 14 total cases. Given the increased number of APL cases, we studied 33 additional APL cases and identified a significant increase in cCD3 expression. Of the 33 cases, 14 were positive for cCD3. Interestingly, dim cCD3 expression was frequent in the APL cases containing a FLT3-internal tandem duplication (FLT3-ITD) mutation (10 of 14, 71%), but not as frequent in APL cases without the FLT3-ITD mutation (4 of 19, 21%) (p-value <0.001). However, as initially noted, there was no effect on prognosis among the cases of non-APL AMLs or within APLs treated with ATRA therapies.



Conclusions: Our data reveals that overall survival and prognosis is not altered based on cCD3 expression. As such, our study supports the 2016 revised WHO criteria in that expression of dim cCD3 should not be used as lineage defining criteria. Finally, our findings suggest that dim cCD3 expression is significantly associated with APL with FLT3-ITDs.

1487 Hairy cell leukemia expresses Programmed death 1 (PD-1): a new diagnostic marker

Priyadarshini Kumar¹, Janine D Pichardo¹, Natasha Lewis¹, Alex Chan¹, Qi Gao¹, Mikhail Roshal¹, Ahmet Dogan¹. ¹Memorial Sloan Kettering Cancer Center, New York, NY

Background: Programmed death 1 (PD-1) is a lymphoid receptor that negatively regulates immune responses. PD-1 is mainly expressed in reactive T cells; but reports of expression were also noted in neoplastic B cells from small lymphocytic lymphoma/chronic lymphocytic leukemia (SLL/CLL), rare cases of follicular lymphoma and diffuse large cell lymphoma. In contrast, neoplastic B cells from mantle cell lymphoma, marginal zone lymphoma, Burkitt lymphoma, and most follicular lymphomas are PD-1 negative. In SLL/CLL, PD-1 expression is associated with a mutated immunoglobulin heavy chain variable gene (*IGHV*). Classical hairy cell leukemia, which is mainly prone to peripheral blood circulation, splenomegaly and bone marrow involvement, also shows somatic hypermutations in the *IGHV*. In this study we examined PD-1 expression in hairy cell leukemia using immunohistochemistry (IHC) and flow cytometry.

Design: A series of 27 patients with a diagnosis of HCL were identified and PD-1 (CD279) expression was assessed by flow cytometry on peripheral blood samples or bone marrow aspirates, and PD-1 and PD-L1 expression by IHC on bone marrow biopsies. In addition ten cases of marginal zone lymphoma were analyzed for comparison.

Results: PD-1 expression was identified on 26 of 27 HCL samples with an average mean fluorescence index (MFI) of 126868 as compared to control B cells with an average MFI of 102766. The expression level was similar to that observed in CLL/SLL or in exhausted T-cells. As expected, none of the 10 cases of marginal zone lymphoma were positive for surface expression of PD-1. IHC for PD-1 staining was positive in 2 of 20 cases of hairy cell leukemia. PD-L1 staining was positive in none. All cases of marginal zone lymphoma were negative for PD1 and PD-L1 expression.

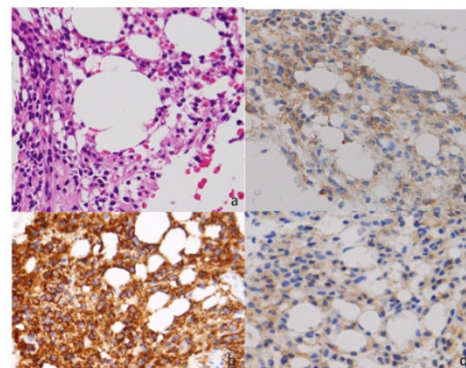


Figure 1. Bone marrow biopsy extensively involved by Hairy cell leukemia, a) H&E; b) CD20; c) PD-1; d) CD103

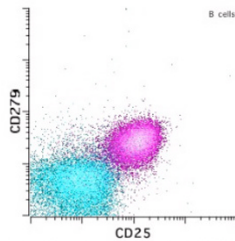


Figure 2. CD19+ B cells showing aberrant expression of CD25 and CD279 (pink), normal B cells (blue)

Conclusions: This is the first report to show uniform surface expression of PD-1 (CD279) on hairy cell leukemia to our knowledge. The discrepancy between PD-1 surface expression by flow cytometry and immunohistochemistry is most likely a consequence of the lower sensitivity of the PD-1 IHC assay in decalcified marrow biopsies. Although biological significance of this finding is not yet known, flow cytometric evaluation of PD-1 expression provides a useful tool to separate hairy cell leukemia from other low grade B cell lymphomas that appear in the differential including marginal zone lymphoma. The expression of PD-1 in hairy cell leukemia may be important in tumor immune escape and could be a useful therapeutic target.

1488 Identification of Early Hematogones in the Peripheral Blood

Jason H Kurzer¹, Olga K Weinberg². ¹Stanford University School of Medicine, Stanford, CA, ²Children's Hospital Boston, Boston, MA

Background: Early B-cells, "hematogones", pass through multiple maturation stages within the bone marrow that can be defined by immunophenotypic changes. Stage 1 hematogones express CD34, TdT, CD10, and lack CD20, stage 2 cells lack CD34 and upregulate CD20, while those in stage 3 retain CD10, have full CD20 expression, and express surface light chain. Previous reports indicate that only stage 3 hematogones circulate. However, as stage 1 and 2 hematogones share morphologic and immunophenotypic similarities with neoplastic B-lymphoblasts, the presence of earlier hematogones in the peripheral blood could pose a substantial diagnostic challenge. We therefore performed a multi-institutional review to assess for circulating early hematogones and to uncover discriminatory factors between these precursors and their neoplastic counterparts.

Design: We retrospectively searched our institutional databases for peripheral blood samples submitted for flow cytometric immunophenotyping that contained the terms, "hematogones" and "immature cells" within the associated pathology reports. We then reviewed the scatter plots to identify cases containing stage 1 and/or stage 2 hematogones. Clinical histories were reviewed for positive cases.

Results: Our search yielded a total of 518 reports, 13 of which contained stage 1 and 2 hematogones. The patients ranged in age from 15 days to 85-years old, with 4 (31%) patients <1 year of age and 6 (46%) adults. All positive cases demonstrated a maturation curve when examined by a plot of CD20 vs CD10 expression, with no cases showing stage 1 hematogones in isolation. 8 cases (62%) showed <1% early hematogones in the circulation, while 1 case showed 2.9%, and 4 (31%) showed >1% stage 1 hematogones. The patients demonstrated a range of associated clinical histories, including osteopetrosis, lymphoma, hepatitis C, prior B-ALL, and Noonan's syndrome.

Conclusions: While rare, our study shows that earlier hematogones can be found circulating in both children and adults. It is likely that the increased number of cases screened, and the increased events collected accounts for the difference from prior reports. Of importance, the presence of circulating early hematogones raises a challenge for potential MRD studies looking for small populations of B-lymphoblasts. To this end, all cases with stage I and/or II hematogones showed an associated maturation curve, contrasting these cases with cases of typical of B-ALL.

1489 A p63 Immunostain is Frequently Positive in Hematolymphoid Neoplasms, while p40 is Uniformly Negative: Another Justification for Adopting p40 as the Primary Marker of Squamous Differentiation

John Lee¹, Andrew Bellizzi¹. ¹University of Iowa Hospitals and Clinics, Iowa City, IA

Background: p63 exists as isoforms containing (TAp63) or lacking (Δ Np63) a transactivating domain. While Δ Np63 is narrowly expressed by squamous epithelium, urothelium, myoepithelial cells, and basal cells, TAp63 is more widely expressed. The most widely utilized p63 antibody (clone 4A4) recognizes an epitope in the core domain of both isoforms, while p40 recognizes a Δ Np63-specific epitope. p63-positivity has been noted in 15-60% of lung adenocarcinomas, attributable to detection of TAp63. We recently encountered

a sarcomatoid neoplasm presenting as a lung mass invading the chest wall in which a diagnosis of sarcomatoid carcinoma was initially favored, based in part on strong p63 expression, before a diagnosis of diffuse large B-cell lymphoma (DLBCL) was ultimately confirmed. The purpose of this study is to document the frequency/extent of p63 vs. p40 staining across a broad range of hematolymphoid neoplasms.

Design: IHC with mouse monoclonal antibodies to p63 (clone 4A4) and p40 (clone BC28) was performed on tissue microarray slides (triplicate 1 mm cores) from 459 hematolymphoid neoplasms. Tumors were assessed for intensity (0, 1+, 2+, 3+) and extent (0-100%) of expression with an H-score calculated (intensity*extent).

Results: p63 expression was seen in 45% of 459 tumors, with particularly strong expression in DLBCL and marginal zone lymphoma (mean H-scores >100), while, remarkably, **p40 expression was not detected (0%)**. Detailed p63 data are presented below:

Tumor	% + (H-score \geq 1)	Mean H-score (if +)
DLBCL, activated B-cell (51)	86%	109
Anaplastic large cell lymphoma, ALK+ (6)	83%	32
Follicular lymphoma (50)	82%	31
DLBCL, germinal center (77)	55%	99
B-lymphoblastic lymphoma (6)	50%	64
Anaplastic large cell lymphoma, ALK- (15)	47%	68
Angioimmunoblastic T-cell lymphoma (11)	45%	87
Burkitt lymphoma (35)	43%	27
T-lymphoblastic lymphoma (10)	40%	2.5
Mantle cell lymphoma (12)	33%	3.75
Classical Hodgkin lymphoma (52)	27%	48
Chronic lymphocytic leukemia (33)	24%	40
Granulocytic sarcoma (21)	24%	5
T-cell lymphoma, NOS (32)	19%	79
Marginal zone lymphoma (37)	14%	127
Plasma cell myeloma (11)	0%	NA

Conclusions: Frequent p63-positivity in lymphoma represents a significant diagnostic pitfall, providing additional justification for adopting p40.

1490 PHF6 Mutations Define a Subgroup of Mixed Phenotype Acute Leukemia with Aberrant T-Cell Differentiation

Natasha Lewis¹, Friederike Pastore¹, Priyadarshini Kumar¹, Bartlomiej Getta¹, Anne Hultquist¹, Brian Shaffer¹, Sergio Giral¹, Raajit Rampal¹, Maria Arcila², Ross Levine¹, Mikhail Roshal¹, Wenbin Xiao¹. ¹Memorial Sloan Kettering Cancer Center, New York, NY, ²New York, NY

Background: Mixed phenotype acute leukemia (MPAL) is rare, comprising 2% of acute leukemias. Except for few with *BCR/ABL1* or *MLL* fusions (~15%), genetic aberrations in MPAL are largely unknown. Somatic *PHF6* mutations are common in T lymphoblastic leukemia/lymphoma (up to 30%) and rare in acute myeloid leukemia (AML) (~3%). Here we report a high frequency of *PHF6* mutations in MPAL.

Design: We sequenced 1329 patients with myeloid neoplasms (2013-2016; targeted next-generation sequencing [NGS] panel) and recorded diagnoses among *PHF6* mutated (*PHF6*-m) cases. 24 MPAL patients (2013-2016; AML with myelodysplasia-related changes [AML-MRC] and therapy-related AML [t-AML] excluded) were also evaluated for genetic alterations (NGS panel), phenotype (flow cytometry; BD Biosciences, San Jose, CA) and outcomes (medical records). Flow cytometric immunophenotype of *PHF6*-m AMLs was determined. Statistical analysis used Fisher's exact test.

Results: We identified 38 significant *PHF6* mutations in 33 patients (2.5%) (10 frameshift, 11 nonsense, 1 splice site, 16 missense; MPAL [n=5], AML [n=19], myelodysplastic syndrome [n=5], myeloproliferative neoplasm [n=4]). *RUNX1* was most commonly co-mutated (30%, 11/37); no *TP53* mutations were found. Among 24 MPAL cases, 3 (12%) *BCR-ABL1* (p190) fusions, 1 (4%) *MLL* fusion and 5 (21%) *PHF6* mutations were seen (all mutually exclusive). 4/5 *PHF6*-m MPALs had T-cell differentiation while *BCR-ABL1* and *MLL* cases had B/myeloid. *PHF6*-m MPALs had lower 2-year overall survival than unmutated ones (40% vs. 100%; p=0.005). Of all AML, *PHF6* mutations occurred predominantly in secondary AML (sAML) (12%, 11/88 of AML-MRC, 7%, 6/84 of t-AML, 1 de novo AML). SAMLs often expressed T-cell markers regardless of *PHF6* mutational status (56%, 9/16 vs. unmutated 51%, 36/70). *PHF6*-m AMLs were more often negative for CD33 (69%, 11/16 vs. 28%, 20/70; p=0.004) and CD38 (44%, 7/16 vs. 17%, 12/70; p=0.04) than unmutated cases, suggestive of a stemness phenotype with aberrant T-cell differentiation.

Conclusions: *PHF6* mutations are the most common somatic alteration in MPAL and define a MPAL subgroup with altered T-cell differentiation and inferior outcome. *PHF6* mutations are predominant in sAML and associated with T-cell antigen expression and more primitive progenitor immunophenotype. They co-exist with *RUNX1*

mutations but are mutually exclusive of *TP53* mutations. *PHF6* mutations may provide a genetic and functional link between MPAL with poor outcome and sAML and insight into shared transformation mechanisms.

1491 Myeloid Neoplasms With Features of Both Myelodysplastic/Myeloproliferative Neoplasm With Ring Sideroblasts and Thrombocytosis and Myelodysplastic Syndrome With Del(5q)

Natasha Lewis¹, Jinjuan Yao¹, Yanming Zhang¹, Mikhail Roshal¹, Wenbin Xiao¹. ¹Memorial Sloan Kettering Cancer Center, New York, NY

Background: The World Health Organization accepted myelodysplastic/myeloproliferative neoplasm with ring sideroblasts and thrombocytosis (MDS/MPN-RS-T) as a full entity in the 2016 revision. It is characterized by thrombocytosis, anemia and bone marrow with dyserythropoiesis, megakaryocytic hyperplasia and atypia similar to that in primary myelofibrosis or essential thrombocythemia and >15% ring sideroblasts. Most harbor mutations of *SF3B1* as well as *JAK2* V617F, *MPL* or *CALR*. Chromosome 5q deletion (del(5q)) excludes this diagnosis, its presence suggesting a diagnosis of myelodysplastic syndrome (MDS) with isolated del(5q). MDS with isolated del(5q) is also characterized by anemia and thrombocytosis but marrow often shows many small, hypolobated megakaryocytes without significant myeloid/erythroid dysplasia. It is defined by a del(5q) while *JAK2*, *MPL*, and *CALR* mutations are rare. We describe 3 cases with morphologic and molecular features of MDS/MPN-RS-T that also have del(5q), raising questions of classification and pathobiology.

Design: Consultation cases from 3 patients were acquired from our hematopathology files. Clinical and pathologic data were obtained from pathology reports and medical records. Cytogenetic and molecular (targeted next-generation or capillary electrophoresis-based DNA sequencing) tests were performed at outside and/or our institution.

Results: Clinical, morphologic and genetic findings from 3 patients are described below (table). Bone marrow morphology summarizes all available biopsies from outside reports and our evaluation. All patients had thrombocytosis, anemia and MDS/MPN-RS-T-like marrow morphology. 2 patients had *SF3B1* mutations and all 3 had *MPL* mutations and del(5q). 2 patients had thrombotic events, splenomegaly, progressive anemia despite therapy and died of disease.

Clinical, morphologic and genetic characteristics of 3 patients with myeloid neoplasms with features of both MDS/MPN-RS-T and MDS with del(5q)

(AML indicates acute myeloid leukemia; FISH, fluorescent in situ hybridization; Hgb, hemoglobin; MCV, mean corpuscular volume; Plt, platelet count; VAF, variant allele frequency; WBC, white blood cell count)

	Patient 1	Patient 2	Patient 3
Date of diagnosis	7/16/2015	11/15/2010	12/22/2011
Age at diagnosis/Sex	76 male	62 male	71 male
CBC at/near diagnosis	WBC 7 k/ μ L Hgb 10.8 g/dL MCV 95 fL Plt 1,486 k/ μ L	WBC Normal Hgb 10.1 g/dL Plt 783 k/ μ L	WBC 9.0 k/ μ L Hgb 12.1 g/dL MCV 103 fL Plt 778 k/ μ L
Bone marrow morphology	Cellularity 60-70% Dyserythropoiesis Megakaryocytic hyperplasia and atypia (hyperlobulated) Ring sideroblasts (>50%) 1+ reticulin fibrosis <5% blasts	Cellularity >95% Megakaryocytic hyperplasia and atypia (hyperlobulated) Myeloid hyperplasia with left-shifted maturation Ring sideroblasts (reported) 2-3+ reticulin fibrosis <5% blasts	Cellularity >90% Megakaryocytic hyperplasia and atypia (hyperlobulated) Mild dysgranulopoiesis Ring sideroblasts (5% on suboptimal aspirate) 2+ reticulin fibrosis <5% blasts
Karyotype	46,XY,del(5)(q31q31)[9]/46,XY[11]	Normal	46,XY,del(5)(q22q35)[17]/46,idelm,del(20)(q11.2)[3]
FISH	Del(5q31) (83% of cells)	Del(5q) of cells (10%) Del(17p13) of cells (10%) Del(17q11) not provided (%)	Del(5q31) (92% of cells) Del(20q) (15% of cells)
Molecular alterations	SF3B1 p.K666Q (VAF 46%) MPL p.W515S (VAF 39%)	MPL p.W515L	SF3B1 p.K666N (VAF 42%) MPL p.W515L (VAF 45%) IDH1 p.R132C (VAF 9%)
Complications	Progressive fatigue Progressive anemia	Transient ischemic attacks, deep vein thrombosis, hepatosplenomegaly Bone pain, fever, night sweats, fatigue, early satiety, weight loss Progressive transfusion-dependent anemia and leukocytosis	Retinal vein occlusion, splenomegaly Fatigue Progressive transfusion-dependent anemia
Therapies	Anagrelide Lenalidomide	Hydroxyurea Lenalidomide Darbepoetin Ruxolitinib	Hydroxyurea Lenalidomide Darbepoetin
Outcome	Alive	Dead of disease	Progressed to AML Dead of disease
Time to last follow up (months)	18	63	64

Conclusions: Myeloid neoplasms with features of MDS/MPN-RS-T and MDS with del(5q) are rare and poorly understood. Whether they represent true overlap disease, two separate, concurrent processes or belong in one diagnostic category is unknown. Although 2 cases had high *SF3B1* and *MPL* variant allele frequencies and percentages of cells with del(5q) by fluorescent in situ hybridization, the sequence of these genetic alterations and whether any were subclonal is unclear. The suboptimal response to lenalidomide, thrombotic events and fairly short survival in 2 patients suggests these neoplasms may not be best diagnosed as MDS with isolated del(5q). Additional studies to better define these rare lesions are needed.

1492 Revisiting Diagnostic Criteria for Myelodysplastic and Myeloproliferative Neoplasms with Ring Sideroblasts and Thrombocytosis: Borderline Cases without Anemia Exist

Peng Li¹, Robert S Ohgami². ¹University of Florida, Gainesville, FL, ²Stanford University

Background: Myelodysplastic and myeloproliferative neoplasm with ring sideroblasts and thrombocytosis (MDS/MPN-RS-T) is a rare disease in the 2016 revised World Health Organization (WHO) classification. Diagnostic criteria include: persistent thrombocytosis (>450 x 10⁹/L) with clustering of atypical megakaryocytes, refractory anemia, dyserythropoiesis with ring sideroblasts, and the presence of the spliceosome factor 3b subunit (*SF3B1*) mutation.

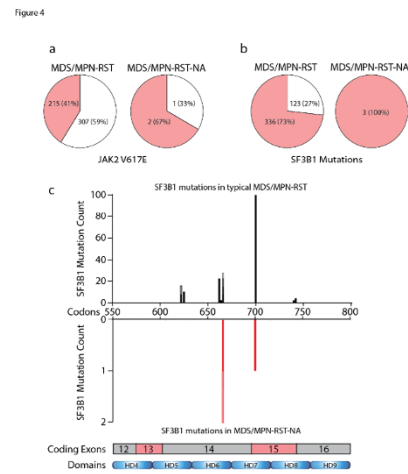
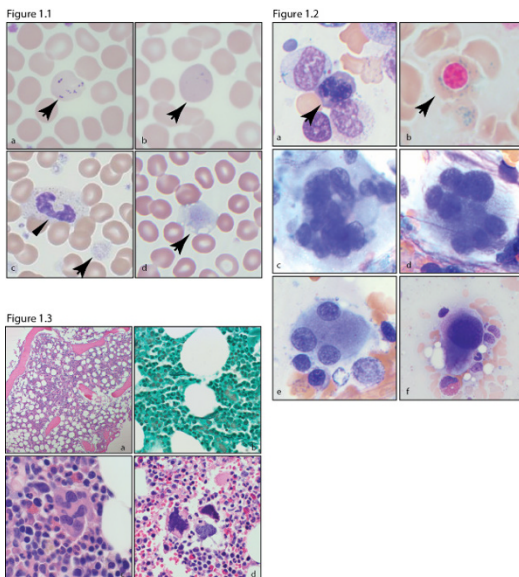
Design: In the current study, we report on three cases of borderline-MDS/MPN-RS-T, in which anemia was absent (b-MDS/MPN-RS-T-NA) in which refractory anemia was absent at diagnosis, resulting in difficulty in establishing not only the correct diagnosis, but also the subsequent appropriate therapeutic approach. Not only do we summarize and describe in detail these cases, but also compare the mutational *JAK2* and *SF3B1* findings to those of 500 typical MDS/MPN-RS-T cases reported in the literature.

Results: Our comparative analysis demonstrates that compared to classic cases of MDS/MPN-RS-T, borderline cases without anemia show a younger median age at diagnosis, 55.5 years versus 71–75 years. Other morphologic, laboratory, cytogenetic, and molecular findings in b-MDS/MPN-RS-T-NA cases were otherwise classical for MDS/MPN-RS-T. Our findings suggest that b-MDS/MPN-RS-T-NA may represent the most “benign” end of the spectrum of MDS/MPN-RS-T and anemia should not be required for the diagnosis of MDS/MPN-RS-T.

Table 1. Clinical and hematologic features of patients with borderline MDS/MPN-RS-T-NA and their documented *JAK2* V167F mutation status.

Cases	1	2	3
Age	57	54	82
Gender	F	M	F
HGB (g/dL)	14.3	14.8	12.5
MCV (fL)	91.2	95.0	90
PLT(K/uL)	626	652	>450
Cellularity	Normocellular	Normocellular	Hypercellular
>5% blasts in BM	No	No	No
Dyspoiesis	Yes ²	Yes ¹	Yes ¹
Ring sideroblasts	+ (15%)	+ (5%)	+ (>15%)
Myelofibrosis	0	0-1	n/a
Karyotype	Normal	Normal	n/a
<i>JAK2</i>	-	+	+
Follow up(yrs)	1	19	n/a

BM = bone marrow; 1, dysmegakaryopoiesis; 2, dyserythropoiesis and dysmegakaryopoiesis



Conclusions: In summary, this study supports the finding that anemia may not be necessary for the diagnosis of MDS/MPN-RS-T. b-MDS/MPN-RS-T-NA belongs to the most benign end of the MDS/MPN-RS-T spectrum—namely, the low risk group of myeloid dysplastic neoplasms. Careful review of clinical and laboratory data, thorough evaluation of peripheral blood and bone marrow morphologic and cytogenetic findings, and molecular analysis of *SF3B1* and *JAK2* mutations are required for the diagnosis and precise classification of this rare disorder.

1493 Pathogenic Mutations and Atypical Flow Cytometric Findings Characterize the Majority of Myelodysplastic/Myeloproliferative Neoplasms (MDS/MPN)

Yanchun Li¹, Rose Beck¹, Erika M Moore¹. ¹University Hospitals Cleveland Medical Center, Cleveland, OH

Background: MDS/MPN are a group of rare & heterogeneous diseases often difficult to diagnose. Chronic myelomonocytic leukemia (CMML) & MDS/MPN with ring sideroblasts & thrombocytosis (MDS/MPN-RS-T) have relatively clear diagnostic criteria, while atypical chronic myeloid leukemia (aCML) & MDS/MPN, unclassifiable (MDS/MPN-U) are not well characterized. Diagnoses can be morphologically challenging & abnormal cytogenetic (CG) findings are inconsistent and variable. We sought to determine the usefulness of flow cytometry (FC) and next generation sequencing (NGS) in the diagnosis and classification of this challenging group of neoplasms.

Design: We assessed clinical, morphologic, FC, CG, & molecular features of 18 consecutive MDS/MPN cases assessed during a 1.5 year period. A 31 gene panel was used for most cases.

Results: Cases included 6 CMML, 2 MDS/MPN-RS-T, 2 aCML, & 8 MDS/MPN-U, including 3 in transformation with overlapping MDS & MPN features. Table 1 lists detailed features for each case.

All had at least one cytopenia & 13 had at least one cytosis, with bone marrow (BM) hypercellularity observed in all cases. 13 had M:E ratio >3.5:1. Dysplasia in at least one cell line was observed in PB or BM in all cases. All but one case had FC abnormalities. Every case had at least one CG or molecular abnormality, but mutations were more prevalent than abnormal CG, with 17 having at least one mutation, versus 8 with abnormal CG. 4/6 CMML had normal CG but 6/6 had mutations in at least 2 genes, including *ASXL1* (2), *SETBP1* (2), *SRSF2* (3), *TET2* (2), & *CBL* (2). Of 2 aCML, one had multiple CG abnormalities & a *TP53* mutation (limited panel) & the other had normal CG but multiple mutations including *SETBP1* & *GATA2*. Both MDS/MPN-RS-T had *SF3B1* & *DNMT3A* mutations but normal CG. All CMML, aCML, & MDS/MPN-RS-T had abnormal FC, including CD5 & CD7 expression on myeloblasts &/or CD56 expression on grans &/or monos. 7/8 MDS/MPN-U had mutations including 6/8 in at least two genes, the most common being *SRSF2* (4) & *JAK2* (4). 7/8 had CG abnormalities & 7/8 had FC abnormalities.

FOR TABLE DATA, SEE PAGE 570, FIG. 1493

Conclusions: Mutation analysis and FC aid in the evaluation of MDS/MPN disorders. 94% of cases had FC abnormalities or mutations, while only 44% had clonal CG abnormalities. Mutations in CMML & MDS/MPN-RS-T cases were consistent with previous reports. The most commonly mutated genes in MDS/MPN-U were *SRSF2* & *JAK2*. More data is needed to identify genes that may be specific to MDS/MPN-U & possibly help subcategorize this diverse group of disorders.

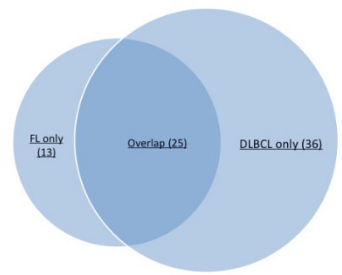
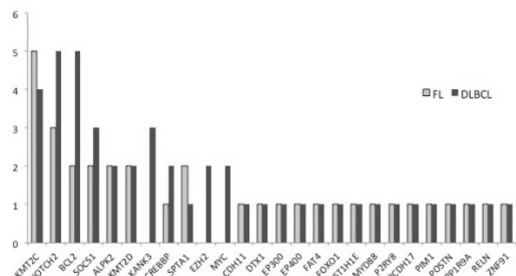
1494 A whole exome sequencing analysis of diffuse large B-cell lymphoma arising from topologically adjacent follicular lymphoma reveals an intimate and distant relationship

Chieh-Yu Lin¹, Alexandra Nagy¹, James L Zehnder², Dennis P O'Malley³, Robert Ohgami¹. ¹Stanford University Medical Center, Stanford, CA, ²Stanford University School of Medicine, ³NeoGenomics Laboratories

Background: The transformation of diffuse large B-cell lymphoma (DLBCL) from follicular lymphoma (FL) represents an aggressive process which is believed to result from acquisition of driver mutations and other genetic changes. However, next generation sequencing studies to date have assessed this transformational process in patient tissues from disparate anatomic locations, and/or frequently in disparate temporal sequences. We sought to understand the transformational process of DLBCL arising from histologically adjacent FL.

Design: We identified and studied 7 cases of transformed DLBCL arising from adjacent FL in the same slide/block from two major institutes. 1 case of DLBCL showed a MYC translocation which was not present in the FL component. Areas of DLBCL and FL were microdissected, and DNA extracted for whole-exome sequencing (average depth of coverage: 180-fold). Alignment was performed using BWA-MEM and variant calling by Surecall (version 3.5.1.46, Agilent Technologies) and GATK with variant annotation by interrogating multiple open-resource databases to determine pathogenicity.

Results: In total, 99 calls passed the filter. Some of the variants as recurrent events (Figure 1). The majority of variants were categorized as variants of unknown significance (82.8%), with some as pathogenic/likely pathogenic (11.1%) or benign/likely benign (6.1%). In average, 5.4 variants/case [1-13 variants] were identified in FL, and 8.7 variants/case [3-17 variants] were identified in DLBCL. The increased mutational burden in DLBCL compared with paired FL was statistically significant (p=0.02). While in many cases, the DLBCL and adjacent FL shared variants, unique variants were identified not only in DLBCL but also in FL, suggesting that loss of variants may also be a pathway to transformation. In average, 59.6% of variants identified in FL were shared between FL and DLBCL [0-100%] (Figure 2). The case of DLBCL with MYC translocations showed similar numbers of variants compared to those without a MYC translocation (8 variants/case vs 8.3 variants/case).



Conclusions: DLBCL arising from histologically adjacent FL typically exhibits a higher mutational burden, though some significant genetic changes are seen only in FL and not in the DLBCL component. That these cases of FL and DLBCL share some but not all altered genomic events is overall supportive of a common ancestor clone which undergoes both gains and losses of genetic mutation leading to transformation.

1495 Primary Breast Lymphoma: a Clinicopathologic Study of 13 Cases

Jianping Lin¹, Qinglong Hu², Ji Yuan¹, Catalina Amador¹, Hina N Qureshi¹, Philip J Bierman¹, Timothy Greiner¹, Kai Fu¹. ¹University of Nebraska Medical Center, Omaha, NE, ²Carondelet St Joseph Hospital, Tucson, AZ

Background: Primary breast lymphoma (PBL) is an infrequent neoplasm, representing less than 0.5% of all malignant breast tumors.

It is defined as a primary malignancy originating from the breast in the absence of previously diagnosed lymphoma. The pathologic features of PBL have been rarely reported. We did a retrospective review of the clinicopathologic features of PBL to gain a better understanding of this rare entity.

Design: Total 13 cases of PBL were retrieved from our pathology files from 1988 to 2017. These cases were reviewed. Clinical information and pathologic characteristics were collected and analyzed.

Results: From a total of 4895 archived lymphoma cases from 1988 to 2017, 13 patients (0.27%) with a PBL diagnosis were identified (all females, mean age: 70y, range: 49-86y). Indolent lymphomas were present in six of 13 (46%) patients with five cases of extranodal marginal zone B-cell lymphoma (B-MZL) and one case of low grade follicular lymphoma (FL). Seven of 13 (54%) patients presented with aggressive lymphomas including six cases of diffuse large B cell lymphoma (DLBCL) and one case of high grade FL. Tumor sizes ranged from 1.6 to 9 cm with DLBCL presenting the largest mass (mean=4.5 cm) and FL with the smallest mass (mean=1.8 cm). 11 of 13 (85%) of tumors were unilateral and unifocal, but two of 13 (15%) tumors presented in bilateral breasts, both of which showed B-MZL. Histologically, the patterns of involvement included diffuse in seven of 13 (54%), aggregates in three of 13 (23%) and the mixed in three of 13 (23%) cases. Two of 13 (15%) tumors invaded breast ducts and lobules. There was no concurrent breast adenocarcinoma identified. 12 of 13 (92%) patients present at low clinical stages (I or II). Clinically, there were no systemic symptoms and no skin changes. Treatment primarily included the standardized chemotherapy/radiation based on the types of lymphoma. 10 of 13 (77%) patients achieved complete response. Relapse was seen in only one of 13 (8%) cases with bilateral B-MZL. The event free survival was 65.9 months and overall survival was 88 months.

Conclusions: Both indolent and aggressive lymphomas can present in the breast. The majority of PBL present as localized disease except for B-MZL which is more prone to occurring in bilateral breasts. Most of patients presented at low clinical stage and responded very well to treatment.

1496 Molecular Genetic Characterization of Follicular Dendritic Cell Sarcoma Using Targeted Next Generation Sequencing Analysis

Jianping Lin¹, Courtney Schweikart¹, Kai Fu¹, Allison Cushman-Vokoun¹, Timothy Greiner¹. ¹University of Nebraska Medical Center, Omaha, NE

Background: Follicular dendritic cell sarcoma (FDCS) is a very rare malignant neoplasm with a variable clinical course, no uniform treatment strategy and a high recurrence rate. However, the pathogenesis and molecular genetics underlying FDCS are not well understood. Previous sequencing studies of small series of FDCS have identified mutations in BRAF, NF-κB1A and deletions involving some genes including CDKN2A, RB1, B1RC3 and CYLD. Our goal was to identify additional genetic mutations using Next Generation Sequencing (NGS) analysis.

Design: Formalin-fixed paraffin-embedded tissues from four cases of confirmed FDCS were retrieved from departmental archives. The cytogenetic karyotypes were reviewed on the four cases. NGS was performed on all cases using the Ion Torrent Ampliseq Cancer Hotspot Panel V2.0 with 50 genes on the Ion Torrent Personal Genome Machine. Sequence data were analyzed using Variant Caller Ion Torrent and Integrative Genomics Viewer (MIT).

Results: The patient cohort included 4 females ranging in age from 42 to 59. The size of the tumor ranged from 5 to 13 cm. All cases developed metastases including lung, liver, bone and chest wall, with lung as the most common site (3 of 4 cases). Cytogenetic analysis in 4 cases revealed either complex hyperdiploid karyotypes (2) including: +X, +6, +7, +18, +20 or hypodiploid karyotypes (2) including: -3, -5, -6, -9, -14, -22. The average NGS read coverage was 2,477 reads. The NGS results showed mutations in an oncogene, CTNNB1, and in two tumor suppressor genes, VHL and TP53. Case 1 had a missense mutation in CTNNB1 (TCA>TAA, p.Ser45Tyr) at 19.4% allele frequency. Case 2 had a missense mutation in VHL (GAT>CAT, p.Asp126His) at 7.9% allele frequency and a nonsense mutation in TP53 (GAG>TAG, p.Glu298Stop) at 13.4% allele frequency. Case 3 had a nonsense mutation in TP53 (CGA>TGA, p.Arg213Stop) at 17% allele frequency. Case 4 had no mutations identified in the 50 genes analyzed. Partial deletions of the 3' end of both CDKN2A and RB1 in all 4 cases were indicated by low read coverage in CDKN2A (mean: 254, range: 98-359) and RB1 (mean: 162, range: 130-198).

Conclusions: In addition to complex cytogenetic abnormalities, our small series shows that FDCS can have a mutation in an oncogene (CTNNB1) and mutations/deletions in tumor suppressor genes (VHL, TP53, RB1 and CDKN2A). Recurrent aberrations were observed in CDKN2A, RB1 and TP53. These molecular genetic results provide a foundation for a better understanding of the underlying pathophysiology of FDCS.

1497 **Clinicopathologic Characterization of Acute Myeloid Leukemia with Isolated Deletion of Chromosome 5q**

Yen-Chun Liu¹, Nidhi Aggarwal², Svetlana Yatsenko¹, Nathanael Bailey¹. ¹University of Pittsburgh School of Medicine, Pittsburgh, PA, ²Pittsburgh, PA

Background: Myelodysplastic syndrome (MDS) with isolated del(5q) is a well-recognized entity with a relatively favorable prognosis. Haploinsufficiency of the tumor suppressor genes in the commonly deleted region of 5q and their pathways have been implicated in the pathogenesis of MDS with del(5q) and in its response to lenalidomide. Isolated del(5q) in acute myeloid leukemia (AML) is rare. Del(5q) has been shown as a poor prognostic marker in AML based on multivariable analysis in cohort studies containing mostly cases with del(5q) as part of multiple abnormalities. To further characterize AML with isolated del(5q), clinicopathologic characterization including mutation analysis was performed.

Design: 14 AML with isolated del(5q) (AML-5q), 11 AML with del(5q) and one additional chromosome abnormality not involving chromosome 7 (AML-5q plus) and 123 AML with complex karyotype containing del(5q) (AML-5q complex) were identified during 2008-2017. Review of the clinical records and pathology material was performed. Next generation sequencing mutation analysis using amplicon target enrichment of coding and non-coding regions of 37 genes recurrently mutated in myeloid neoplasm was performed on a subset of cases.

Results: The demographic profile of AML-5q (M:F 8:6; 51-83 y/o) was not significantly different from the other 2 groups. 2 AML-5q cases with a history of myeloproliferative neoplasm and 1 case with a history of AML carrying normal karyotype were excluded from further analysis. Many AML-5q cases (67%) demonstrated small/hypolobated megakaryocytes and the average platelet count at initial presentation was 111 K/ μ l (28-279), which was not significantly different from AML-5q plus. 0/11 AML-5q cases but 32/123 AML-5q complex cases were therapy-related ($p=0.06$). AML-5q cases, not AML-5q plus, demonstrated a trend toward better survival when compared with AML-5q complex cases ($p=0.046$ including t-AML; $p=0.078$ excluding t-AML). TP53 mutations were found in 2/7 AML-5q cases and 8/10 AML-5q complex cases ($p=0.058$). 5/11 AML-5q patients received lenalidomide during their disease course.

Conclusions: AML-5q appeared less

likely when compared with AML-5q complex, despite demonstrating a similar demographic profile. A subset of AML-5q cases carried TP53 mutation but the incidence was likely lower than that in AML-5q complex. Mutation analysis of additional cases is in progress. Further validation of our findings will be important.

1498 **MYC-Rearrangement and MYC/BCL2 Double Expression but not Cell-of-Origin Predict Prognosis in de novo Diffuse Large B-Cell Lymphoma Treated with R-CHOP**

Jing-Lan Liu¹, L. Jeffrey Medeiros¹, Wenting Huang¹, Timothy McDonnell¹, Roberto Miranda¹, Carlos Bueso-Ramos¹, Ellen Schlette¹, Pei Lin¹, Shaoying Li¹. ¹The University of Texas MD Anderson Cancer, Houston, TX

Background: Diffuse large B-cell lymphoma (DLBCL) can be classified as germinal center B cell-like (GCB) or activated B cell-like/non-GCB based on cell-of-origin (COO) classification. It is well reported that patients with GCB type DLBCL have a better prognosis than those with non-GCB type. However, a recent large prospective study showed that COO failed to predict prognosis in R-CHOP treated DLBCL patients.

Design: We performed a retrospective study to evaluate the prognostic significance of COO classification in 280 patients diagnosed with *de novo* DLBCL who received R-CHOP. CD10, BCL6, MUM1, MYC and BCL2 were assessed by immunohistochemistry with positive cut-offs of 30%, 30%, 30%, 40%, and 50%, respectively. Cases were divided into GCB and non-GCB types according to the Hans algorithm. MYC, BCL2 and BCL6 rearrangements were evaluated by fluorescence in situ hybridization. Overall survival (OS) was analyzed by Kaplan-Meier method and compared with log-rank test.

Results: There were 165 (66%) GCB type DLBCL, 85 (34%) non-GCB type, and 30 unclassifiable or lacked adequate data for classification. The study has focused on the 250 patients with COO defined. There were 162 men and 88 women with a median age of 62 years (range, 18-86). 45/250 (18%) cases harbored MYC-rearrangement (R), including 28 MYC/BCL2 double hit lymphoma (DHL) (of which 5 were triple hit lymphoma), 5 MYC/BCL6 DHL, 12 cases with only MYC-R or BCL6 not tested. The frequency of MYC-R was much higher in GCB than in non-GCB tumors (40/165, 24% versus 5/85, 6%) ($p=0.0001$). MYC/BCL2 double expression (DE) was observed in 53/130 (41%) cases. Survival analysis showed that COO classification failed to predict OS in DLBCL patients ($p=0.07$), and

surprisingly, GCB type had a tendency toward poorer OS, likely related to the significantly higher frequency of MYC-R in the GCB group. When cases with MYC-R were excluded, COO still did not correlate with OS ($p=0.27$). In contrast, MYC-R and MYC/BCL2 DE significantly correlated with inferior OS ($p=0.0001$ and $p=0.001$ respectively). Within the GCB group, BCL2-R was associated with a worse OS ($p=0.02$), however, the prognostic effect was lost when cases with MYC-R were excluded ($p=0.31$).

Conclusions: In this retrospective study, COO classification failed to stratify the outcomes of DLBCL patients treated with R-CHOP. In contrast, MYC-R and MYC/BCL2 double expresser were significant adverse prognostic factors for DLBCL patients.

1499 **Primary bone lymphoma: Clinicopathologic analysis of 18 cases**

Xin Liu¹, Catherine Luedke², Rachel Jug³, Anand Lagoo², Endi Wang⁴. ¹Duke University Medical Center, Cary, NC, ²Duke University Medical Center, Durham, NC, ³Duke Health, Durham, NC, ⁴Duke University Medical Center

Background: Primary bone lymphoma (PBL) comprises <1% of non-Hodgkin lymphoma, and the majority are diffuse large B-cell lymphoma (DLBCL). The pathologic diagnosis is sometimes difficult due to distorted morphology and absent flow cytometric analysis in many cases.

Design: Eighteen cases of PBL were identified from our databases (2014-2016), and retrospectively analyzed.

Results: Of the 18 cases of PBL, 15 (83%) were DLBCL, 2 (11%) were follicular lymphoma, and 1 (6%) was unclassifiable small B-cell lymphoma (SBCL). Among DLBCLs, 7 (47%) were non-germinal center type, 4 (27%) were germinal center type, and 4 (27%) were unclassifiable. The median age was 55 years with a range of 20-86. Male/female ratio was 2:1. Fourteen patients presented with localized bone pain, 4 patients had systemic symptoms as initial complaint. At diagnosis, 69% (9 out of 13) patients had anemia, 23% (3 out of 13) had thrombocytopenia, and 45% (5 out of 11) had elevated LDH. None had serum hypercalcemia. Radiographic imaging demonstrated femoral/pelvic bone lesions in 61%, and 62% of the cases showed ≥ 2 lesional sites. Because lymphoma was not a major consideration, flow cytometry was not included on 50% of the cases. Histologic section showed distorted morphology and extensive necrosis in 50% of the cases, and neoplastic large cells were scattered and obscured by intense reactive small lymphocytes in 40% of DLBCLs. Nonetheless, the lymphomatous involvement was highlighted by immunohistochemistry in all except for one case (SBCL). Three cases had IGH/K gene rearrangement analysis performed, and all were positive. Flow cytometry detected clonal populations in 8 out of 9 (89%) cases. All DLBCLs and one follicular lymphoma were treated with standard DLBCL regimens, and two of them received chemoradiation therapy. The other 2 cases were treated with an indolent B-cell protocol. Twelve (67%) patients achieved clinical remission, 5 (28%) died of disease recurrence/complications, and 1 patient was lost to follow up. At a median follow-up of 16 months, the progression-free survival was 62%.

Conclusions: Because of nonspecific radiographic features and often distorted histology, diagnosis of PBL needs a multidisciplinary approach. Immunohistochemistry seems most critical for the diagnosis, but careful evaluation is required to overcome morphologic distortion in certain cases. Our data suggests PBL responds to therapy similarly to the conventional DLBCL; though a conclusive comparison requires a longer follow up.

1500 **Type-I Interferon Signature in Cutaneous Blastic Plasmacytoid Dendritic Cell Neoplasm**

Luisa Lorenzi¹, Donatella Vairo¹, Andrea Bernardelli¹, Silvia Lonardi¹, Simona Fisogni¹, Mattia Bugatt¹, Sara Licini¹, Silvia Giliani¹, Fabio Facchetti¹. ¹University of Brescia, Brescia, Lombardia, ²Spedali Civili di Brescia

Background: Blastic Plasmacytoid Dendritic Cell Neoplasm (BPDCN) is an aggressive disease due to clonal proliferation of Plasmacytoid Dendritic Cells (PDC) precursors. PDC are specialized type-I interferon (IFN-I) producing cells and accumulate in tissues in IFN-related diseases e.g. Lupus Erythematosus (LE). Expression studies of IFN-I stimulated genes (ISG) on peripheral blood (IFN-I signature, IFN-S), correlate with disease activity in LE patients. IFN-I production in BPDCN is debated; neoplastic cells produce IFN-I at low levels, after *in vitro* stimulation. BPDCN express the IFN-induced protein MxA, however, on skin, its stain is limited to neoplastic infiltrate and absent in the epidermis, differently from cutaneous LE.

Design: By immunohistochemistry, we scored MxA and phosphorylated-STAT1 (pSTAT1) expression, in dermal infiltrate and epidermis, on 71 FFPE skin biopsies including 18 cutaneous BPDCN (cBPDCN), 24 cLE, 16 Acute Myeloid Leukemia (cAML) and 13 unaffected skin (US). Evaluation of IFN-S by qRT-PCR of 7 ISG (RSAD2, IFI27, IFIT1, MXA, ISG15, SIGLEC1, STAT1) was performed in 23 cases: 5cBPDCN, 7cLE, 5cAML and 6 US.

Results: cLE showed high expression (score 3-4 over 4) of both MxA and pSTAT1 on dermal infiltrate (92% and 71%) as well as on the above

epidermis (92% and 88%). On BPDCN MxA was high on tumor cells in 78% of cases while the epidermis was negative in more than half (score 0 in 53%); adversely, pSTAT1 was low or negative (score 0-2) in both cell subsets (83% and 88%, respectively). MxA and pSTAT1 were expressed at low levels (score 0-2) in cAML on tumor cells (75%, 100%) as well as on keratinocytes (80%, 80%). cBPDCN IFN-S showed high expression of 6/7 ISG compared with US ($p < .05$), however, compared with cLE, BPDCN had lower expression of *RSAD2* and *IFIT1* ($p = .0013$). cBPDCN levels of *MXA* and *ISG15* were absolutely higher than in cAML ($p < .05$).

Conclusions: BPDCN is associated with expression of IFN-I related markers, confirming its PDC derivation, but its profile differs from what observed in cLE. On cBPDCN MxA and pSTAT1 expression is limited to tumor infiltrate and not induced in the overlying epidermis. Furthermore, BPDCN has deficient gene expression of *RSAD2* and *IFIT1* while scoring high levels of *MXA* and *ISG15*. These data suggest that BPDCN is associated with an incomplete IFN-S which may be due to a "resting" stage of neoplastic PDC and explains the lack of IFN related symptoms in these patients.

1501 IgM Plasma Cell Myeloma: Clinicopathologic and Molecular Evaluation of a Rare Entity

Haiyan Lu¹, Lisa Durkin², Xiaoxian Zhao², Megan Nakashima²
¹Cleveland Clinic, Beachwood, OH, ²Cleveland Clinic, Cleveland, OH

Background: Immunoglobulin M plasma cell myeloma (IgMPCM) is a rare entity which may be difficult to distinguish from other IgM-related neoplasms. The study aims to characterize the clinicopathologic features of IgMPCM, including *MYD88* mutation status.

Design: We searched our institutional archives for cases diagnosed with IgMPCM from 1/1/2008-6/1/2017. Cases were reviewed and additional information retrieved from the electronic medical record. *MYD88* L265P mutation analysis was performed by allele-specific PCR.

Results: Eight cases of IgMPCM were identified. Gender distribution was equal. Median age at diagnosis was 63 years (range 39-85). Initial presenting symptoms included pathologic fractures/lytic lesions (3/8, 37.5%), renal dysfunction (3/8, 37.5%), excess wound bleeding (1/8, 12.5%) and pancytopenia (1/8, 12.5%). Seven patients met criteria for symptomatic myeloma: hypercalcemia (3/8, 37.5%), renal dysfunction (3/8, 37.5%), and lytic bone lesion (3/8, 37.5%). The remaining patient was positive for t(11;14).

Serum monoclonal protein analysis showed an IgM paraprotein in seven (87.5%) cases, the eighth had serum free lambda light chain and plasma cells were positive for IgM by immunohistochemistry. CD138-positive plasma cell burden at diagnosis ranged from 5-80% (average 36.25%). Five cases (62.5%) had lymphoplasmacytic cytology. Cyclin D1 expression was common (6/8, 75%), including two which were positive for t(11;14) by FISH. Among the other two cases with FISH testing was one del13q14. Seven patients (88%) were given myeloma immunochemotherapy with three also receiving autologous stem cell transplant. Median follow up was 68 months (range 11-120). All patients were alive at last follow-up except one patient who received rituximab, cyclophosphamide, vincristine and transplant. Two tested cases were negative for *MYD88* L265P mutation; the remaining cases are pending.

Conclusions: Currently distinguishing IgMPCM from other IgM-related disorders requires correlation with clinical, laboratory, and radiologic findings. Prognosis in our patients was good when treated with myeloma-directed protocols suggesting these lesions are biologically more similar to other (IgG, IgA) myelomas than B-cell lymphomas. Exclusion of *MYD88* L265P may be useful for diagnosing IgMPCM, and be further evidence of its biological nature.

1502 TOX expression correlates with nodal progression of cutaneous T cell lymphoma

Ying Lu¹, Rekha Bhat¹, Eric Vonderheid¹, J. Steve Hou¹. ¹Drexel University College of Medicine, Philadelphia, PA

Background: Cutaneous T-cell lymphomas (CTCL) are a heterogeneous group of T-cell lymphoproliferative disorders involving the skin, with skin-associated peripheral lymph nodes involvement. Thymocyte selection associated high mobility group box protein (TOX) is a transcription factor with a role in the development of CD4+ T cells, including downstream effects on the expression of RUNX 3, a well-known tumor suppressor gene. Multiple immune checkpoint proteins, such as Lymphocyte-activation gene 3 (LAG-3), PD-1, PD-L1 have been reported as therapeutic targets for clinical trials for multiple tumor types. The aim of this study is to examine the expression of TOX, LAG-3, PD-1 and PDL-1 in detecting early nodal involvement and disease progression in CTCL.

Design: 52 lymph nodes from patients with a history of CTCL as well as 21 reactive lymph nodes from patients without history of hematopoietic disease were evaluated by immunohistochemistry (IHC) with tissue microarray. 18 of 52 lymph nodes were involved by CTCL and 34 of 52 lymph nodes did not show morphologic,

immunohistochemical and flow cytometry evidence of disease, diagnosed as dermatopathic lymphadenopathy (DL). The expression of TOX, LAG-3, PD-1 and PDL-1 were reviewed by 3 independent pathologists and scored as negative (less than 5% of tumor cells with staining), focal positive (5% to 20% of tumor cells with staining), or diffuse positive (more than 20% of tumor cells with staining). Staining intensity was scored as negative, intermediate and strong.

Results: TOX showed diffuse and intense nuclear positivity in the neoplastic cells in 16 of 18 lymph nodes involved by CTCL, and 8 of 34 lymph nodes without CTCL involvement; focal positivity was seen in 18 of 34 lymph nodes without CTCL involvement. Reactive lymph nodes showed focal intermediate nuclear TOX positivity in follicle and interfollicular area. For CTCL with nodal involvement, LAG3 was diffusely positive (2/18) and focally positive (4/18). For DL lymph nodes, LAG3 was focally positive (17/34). Only few lymph nodes with CTCL involvement were positive for PD-1 and PDL-1.

Conclusions: TOX expression is increased in neoplastic cells of CTCL with correlation with nodal progression. LAG-3 might be another potential marker. Further studies involving larger data sets and clinical correlation may provide validation for the utility of TOX and LAG-3 analysis as early detection marker of disease progression and possible therapeutic target.

1503 Persistent Clonal Cytogenetic Abnormalities in "Normal" Bone Marrow Status Post Chemotherapy for Acute Leukemia: Evidence of Occult Myelodysplastic Syndrome and Predictor of Dismal Clinical Outcomes

Catherine Luedke¹, Rachel Jug², Xin Liu³, Chad McCall¹, Anand Lago¹, Endi Wang⁴. ¹Duke University Medical Center, Durham, NC, ²Duke Health, Durham, NC, ³Duke University Medical Center, Cary, NC, ⁴Duke University Medical Center

Background: In acute leukemia (AL) arising from myelodysplastic syndrome (MDS), chemotherapy rarely induces return to a preexisting chronic, MDS phase. In addition, cases of de novo AL regressing to MDS after therapy are seldom noted, resulting in little understanding of this phenomenon in the literature.

Design: We identified 4 cases with morphologic remission but with sustained clonal cytogenetic abnormalities status post chemotherapy for de novo AL. These were retrospectively analyzed.

Results: All 4 patients were male. The median age was 67 years, ranging from 23-76, at the time of initial diagnosis. Three patients (cases 2-4) presented with leukocytosis and anemia/thrombocytopenia, while the other (case 1) had pancytopenia. All 4 cases showed replacement of bone marrow with blasts that were confirmed to be B-lymphoblasts (B-ALL) in cases 1 and 2 and predominantly promonocytes (AML-M5b) in cases 3 and 4. Clonal cytogenetic abnormalities were detected in all cases, including complex abnormalities with subclone heterogeneity in cases 1 and 2, -7/+11 in case 3, and t(10;14) in case 4. After chemotherapy, all cases demonstrated trilineage hematopoiesis with no appreciable leukemia by morphology or flow cytometry. However, conventional cytogenetics detected persistent stem line clones in cases 1 and 2, +8, a novel abnormality, in case 3, and the original clone in case 4. High fractions of these abnormalities were confirmed by FISH analysis. Patients 1-4 relapsed in 6.5, 10, 13.7, and 3.5 months, respectively, following induction. Of these 4 cases, cases 1 and 2 demonstrated lineage switch at relapse, converting from B-ALL to AML. Cytogenetic studies demonstrated persistent stem line abnormalities in all 4 cases with evidence of continued clonal evolution in cases 1-3. Patients 1-3 died 59, 4, and 106 days after relapse, respectively, while patient 4 is currently being considered for stem cell transplant.

Conclusions: The frequent complex cytogenetic abnormalities with evidence of clonal evolution suggest genomic instability whereby stem line abnormalities occur at an early hematopoietic progenitor stage followed by the generation of heterogeneous subclones with various differentiation potentials that could be selected by certain therapies. Furthermore, retention of cytogenetic abnormalities in morphologic "remission" marrow status post chemotherapy for AL may suggest a preceding, occult MDS and predict early relapse with dismal clinical outcomes.

1504 Myeloid Neoplasms (MN) Associated with Chronic Lymphocytic Leukemia/Small Lymphocytic Lymphoma (CLL/SLL) and Other Indolent B-Cell Lymphomas (iBCL): A Clinicopathologic Study of 32 Cases

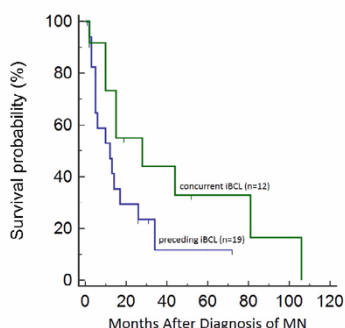
Catherine Luedke¹, Lianhe Yang², Rachel Jug³, Jonathan Galeotti⁴, Endi Wang⁵. ¹Duke University Medical Center, Durham, NC, ²Duke Health, ³Duke Health, Durham, NC, ⁴University of North Carolina, ⁵Duke University Medical Center

Background: While MNs, either subsequent to or concurrent with iBCLs, are unusual, they do occur. Studies comparing therapy-related and concurrent MNs in this setting are rare, resulting in decreased

understanding of pathogenesis and outcomes.

Design: We identified 32 cases of MNs in patients with preceding or concurrent iBCL over a 17 year period from 1999 to 2016. The clinicopathologic features were retrospectively analyzed.

Results: Of 32 cases, 22 were male, and 10 were female. The median age was 66.5 (range: 32-91) at the time of iBCL diagnosis, and 70.5 (range: 35-91) at the time of MN diagnosis. 19 of the cases had MNs diagnosed following an iBCL, while the remaining 13 cases had concurrent diagnoses. For cases with a preceding iBCL, the median interval between diagnoses was 72 months (range: 3-276), while the median interval between treatment and the development of MN was 56 months (range: 6-204). 22 of the iBCLs were CLL, while the remaining 10 cases involved others. The majority of iBCL treatment involved variable combinations of chlorambucil, bendamustine, cyclophosphamide, fludarabine, and rituximab. The types of MNs included myelodysplastic syndrome (MDS) in 12 cases, acute myeloid leukemia (AML) in 10 cases, myeloproliferative neoplasm (MPN) in 8 cases, and MDS/MPN in 2 cases. Documented cytogenetic studies were found in 27 of the total cases. Of those documented cases with preceding iBCL, 88% (15/17) showed clonal cytogenetic abnormalities, including 76% (13/17) with -7/7q-, 5q-, or complex cytogenetics, whereas those with concurrent iBCL exhibited clonal cytogenetics in 60% (6/10) of cases, of which 30% (3/10) were -7/7q-, 5q-, or complex cytogenetics (OR= 7.58, CI= 1.3-43.9, p= 0.02). Follow-up information was available in 19 and 12 cases, respectively, with median follow-up of 12 months (range: 1-81). Median overall survival for patients with preceding iBCL was 10 months, (95% CI= 5-26) in contrast to 17 months (95% CI= 10-81) for those with concurrent iBCL.



Conclusions: While the use of treatments such as alkylating agents in iBCLs has been implicated in the development of MNs, therapy-related MNs remain low despite frequent use, and the mechanism is uncertain. We found the percentage of adverse cytogenetics and outcomes in those with preceding iBCL more comparable to other therapy-related MNs than those with concurrent iBCL, which resembled de novo MNs. While treatment appears to play a role, the degree of intrinsic predisposition of iBCLs for certain MNs requires further study.

1505 IDH2 R172 Mutated Myeloid Malignancies Show Distinct Mutational Profiles Compared to Cases with IDH1 and IDH2 R140 Mutations

Nick Luem¹, Philippe Szankas², Todd Kelley³, Jay L Patel⁴. ¹University of Utah, Salt Lake City, Utah, ²ARUP Laboratories, ³ARUP Laboratories and University of Utah, Salt Lake City, UT, ⁴University of Utah and ARUP Laboratories, Salt Lake City, UT

Background: IDH1 and IDH2 mutations are seen across the spectrum of myeloid malignancies and characteristically occur in one of three hotspots centered on arginine residues in the active site: R132 in IDH1, and R140 or R172 in IDH2. Although each of these mutations results in abnormal accumulation of the oncometabolite 2-hydroxyglutarate, prior studies hint that IDH2 R172 mutations may tend to occur in a distinct genetic context. We analyzed the mutation pattern of IDH2 R172 cases and compared to cases with IDH1 R132 or IDH2 R140 mutations in a large series of myeloid malignancies.

Design: This study was approved by the University of Utah IRB. Diagnostic peripheral blood or bone marrow samples from patients with IDH1 or IDH2 mutations (n=373) were subjected to targeted sequencing of a panel of fifty-seven genes known to be mutated in myeloid malignancies. Briefly, genomic DNA was extracted from bone marrow or peripheral blood leukocytes by the Puregene method (Qiagen), followed by library preparation and enrichment for regions of interest by solution capture (SureSelect, Agilent). Massively parallel sequencing was performed on Illumina platforms. Genetic variants were identified by the FreeBayes (single nucleotide variants and small insertions/deletions) and Pindel (larger insertions/deletions) software programs. Variants detected were subjected to a rigorous manual curation process.

Results: All IDH1 or IDH2 mutated cases showed co-mutation of one or more sequenced genes. Mutations in IDH1 or IDH2 R140 demonstrated median VAFs higher (39.8%) than IDH2 R172 (24.5%). No cases of co-mutation of NPM1 and IDH2 R172 were observed (p<.001). IDH2 R172 mutated cases showed preferential co-mutation of cell-signaling genes such as BCOR/BCORL1 (43%, p<.001). Spliceosome (e.g. SF3B1, SRSF2, U2AF1, ZRSR2) and cohesin complex (e.g. RAD21, SMC1A, SMC3, STAG2) genes were rarely co-mutated with IDH2 R172. Only one case of concurrent IDH1 and IDH2 R140 mutations were observed.

Co-mutated Gene	IDH1 R132 n=149	Median VAF (%)	IDH2 R140 n=189	Median VAF (%)	IDH2 R172 n=35	Median VAF (%)
ASXL1	38 (25.5%)	18.1	45 (23.8%)	22.8	6 (17.1%)	16.0
BCOR	12 (8.1%)	44.5	14 (7.4%)	69.3	11 (31.4%)	33.7
BCORL1	6 (4.0%)	10.9	1 (0.5%)	5.2	4 (11.4%)	2.5
CALR	0	0	1 (0.5%)	3.0	0	0
CBL	4 (2.7%)	2.2	10 (5.3%)	37.9	0	0
CEBPA	4 (2.7%)	9.6	9 (4.8%)	13.6	0	0
CSF3R	1 (0.7%)	3.6	5 (2.6%)	19.8	2 (5.7%)	9.6
DNMT3A	48 (32.2%)	39.6	49 (25.9%)	37.3	17 (48.6%)	33.7
EZH2	5 (3.4%)	35.8	4 (2.1%)	35.4	1 (2.9%)	24.7
FLT3-ITD	11 (7.4%)	12	23 (12.2%)	7.0	4 (11.4%)	31.3
FLT-TKD	9 (6.0%)	11.3	12 (6.3%)	12.0	0	0
IDH1 R132	149 (100%)	34.1	1 (0.5%)	15.3	0	0
IDH2 R140	1 (0.7%)	20.9	189 (100%)	41.8	0	0
IDH2 R172	0	0	0	0	35 (100%)	24.5
JAK2	10 (6.7%)	18.9	19 (10.1%)	65.3	1 (2.9%)	22.5
KIT	1 (0.7%)	12.6	2 (1.1%)	55.5	0	0
KRAS	7 (4.7%)	12.9	12 (6.3%)	31.7	0	0
MPL	1 (0.7%)	23.3	4 (2.1%)	37.8	0	0
NPM1	39 (26.2%)	16.3	48 (25.4%)	17.3	0	0
NRAS	20 (13.4%)	14.9	29 (15.3%)	13.2	6 (17.1%)	10.9
PTPN11	16 (10.7%)	6.6	7 (3.7%)	13.4	0	0
RAD21	2 (1.3%)	26.5	0	0	0	0
RUNX1	28 (18.8%)	34	25 (13.2%)	18.3	7 (20%)	18.3
SETBP1	2 (1.3%)	43.2	3 (1.6%)	5.4	0	0
SF3B1	5 (3.4%)	36.8	6 (3.2%)	27.2	1 (2.9%)	19.7
SMC1A	3 (2.0%)	5.0	4 (2.1%)	32.1	0	0
SMC3	2 (1.3%)	28.0	6 (3.2%)	35.5	0	0
SRSF2	40 (26.8%)	34.4	85 (45%)	40.2	0	0
STAG2	9 (6.0%)	36.3	32 (16.9%)	38.4	2 (5.7%)	41.8
TET2	15 (10.1%)	27.7	12 (6.3%)	23.4	4 (11.4%)	1.3
TP53	12 (8.1%)	52.1	14 (7.4%)	44.6	3 (8.6%)	40.5
U2AF1	6 (4.0%)	34.5	7 (3.7%)	40.5	3 (8.6%)	13.0
ZRSR2	4 (2.7%)	71.2	1 (0.5%)	61.0	0	0

Conclusions: These data show that IDH2 R172 mutated myeloid neoplasms show different patterns of co-mutated genes compared with IDH1 R132 or IDH2 R140-mutated cases. Analysis of VAFs suggests that IDH2 R172 mutations are subclonal and may represent secondary events preceded by founder mutations in genes associated with recently described preclinical states such as clonal hematopoiesis of indeterminate significance. Gene-gene interactions are likely at work in the pathogenesis of myeloid neoplasms with mutated IDH2 R172.

1506 Prevalence, Clinical Characteristics and Prognosis of EBV-Positive Follicular Lymphoma

Nicholas Mackrides¹, Jennifer Chapman², Melissa C Larson³, Andrew Feldman⁴, Izidore S Lossos⁵, Offiong F Ikpat⁶, Yaohong Tan⁷, Sergei Syrbul⁸, Stephen M Ansell⁹, Thomas M Habermann¹⁰, Brian K Link¹¹, James R Cerhan¹², Francisco Vega¹³. ¹University of Miami/Sylvester Cancer Center, Hallandale Beach, FL, ²University of Miami/Sylvester Cancer Center, Miami Shores, FL, ³Mayo Clinic, ⁴Mayo Clinic, Rochester, MN, ⁵University of Miami/Sylvester Cancer Center, ⁶Univ. of Iowa, Iowa City, IA, ⁷Mayo Clinic, ⁸University of Iowa, ⁹University of Miami/Sylvester Cancer Center, Coral Gables, FL

Background: We recently reported that 2.6% of follicular lymphoma (FL) cases in a clinical series of 382 patients were EBV+ (Mod Pathol 2017;30:519-29). In that study, the EBV+ FL progressed to either a higher grade FL or to diffuse large B-cell lymphoma (DLBCL), raising the question of whether EBV+ FL represents a more aggressive FL subgroup. The goal of this study was to confirm the prevalence of EBV in a cohort of community-based patients with FL and correlate EBV status with clinicopathological features and prognosis.

Design: Patients with FL were prospectively enrolled in the University of Iowa/Mayo Clinic SPORC Molecular Epidemiology Resource (MER) cohort study from 2002-2015. Tissue microarrays (N=25) were assembled using tissue from diagnostic biopsies. HIV patients were excluded, as were cases with a second histology. TMA were stained for EBER by in situ hybridization, and for LMP1 and EBNA2 by IHC. EBV+ FL were those with tumor cells positive for one or more markers. Cases with staining of only 'bystander' non-neoplastic lymphocytes were considered negative. Event-free survival (EFS) was defined as time from diagnosis to relapse/progression, retreatment, or death due to any cause. Early events were defined as failing to achieve EFS at 12 months (EFS12). We estimated hazard ratios (HRs) and 95% CIs for EFS and overall survival (OS) from Cox models, adjusted for age and sex.

Results: 491 cases were available for analysis, of which 43 (8.9%) were EBV-positive, 418 (85%) were EBV-, and 30 (6.1%) were equivocal and were excluded from further analysis. The mean age was 63 years for EBV+ compared to 58 years for EBV- FL (P=0.036). There was no association of EBV status with gender, grade, stage, LDH, performance status, number of nodal groups or FLIPI (Table). Initial therapy included immunochemotherapy (41%), observation (34%), R-monotherapy (11%), and radiotherapy only (6%). Through 2017, there were 295 events and 95 deaths. EBV+ status was not associated with EFS (HR=1.00, 95% CI 0.67-1.50) or OS (HR=1.41, 95% CI 0.82-2.43) overall or among those treated initially with immunochemotherapy. There was also no association of EBV status with EFS12 (P=0.45).

Characteristic	EBV- (N=418)	EBV+ (N=43)	P-value
Gender			0.86
Female	193 (46%)	21 (49%)	
Male	225 (54%)	22 (51%)	
Grade			0.24
I-II	352 (84%)	33 (77%)	
IIIa/b	66 (16%)	10 (23%)	
Stage			1.0
I-II	130 (31%)	13 (30%)	
III-IV	288 (69%)	30 (70%)	
LDH			0.83
≤Normal	278 (75%)	29 (78%)	
>Normal	91 (25%)	8 (22%)	
Performance Status			0.23
<2	395 (94%)	43 (100%)	
2+	23 (6%)	0 (0%)	
# Nodal Groups			1.00
≤4	249 (61%)	25 (60%)	
>4	161 (39%)	17 (40%)	
FLIPI			0.65
0	53 (13%)	3 (7%)	
1	105 (25%)	11 (26%)	
2	153 (37%)	14 (33%)	
3	79 (19%)	11 (26%)	
4	24 (6%)	4 (9%)	
5	4 (1%)	0 (0%)	

Conclusions: The prevalence of EBV+ FL was 8.9%, considerably higher than the 2.6% in our previous study. Beyond older age of EBV+ cases, there was no correlation with clinical characteristics, disease progression, or OS. Similar to DLBCL, EBV does not appear to correlate with disease aggressiveness in immunocompetent North American patients.

1507 Metabolomic Profiling of Follicular Lymphoma: A Proof-of-Principle Study

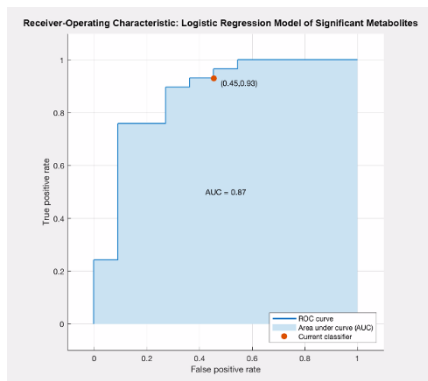
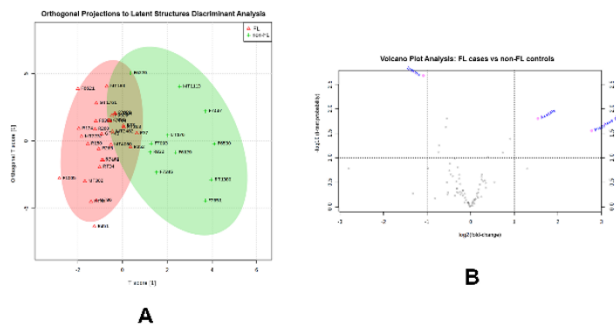
Etienne Mahe¹, Mohammad M Banoee², Adnan Mansoor¹, Hamid Habib³, Douglas Stewart⁴, Meer-Shabani Taher-Rad⁵. ¹University of Calgary, Calgary, AB, ²University of Calgary, ³University of Calgary/Calgary Laboratory Services

Background: Follicular lymphoma (FL) is one of the most commonly diagnosed lymphomas. Recent decades have led to better understanding of FL, especially in areas of molecular biology. While molecular changes might presume to result in metabolic derangement, efforts to study the metabolomics of FL are lacking. Metabolomics is the study of sets of metabolites present in a tissue; as applied to cancer research, these can provide a snapshot of metabolic derangement with a potential for biomarker discovery.

Design: We sought to identify an FL metabolomic signature by comparing a set of FL cases to non-FL controls. In partnership with the Alberta Cancer Research Biobank (ACRB), high-quality cryopreserved lymph node samples were studied. These were homogenized and subjected to methanol/chloroform extraction. Quantitative 1H-NMR spectroscopy was performed; signals were assigned to metabolites using the Chenomx NMR Suite (Edmonton, AB). Unsupervised analysis employed Orthogonal Projections to Latent Structures Discriminant Analysis (OPLS-DA). Using diagnosis classification, Volcano Plot Analysis was performed (p<0.05, fold-change>2). Significant features were input to logistic regression (with 5-fold cross-validation); results were assessed using Receiver-Operator Characteristic (ROC) analysis. MetaboAnalyst (v3.0, McGill University) and MATLAB (vR2016b, MathWorks, Natick, MA) software suites were employed.

Results: We obtained 29 FL and 11 non-FL specimens in the ACRB biobank. Clinical data were available for all but 3 FL cases, summarized in Table 1. Metabolomic analysis identified 75 metabolite signals. These data were input to OPLS-DA, Figure 1A, highlighting segregation of FL cases from non-FL controls. Volcano plot analysis is highlighted in Figure 1B, yielding a list of differentially-enriched metabolites (FL vs non-FL); the most significantly differentially-enriched metabolites included inosine, acetate and propylene glycol. With these metabolite concentrations as variables, logistic regression yielded the ROC curve of Figure 2, with an Area-Under the curve of 0.87.

Parameter	Available Clinical Data, n=26	
Age	Mean	58.5 years
	Median	57 years
	Range	31-83 years
Sex	Female	11 (42%)
	Male	15 (58%)
Grade	1-2	22 (84%)
	3	2 (8%)
	Not Available	2 (8%)
Clinical Stage	I/II	7 (27%)
	III/IV	18 (69%)
	Unknown	1 (4%)
FLIPI	Low-risk	17 (65%)
	Intermediate-risk	6 (23%)
	High-risk	3 (12%)
Lymph Node Bulk	All nodes ≤ 6 cm	11 (42%)
	Any node > 6 cm	7 (27%)
	Unknown	8 (31%)
Median Clinical Follow-up		53 months
Median Time-to-Treatment		8.5 months
Deaths	Total	4 (16%)
	From Disease	2 (8%)



Conclusions: We have performed, to our knowledge, the first metabolomic study of follicular lymphoma. Our results suggest that an FL-specific metabolomic signature exists, however additional studies comparing the metabolomic profile of FL relative to more aggressive lymphomas are needed. These results might motivate the future metabolomic analysis of peripheral blood, perhaps as a means of non-invasive disease assessment.

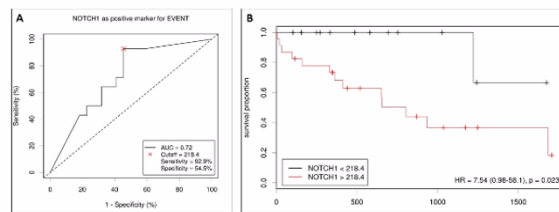
1508 Prognostic Implications of Notch1 Activation Through Non-canonical Pathway Among Young Patients with Normal Karyotype Acute Myeloid Leukemia (AML)

Mohammad O Mansoor¹, Ghaleb Elyamany², Fahad Farooq¹, Mohammad K Mughal¹, Meer-Shabani Taher-Rad³, Ariz Akhter¹. ¹University of Calgary, ²Prince Sultan Military Medical City, Riyadh, ³University of Calgary/ Calgary Laboratory Services

Background: Genetic heterogeneity drives clinical variation in AML patients with normal cytogenetics. Mutational analysis (FLT3/NPM1/CEBPA) has improved risk stratification but the response to conventional therapy is variable with frequent relapses. FLT3 targeted therapies are showing variable therapeutic responses. Hence, improved insight into the biology of AML, especially with normal cytogenetic is warranted to explore new therapeutic targets. Notch 1 is now established to play a key role in the prognosis of several hematological malignancies, however, its role in AML remains controversial. In this pilot study, we correlated Notch1 and associated pathway expression patterns with hematological data and overall survival (OS) among young AML patients with normal cytogenetics.

Design: RNA from diagnostic BM biopsies (n=36) were subjected to expression analysis employing nCounter Pan-Cancer pathway panel by Nanostring technologies. Laboratory and clinical data were correlated with expression of Notch1 and associated molecules.

Results: 36 AML patients (median age 56 yrs., range 18-66 yrs.) were dichotomized into low Notch1 (13/36;37%) and high Notch1 (23/36;63%) groups based on ROC curve analysis (72% AUC; 93% sensitivity /55% specificity). Age, gender, hematological data or molecular risk factors (FLT3/NPM1 mutation) exposed no significant differences across these two distinct Notch1 expression groups (P<0.483). Notch ligands (Delta-like 1,3,4 and Jagged 1,2) did not show significant differential Notch1 expression across two groups (P=0.1492); suggesting a non-canonical pathway of Notch1 activation in this pilot study. High expression of Notch1 correlated with Wnt signaling pathway modulator- Secreted-frizzled related protein 4 (SFRP-4) (>2.0 fold ; P<0.001) and several genes associated with micro-environment like Osteopontin, bone sialoprotein- IBSP, MMP-9 (>2.0 fold ; P<0.001) . High Notch1 was associated with high mortality (13/23 (57%) vs. 1/13; (8%) P<0.0048). Low Notch1 expressers showed better OS {740 days vs. 579 days; log-rank P=<0.023; HR 7.54 (0.98-54.1)}



Conclusions: Our pilot study identified high Notch1 expression through non-canonical pathway as an important poor prognostic marker among AML patients with normal cytogenetics. Notch1 expression is independent of conventional risk parameters and can be a potential therapeutic target.

1509 Leukemic transformation of Ph- MPN is associated with myelofibrosis, SRSF2 mutation and poor prognosis

Elizabeth Margolske¹, Leonardo Boiocch², Robert Hasserjian², John Philip³, Daniel Arber³, Attilio Orazi⁴. ¹NYP/Weill Cornell Medical College, New York, NY, ²Massachusetts General Hospital, Boston, MA, ³University of Chicago, Chicago, IL, ⁴Weill Cornell Medical College/ NYP, New York, NY

Background: The Philadelphia chromosome negative myeloproliferative neoplasms (Ph- MPN: Polycythemia vera [PV], essential thrombocythemia [ET], and primary myelofibrosis [PMF]) are chronic hematopoietic stem cell neoplasms with variable potential for progression to acute leukemia, also known as “blast phase” (MPN-BP). Little is known about the pathologic and molecular features of MPN-BP. We sought to investigate the clinical, laboratory, and genetic features of Ph- MPN-BP and compare them to a control group of de novo AML.

Design: We retrospectively identified cases of PV, ET, and PMF with transformation to acute leukemia (i.e. ≥20% blasts in peripheral blood or bone marrow). We excluded patients with concomitant malignancies, age <18, history of cytotoxic or radiotherapy, or patients with MDS/MPN. A control group of de novo AML was also identified. Appropriate statistical analyses were performed using R software for Windows.

Results: 34 cases of MPN-BP were identified (14 arising from PV, 12 ET and 8 PMF). The median age at transformation was 74 (range: 44-88). There were 17 men and 17 women. The median time to transformation was 5.7 years after diagnosis of an MPN. 42% had splenomegaly. Of the ET/PV patients, 42% had progressed to myelofibrosis at the time of transformation. Overall, 18 patients died of disease (6/12 PV; 7/12 ET; 5/8 PMF; p>0.05). At the time of transformation, the median overall survival was 1.6 years. In comparison to AML, NOS, there was no statistically significant differences in survival for MPN-BP. MPN driver mutations were seen in 82% of cases (JAK2 70%, CALR 6%, MPL 6%). The most common additional mutations were SRSF2 (33%), TET2 (26%), and TP53 (20%). NPM1 and CEBPA mutations were not identified in any case.

Conclusions: Blast phase or leukemic transformation is a late complication of chronic Ph- MPN associated with bone marrow fibrosis and splenomegaly. Assessment of prognosis in this study is limited due to the retrospective nature and the variable chemotherapy regimens. The prognosis appears poor, regardless of the initial subtype of MPN. Mutations in spliceosome genes such as SRSF2 at codon 95 were the most commonly observed genetic alterations in MPN-BP.

1510 Pathologic and Cytogenetic Characterization of Aggressive B-Cell Lymphomas with MYC Amplification

Lisa Marinelli¹, Rhett P Ketterling¹, Reid G Meyer¹, Ellen McPhail¹, Paul Kurtin¹, Rebecca L King¹. ¹Mayo Clinic, Rochester, MN

Background: While MYC translocation in B cell lymphoma (BCL) has been extensively studied, little is known about the significance of MYC amplification (amp), partly due to variable definitions used for “amp.” Recent studies have described increased aggressiveness in BCL with increased MYC copy number (3-10 copies per cell), suggesting alternative means of MYC overexpression may have prognostic significance. The goal of this study was to characterize the pathologic and cytogenetic features of patients with BCL showing MYC amp.

Design: We retrospectively reviewed the Mayo Clinic cytogenetic database for all cases of BCL with MYC amp seen by FISH from 2010 to 2017. MYC amp was defined as having increased MYC signals beyond 20 (ie. uncountable number of signals). All FISH studies reported as MYC amp were re-reviewed by a cytogeneticist to verify the level of amplification and the MYC probes involved in the amplicon.

Results: FISH analysis for MYC aberrations identified 39/7690 (0.5%)

cases with *MYC* amp. Of cases with available H&E, the most common diagnosis was diffuse large BCL (DLBCL)(83%; 24/29), followed by high grade BCL (14%, 4/29) and plasmablastic lymphoma (3%; 1/29). Among the 22 cases with Hans algorithm immunohistochemistry (IHC), 20(91%) were germinal center B-cell-like(GCB), and 2 (9%) were non-GCB. 18/24 (75%) cases were positive for BCL2 by IHC. *MYC* by IHC was $\geq 40\%$ in 9/12 (75%), $<40\%$ in 3, and not available in 27 cases. *MYC* amp probe signals appeared in a cloud-like distribution (possible double minutes or episomes) (77%) or in a single homogenous staining region (23%). Among 34 cases with amp in a *MYC* breakpoint probe, 18 (53%) had amp of 5' probe alone, 14 (41%) had amp of intact probes, and 2 (6%) had amp of the 3' probe alone. Four cases also had a *MYC-IGH* fusion, in addition to *MYC* amp. *BCL2* rearrangement was seen in 14/35 (40%) cases, and *BCL6* rearrangement in 2/32 (6%).

Conclusions: To our knowledge, this is the first study to characterize the pathologic and genetic features of BCL with strictly-defined *MYC* amp identified by FISH. These cases are usually DLBCL, GCB type, and may be *MYC* negative by IHC. The 5' signal alone, or the intact probe are most frequently amplified, and two distinct patterns of amp can be seen. A significant % of cases with *MYC* amp also have *BCL2* or *BCL6* translocation raising the question of whether this group could be similar to true "double-hit" lymphomas. Further research is warranted to understand the clinical significance of true *MYC* amp in BCL.

1511 Impact of Bone Marrow Biopsy Operator Experience on Biopsy Quality and Ancillary Testing Utilization

Lisa Marinelli¹, Hong Fang¹, Matthew Howard¹, Curtis Hanson¹, Rebecca L King¹. ¹Mayo Clinic, Rochester, MN

Background: Adequate bone marrow (BM) biopsies and aspirates are essential to the diagnosis and management of many hematologic diseases. Past research suggests a relationship between BM biopsy operator experience, length of interpretable marrow, and rate of correct diagnosis. Our study sought to compare the quality of BM biopsies and aspirates obtained by a trained team of nurses within our institution with those referred by outside institutions. In addition, we examined the relationship between the quality of BM and the use of ancillary studies.

Design: We evaluated all referred and in-house BM over a contiguous six week period. BM biopsies were assessed for the length of interpretable marrow, excluding artifact. Aspirates were assessed for the presence of spicules and BM elements. Sub-group comparisons included in-house (IH) BM obtained by a trained group of nurses within our institution, patients clinically referred (CR) to our institution whose outside-obtained BM specimens were evaluated at our institution, and outside pathologist referred (PR) pathology consultation cases. Ancillary study usage was compared between the first 100 cases of each group.

Results: A total of 1190 BM were analyzed, including 600 IH, 288 CR, and 303 PR cases. The average interpretable biopsy lengths of IH, CR, and PR cases were 17.1mm, 10.3mm, and 8.9mm respectively ($p<0.0001$). WHO recommended length of ≥ 15 mm was achieved in 61.4%, 26.6%, and 19.1%, respectively ($p<0.0001$). Of the aspirates analyzed among IH, CR, and PR cases, 93%, 71.3%, and 73.5% contained spicules respectively ($p<0.0001$). Among the cases assessed for ancillary testing, quality metrics were statistically similar to the entire cohort. Percent of cases with use of any IHC, flow cytometry, karyotype, and FISH was higher in CR and PR cases than in IH cases (all $p<0.05$). The average number of immunohistochemistry (IHC) stains was 1.5, 2.8, and 4.8 respectively ($p<0.0001$).

Conclusions: Operator experience significantly correlates with biopsy and aspirate quality. Increased use of ancillary testing correlates with, and is likely at least partly a result of, inferior specimen quality. While quality of preparation and stain are also important, having an adequate sample is an essential part of BM diagnostics and increased attention should be paid to ensuring quality samples via proper education and training.

1512 Expression of Myeloid cell Nuclear Differentiation Antigen (MNDA) in Nodal Marginal Zone Lymphoma (NMZL) and Follicular Lymphoma (FL)

Javier Martín López¹, Marcos Mauricio Siliézar², Santiago Montes-Moreno³, Laura Cereceda⁴, Miguel A Piris⁵. ¹Hospital Universitario Marqués De Valdecilla, Santander, Cantabria, ²Instituto de Cancerología de Guatemala, Guatemala, ³Hospital Universitario Marqués de Valdecilla/Idival, Santander, Cantabria, ⁴Hospital Universitario Fundación Jiménez Díaz, Madrid, Spain, ⁵Fundación Jiménez Díaz

Background: The diagnosis of Nodal Marginal Zone Lymphoma (NMZL) lacks reproducibility because of the absence of diagnostic immunohistochemical or molecular markers. Recently, new positive markers for marginal zone cell lymphoma have been reported that could help in the recognition of NMZL such as MNDA and immunoglobulin superfamily receptor translocation-associated 1

(IRTA-1). MNDA is expressed by cells of the myelomonocytic lineage, but has also been shown to be expressed by a B-cell subset that is located around the germinal center and inter-follicular regions.

We analyzed the immunohistochemical expression of MNDA in a large series of NMZL and Follicular Lymphoma (FL), and correlated the expression with other phenotypic, molecular or clinical markers.

Design: Biopsies of 80 NMZL and 80 FL were included in this study from the tissue archives of the Hospital Marqués de Valdecilla. The diagnosis was confirmed in all cases by a central review using standard tissue sections. By using the tissue microarray technique, we performed an immunohistochemical evaluation of BCL2, BCL6, CD10 and MNDA. Each case was scored for MNDA as negative, low expression (0-15% positive tumor cells) and high expression (15-100% positive tumor cells).

Results: MNDA positive neoplastic cells were identified in 59 NMZL (73,75%). In 46 out 59 (57,5%) cases the expression was strong and diffuse, in most cases delineating a nice pattern surrounding reactive germinal centres. The total amount of NMZL cases negative for MNDA was 21 (26,25%). MNDA expression was shown in only 7 (8,75%) FL, 6 of them with high expression. The majority of FL (91,25%) cases was negative for MNDA. MNDA positive FL cases were positive for BCL2, BCL6 and CD10.

Conclusions: According our results MNDA is frequently expressed in NMZL (in 73,75% cases), but only rarely in FL (in 8,75 %). MNDA expression constitutes a marker differentially expressed in NMZL and FL. MNDA expression is useful for the diagnosis of NMZL.

MNDA staining in a subset of FL cases allows also to investigate the clinical and molecular heterogeneity of FL cases.

1513 Identification of Genetic and Phenotypic Diversity Within NPM1-Mutated Acute Myeloid Leukemia With Biologic and Prognostic Implications

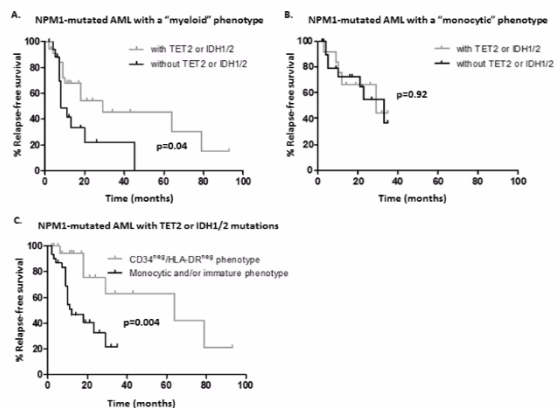
Emily Mason¹, Frank Kuo², Robert Hasserjian³, Adam Seegmiller¹, Olga Pozdnyakova⁴. ¹Vanderbilt University Medical Center, Nashville, TN, ²Brigham and Women's Hospital, Boston, MA, ³Massachusetts General Hospital, Boston, MA, ⁴Brigham and Women's Hospital, Southborough, MA

Background: Recent work has identified distinct molecular subgroups of acute myeloid leukemia (AML) with implications for disease classification and prognosis. *NPM1*-mutated AML now represents a distinct entity in the 2016 WHO classification. *NPM1* mutations are frequently associated with monocytic differentiation and often co-occur with mutations in genes that regulate DNA methylation, such as *DNMT3A*, *TET2*, and *IDH1/2*. However, despite much characterization of *NPM1*-mutated AML as a whole, relatively little work has examined the genetic and phenotypic heterogeneity within this group.

Design: We reviewed sequential (between 2014-2017) *NPM1*-mutated AML cases with flow cytometric, cytogenetic, and next generation sequencing (NGS) data collected as part of the clinical work-up at multiple institutions and correlated sequencing data with immunophenotypic and clinical findings.

Results: We identified 133 cases of *NPM1*-mutated AML (AML-NPM1), 130 of which showed additional pathologic variants in 26 genes. 49 (37%) showed monocytic differentiation by flow cytometry, while 84 (63%) lacked monocytic features (termed "myeloid AML-NPM1"). Mutations in genes that regulate DNA methylation were present in 79% of cases, with *TET2* and *IDH1/2* mutations being significantly more common in myeloid vs. monocytic AML-NPM1 (67% vs. 43%; $p=0.01$) and *DNMT3A* mutations being significantly less common in myeloid vs. monocytic AML-NPM1 (30% vs. 57%; $p=0.003$). *TET2* or *IDH1/2* mutations were associated with significantly longer median relapse-free survival (RFS) among cases of myeloid (29 mo vs. 8 mo; $p=0.04$) but not monocytic AML-NPM1 (Figure 1A-B). Myeloid AML-NPM1 with *TET2/IDH1/2* mutations frequently showed a unique CD34-negative, HLA-DR-negative phenotype (70% vs. 4% of myeloid AML-NPM1 lacking *TET2/IDH1/2* mutations and 4% of monocytic AML-NPM1; $p<0.001$), suggesting a more mature stage of blast differentiation in this subgroup. Importantly, these cases showed significantly longer median RFS compared both to *TET/IDH1/2*-mutated cases lacking this mature phenotype (64 mo vs. 12 mo; $p=0.004$) (Figure 1C) and to all other cases of *NPM1*-mutated AML (64 mo vs. 18 mo; $p=0.004$).

Figure 1. Relapse-free survival of NPM1-mutated AML



Conclusions: We show that *NPM1*-mutated AML harboring *TET2/IDH1/2* mutations shows significantly longer RFS when associated with a myeloid but not monocytic phenotype and that these cases are often characterized by a unique, mature immunophenotype. Our findings highlight biologic differences within *NPM1*-mutated AML that may impart prognostic significance.

1514 Clinical and Pathological Characterization of Immunophenotypic Variants of Mycosis Fungoides: A Single Institutional Experience

Tania Mendoza¹, Ling Zhang², Xiaohui Zhang³, Lubomir Sokol¹. ¹Moffitt Cancer Center and Research Institute, Tampa, FL, ²Tampa, FL, ³H. Lee Moffitt Cancer Center, Tampa, FL

Background: Mycosis fungoides (MF), a distinctive neoplasm of the skin effector memory T-cells, is the most common form of cutaneous T-cell lymphoma. Several clinical and pathologic/immunophenotypic variants of MF with specific therapeutic and prognostic implications have been described. We present clinicopathologic findings in 20 cases of mycosis fungoides with divergent phenotypes.

Design: MF cases with rare immunophenotypes were identified from the institutional pathology database (2014 – 2017). Integumentary examination, clinical course, treatment and patient outcome were analyzed; pathology glass slides including ancillary studies were reviewed.

Results: A total of 143 MF cases were identified. Of these cases, 20 showed immunophenotypic variants, including 15 CD4-/CD8+ cases and 5 CD4-/CD8- cases. There were 11 females and 9 males (M:F ratio = 1.2). Age at presentation ranged from 13 to 69 years (median 49 years). Site of Involvement, morphologic presentation of lesions, and clinical stage are listed in Table I. Morphologically, four patterns were observed: superficial dermal atypical lymphoid infiltrate (n=11), pagetoid reticulosis pattern (n=3), increased large cells (n=3) and dense dermal infiltrate (n=2). Phenotypically, the aberrancies included CD7 loss or partial loss (82%), CD5 loss (61.5%), and CD2 loss (40%). CD30 partial expression was present in 3 cases. Clonal T cell receptor gene rearrangement was observed in 13 of 15 tested cases. The patients received skin directed therapy, local radiation therapy, or systemic therapies. Three of the 15 CD4-/CD8+ cases showed disease progression, including the 2 cases with large cell transformation; of the 5 CD4-/CD8- cases, 4 cases demonstrated disease progression to multiple lesions, disease dissemination to soft tissue or brain, and systemic disease, and 2 patients succumbed to their disease.

Table 1. Clinical features of patients with immunophenotypic variants of MF

Site of involvement (n, %)	Presentation of lesions (n, %)	Clinical stage (n, %)
Lower extremities (10, 50%)	Erythematous (17, 85%)	IA (9, 45%)
Upper extremities (7, 35%)	Plaque and patches (13, 65%)	IB (6, 30%)
Abdomen (4, 20%)	Papules (1, 5%)	IIB (2, 10%)
Trunk/buttocks (3, 15%)	Tumor lesions (2, 10%)	IVA (1, 5%)
Foot (2, 10%)	Solitary nodule (2, 10%)	IVB (2, 10%)
	Poikilodermatous (1, 5%)	
	Blister like (1, 5%)	

Conclusions: Our study found that CD4-/CD8+ and CD4-/CD8- phenotypes are the most common MF immunophenotypic variants. A small subset of CD8+ MF cases may have a progressive course. The

rare cases with CD4-/CD8- phenotype demonstrate a more aggressive clinical course. Further clinicopathologic characterization is warranted for these unusual MF variants.

1515 PREVIOUSLY PUBLISHED

1516 Myeloid Blasts in Myeloid Neoplasm with Mutated NPM1 have a Characteristic Immunophenotype

Andres Moon¹, Xueyan Chen², David Wu¹, Jonathan Fromm¹, Lorinda Soma², Yi Zhou¹. ¹University of Washington, Seattle, WA, ²Seattle, WA

Background: AML with mutated *NPM1* shares a common genetic driver in leukemogenesis, and is now recognized as a distinct subtype in the revised WHO. However, unlike t(8;21) or inv(16), mutated *NPM1* is not considered an AML defining genomic lesion. In addition to AML, mutated *NPM1* is detected in other types of myeloid neoplasms that usually imminently progress to AML. Herein, we investigated whether myeloid neoplasms with mutated *NPM1* share common immunophenotypic abnormalities.

Design: Patients with mutated *NPM1* were identified in our molecular database. Only patients who had bone marrow biopsy with morphologic and in-house flow cytometric examination at initial diagnosis were analyzed. Morphologic and immunophenotypic features were reviewed in samples collected at diagnosis, after therapy and at relapse, if available. The myeloid neoplasms at diagnosis were classified based on the WHO criteria. Immunophenotyping was performed on a 10-color flow cytometer.

Results: Our cohort included 53 patients with a median age 59 years old (range 21-80). At diagnosis, there were 44 AML, 7 MDS with excess blasts and 2 secondary AML arising from myelofibrosis. Among 59 cases, 13 had FLT3-ITD and 3 had abnormal karyotype. Irrespective of morphologic enumeration of blasts and variable expansion of immature monocytes, common immunophenotypic abnormalities were detected on myeloid blasts in 52 of 53 cases. The abnormal immunophenotype was characterized by CD117-positive blasts with increased CD33 and CD123, variable CD7 and CD34, dysynchronous CD13 and HLA-DR and absence of CD15 and CD64. This abnormal immunophenotype on myeloid blasts was also present at disease relapse.

Conclusions: Myeloid blasts in AML and non-AML myeloid neoplasms with mutated *NPM1* appear to share a common immunophenotype indicative of disrupted myelomonocytic differentiation. While the clinical and morphologic features appear different in subtypes of diseases, the phenotypic variation may simply reflect differential myelomonocytic maturation from common leukemic blasts. This finding suggests that myeloid neoplasms with mutated *NPM1* likely represent a continuum of a common disease process that is detected at various stages of disease progression.

1517 Genetic Profiling of Pediatric Large B-cell Lymphoma

Ali Nael¹, Dolores B Estrine², Gordana Raca², Matthew Hiemenz², Jianling Ji², Ashley Hagiya³, Matthew J Oberley². ¹Los Angeles, CA, ²Children's Hospital Los Angeles, Los Angeles, CA, ³Pasadena, CA

Background: Diffuse large B-cell lymphoma (DLBCL) is a genetically heterogeneous mature B-cell neoplasm that occurs in all age groups. While overall survival is better for children than adults, novel, less toxic therapies are needed, and children who relapse face poor outcomes. Small studies to date suggest that significant genetic differences exist between pediatric and adult DLBCL. To further examine this, we have created a cohort of pediatric DLBCL cases for genetic profiling.

Design: 34 cases of B-cell NHL between 1992 and 2016 were identified from the CHLA archives. These cases were assembled into tissue microarrays and characterized using 2016 WHO diagnostic criteria. Chromosomal microarray (CMA) analysis was performed using the OncoScan platform and analyzed with Chromosome Analysis Suite software (Affymetrix). DNA sequencing was performed with the OncoKids panel (CHLA) on the Ion Torrent platform (Life Tech). Sequencing data was analyzed and curated with customized analysis software.

Results: Cases were categorized as: Germinal center B-cell (GCB; 13 cases) and activated B-cell (ABC; 8 cases) type DLBCL, Primary Mediastinal Large B-cell Lymphoma (PMLBCL; 7 cases), Mediastinal Grey Zone Lymphoma (3 cases), and IRF4-rearranged lymphoma (IRL; 3 cases). The median age for all cases was 14 years old, and deaths occurred in 32% of all cases. Known immunodeficiencies were present in 12% of cases. CMA testing identified multiple copy number alterations described previously in pediatric DLBCL cases and those described in both pediatric and adult DLBCL cases. Recurrent findings included gains at 9p24 (PDL1) in 57% of PMLBCL cases, 6p loss of heterozygosity (HLA loci) in 26% of all cases, and 12p gain in 32% of all cases (Figure 1). DNA sequencing of 7 cases to date has identified several mutations including EZH2 in DLBCL-GCB and MAP2K1 in IRL.

Recurrent likely germline variants were identified in PTEN and KMT2D.

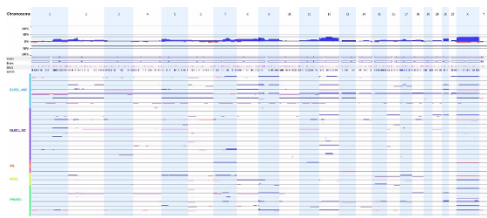


Figure 1. Chromosomal microarray analysis identifies multiple recurrent copy number gains, losses, and loss of heterozygosity in pediatric large B-cell lymphoma. Blue bars represent gains, Red bars represent losses, and purple represent loss of heterozygosity (LOH). Recurrent findings include: LOH: 92q24 gains in PMBCL and 12p gains among others; DLBCL: ABC: Diffuse large B-cell lymphoma, activated B-cell type; DLBCL: GC: Diffuse large B-cell lymphoma, germinal center B-cell type; IR: IR64: rearranged large B-cell lymphoma; MZL: Medial/interstitial grey zone lymphoma; PMBCL: Primary mediastinal large B-cell lymphoma.

Conclusions: Our cohort had a higher percentage of DLBCL-ABC cases relative to GCB cases than reported in the literature. Molecular subtyping of cases is underway by RNA expression analysis to confirm cell of origin results by immunohistochemistry. We identified recurrent copy number abnormalities and DNA mutations, some of which are enriched in pediatric lymphoma relative to adult cases. Recurrent alterations include 6p loss of heterozygosity which is postulated to result in immune escape by lymphoma cells. Additional DNA sequencing and RNA expression analysis is currently underway.

1518 Mutational Profile and Clinical Outcome in RUNX1-Mutated Acute Myeloid Leukemia, Not Otherwise Specified (AML, NOS) and Acute Myeloid Leukemia with Myelodysplastic-Related Changes (AML-MRC)

Lynh Nguyen¹, Ling Zhang², Xiaohui Zhang¹, Jinming Song³, Diana S Braswell⁴. ¹H. Lee Moffitt Cancer Center, Tampa, FL, ²Tampa, FL, ³Moffitt Cancer Center, Tampa, Florida, ⁴University of South Florida, Tampa, FL

Background: Acute myeloid leukemia with mutated RUNX1 is a new provisional entity in the WHO classification associated with worse prognosis in de novo AML, NOS with non-complex karyotype. Studies focusing on RUNX1 mutation in acute myeloid leukemia with myelodysplasia related changes (AML-MRC) are limited. This study aims to compare the clinical outcome and overall survival (OS) of patients with AML, NOS with mutated RUNX1 to those with AML-MRC with RUNX1 mutation.

Design: Retrospectively, 127 patients (2012-2017) with NGS data showing RUNX1-mutated AML were reviewed. Information on patients' initial bone marrow diagnosis, laboratory parameters, and molecular data were collected. Patients were further categorized as de novo AML, NOS or AML-MRC and compared. Paired t-test and Kaplan-Meier log rank analysis were used for statistical analysis.

Results: Of 127 patients, 61 were diagnosed with de novo AML, NOS and 66 with AML-MRC. Patients with de novo AML, NOS had a median age of 64 years (range 21-86) and were predominantly male (M:F, 42:19) while patients with AML-MRC had a median age of 73.5 years (range 26-91) also showing male predominance (M:F, 41:25). AML-MRC patients showed slightly shorter OS than de novo AML, NOS (median survival 11±3.3 months vs 19±7.1 months, p=0.265). When stratified for complex cytogenetics (≥3 cytogenetic aberrations) (AML-MRC, n=6; de novo AML, NOS n=6), the results were similar. The most frequently mutated genes in AML-MRC were DNMT3A (39.3%), SRSF2 (29.5%), ASXL1 (26.2%), and IDH2 (23.0%), while in de novo AML, NOS the common mutations were ASXL1 (42.4%), SRSF2 (27.3%), TET2 (19.7%), IDH2 (18.2%), and DNMT3A (15.2%). When the data was stratified for concurrent mutated genes, ASXL1 and TET2 mutations appeared to adversely affect OS in AML-MRC, but not de novo AML, NOS (RUNX1 vs RUNX1+ASXL1, p=0.019; RUNX1 vs RUNX1+TET2, p=0.001). DNMT3A mutation however, had increased negative impact on OS in de novo AML, NOS (RUNX1 vs RUNX1+DNMT3A, p=0.044) compared to AML-MRC (RUNX1 vs RUNX1+DNMT3A, p=0.126). Other concurrent gene mutations showed no effect on OS in

Conclusions: Patients with RUNX1-mutated de novo AML, NOS showed slightly superior OS over AML-MRC patients harboring RUNX1 mutation. Concurrent ASXL1 or TET2 mutation conferred worse OS in RUNX1-mutated AML-MRC; while co-mutation with DNMT3A had negative impact on de novo AML, NOS. Given the results of our pilot study, further investigation in larger multicenter cohorts is warranted.

1519 TP53 Protein Expression, But Not 17p13 Deletion, is Useful in Rapid Screening and Triage of TP53 Mutation in Acute Myeloid Leukemia

Nneamaka Nwaoduah¹, Belen Quereda Bernabeu¹, Zixuan Wang¹, Jinglan Liu¹, Guldeep Uppla², Stephen Peiper³, Jerald Gong¹. ¹Thomas Jefferson University Hospital, Philadelphia, PA, ²Glen Mills, PA, ³Sidney Kimmel Medical College, Philadelphia, PA

Background: TP53 mutation is associated with unfavorable cytogenetic

risk and poor clinical outcome in acute myeloid leukemia (AML). In a recent study by Welch et al, high risk AML patients (>60 years or relapsed) with TP53 mutations treated with single agent decitabine instead of standard anthracycline and cytarabine were found to achieve improved response and survival. In this study, we investigate the utility of TP53 expression and 17p13 deletion as rapid screening tools to predict TP53 mutational status and triage for further next generation sequencing (NGS) analysis in patients with AML and as such, facilitate the choice of induction therapy for these patients.

Design: We reviewed TP53 immunohistochemistry (IHC), fluorescence in situ hybridization (FISH) and NGS in 64 bone marrow cases with a diagnosis of AML. The cases included de novo AML (58/64), secondary AML (5/64), and therapy-related AML (1/64). The intensity of TP53 staining was graded on a scale of 0-3+ and percent of positive cells was graded in 5% increments. A cutoff of equal to or greater than 5% cells with 1+ or more intensity was considered as positive TP53 expression.

Results: Of the 64 cases, 31 (48%) were positive for TP53 expression, 21 (33%) were positive for 17p13 deletion, and 8 (12.5%) were positive for TP53 mutation. Fifteen cases (15/64) had both TP53 expression and 17p13 deletion. Of the 8 TP53 mutated cases, 5 cases had both positive IHC and FISH, 1 case had positive IHC but negative FISH, and the remaining 2 cases had both negative IHC and FISH. In the 1 case with positive IHC but negative FISH, there were double TP53 mutations indicating biallelic mutations, which correlated with the overexpression of p53 by IHC in the absence of 17p13 deletion. In the 2 TP53 mutated cases with negative IHC and FISH, 1 case showed a normal FISH pattern and the second case showed 3-4 copies of 17p13, consistent with heterozygous mutation. The results are summarized in the Table.

	Diagnosis	IHC for TP53 (% and intensity)	FISH for 17p13 deletion (%)	NGS for TP53 (VAF)
1	AML	Negative	Normal	c.638G>A (5%)
2	AML	10% 3+	Positive (11%)	c.830G>T (42.7%)
3	2 nd AML	60% 3+	Normal	c.672+1G>A (43.6%); c.488A>G (38.4%)
4	AML	Negative	Amplified 3-4 copies	c.548C>G (61.6%)
5	AML	95% 3+	Positive (95%)	c.743G>A (82%)
6	AML-MRD	10% 1+	Positive (100%)	c.1006G>T (84.7%)
7	AML	90% 3+	Positive (76%)	c.818G>A (84.2%)
8	AML	40% 3+	Positive (92%)	c.818G>A (78.7%)

Conclusions: Using a cutoff of 5%, immunohistochemistry for TP53 is effective in rapid screening to guide NGS mutational analysis. All the cases with TP53 mutations accompanied by 17p13 deletion had positive TP53 expression. Because TP53 inactivation requires mutation and/or deletion of both alleles, negative IHC is useful to clarify heterozygous mutation in cases with a preserved normal allele. FISH for 17p13 deletion is not an effective screening tool for TP53 mutation since cases with double mutations in both alleles may have normal FISH pattern.

1520 Acute Myeloid Leukemia with Mutated Runx1 Shows Characteristic Clinicopathological Features

Nneamaka Nwaoduah¹, Lindsay Wilde¹, Zixuan Wang¹, Jinglan Liu¹, Stephen Peiper², Jerald Gong¹, Guldeep Uppla³. ¹Thomas Jefferson University Hospital, Philadelphia, PA, ²Sidney Kimmel Medical College, Philadelphia, PA, ³Glen Mills, PA

Background: Runt-related transcription factor 1 (RUNX1) mutations have been identified in various myeloid neoplasms including acute myeloid leukemia (AML). The addition of the provisional entity of AML with mutated RUNX1 in the WHO 2016 classification calls for further characterization of these cases.

Design: We reviewed 66 AML cases with accompanying cytogenetic studies (FISH and chromosomal analysis) and Next-Generation Sequencing (NGS) analyses with a myeloid gene panel. The cohort included 50 AML-NOS, 8 AML-MRC, 7 AML with recurrent genetic abnormalities and 1 therapy-related AML diagnoses according to the WHO 2016 classification. Fifty-nine cases were de novo AML and 7 were secondary AML.

Results: 11 cases were positive for RUNX1 mutations (17%) including 6 females (54%) and 5 males (45%) with a median age of 69 years. Ten of the cases were de novo AML and 1 was a secondary AML. Of all RUNX1 mutations, 7 were frameshift, 2 were nonsense, 1 was missense mutation and 1 was a splice site mutation. Additional mutations were present in 9 cases. The most frequent additional mutations were identified in the genes ASXL1, NRAS, BCOR and BCORL1. Three cases were positive for the FLT3-ITD mutation. Among cases with an AML-RUNX1mut, 5 showed a normal diploid karyotype (45%), 2 demonstrated one clonal cytogenetic abnormality (18%) and

4 exhibited 2 or more clonal abnormalities (36%). The most frequent cytogenetic abnormality detected by FISH was deletion 17p (6/11, 54%) followed by deletion 7q/monosomy 7 (3/11, 27%). When categorizing the 10 de novo AML cases based on cytogenetic features, 6 cases fell under into the adverse risk group, and 4 cases fell under into the intermediate risk group. The cases showed relative phenotypic uniformity by flow cytometry (CD34+, CD117+, and MPO-).

Conclusions: AML-RUNX1mut tends to occur in older patients, shows a characteristic immunophenotype with minimal or no maturation (CD34+, CD117+, MPO-), and are frequently associated with intermediate and adverse prognostic subgroups. Mutations in NPM1 were conspicuously absent in our study and, in addition to ASXL1, mutations in BCOR and BCORL1 were frequently present.

1521 Clinicopathologic Features of Large B-cell Lymphoma with Overexpression or Genetic Alterations in MYC and BCL2

Christopher J O'Connor¹, Iván González¹, Friederike Kreisel¹, John Frater¹, Eric J Duncavage¹, Marianna Ruzinova¹, Anjum Hassan¹, Yi-Shan Lee¹. ¹Washington University, St Louis, MO

Background: DLBCL has heterogenous morphologic, immunophenotypic and genetic features as well as clinical outcomes. Double-hit lymphoma (DHL), defined as large B-cell lymphoma (LBCL) with concurrent rearrangement of MYC and BCL2/or BCL6, has a more aggressive clinical course and high rate of disease relapse compared to nonDHL. Double-expressor lymphoma (DEL), defined as LBCL with overexpression of both bcl2 and c-myc, has also been shown to have a worse clinical outcome compared to nonDEL. Additionally, although not recapitulated in our single institution cohort, one recent study showed LBCL with copy number gains (CNG) of either BCL2 or MYC had a similarly worse clinical outcome compared to DHL. In this study, we aim to further analyze the clinicopathologic features of LBCL based on overexpression or genetic alterations in MYC and BCL2.

Design: We retrospectively identified 177 cases of DLBCL in our institution from 2013 to 2015, with informative MYC and IgH-BCL2 status by FISH testing. Diagnoses and histologic features including cell of origin were confirmed by re-review of the cases. 93 cases had bcl2 and c-myc immunostains available. The clinical data and cytogenetic features were collected from our institutional databases. Statistical analysis was performed using software R 3.1.1 (Vienna, Austria).

Results: We identified 9 patients with DHL (5%), 50 patients with CNG/nonDHL (28%), 118 patients with nonCNG/ nonDHL (67%), 44 patients with DEL (47%) and 49 patients with nonDEL (53%). The clinical characteristics and outcomes based on FISH findings and bcl2/c-myc expression are summarized in Table-1, 2 and 3. Patients with DHL and/or DEL had worse clinical outcomes. No statistically significant difference in disease relapse were identified between CNG/ nonDHL and nonCNG/nonDHL. The nonDHL patients with CNG and/or DEL had statistically significant higher rate of relapse compared to those without either CNG or DEL.

	DHL	CNG/nonDHL	nonCNG/nonDHL	P-value
N	9	50	118	
Gender (M:F)	5:4	29:21	51:59	
Age (mean)	64.6	65.2	61.2	
GCB n (%)	9 (100%)	33 (66%)	64 (54%)	
DE n (%)	5/5 (100%)	13/29 (45%)	26/59 (44%)	
Relapse n (%)	8 (89%)	21 (42%)	34 (29%)	0.0096*, 0.0002*, 0.0959*
Death n (%)	1 (11%)	2 (4%)	16 (14%)	0.3713*, 0.8359*, 0.0670*

^: DHL vs CNG/nonDHL, #: DHL vs nonCNG/nonDHL, &: CNG nonDHL vs nonCNG/nonDHL

	DEL	nonDEL	P-value
N	44	49	
Gender (M:F)	18:26	25:24	
Age (mean)	65	59.7	
GCB n (%)	20 (45%)	36 (73%)	0.0059
Relapse n (%)	21 (48%)	14 (29%)	0.0569
Death n (%)	7 (16%)	4 (8%)	0.248

	CNG and/or DEL	Without CNG or DEL	P-value
N	79	94	
Gender (M:F)	40:39	40:54	
Age (mean)	65	60.2	
GCB n (%)	45 (57%)	55 (59%)	
Relapse n (%)	35 (44%)	19 (20%)	0.0007
Death n (%)	6 (8%)	13 (13%)	0.1914

Conclusions: Patients with DHL or DEL have statistically significant higher rate of disease relapse compared to nonDHL or nonDEL, respectively. CNG/nonDHL is not associated with higher rate of disease recurrence. However, nonDHL patients with either CNG or DEL have higher rate of disease relapse compared with those without either DEL or CNG. The findings suggest status of overexpression or genetic alterations of BCL2 and/or MYC provide useful clinical prognostic values in the setting of DLBCL.

1522 Genetic Subtyping of Breast Implant-associated Anaplastic Large Cell Lymphomas

Naoki Oishi¹, Garry Brody², Rhett P Ketterling³, Christopher A Sattler³, Rebecca L Boddicker³, N N Bennan², L. Jeffrey Medeiros⁴, Roberto Miranda⁴, Andrew Feldman¹. ¹Mayo Clinic, Rochester, MN, ²Keck School of Medicine at USC, ³Mayo Clinic, ⁴The University of Texas MD Anderson Cancer Center, Houston, TX

Background: Anaplastic large cell lymphomas (ALCLs) represent a group of CD30-positive T-cell lymphomas with marked genetic heterogeneity. ALK-positive ALCLs consistently bear ALK rearrangements, whereas some systemic and primary cutaneous ALK-negative ALCLs bear rearrangements of DUSP22 or TP63. The 2016 revision of the World Health Organization classification of lymphoid neoplasms recognizes a new provisional subtype of breast implant-associated (BIA) ALCL with unique clinical features. However, the genetic features of these cases remain incompletely characterized.

Design: We evaluated pathologic and genetic features in 35 BIA ALCLs. ALK status was evaluated by immunohistochemistry (IHC). DUSP22 and TP63 rearrangements were evaluated using a combination of screening IHC for p63 and breakapart and/or dual-fusion fluorescence *in situ* hybridization. We also performed IHC for phosphorylated STAT3 (pSTAT3; Tyr705) in 25 available cases.

Results: All patients were women, with a mean age of 56 years (range, 33-76 years). Morphologically, all cases showed large, pleomorphic cells with abundant cytoplasm and often multilobated or wreath-like nuclei. All cases were ALK-negative by IHC and in addition all cases lacked rearrangements of DUSP22 and TP63 (triple-negative genetics). pSTAT3 was positive by IHC in all 25 cases tested, with staining seen in 30-100% of tumor cell nuclei.

Conclusions: In contrast to the heterogeneity observed in other ALK-negative ALCL subtypes, BIA ALCLs consistently demonstrate triple-negative genetics, pleomorphic cytology, and expression of pSTAT3. Systemic and cutaneous ALK-negative ALCLs have DUSP22 rearrangements in 28-30% of cases and TP63 rearrangements in 5-8%; show variable cytologic features; and are negative for pSTAT3 in more than half of cases. These findings indicate that, in addition to its distinct clinical presentation, BIA ALCL has strikingly consistent pathological features, supporting its classification as a distinct entity. Furthermore, this relative homogeneity suggests that BIA ALCLs may share a unifying pathogenetic mechanism, likely related to the inflammatory milieu in which they arise.

1523 PD-L1 Expression Correlates with Genetic Subtype and Predicts Outcome in Anaplastic Large Cell Lymphoma

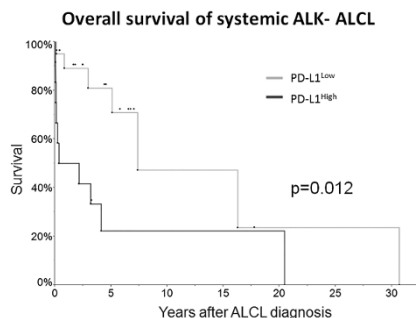
Naoki Oishi¹, Rebecca L Boddicker², Stephen M Ansell², Surendra Dasari², Karen Rech², Andrew Feldman². ¹Mayo Clinic, Rochester, MN, ²Mayo Clinic

Background: Anaplastic large cell lymphomas (ALCLs) are CD30+ T-cell lymphomas that vary widely in their genetics and prognosis. Programmed cell death ligand 1 (PD-L1) is expressed by a variety of cancers and promotes immune evasion by binding the inhibitory receptor PD-1 on reactive cells in the tumor microenvironment. PD-L1 expression has been observed in some ALCLs, but its associations with WHO subtype, genetics, PD-1 expression, and outcome remain incompletely understood.

Design: We evaluated 93 ALCLs (20 ALK+, 45 ALK-, 20 cutaneous, and 4 breast implant-associated [BIA]) using immunohistochemistry for PD-L1, PD-1 (evaluable in 90) and phosphorylated STAT3 (pSTAT3;

Tyr705; evaluable in 87). PD-L1 and pSTAT3 were scored as percent positive tumor cells, and PD-1 as positive infiltrating non-neoplastic cells per high power field (hpf). Genetic subtype was categorized in all cases as ALK, *DUSP22*, TP63, or triple-negative, using fluorescence *in situ* hybridization to detect *DUSP22* and *TP63* rearrangements. Outcome was assessed as overall survival (OS) from diagnosis.

Results: Mean age was 54 years (range, 4-96 years; M:F, 51:42). Some degree of PD-L1 staining was seen in 75/93 cases (81%). Mean \pm SD staining by WHO subtype was: ALK+, 64 \pm 32%; ALK-, 35 \pm 34%; cutaneous, 29 \pm 31%; and BIA, 90 \pm 14% ($p=0.0003$, Wilcoxon test). Staining by genetic subtype was: ALK, 64 \pm 32%; *DUSP22*, 10 \pm 9%; TP63, 27 \pm 31%; and triple-negative, 48 \pm 36% ($p<0.0001$). Using a cutoff for PD-L1 of 30% (median value), staining for pSTAT3 was 21 \pm 31% vs. 71 \pm 24% in PD-L1^{low} and PD-L1^{high} ALCLs, respectively ($p<0.0001$). Among 32 systemic ALK- ALCLs with follow-up data, median OS was 7.4 years vs. 1.3 years in PD-L1^{low} and PD-L1^{high} ALCLs, respectively ($p=0.012$, log-rank test). PD-1 was expressed in an average of 101 cells/hpf (range, 0-663) in the microenvironment and was not significantly associated with WHO subtype, genetic subtype, PD-L1 or pSTAT3 staining, or OS.



Conclusions: PD-L1 expression correlates with WHO subtype, genetic subtype, pSTAT3 expression, and prognosis in ALCL. Of note, *DUSP22*-rearranged ALCLs express minimal PD-L1 compared to other genetic subtypes. These cases have excellent outcomes, which might be partly attributable to a more effective anti-tumor immune response. Conversely, PD-L1 may facilitate immune evasion by ALK+ ALCLs, BIA ALCLs, and ALK- ALCLs with triple-negative genetics, providing a potential rationale for immune checkpoint blockade in these ALCL subtypes.

1524 SOX9 Expression in Lymphoid Tissues and Lymphomas

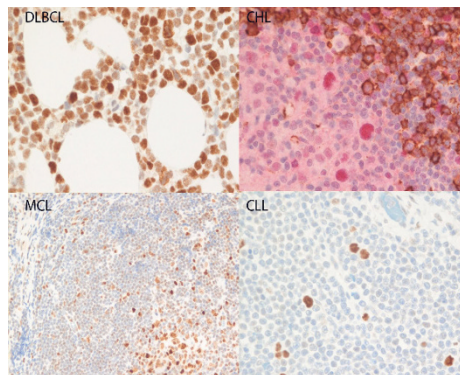
Megan M Parilla¹, Paola Dama², Sonali Smith³, Elizabeth Hyjek¹, Girish Venkataraman⁴. ¹University of Chicago, Chicago, IL, ²University of Chicago, Chicago, ³University of Chicago Medicine, ⁴The University of Chicago Medical Center, Chicago, IL

Background: SOX9 is a highly conserved transcription factor critical for development of mesenchymal and epithelial tissues during embryogenesis and has been implicated in the formation and growth of number of tumors. However, very little is known about its role in lymphomagenesis. Herein, we evaluated expression of SOX9 in lymphoid tissues as well as B- and T-cell lymphomas.

Design: We retrieved paraffin embedded whole sections (n=22) and duplicate 0.8 mm² tissue microarray (n=62) material from the department archives and Lymphoma Biobank representing a range of benign (tonsils and reactive nodes) and malignant (B-cell and T-cell lymphomas) collected over 16 years. After diagnostic confirmation on H&E stain, Sox9 (Abcam 3C10 monoclonal at 1:5000) immunostaining was performed with additional double staining for CD20/SOX9 in a subset of cases. Only strong nuclear SOX9 expression was considered as positive.

Results: In normal lymph nodes/tonsils, SOX9 nuclear expression is restricted to the centroblast-rich, "dark zone" of the germinal center (GC), mitotically active cells and perfollicular immunoblasts as well as some plasma cells. GCB light zone cells, mantle zone, marginal zone and most T-cell areas were negative. Table 1 depicts staining pattern in lymphoma tissues. Figure 1 depicts a large B-cell lymphoma and classical Hodgkin lymphoma (CD20/SOX9+ HRS cells) both positive for SOX9 while Mantle cell lymphoma and small lymphocytic lymphoma (SLL) are both negative with scattered larger SOX9+ paraimmunoblasts in CLL/SLL. Hodgkin lymphoma background milieu frequently contained SOX9+ lymphoid cells.

Lymphoma Subtype	Positive
Diffuse Large B cell lymphoma	13/13
Hodgkin Lymphoma	13/14
T-cell lymphomas	4/6
Follicular Lymphoma	11/19
Chronic Lymphocytic Leukemia	5/10
Marginal zone lymphoma	0/8
Mantle cell lymphoma	0/3



Conclusions: Most large B-cell lymphomas express SOX9 irrespective of cell of origin. Among low-grade BCL, there is differential expression of SOX9 restricted to scattered centroblasts of follicular lymphoma and paraimmunoblasts of CLL/SLL with acquisition of SOX9 at transformation in one case of Richter transformation. The expression or lack of SOX9 in various B- or T-cell entities may have differing implications for prognostication of certain subsets of lymphomas and we are examining a larger cohort to evaluate this aspect.

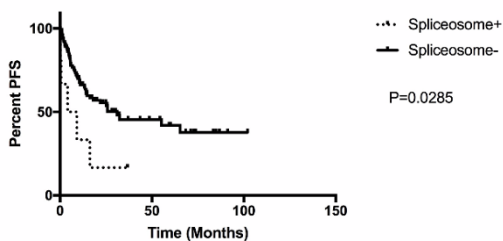
1525 Clinical Impacts of Co-Occurring Mutations in De Novo Acute Myeloid Leukemia with Mutated NPM1

Sanjay S Patel¹, Frank Kuo¹, Robert Hasserjian², Olga K Weinberg³. ¹Brigham & Women's Hospital, Boston, MA, ²Massachusetts General Hospital, Boston, MA, ³Children's Hospital Boston, Boston, MA

Background: Acute myeloid leukemia (AML) with *NPM1* gene mutation is a new diagnostic entity in the revised 2016 WHO classification. The mutational landscape in this leukemia subtype has not yet been fully explored. In this study, we examined a series of *NPM1*-mutated de novo AML patients to identify any effects on patient outcome and other clinical parameters conferred by co-mutation(s).

Design: 110 cases of de novo AML with *NPM1* mutations and available clinical outcome data were identified from three institutions between 2008-2017. All patients were treated with standard induction chemotherapy, with or without subsequent allogeneic stem-cell transplant (SCT). Next-generation sequencing was performed to interrogate for the presence of 95 mutations known to be associated with myeloid neoplasms. Mutations were segregated by pathway: DNA methylation, epigenetic regulation, tumor suppressor, transcription factors, protein kinase, protein phosphatase, RAS, and spliceosome. Relapse-free survival (RFS) and multivariable analysis using a Cox proportional hazards model was performed; patients were censored at the time of any SCT.

Results: 95 cases (86%) had a normal karyotype. The most common co-occurring mutations included *DNMT3A* (49%), *FLT3-ITD* (32%), *TET2* (28%), *NRAS* (24%), *FLT3-TKD* (25%) and *PTPN11* (23%). The *NPM1* mutation position in the clonal hierarchy, as either a potential founder (22%) or subclone (31%), had no impact on outcome. 6 cases (5.5%) had co-occurring spliceosome pathway mutations mostly involving the *SRSF2* gene (5/6), and all of these had a normal karyotype. Clinically, these patients were characterized by older age ($p=0.0010$) and lower platelet counts ($p=0.0303$) at diagnosis. Both older age ($p < 0.0001$) and spliceosome mutations ($p=0.0285$) were associated with shortened relapse-free survival (RFS) (Figure 1). 29 cases (26%) had co-occurring *NRAS* or *KRAS* mutations. Clinically, these patients had lower white blood cell counts ($p=0.0195$), fewer peripheral blasts ($p=0.0003$), and less cellular bone marrows ($p=0.0203$) at diagnosis, with a prolonged RFS ($p=0.04$). In multivariable analysis, only age remained significant.



Conclusions: In cases of de novo AML with mutated *NPM1*, co-occurring spliceosome pathway mutations are associated with older age and shorter RFS, while *KRAS* or *NRAS* mutations are associated with longer RFS. On multivariable analysis, the prognosis of AML with mutated *NPM1* is adversely influenced only by older age and not by co-mutations.

1526 Microarray CGH-SNP Analysis Detects Frequent Chromosomal Abnormalities Indicating Clonal Cytopenia(s) in Patients With Indeterminate Bone Marrow Dysplasia - An Institutional Study Of 94 Cases

Nisha Patel¹, Michelle Pitch², Andrew G Evans², M. Anwar Iqbal².
¹Rochester, NY, ²University of Rochester Medical Center, Rochester, NY

Background: Disorders of ineffective clonal hematopoiesis can present with indolent clinical presentations, subtle morphologic bone marrow changes, and subdiagnostic cytogenetic abnormalities that can cause diagnostic uncertainty. While conventional karyotype and fluorescence in-situ-hybridization (FISH) are considered standard in evaluating cytogenetic abnormalities, emerging data shows comparative genomic hybridization (CGH) and single nucleotide polymorphism (SNP) array can potentially identify clinically significant genetic lesions. We examined the ability of combined-microarray CGH-SNP analysis (aCGH-SNP) to detect DNA copy number variations (CNVs) and regions of homozygosity (ROH) in normal karyotype individuals undergoing evaluation for unexplained cytopenias.

Design: Ninety-four (94) bone marrow samples deemed indeterminate for dysplasia were collected over a 3 year period (2014-2017) from patients referred for unexplained cytopenias. Inclusion criteria included "normal" or non-clonal karyotype abnormalities by standard cytogenetics. aCGH-SNP analysis was performed using a cancer targeted array (4x180K - Agilent Technologies) designed by the Cancer Genomics Consortium. The platform contains approximately 120K oligonucleotides that provide high-density coverage for clinically relevant oncogenes, telomeres and pericentromeric regions, and 60K SNP probes (MAF >5.0), providing resolution of 5-10 Mb for ROH. The cut-off for CNVs was 250kb, containing at least one targeted gene, with confirmation by FISH. Results were compared to 18 normal bone marrow controls.

Results: Thirty-seven (37) patients (39% of total) were positive for a chromosomal abnormality by aCGH-SNP analysis. Twenty cases (21% of total) were positive for CNVs, and 17 cases (18% of total) were positive for ROH alone. CNVs among patients included a 555 kb deletion at 4q24 (TET2 gene); a 6.4 Mb deletion at 12p13.31 (ETV6 gene); a 25.8 Mb loss at 20q11.23; a 91.8 Mb ROH (UPD7q; EZH2 gene) and 135.9 Mb ROH (UPD4q; TET2 gene), and all of these regions are implicated in MDS pathogenesis.

Conclusions: More than a third of patient samples were found positive for CGH-SNP findings in the presence of a normal karyotype, including causative genes associated with MDS. Our data supports utilization of microarray CGH and SNP array in evaluating unexplained cytopenias. Furthermore, it suggests an alternative approach to detect clonal cytopenias of uncertain significance, and has implications for early detection of myelodysplastic syndromes.

1527 Novel Immunophenotypic Findings in Hypodiploid B-Acute Lymphoblastic Leukemia

Smita Patel¹, Murty Vundavall², David Park². ¹Columbia University Medical Center, New York, NY, ²Columbia University College of Physicians & Surgeons

Background: Hypodiploid B-acute lymphoblastic leukemia (B-ALL) has cytogenetically and molecularly defined subgroups but without reported distinct immunophenotypic profiles. Therefore, we investigated if comprehensive flow cytometric immunophenotypic panels could uncover correlative patterns of antigen expression with hypodiploid subgroups of B-ALL.

Design: We searched for all hypodiploid B-ALL cases in the last 5 years and retrospective analysis of flow cytometry, cytogenetics, molecular, and clinical data was performed. Antigen expression in

>10% blasts was considered inclusion criteria.

Results: Ten cases were identified that include 6 near-haploid (NH), 1 low-hypodiploid (LH), and 3 high-hypodiploid (HH). All NH cases showed an evidence of whole genome endoreduplication. Clinical and immunophenotypic features are described in Table 1. Only pediatric cases showed absent CD34 or CD45 expression in 50% and 62% cases, respectively; and CD13 and/or CD33 expression without MPO in 62% cases. All NH cases with an endoreduplicated and NH clone and a HH case expressed CD13 and/or CD33, while all NH cases with only an endoreduplicated clone showed no CD13 or CD33 expression. Only adult cases showed partial MPO expression. NH cases retained both homologs of chromosomes 6, 14, 18, 21, X, and Y as previously reported. However, 1 NH case was found to have a structural abnormality, t(2;14). Frequent structural and numerical abnormalities in other hypodiploid cases included 14q32 rearrangements [3], p16 deletion [2], t(12;21) [1], and loss of 17 [3]. We found TP53 and DDB2 mutations (LH with MPO expression) and CREBBP mutations (NH) in keeping with recent reports.

Feature	Near-Haploid (n = 6)	Low hypodiploid (30-40) (n = 1)	High hypodiploid (41-45) (n = 3)
Adult/pediatric (<15 yrs)	0/6	1/0	1/2
Male/female	4/2	1/0	1/2
Mean age (yr)	6	68	30
Phenotype:			
Early pre-B	0	1	0
Common B	5	0	2
Pre-B	1	0	1
CD45 (absent)	5	0	0
CD34 (absent)	4	0	0
CD117	0	0	0
CD43	6	1	2
CD25	2	1	1
CD13	1	0	1
CD33	3	0	1
CD11c	2	0	1
MPO (isolated)	0	1	1
CD4	0	0	2
CD5	1	0	0
s/c CD3	0	0	0
Somatic mutations by NGS (2/10)	1 (CREBBP)	1 (TP53, DDB2)	-
Outcome (median follow-up 24 months):			
Remission	6	1	1
Marrow relapse (median 22.5 months)	4	1	3 (1 with monosomy 7 relapsed as therapy-associated myeloid neoplasm with KMT2A rearrangement)
Death	1	1 (5 months from the diagnosis)	1

Conclusions: Hypodiploid B-ALL is a very rare subtype and has been shown to have equal incidence in males and females while we noted a slight male excess. Our study demonstrates frequent myeloid and/or T-cell associated antigen expression and absent CD34 or CD45 in pediatric cases with an apparent good correlation with cytogenetically-defined hypodiploid groups. Furthermore, due to frequent aberrant expression myeloid-associated antigens and rarely MPO, caution must be taken to avoid incorrectly assigning these cases as mixed-phenotype acute leukemia. Previously unreported CD25 expression in hypodiploid B-ALL seen in our study also suggests that it may not be specific to BCR-ABL1 B-ALL, as previously thought. Our findings highly suggest hypodiploid B-ALL has distinctive immunophenotypic profiles, but require additional cases to confirm our findings.

1528 Single Cell RNA Sequencing Dissects through the Microenvironment and Highlights Transcriptional Heterogeneity of the Hodgkin/Reed Sternberg Cell in Classical Hodgkin Lymphoma

Nikhil Patkar¹, Stephen Salipante², William J Valente³, Kelsi M Penewit⁴, Jason H Bielas³, Brent Wood⁵, David Wu⁶, Jonathan Fromm⁶. ¹Tata Memorial Centre, Navi Mumbai, Maharashtra, ²UWMC, Seattle, WA, ³Fred Hutchinson Cancer Research Center, ⁴University of Washington, ⁵University of Washington, Redmond, WA, ⁶University of Washington, Seattle, WA

Background: Classical Hodgkin lymphoma (cHL) is a lymphoma in which neoplastic Hodgkin/Reed-Sternberg (HRS) cells are infrequent,

being outnumbered by an ineffective immune response. As a result, flow cytometric cell sorting or microdissection of HRS has been required to study the biology of this disease. A representative transcriptomic analysis of cHL requires sampling of individual cells, not bulk averaged sampling. Here, we employ single cell RNA sequencing (scRNA-seq) to provide a transcriptome-based description of HRS cells and the microenvironment.

Design: Seven cHL lymph nodes were processed using a microfluidics system to bar-code single cell mRNA transcripts for reverse transcription with semi-quantitative sequencing. Data was then mapped to create an aggregated cell-transcript expression matrix. Secondary analysis was performed to identify highly variable transcripts among cells to compute principal components. Graph-based analysis was used to cluster cells with similar transcriptomic characteristics. Validation was performed using reactive lymph nodes and single cell suspensions of 3 HRS cell lines (L1236, L428, KMH2).

Results: Over the 7 CHL cases, ~28K cells were evaluated with approximately 16K transcripts mean reads/cell (median of 377 unique genes/cell). With these data, we could annotate the immune response in the microenvironment of CHL, including lymphocytes, dendritic cells, plasma cells and macrophages and find that the majority of lymphocytes were CD4+ T-regulatory cells including a subset of effector T-regulatory cells. Interestingly, macrophages showed transcriptional heterogeneity with overexpression of genes encoding chemokines and metalloproteins. In all cases, we could identify HRS cells with strong *CCL17*, *TXN*, *LGALS1*, *MGST2* and *RAB13* expression (top overexpressed transcripts). Further analysis shows that HRS cells can exist in at least 4 transcriptionally distinct states. Notably, in all cases, we detected multiple invariant transcriptional states. Comparative analysis of scRNA-seq data from HRS cell lines and published literature confirmed the majority of these overexpressed genes seen in the primary cHL cases.

Conclusions: scRNA-seq can dissect the complex microenvironment of cHL and identify novel transcripts affecting biological pathways in HRS cells. We find that HRS cells in clinical samples exist in transcriptionally heterogeneous states that may define the pathobiology and immune response in CHL.

1529 Targeting CD47 by MiR-155 Promotes Phagocytosis and Inhibits Cell Growth in Multiple Myeloma

Maryam Pourabdollah¹, Nasrin Rastgoo², Hong Chang³
¹University of Toronto, Toronto, ON, ²University Health Network, ³Toronto General Hospital, Toronto, ON

Background: CD47 is a transmembrane glycoprotein which acts as a ligand for several receptors, including signal regulatory protein alpha (SIRP α). CD47-SIRP α signaling on macrophages results in inhibition of phagocytosis. It has been shown that CD47 is highly expressed on multiple myeloma (MM). However, the underlying mechanism for CD47 overexpression and its role in myeloma drug resistance are not known.

Design: CD47 level was assessed in drug resistant cell lines (8226-R5 and MM1.R) in comparison to their parental sensitive cells (8226 and MM1.S). Several miRNA-target prediction algorithms were used to identify miRNA candidates that can potentially target *CD47*. Functional assays including MTT and phagocytosis assays were performed on miR transfected cells to examine the functional effect of *CD47* targeting on phagocytosis by macrophages and myeloma cell proliferation.

Results: CD47 protein level was higher in drug resistant cell lines in comparison to their parental cells and its mRNA level was significantly upregulated in relapsed patients compared to newly diagnosed MM patients and normal plasma cells. We also observed that miR-155 expression was dramatically downregulated in drug resistant cell lines and stage III of MM relative to parental cell lines and stage I/II of MM, respectively. Our datasets analysis indicated a significant negative correlation between CD47 and miR-155 level in MM patients. Moreover, overexpression of miR-155 significantly decreased CD47 protein level in MM resistant cells confirming the direct targeting of CD47 by miR-155. FACS analysis also showed the level of CD47 on MM cell surface was decreased after miR-155 overexpression. In addition, overexpression of miR-155 in drug resistant cell lines sensitized them to bortezomib, suggesting that downregulation of miR-155 is associated with bortezomib-resistance in MM. Importantly, we demonstrated that targeting *CD47* by miR-155 abrogated the protection against phagocytosis and promoted the phagocytosis of MM cells by macrophages.

Conclusions: In conclusion, our data indicate that miR-155 is downregulated in drug resistant MM cell lines and primary MM cells, which contributes to the drug resistance of MM through upregulation of CD47. Moreover, regulatory interaction between miR-155 and CD47 provides the rationale that restoration of miR-155 may serve as a promising therapeutic approach by targeting CD47 in patients with refractory/relapsed MM.

1530 DDX41 Mutations in Myeloid Neoplasms Are Associated with Male Predominance, TP53 mutation and a High Risk of Progression to AML

Andres E Quesada¹, Courtney DiNardo¹, Mark Routborf², Carlos Bueso-Ramos¹, Rashmi Kanagal-Shamanna³, Zhuang Zuo¹, C. Cameron Yin¹, Sanam Loghavi⁴, Chi Young Ok¹, Sa Wang¹, Christopher Benton¹, Hagop M Kantarjian¹, Rajyalakshmi Luthra¹, L. Jeffrey Medeiros¹, Keyur Patef⁵. ¹The University of Texas MD Anderson Cancer Center, Houston, TX, ²Bellaire, TX, ³The University of Texas M.D. Anderson Cancer Center, Bellaire, TX, ⁴Houston, TX, ⁵UT-MD Anderson Cancer Center, Sugar Land, TX

Background: Myeloid neoplasms with germline predisposition as a result of germline mutations in *DDX41*, a DEAD-Box helicase (chr:5q35), have been incorporated into the 2016 revision of WHO classification. Limited studies describing the clinicopathologic features and mutation profile of this entity are available. We describe 19 patients with myeloid neoplasms associated with *DDX41* mutations.

Design: We searched the archives for cases tested by next-generation sequencing using MiSeq (Illumina, San Diego, CA) and an 81-gene panel over a 5 month interval. All cases in which a *DDX41* gene mutation formed the study group.

Results: We identified 19 patients with myeloid neoplasms associated with *DDX41* abnormalities. There were 16 men and 3 women with a median age of 71 years (range, 57 – 81). The diagnoses of the myeloid neoplasms were: AML (n=12), MDS (n=4), and MPN (n=3). A total of 33 *DDX41* variants were detected: 14 (42%) appeared to be somatic mutations (VAF: <25%) and 19 (57%) were presumably germline mutations based on populations studies and near heterozygous VAF (~50%), although definitive testing was not performed. A detailed summary is shown in table 1.

16 other genes were mutated concomitantly but only *TP53* (n=6, 32%), *ASXL1* (n=3, 16%), and *JAK2* (n=3, 16%) were recurrent. 11 (58%) patients showed diploid cytogenetics; 2 (11%) patients had a der(1;7) (q10;p10); 2 (11%) patients had a complex karyotype, 1 (5%) patient had del5q and 1 (5%) patient had del20q. 11 of 12 (92%) patients with AML showed deleterious (frameshift or nonsense) mutations in their germline *DDX41* polymorphisms. In contrast, only 2 of 7 (29%) patients with MDS or MPN showed deleterious mutations; the remaining 5 had missense polymorphisms (p=0.01). In patients with AML, 10 (91%) had both a somatic and germline alteration in contrast to 3 of 8 (37.5%) patients with a myeloid neoplasm without increased blasts (p=0.04).

FOR TABLE DATA, SEE PAGE 573, FIG. 1493

VAF, variant allele frequency; MS, Missense; SCL, start codon loss; FS, frameshift; NS, nonsense

Conclusions: Patients with myeloid neoplasms carrying *DDX41* mutations show a striking male predominance and higher age at presentation. Deleterious germline variants and concomitant somatic + germline variants are associated with AML. There appears to be an association between *TP53* mutation and a risk of progression from MDS to AML. These findings support the recognition of myeloid neoplasms with *DDX41* mutation as a unique entity and the need for confirmation of germline status, as well as further assessment family members.

1531 RUNX1 Mutations in Myelodysplastic Syndrome

Andres E Quesada¹, Mark Routborf², Rajyalakshmi Luthra¹, Keyur Patef³, Juliana E Hidalgo-Lopez¹, Carlos Bueso-Ramos¹, L. Jeffrey Medeiros¹, Rashmi Kanagal-Shamanna⁴. ¹The University of Texas MD Anderson Cancer Center, Houston, TX, ²Bellaire, TX, ³The University of Texas MD Anderson Cancer Center, Sugar Land, TX, ⁴The University of Texas MD Anderson Cancer Center, Bellaire, TX

Background: *RUNX1* mutations occur in a subset of myelodysplastic syndrome (MDS) and acute myeloid leukemia (AML) and predict for a poor survival. 2016 WHO has included AML with mutated *RUNX1* in a *de novo* setting as a provisional entity due to distinct biologic features and worse outcome. The purpose of this study was to explore the somatic *RUNX1* mutations in MDS and correlate with clinicopathologic features.

Design: We identified MDS cases with *RUNX1* mutations detected by an NGS-based comprehensive myeloid gene panel. We compared the clinical, morphologic and genetic findings between MDS with and without somatic mutations in *RUNX1* gene.

Results: Of a total of 154 MDS patients, we identified *RUNX1* mutation in 10% of cases, 14% of MDS with a splicing factor (SF) gene mutation, and 18% of MDS with *SF3B1* mutation. The study group included 8 (53%) men and 7 (47%) women with a median age of 73 years (range, 45-82). Distribution by 2016 WHO subtype at the time of presentation included 7 MDS with multilineage dysplasia (MLD, n=7, 47%), 5 MDS with excess blasts [2 MDS-EB-2; 3 MDS-EB-1] and 3 MDS with ring sideroblasts with MLD (20%). We found a total of 22 *RUNX1*

mutations, including a high proportion of deleterious frameshift or nonsense mutations (n=15, 68%). The median variant allele frequency was 14.44 (range, 2.1 – 42.28); in 6 patients (40%), *RUNX1* mutation was seen in sub-clonal population (<50% VAF of driver mutant gene). The most frequent co-mutated genes included: *SF* (n=11, 73%; 6 *SF3B1* (4 of which met the criteria for MDS-RS based on at least 5% ring sideroblasts), 3 *SRSF2* and 2 *U2AF1*, *ASXL1* (n=8, 53%), *STAG2* (n=4, 27%), *BCOR* (n=3, 20%), and *TET2* (n=3, 20%). Compared to MDS with wild-type *RUNX1*, *RUNX1* mutated MDS showed a significantly higher frequency of *ASXL1* (53% vs. 18%, p=0.02) and *STAG2* (27% vs. 0, p=0.004) mutations, and showed exclusivity with *TP53* mutations (0 vs. 23%, p=0.05). Cytogenetics (CG) showed a diploid karyotype in 6 (40%) patients. *RUNX1* mutations were not seen in MDS patients with del(5q) or complex karyotype (0 vs. 24%, p=0.08). The median follow-up of 13.9 months, 1 patient died.

Conclusions: *RUNX1* mutations are seen in 10% of all MDS and are enriched in *SF3B1* mutated MDS. A high proportion of mutations are deleterious (frameshift or nonsense) and subclonal. *RUNX1* mutation co-occurs with mutations in *SF* genes, *ASXL1* and *STAG2*, and is exclusive with *TP53* mutations.

1532 Next Generation Sequencing (NGS) Identifies Frequent Somatic Mutations in Acute Promyelocytic Leukemia

Nina Rahimi¹, Amir Behdad², Xinyan Lu², Yi-Hua Chen³, Juehua Gao⁴. ¹Northwestern Memorial Hospital, Chicago, IL, ²Northwestern University Feinberg School of Medicine, Chicago, IL, ³Northwestern University, Chicago, IL, ⁴Northwestern Memorial Hosp, Chicago, IL

Background: Acute promyelocytic leukemia (APL) is characterized by blasts/abnormal promyelocytes and genetic alteration of t(15;17) *PML-RARA*. Recent studies have shown that additional somatic mutations cooperate with *PML-RARA* in the leukomogenesis, but the data on the recurrent somatic mutations in APL is limited.

Design: A database search identified 18 patients with initial diagnosis of APL at our hospital (12 females, 6 males, median age 50) with cytogenetic/molecular confirmation. DNA samples extracted from bone marrow aspirate were sequenced using a targeted NGS panel of 33 genes including: *ASXL1*, *BRAF*, *CALR*, *CBL*, *CSF3R*, *DNMT3A*, *FLT3*, *GATA1*, *GATA2*, *HRAS*, *IDH1*, *IDH2*, *JAK2*, *JAK3*, *KIT*, *KRAS*, *MPL*, *NPM1*, *NRAS*, *PTPN11*, *SETBP1*, *SF3B1*, *SRSF2*, *TET2*, *TP53*, *U2AF1*, *WT1*, *CEBPA*, *ETV6*, *EZH2*, *IKZF1*, *PHF6*, and *RUNX1*.

Results: 11/18 cases (61%) showed somatic mutations including 3 cases (27%) with 1 mutation, 4 cases (36%) with 2 mutations, and 4 cases (36%) with 3 or more mutations. The most common mutations were *WT1* and *FLT3*. All *WT1* mutations (5/18; 28%) were single nucleotide substitution in exon 9 (4/5) or exon 7 (1/5). *FLT3* mutations (5/18; 28%) included 3 internal tandem duplication and 2 tyrosine kinase domain mutations (codons 835 and 839). *ETV6* mutations were present in 3/18 cases (17%) including 2 frameshift and 1 substitution. 3/18 cases (17%) showed *RAS* mutations (2 *NRAS* and 1 *KRAS*). Mutations involving epigenetic modifiers (*TET2*, *EZH2*, *DNMT3A*) were identified in 3 cases, all co-existed with either *WT1* or *FLT3* mutations and presented with lower variant allele frequencies indicating their presence as subclones. A *TP53* mutation was present in only 1 case (6%). Out of 18 patients, two were clinically classified as intermediate risk, one had no somatic mutations and the other had *WT1* and *RAS* mutations. Three were classified as high risk, including one with no mutations, the other two had *FLT3* mutations among others.

Conclusions: Our study demonstrated that APL is a genetically heterogeneous disease and harbors many co-occurring mutations commonly associated with other myeloid leukemias. Common mutations include activated signaling (*FLT3*, *RAS*), tumor suppressor (*WT1*, *TP53*), transcription factor (*ETV6*) and epigenetic modulation (*TET2*, *EZH2*, *DNMT3A*). Mutations involving epigenetic modulation likely represent a secondary event in APL. Large studies are needed to evaluate the prognostic significance of the somatic mutations in APL.

1533 Aberrant Cytokeratin Expression in Acute Myeloid Leukemia is Associated with Complex Karyotype and TP53 Alterations

Haitham Rahman¹, Joseph Khoury¹, Carlos Bueso-Ramos¹, Timothy McDonnell¹, Alireza Saleem², Sa Wang¹, Tariq Muzzafar¹, Michael Tetzlaff¹, Diana Bell¹, Haitham Khogeer³, Evgeniya Angelova¹, Shaoying Li¹, Guilin Tang¹, Shimin Hu¹, Keyur Patel⁴, Mark Routbor⁵, Rajyalakshmi Luthra¹, Pei Lin¹, L. Jeffrey Medeiros¹, Sanam Loghavi². ¹The University of Texas MD Anderson Cancer Center, Houston, TX, ²Baylor University Medical Center, ³Houston, TX, ⁴The University of Texas MD Anderson Cancer Center, Sugar Land, TX, ⁵Bellaire, TX

Background: Aberrant cytokeratin expression has been reported rarely in hematopoietic malignancies including mantle cell lymphoma, chronic lymphocytic leukemia/small lymphocytic lymphoma, peripheral T-cell lymphoma, diffuse large B-cell lymphoma, Hodgkin lymphoma, plasma cell myeloma and rarely (<1%) in acute myeloid

leukemia (AML) and may introduce a potential diagnostic pitfall. We assessed the frequency of aberrant cytokeratin (CK) expression in AML and correlated the results with clinicopathologic features and cytogenetic and molecular findings.

Design: We assessed CK expression by immunohistochemistry using a pancytokeratin antibody cocktail against AE1/AE3, CAM5.2 and MNF116 in 163 cases of AML including 100 *de novo* cases with a diploid karyotype and 63 therapy-related (t-AML). The percentage of CK positive cells was semi-quantitatively assessed and recorded in increments of 5%. Conventional cytogenetic analysis was performed on unstimulated cultured BM aspirate specimens using standard GTG-banding. Next-generation sequencing-based mutation analysis (Illumina, San Diego CA, USA) was performed using DNA extracted from BM aspirate samples. Clinical and laboratory data were obtained from the electronic medical records.

Results: Aberrant CK expression was seen in 15 of 163 (9%) cases, all confined to the t-AML group (15/63; 24%); all *de novo* AMLs were negative for CK (p=<0.0001). All positive cases showed a perinuclear dot-like pattern of staining; the median percentage of CK positive cells was 10% (range, 1% to 80%). Patients with CK+ t-AML included 8 (53%) men and 7(47%) women with a median age of 65 years (range, 43-89) at AML diagnosis. The most common antecedent malignancies included B-cell lymphoma (n=6; 40%) and breast carcinoma (n=4; 27%). All CK+ t-AML cases had a complex karyotype (p=<0.0001) *TP53* alterations (mutation and/or deletion) were more common in CK+ cases compared with CK-negative t-AML (12/15; 80% vs. 18/48, 34%; p=0.007). There was no association between other gene mutations and CK expression.

Conclusions: Aberrant CK expression occurs in a subset of AML and is associated with poor-risk cytogenetic and molecular features including a complex karyotype and *TP53* abnormalities. The etiology of aberrant CK expression in t-AML is unknown, but earlier studies have shown that functional wild-type p53 is able to repress CK expression. Functional studies are required to further investigate a potential biologic link between *TP53* alterations and aberrant CK expression in AML.

1534 H3K27me3 Expression in T-cell Lymphomas

Emilio Ramos¹, Melike Pekmezci¹, Linlin Wang¹. ¹University of California, San Francisco, San Francisco, CA

Background: Histone 3 trimethylation at lysine 27 (H3K27me3) is an epigenetic modification associated with gene silencing, loss or aberrant expression of which has been described in tumorigenesis. Deregulation of H3K27me3 via enhancer of zeste homologue 2 (EZH2) is suggested to play a critical role in hematologic malignancies. H3K27me3 expression in T-cell lymphomas (TCLs) has not been studied.

Design: Immunohistochemistry (IHC) for H3K27me3 (clone C36B11, Cell Signaling, Leica Bond III) was performed on 44 cases of TCLs. H3K27me3 IHC was reviewed by 2 pathologists and scored using the following criteria: Strong (3+): dark staining that is easily visible at low power and involves >50% of cells; Moderate (2+): focal dark staining areas (5-50% of cells) or moderate staining of >50% of cells; Weak (1+): focal moderate staining in 5-50% of cells or pale staining in > 5% of cells not easily seen at low power; Negative: less than 5% of tumor cells with staining.

Results: TCLs in this study include ALK+ anaplastic large cell lymphoma (ALCL)(n=5), ALK- ALCL (n=9), angioimmunoblastic T-cell lymphoma (AITL)(n=12), peripheral T-cell lymphoma not otherwise specified (PTCL NOS)(n=10), mycosis fungoides (MF)(n=2), NK/T-cell lymphoma (NKTL)(n=2), enteropathy-associated T-cell lymphoma (EATL)(n=3) and subcutaneous panniculitis-like T-cell lymphoma (SPTL)(n=1). 7/44 (16%) of TCLs show loss of expression, 37/44 (84%) show weak (12/44, 27%), moderate (7/44, 16%) and strong (18/44, 41%) expression. ALK+ ALCL predominantly shows loss (4/5, 90%) or weak expression (1/5, 10%). ALK-ALCL shows predominantly weak expression (6/9, 67%) or loss of expression (2/9, 22%), with one case (1/9, 11%) showing strong expression. PTCL NOS shows strong expression in all cases (10/10, 100%). AITL shows strong (4/12, 33%), moderate (4/12, 33%) or weak expression (4/12, 33%). MF shows strong expression in 2 cases (2/2). NKTL shows no expression in 1 case (1/2) and strong expression in another case (1/2). EATL shows strong (1/3, 33%), moderate (1/3, 33%) and weak expression (1/3, 33%). SPTL shows strong expression in 1 case (1/1).

Conclusions: H3K27me3 expression is predominantly lost or at low level in ALCL, especially in ALK+ ALCL. In contrast, PTCL NOS shows strong expression of H3K27me3. The findings suggest that different epigenetic mechanisms may exist between ALCL and PTCL NOS. In addition, strong H3K27me3 expression in PTCL NOS may suggest H3K27me3/EZH2 pathway as a potential therapeutic target using EZH2 inhibitors.

1535 Molecular targeting of MCL1 to overcome chemoresistance in diffuse DLBCL

Candace Reveles¹, Danzhou Yang², Samantha Kendrick³, Samantha Kendrick³. ¹University of Arizona, Tucson, AZ, ²University of Arizona, ³University of Arkansas for Medical Sciences, Little Rock, AR

Background: Myeloid cell leukemia-1 (MCL1) is an anti-apoptotic member of the BCL2 family that is upregulated in various malignancies. High expression of MCL1 is especially notable at the time of relapse and in particular, is shown to confer chemoresistance in DLBCL. These findings underscore the potential value in therapeutic exploitation of MCL1 inhibition. In this project we aim to develop an alternative approach to targeting MCL1.

Design: DNA secondary structures are targetable motifs that arise from contiguous runs of guanines or cytosines. These structures (G-quadruplex or i-motif) are known to regulate transcription and can be modulated with small molecules. Using the i-motif forming sequence of the MCL1 promoter as molecular bait, we performed a fluorescence based high-throughput screening assay of 1596 compounds from the NCI Diversity library to identify potential small DNA secondary interactive molecules. Candidate compounds were selected and their IC₅₀ concentrations were determined using the MTS cytotoxicity assay in 4 well-established DLBCL lines. The effects of these novel inhibitors on MCL1 gene expression were then evaluated following 24-hour treatment in the DLBCL lines. RNA extraction was performed using the Roche High Pure RNA Isolation kit and reverse transcription was then performed on the extracted RNA using the BioRad iScript RT kit. The synthesized cDNA was subjected to real-time qPCR on the BioRad CFX96 Touch real-time instrument following the BioRad Sso Advanced qPCR protocol. Experiments were repeated 3 times and data is represented by the mean.

Results: During our high-throughput screening assay, we identified 2 likely candidates, which resulted in a 2 to 6-fold increase in fluorescence relative to the MCL1 probe alone indicating significant destabilization of the i-motif. Both compounds exhibited an IC₅₀ within the 50-100 μ M range in all 4 DLBCL lines and concentrations below the IC₅₀ were then used to test whether the i-motif interactive compounds could repress MCL1 gene expression. We observed lowering of MCL1 mRNA levels by ~20% in DLBCL cells treated with NSC3064 and up to 40% with NSC50572.

Conclusions: Our findings suggest that destabilization of the MCL1 i-motif may repress gene expression and thus be a target for MCL1 inhibition. Follow-up studies are ongoing to validate these compounds and to determine if lower mRNA translates to a reduction in MCL1 protein expression.

1536 Next Generation Sequencing-Assays Detect B-Lymphocyte Clonality in Formalin-Fixed Paraffin Embedded Specimens of Classical Hodgkin Lymphoma without Microdissection

Cynthia Reyes Barron¹, Andrew Campbell², Paul G Rothberg², Richard Burack³, Yi Ding⁴. ¹University of Rochester Medical Center, Victor, NY, ²University of Rochester Medical Center, ³University of Rochester, Rochester, NY, ⁴University of Rochester Medical Center, Rochester, NY

Background: The diagnosis of Hodgkin lymphoma (HL) is primarily made in tissue sections as attempts to identify neoplastic Hodgkin and Reed Sternberg (RS) cells by flow cytometry is usually unsuccessful. Routine assessment of immunoglobulin heavy chain (IGH) clonality has traditionally relied on PCR based methods. This approach may show limited sensitivity for low abundance tumor clones, such as in HL cases. While methods for the detection of B cell clonality could aid in the diagnosis of HL, microdissection is not practical in most clinical settings. Here we assess the utility of Next Generation Sequencing (NGS) based clonality assays applied to formalin-fixed paraffin embedded (FFPE) Hodgkin lymphoma specimens without microdissection.

Design: Thirty-three cases with diagnoses of classical Hodgkin lymphoma (cHL) were retrieved and confirmed by histologic and immunohistochemical study review. The median tumor cellularity (number of RS cells and mononuclear variants) was 5% (range <1% to 15%). DNA was isolated, amplified and sequenced on MiSeq NGS platform. For comparison, the same set of specimens was tested by the standard BIOMED-2 heteroduplex PCR-based clonality assay for IGH and IGK genes with analysis of the products by gel electrophoresis.

Results: Without microdissection, clonality was detected in 18 of 33 cases (55%) by NGS assays (See Figure 1). IGK assays contributed slightly more positive results than IGH (13 vs. 11 positive cases, with six cases positive in both). There was no significant difference between IGH framework regions (FR1, FR2 and FR3). In comparison, standard PCR-based assays identified a clonal population in eight of 33 cases (24%) and IGK assays contributed significantly more positive results than IGH assays (8 vs. 0 positive cases, respectively).

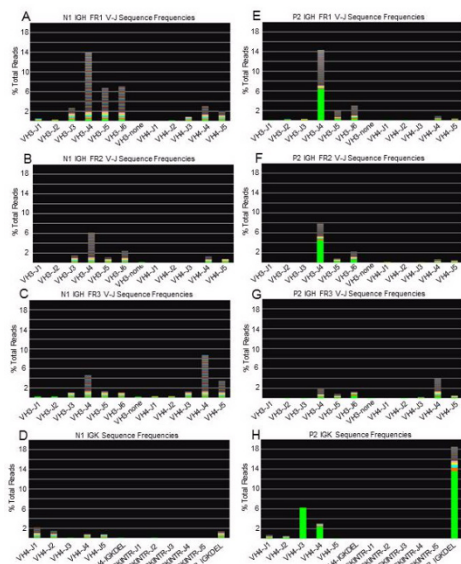


Figure 1. (A-D) Representative case (P21) which shows polyclonal sequences for both IGH and IGK; (E-H) Representative case (P2), monoclonal gene rearrangement in IGH FR1, FR2 and IGK regions and polyclonal in IGH FR3 region.

Conclusions: NGS-based IGH and IGK assays are more robust and sensitive than PCR-based assays in detection of B cell clonality in cHL without microdissection; they also provide valuable information to evaluate the preference in immunoglobulin heavy or light chain segment usage for classification and prognosis correlation purposes. Assessing clonality in both IGH and IGK genes expands the ability to detect clonal neoplasms. The application of NGS-based clonality detection for Hodgkin lymphoma is much less developed, but its role could be more critical than it is for non-Hodgkin lymphomas, especially in the evaluation of the occasional specimen of cHL which does not show typical clinical or histologic features.

1537 Characterization of p53 and CD99 Expression in MYC Rearranged, Increased MYC Copy Number and MYC Negative High Grade B-Cell Lymphomas

Aida Richardson¹, Da Zhang¹, Janet Woodroof², Wei Cu². ¹Kansas University Medical Center, Kansas City, KS, ²University of Kansas Medical Center, Kansas City, KS

Background: Patients with MYC, MYC/BCL-2 or MYC/BCL-6 rearranged B cell lymphomas have an aggressive clinical course. p53 expression and increased MYC copy number have been shown to serve as independent prognostic markers in patients with diffuse large B-cell lymphoma (DLBCL). However expression of p53 in lymphomas with increased MYC copy number has not been explored. Conversely, CD99 expression was shown to have better survival in the germinal center B-cell DLBCL. To the best of our knowledge this is the first study to evaluate p53 expression in lymphomas with increased MYC copy numbers and CD99 expression in relation to MYC status.

Design: We identified 115 patients via keyword search in our electronic record system during 2001-2016. The status of MYC, BCL-2 and BCL-6 rearrangement was identified by fluorescence in situ hybridization (FISH). The patients included MYC negative (n=42), increased MYC copy numbers (n=28), MYC rearranged (n=23) and MYC/BCL-2 and or MYC/BCL6 rearranged (n=22). We retrospectively assessed CD99 and p53 expression by immunohistochemistry using a cut-off of 25% and 50% and correlated CD99 and p53 expression with MYC status. We also analyzed the impact of p53 and CD99 expression on overall survival (OS), progression free survival (PFS) and disease free survival (DFS) in regards to MYC status.

Results: P53 expression was significantly associated with MYC expression, increased MYC copy numbers and MYC rearrangement (p=0.001-0.006). p53 expression showed an adverse impact on OS, PFS and DFS in patients with MYC rearrangement regardless of status of BCL-2 and or BCL-6 rearrangement (p=0.0003-0.04), but no significant impact on survivals in patients with negative MYC rearrangement or increased MYC copy numbers. In addition, patients with p53 expression also showed inferior PFS regardless of MYC status (p=0.007).

CD99 expression on the other hand showed statistically significant association with MYC negative high grade B-cell lymphoma regardless of MYC genetic background or protein level (p=0.0001-0.02). However, CD99 expression had no significant impact on OS, PFS, and DFS (p>0.05).

Conclusions: p53 expression is associated with MYC expression, increased MYC copy numbers and MYC rearrangement while CD99 expression is associated with MYC-negative status. The adverse

impact of p53 expression on survivals in *MYC* rearranged group again demonstrated synergistic effect between p53 and *MYC* rearrangement.

1538 Core binding factor acute myeloid leukemia has favorable clinical outcome regardless of complex karyotype or secondary genetic abnormalities

Heesun Rogers¹, Xiaoqiong Wang¹, Eric Hsi¹, Robert Hasserjian². ¹Cleveland Clinic, Cleveland, OH, ²Massachusetts General Hospital, Boston, MA

Background: Core binding factor acute myeloid leukemia (CBF AML), comprising about 15% of de novo adult AMLs, include AMLs with t(8;21)(q22;q22) [t(8;21)] and inv(16)(p13.1q22) [inv(16)]. t(8;21) and inv(16) AMLs share relatively favorable prognosis and frequent *KIT* mutations; however, they differ in terms of morphology, aberrant immunophenotype, and spectrum of secondary genetic abnormalities. The prognostic significance of these secondary genetic abnormalities is not entirely clear, and there are discrepant findings in the literature.

Design: This retrospective study aims to evaluate clinicopathologic features and clinical outcome of secondary genetic abnormalities in CBF AML patients. CBF AML patients were identified at two centers with local institutional review board approval.

Results: 96 CBF AML patients, including 54 inv(16) and 42 t(8;21) AML, were included. Compared to t(8;21) AML, inv(16) AML patients had significantly higher white blood cell count, blood monocyte count, bone marrow blast and eosinophil count, and the presence of abnormal eosinophils ($p < 0.05$ for all). On Immunophenotyping, CD19 (74%) and CD56 (61%) were commonly expressed in t(8;21) AML, while CD2 (40%) was commonly expressed in inv(16) AML. Considering karyotype, single (inv(16) or t(8;21) alone) and two abnormalities were noted in 48% and 38% of t(8;21) AML and 44% and 19% of inv(16) AML, respectively. Common secondary abnormalities (in decreasing order) were -Y, del(9q), -X and -7/del(7q) in t(8;21) AML and +22, +8, -7/del(7q) and +21 in inv(16) AML. A complex karyotype was more frequent in inv(16) than in t(8;21) AML (37% vs 14%, $p = 0.02$). The incidence of *KIT* mutation was similar in t(8;21) and inv(16) AMLs (26% vs 21%, $p = 0.64$).

There was no significant difference in overall survival (OS) between t(8;21) and inv(16) AML patients (mean 106 vs 124 months, respectively; logrank $p = 0.63$). Within t(8;21) and inv(16) AML patient groups, there was no difference in OS between single cytogenetic abnormality, two abnormalities and complex karyotype (logrank $p = 0.75$ and $p = 0.76$, respectively). Similarly, *KIT* mutation was not associated with OS in either patient group (logrank $p = 0.09$ and $p = 0.96$, respectively).

Conclusions: Despite the limitation of the small numbers, our data demonstrate that both t(8;21) and inv(16) AML patients have similarly favorable clinical outcome. Neither additional secondary cytogenetic abnormalities (including complex karyotype) nor *KIT* mutation adversely affected patient outcome.

1539 Myeloid Neoplasms with t(3;12)(q26.2;p13)/ETV6-EVI1 Rearrangement: A Study of 12 Cases

Arash Ronaghy¹, Zhihong Hu¹, Pei Lin¹, Wei Wang¹, L. Jeffrey Medeiros¹, Shimin Zhu¹. ¹The University of Texas MD Anderson Cancer Center, Houston, TX

Background: *EVI1/3q26.2* rearrangement is observed in various myeloid neoplasms, including cases of acute myeloid leukemia (AML), myelodysplastic syndrome (MDS) and chronic myeloid leukemia (CML), blast phase. Chromosomal translocations involving *EVI1/3q26.2* result in *EVI1* overexpression in most cases. t(3;21)(q26.2;q22) and t(3;12)(q26.2;p13) are the only chromosomal translocations currently known to lead to *EVI1* fusions. Whereas myeloid neoplasms associated with t(3;21) have been studied extensively, myeloid neoplasms associated with t(3;12) have received little attention in the literature.

Design: Patients with myeloid or lymphoid neoplasms associated with t(3;12)(q26.2;p13) diagnosed over a 20-year interval were reviewed. Clinicopathological, genetic and follow-up data were analyzed.

Results: The study group included 12 patients with myeloid neoplasms associated with t(3;12)(q26.2;p13): 5 patients had AML, 5 had MDS (including 3 with *de novo* MDS with excess blasts-2 and 2 with therapy-related MDS), 1 had CML, and 1 had primary myelofibrosis (PMF). No lymphoid neoplasms with t(3;12) were identified. There were 6 men and 6 women with a median age of 48 years (range, 32-63) at initial diagnosis. Eight patients had t(3;12) at initial diagnosis, and 4 patients, including the patients with CML and PMF, acquired t(3;12) after initial diagnosis. In 6 patients, t(3;12) was observed as a sole chromosomal abnormality. Monosomy 7 was observed in 3 patients. Fluorescence *in situ* hybridization analyses for *EVI1* and *ETV6* rearrangements were performed in 6 patients each. Both were positive in all tested patients. A variable degree of dysplasia was observed in 6 of 8 patients with t(3;12) at initial diagnosis, and in other 2 patients, dysplasia couldn't be evaluated at initial diagnosis due to too few non-blast cells. However, both cases showed dysplasia when the blasts were decreased after therapy. Six of 7 patients with an initial

diagnosis of MDS/CML/PMF had follow-up, and 2 developed AML at emergence of t(3;12) and 1 developed AML 20 months later. Follow up was available for 11 patients: 10 received chemotherapy, including one 1 patient who received a stem cell transplant. Six patients had died at last follow-up with a median survival of 17.3 months after emergence of t(3;12).

Conclusions: t(3;12)/*ETV6-EVI1* is a rare translocation associated exclusively with myeloid neoplasms. Morphological dysplasia is common and the overall prognosis of these patients is poor.

1540 Correlation of CD19 and CD22 Expression Level with Response to Novel Immunotherapeutics in B-Lymphoblastic Leukemia

Jaclyn Rosenthal¹, Ammar Naqvi², Gerald Wertheim³, Michele Paessler⁴, Susan Rheingold⁵, Andrei Thomas-Tikhonenko², Vinodh Pilla⁶. ¹University of Pennsylvania Perelman School of Medicine, ²CHOP, ³Swarthmore, PA, ⁴Newtown, PA, ⁵Penn Valley, PA

Background: Targeted immunotherapy has shown higher response rates in the treatment of relapsed/refractory B acute lymphoblastic leukemia (B-ALL) compared to chemotherapy. Blinatumomab and chimeric antigen receptor modified T (CAR) cells are novel immunotherapeutics that target CD19 while Inotuzumab and Moxetumomab are antibody drug conjugates that target CD22. However, significant numbers of patients do not respond or relapse with antigen-negative refractory disease. The level of antigen that is needed for maximum efficacy is not known. Correlation studies are hindered by limited data on antigen levels in de novo and relapsed pediatric B-ALL.

Design: The flow cytometry archives from 2001-2016 were analyzed to identify de-novo and relapsed B-ALL cases. Pure populations of blasts were gated using multiple blast markers. CD19 and CD22 antigen expression in blasts were classified based on comparison to normal B cells as negative, low normal, high normal and bright. Results were correlated with cytogenetics, FISH, whole genome SNP array and NGS sequencing data when available. RNA expression data from the Therapeutically Applicable Research to Generate Effective Treatments (TARGET) study for Pediatric ALL was independently analyzed to identify cases with dim CD19 and CD22 RNA expression compared to pro B cells.

Results: 628 cases of B-ALL were found in the archives out of which 80% were de novo and 20% were relapsed (no prior immunotherapy). 5% of cases showed dim-negative expression of CD19 while 20% were negative for CD22. There was no difference in CD19 and CD22 expression levels between de novo and relapsed cases. CD19 and CD22 expression was correlated with response to immunotherapeutics. 15% of cases also showed significant (>1%) levels of CD19-negative blasts. Evaluation of RNA expression data from the TARGET dataset revealed 18% of cases with low expression of CD19 and 11% with low expression of CD22. Cases with *ETV6-RUNX1* translocation showed high expression of CD19 and CD22 while cases with *MLL* gene translocations showed low expression.

Conclusions: This is the largest pediatric series to quantitatively assess CD19 and CD22 expression in B-ALL by a widely applicable flow cytometry based quantitation system. A significant proportion of de-novo CD19- and CD22-negative cases were found by different methods. Antigen-negative cases were less likely to respond to targeted immunotherapeutics and were correlated with certain cytogenetic abnormalities.

1541 Flow Cytometric Analysis of Expanded and Phenotypically Abnormal NK-Type Large Granular Lymphocytes in Neoplastic and Non-Neoplastic Conditions

Sory J Ruiz¹, Yi-Hua Chen¹, Kristy Wolniak². ¹Northwestern University, Chicago, IL, ²Northwestern University, Evanston, IL

Background: A subset of large granular lymphocytes (LGL) are NK cells. Expansion of LGLs can occur transiently, as a reactive response to other conditions. It does not always indicate neoplasia and that distinction is difficult for pathologists since there are not significant morphologic differences. Prior reports in the literature have described the significance of phenotypically abnormal NK cells with killer-cell immunoglobulin-like receptor (KIR) isoform or lack of detectable KIR.

The aim of this study is to analyze expanded populations of phenotypically abnormal NK LGLs by flow cytometry.

Design: Flow cytometry immunophenotypic data on bone marrow and peripheral blood collected for diagnostic purposes of adult cases of phenotypically abnormal or expanded population of NK cells (>25% of lymphocytes) between 01/01/2007 and 08/30/2015 were identified.

Primary flow cytometry data was re-analyzed on Kaluza software and the expression of CD3, CD4, CD5, CD8, CD16/56, TIA1, granzyme-B, perforin and KIRs (CD158a, CD158b and CD158e) was studied. A retrospective review of the patients' medical records was conducted and the clinical diagnosis was evaluated.

Results: 28 cases of immunophenotypically abnormal or expanded NK LGLs were identified. Ages 26 - 89 (mean 68), 13 were female and 15 male.

In 27/28 cases immunophenotypic abnormalities in NK cells were identified and abnormal expression of KIRs was present in all cases. In one case KIR expression was not performed. 8/27 were NK neoplasia including 3 chronic lymphoproliferative disorder of NK cells (CLD-NK) with cytopenias, 4 CLD-NK without cytopenias and 1 extranodal NK lymphoma.

KIR-restricted expansion associated with non-neoplastic condition were identified: 4 stem cell transplants, 1 kidney transplant, 3 autoimmunity, 4 chemotherapy/radiation, 3 other hematolymphoid conditions.

Conclusions: Non-neoplastic expansions of NK LGLs can occur in a variety of conditions and can be prolonged. Similar immunophenotypic abnormalities can be observed in both neoplastic and non-neoplastic expansion of NK cells.

Adding markers for the identification of KIR antigens to flow cytometry panels is a useful way to identify abnormalities of expanded NK cells. Expression of the 3 KIR antigens tested is a straightforward way to make such identification, and even allows the detection of small abnormal populations.

Clinical correlation remains with clinical and additional laboratory data remains essentially to determine whether a NK cell expansion is neoplastic.

1542 Distinct Genetic Features of Myelodysplastic Syndromes as Defined in the Revised 2016 World Health Organization Classification

Roberto Ruiz-Cordero¹, Juliana E Hidalgo-Lopez¹, Carlos Bueso-Ramos¹, Mark Routbort², Rashmi Kanagal-Shamanna³, Zhuang Zuo¹, C. Cameron Yin¹, Sanam Loghavi⁴, Chi Young Ok¹, Jeff Jorgensen¹, Sa Wang¹, Guilin Tang¹, Rajyalakshmi Luthra¹, L. Jeffrey Medeiros⁵, Keyur Patef¹. ¹The University of Texas MD Anderson Cancer Center, Houston, TX, ²Bellaire, TX, ³The University of Texas MD Anderson Cancer Center, Bellaire, TX, ⁴Houston, TX, ⁵The University of Texas MD Anderson Cancer Center, Sugar Land, TX

Background: Rapidly accumulating genetic information in cases of myelodysplastic syndrome (MDS) along with refinement in morphologic interpretation and assessment of cytopenia(s) form the basis of the revised World Health Organization (WHO) classification of myeloid neoplasms. We present genomic data for MDS cases defined using the new diagnostic categories of the revised 2016 WHO classification.

Design: We identified patients with MDS who had undergone targeted mutation profiling of the DNA extracted from bone marrow aspirates using a MiSeq platform (Illumina, San Diego, CA). The panel included coding and non-coding sequences of 81 genes associated with hematolymphoid neoplasms including: ANKRD26, ASXL1, ASXL2, BCOR, BCORL1, BRAF, BRINP3, CALR, CBL, CBLB, CBLC, CEBPA, CREBBP, CRLF2, CSF3R, CUX1, DDX41, DNMT3A, EED, ELANE, ETK1, ETV6, EZH2, FBXW7, FLT3, GATA1, GATA2, GFI1, GNAS, HNRNP, HRAS, IDH1, IDH2, IKZF1, IL2RG, IL7R, JAK1, JAK2, JAK3, KDM6A, KIT, KMT2A, KRAS, MAP2K1, MPL, NF1, NOTCH1, NPM1, NRAS, PAX5, PHF6, PIGA, PML, PRPF40B, PTEN, PTPN11, RAD21, RARA, RUNX1, SETBP1, SF1, SF3A1, SF3B1, SH2B3, SMC1A, SMC3, SRSF2, STAG1, STAG2, STAT3, STAT5A, STAT5B, SUZ12, TERC, TERT, TET2, TP53, U2AF1, U2AF2, WT1, and ZRSR2. We reviewed clinical and laboratory data, bone marrow pathology reports and ancillary test results.

Results: A total of 114 cases including 79 primary MDS, 20 morphologically normal controls, 12 AML arising from MDS, and 3 MDS/MPN were reviewed. Overall, TP53, splicing factors, and epigenetic modifiers constituted the 10 most commonly mutated genes: TP53 (n=39), SF3B1 (n=31), ASXL1 (n=26), TET2 (n=22), DNMT3A (n=16), SRSF2 (n=14), U2AF1 (n=14), RUNX1 (n=11), SETBP1 (n=9), and STAG2 (n=9). TP53, RUNX1 and STAG2 mutations occurred mainly in therapy-related MDS and MDS with excess blasts (MDS-EB). SF3B1 mutations were most common in MDS with ring sideroblasts (MDS-RS) and MDS with multilineage dysplasia (MDS-MLD). U2AF1 and TP53 mutations were also prevalent in MDS-MLD. The mean number of mutations per case correlated with morphologic dysplasia and an increased blast percentage, ranging from 0.5 in controls (unremarkable by morphology, flow, cytogenetics), to 1.5 in MDS-RS, and >3 mutations per case in MDS-MLD/MDS-EB.

FOR TABLE DATA, SEE PAGE 573, FIG. 1542

Conclusions: MDS entities as defined in the revised WHO classification show distinct genotypes that provide further support for the current categories of MDS and offer additional insights into pathogenesis and clinical behavior.

1543 TP53 Mutations are Common in Mantle Cell Lymphoma, Including the Indolent Leukemic Non-Nodal Variant

Ali Sakhdari¹, Keyur Patef¹, Chi Young Ok¹, Rashmi Kanagal-Shamanna³, C. Cameron Yin¹, Zhuang Zuo¹, Shimin Hu¹, Mark Routbort², Rajyalakshmi Luthra¹, L. Jeffrey Medeiros⁵, Joseph Khoury¹, Sanam Loghavi⁴. ¹The University of Texas MD Anderson Cancer Center, Houston, TX, ²The University of Texas MD Anderson Cancer Center, Sugar Land, TX, ³The University of Texas MD Anderson Cancer Center, Bellaire, TX, ⁴Bellaire, TX, ⁵Houston, TX

Background: Mantle cell lymphoma (MCL) is a B-cell neoplasm usually associated with an aggressive clinical course, but there are clinically indolent subtypes and therefore prognostic biomarkers are needed. Earlier studies have shown that MCL has a unique mutational profile; however, data on the utility of next-generation sequencing (NGS) mutation profiling in the context of routine workup and its role in risk-stratification of MCL patients are limited. In this study, we describe the mutational landscape and clinicopathologic correlates of a series of MCL cases at a single-institution setting.

Design: The study group included 26 MCL patients diagnosed according to World Health Organization criteria. All samples were evaluated by NGS (Illumina, San Diego CA, USA) using DNA extracted from peripheral blood (PB) or bone marrow (BM) with a panel enriched for genes involved in the pathogenesis of B-cell lymphoma. Evaluation of the extent of PB or BM involvement was performed using flow cytometry immunophenotyping. Clinical and laboratory data were obtained from electronic medical records.

Results: There were 17 (65%) men and 9 (35%) women with a median age of 65 years (range, 50-94) at diagnosis. Twenty-one of 26 (81%) patients had classical MCL (C-MCL) and 4 (19%) had the "leukemic non-nodal variant" (L-MCL) defined as cases with BM/PB and/or splenic involvement and not involving lymph node or other extranodal tissues. Mutated genes included TP53 (35%), ATM (27%), CARD11 (8%); and FBXW7, NOTCH1, SPEN, BIRC3 (4% each). Comparison of mutant allele frequency with the extent of sample involvement by MCL showed most mutations were clonal in nature. Ten unique TP53 mutations (7 clonal and 3 subclonal) were identified in 9 samples, including 3 L-MCL cases. There was no difference in the frequency of TP53 mutations between the L-MCL and C-MCL groups (p=0.6) but TP53 mutations were more often subclonal in L-MCL (2/3 cases). Identification of clonal TP53 alterations in 2 L-MCL patients prompted initiation of therapy despite low tumor burden. All TP53 mutant cases had classic MCL morphology; no blastoid or pleomorphic variants were identified. All patients were alive at last follow up (median 11 months, range 1-90 months).

Conclusions: TP53 and ATM are commonly mutated in MCL. TP53 mutations may be clonal or subclonal in nature. Although seemingly indolent, the L-MCL variant may harbor subclonal TP53 mutations which may serve as a useful biomarker for follow-up monitoring and early detection of clonal expansion.

1544 Myelodysplastic Syndromes with EZH2 Mutations Frequently Show Multilineage Dysplasia, Chromosome 7 Alterations and Concomitant Mutations in ASXL1, RUNX1 and TET2

Ali Sakhdari¹, Mark Routbort², Carlos Bueso-Ramos¹, Keyur Patef¹, Rajyalakshmi Luthra¹, Chi Young Ok¹, Sanam Loghavi⁴, Zhuang Zuo¹, C. Cameron Yin¹, Joseph Khoury¹, L. Jeffrey Medeiros⁵, Rashmi Kanagal-Shamanna³. ¹The University of Texas MD Anderson Cancer Center, Houston, TX, ²Bellaire, TX, ³The University of Texas MD Anderson Cancer Center, Sugar Land, TX, ⁴Houston, TX, ⁵The University of Texas MD Anderson Cancer Center, Bellaire, TX

Background: TP53, RUNX1 and EZH2 mutations are independent predictors of survival in myelodysplastic syndrome. EZH2 (7q36) encodes a histone methyltransferase essential for epigenetic silencing during stem cell renewal; as a chromatin regulator, it plays a vital role in myelodysplasia. EZH2 mutation is one mechanism of abnormal EZH2 function. Unlike lymphomas where EZH2 Y641 hot-spot gain-of-function mutation is frequent, MDS cases show a spectrum of mutations. Due to the availability of EZH2-targeted therapies, there is a need for precise evaluation of these mutations in larger cohorts. In this study, we evaluated EZH2 mutations in MDS patients and correlated with clinical, morphologic and genetic findings.

Design: We searched our institutional database for MDS patients with EZH2 mutation detected by targeted NGS using a myeloid gene panel. We evaluated clinical, morphologic, cytogenetic and mutational results.

Results: We identified 34 patients with 39 EZH2 somatic mutations. There were 27 men and 7 women with a median age of 74 years (range, 55-85). Using 2016 WHO cytopenia criteria, 27 (79.4%) had anemia, 21 (61.8%) had thrombocytopenia and 22 (64.7%) had decreased ANC. Fourteen (41.1%) patients had pancytopenia, 9 (26.5%) and 11(32.4%) had bi- and mono-cytopenia, respectively. EZH2 mutations included 24 missense, 6 nonsense and 9 frameshift type; mutations were most frequent in exons 18/19; 16 (41%) mutations were within the catalytic

"SET" domain. Using revised WHO 2016 criteria, the most common subtype was MDS with multilineage dysplasia (MDS-MLD, n=15, 44.1%) followed by MDS-EB-1 (n=6, 17.6%), MDS-EB-2 (n=4, 11.8%), therapy-related MDS (n=3, 8.8%), MDS-RS-MLD (n=2, 5.9%), MDS-SLD (n=2, 5.9%) and MDS-RS-SLD (n=2, 5.9%). The median BM blast% was 4 (0-13); 21 (62%) cases presented with <5% blasts. Eleven (33.3%) patients showed diploid karyotype; 11 (33%) patients had concurrent chromosome 7 alterations. Frequent co-mutated genes were: *ASXL1* (14/34, 41.1%), *RUNX1* (12/34, 35.2%), *TET2* (11, 32.3%) and *TP53* (6/34, 17.6%). The median MAF was 37% (range, 1-90%). Over a median follow-up of 14.1 (1-1347) months,

Conclusions: *EZH2* mutations in MDS span the entire gene. MDS patients with *EZH2* mutations show a male predominance, multilineage dysplasia and frequent co-mutations in *ASXL1*, *RUNX1* and *TET2*. A high proportion (33%) has concurrent chromosome 7 alterations suggesting a tumor suppressor role. The combination of these adverse features may confer poor outcome.

1545 Use of a Blast Dominance-Hematogone Index to Assess Loss of Blast Heterogeneity and Decreased Hematogones in Myelodysplastic Syndrome Versus Normal Bone Marrow

Jason M Schenkel¹, Graham Dudley¹, Karry Charest¹, David Dorfman¹, Betty Li¹. ¹Brigham and Women's Hospital, Boston, MA

Background: Myelodysplastic syndrome (MDS) is a complex and heterogeneous disorder of myelopoiesis, resulting in the inefficient production and cytopenia of at least one myeloid lineage. MDS is diagnosed in roughly 10,000-15,000 people each year. Individuals with certain MDS subtypes are at an increased risk of developing acute myeloid leukemia (AML), and thus identification and tracking of MDS over time could have significant clinical ramifications. Due to the varied causes and manifestations of MDS, diagnosis is often difficult, and relies on histologic and genetic based approaches. Previous work has demonstrated that normal bone marrow contains at least 3 populations of CD34+ blasts based on expression of CD13 and HLA-DR and that MDS patients have a loss of this blast heterogeneity. Additionally, a separate report demonstrated that MDS was correlated with a decrease in hematogones (precursor B cells) in the bone marrow. Loss of blast heterogeneity and loss of hematogones may correlate or even be directly related, but this has not been formally assessed.

Design: Bone marrow samples from patients with known MDS or with no detectable hematologic malignancy were identified and processed for flow cytometry. Two 10 color flow cytometry panels were used to detect blast expression of CD13 and HLA-DR and the fraction of hematogones present within each sample. Flow cytometric analysis was performed using Flowjo.

Results: There was a variable loss of blast heterogeneity for expression of CD13 and HLA-DR in MDS patients (n=30) compared to normal samples (n=16) - the relative size of the dominant blast population was larger in MDS compared to normal (84.8% vs 63.8%, p<0.001). MDS samples also had fewer hematogones compared to normal samples (0.11% vs 0.8%, p<0.001). Dividing the size of the largest blast population by the fraction of hematogones created a blast dominance-hematogone index (BDH), which was significantly larger in MDS compared to normal cases (22588 vs 161.3, p<0.001). Further, using ROC curves, the BDH index had the largest AOC compared to just blast dominance or hematogone size (0.95 vs 0.89 vs 0.93)

Conclusions: Assessment of loss of blast heterogeneity and loss of hematogones has greater sensitivity and specificity for detecting MDS in bone marrow samples than either parameter alone. The blast dominance-hematogone index should be useful in clinical practice to evaluate bone marrow samples for involvement by MDS.

1546 50-dimensional microenvironment analysis of human and mouse bone marrow during malignant transformation

Christian M Schuerch¹, Graham L Barlow¹, Salil S Bhate¹, Nikolay Samusik¹, Garry Nolan¹, Yury Goltsev¹. ¹Stanford University, Stanford, CA

Disclosures:

Nikolay Samusik: *Stock*, Akoya Biosciences; *Consultant*, Akoya Biosciences
Yury Goltsev: *Stock*, Akoya Biosciences; *Consultant*, Akoya Biosciences

Background: Hematopoiesis, the generation of all blood lineages, takes place in the bone marrow (BM). Hematopoietic stem cells (HSCs) are localized in a special BM microenvironment, the HSC niche that regulates their quiescence, proliferation, migration and differentiation. Hematologic cancers have a profound impact on normal HSC and niche function, affecting BM output. A high-dimensional analysis of niche types, their precise spatial interactions with HSCs and their dynamics during the course of a disease will shed light on how

hierarchical BM tissue organization is maintained during homeostasis and altered in malignancy.

Design: We have developed a high-dimensional fluorescent microscopy platform, CO-Detection by antibody indEXing (CODEX) that allows 3D analysis of 50+ parameters in a single tissue section in less than 8 hours. We apply CODEX to BM core biopsies from multiple myeloma patients to characterize how the disease affects the BM microarchitecture. In addition, CODEX is used to analyze BM tissue organization and the HSC niche during cancer development in a murine leukemia model.

Results: We have built an integrated computational pipeline for analysis of high-dimensional CODEX data that enables the identification and characterization, at the single-cell level, of immune and stromal cell subsets and their microenvironmental niches in healthy and diseased immune organs. Analyzing human tonsils, we identified a unique and novel cellular microenvironment for follicular T helper cells. In addition, we investigated spleen tissue architectural rearrangement in a mouse model of autoimmunity and discovered unknown cellular interactions. Furthermore, we applied CODEX to human and mouse bone marrow to simultaneously visualize all major BM cell types as well as their spatial organization, paving the way to study the rearrangement of BM architecture during malignant transformation in multiple myeloma and leukemia.

Conclusions: High-dimensional tissue imaging by CODEX allows studying single cells in their native tissue context in health and disease and facilitates the discovery of novel cellular interactions and cell types.

1547 Immunophenotype signatures for Kikuchi's Disease, Castleman's Disease, and Angiomyomatous Hamartoma: rare diseases drawn out of large-scale normative data using an informatics approach

Gregory D Scott¹, Dita Gratzinger². ¹Stanford University, Stanford, CA, ²Stanford University Medical Center, Stanford, CA

Background: Kikuchi's lymphadenitis, Angiomyomatous Hamartoma, and Castleman's Disease represent important but uncommon potential diagnostic pitfalls when evaluating a clinically suspicious lymph node. The contribution of flow cytometry immunophenotyping in identifying these diseases is poorly understood and prior research is hindered by limited sample sizes of test and control data. Moreover, curation and analysis of such a dataset would require a prohibitive amount of manual labor.

Design: Custom software written in Python, AutoHotkey, and R was created to identify and parse over 370,000 pathology and flow cytometry records for 380 benign excised lymph nodes with paired flow cytometry. Event data for standard clinical B-, T-, and NK-antigen markers were evaluated in the lymphocyte and monocyte gates for diagnosis-specific patterns. Immunophenotype signatures were developed using combinations of markers CD19, CD20, CD10, CD23, CD38, FMC-7, CD4:CD8 ratio, CD7 loss, CD56, and CD57 for Kikuchi's disease (n=14), Angiomyomatous Hamartoma (n=4), or Castleman's Disease (n=17).

Results: The multi-parameter immunophenotype signature for Kikuchi's disease (n=13) versus controls (n=209) identified 84.6% of true positive cases and 99% of true negative cases for a test sensitivity of 84.6%, specificity 99.04%, positive predictive value 84.62%, negative predictive value 99.04%. The immunophenotype signature for Castleman's Disease (n=8) versus controls (n=261) identified 87.5% of true positive cases, 99.2% of true negative cases for a test sensitivity of 87.5%, specificity 99.2%, positive predictive value 77.7%, and negative predictive value of 99.6%. The immunophenotype signature for Angiomyomatous Hamartoma, albeit on a limit number of cases (n=4) detected all positive cases and rejected all negative controls (n=253).

Conclusions: Automated data curation greatly extends a pathologist's reach to evaluate multi-dimensional large-scale data and identify diagnostic aids for rare understudied diseases. Using this method, we found novel signatures in routine flow cytometry immunophenotyping that can significantly aid in flagging rare malignant mimics: Kikuchi's disease, Castleman's Disease, and Angiomyomatous Hamartoma.

1548 Improving Utility of Sequencing Panels Using Morphology-Based Ordering Algorithms in Myeloid Malignancies

Adam Seegmiller¹, Aaron Shaver¹, Cindy Vnencak-Jones¹, David Head¹, Claudio Mosse², Ridas Juskevicius², Mary Zutter¹, Thomas Stricker². ¹Vanderbilt University Medical Center, Nashville, TN, ²Vanderbilt University, Nashville, TN

Background: Next-generation sequencing (NGS) tests to assess for mutations in panels of genes are becoming routine in the diagnostic

work-up of hematolymphoid malignancies. However, their practical utility in the diagnosis and management of these diseases has not been studied extensively. The purpose of this study is to assess the effectiveness of decision-support algorithms based on bone marrow morphology to guide use of NGS testing.

Design: Use of a 37-gene NGS panel focused on myeloid malignancies was incorporated into pre-existing diagnostic management team (DMT) decision-support algorithms for acute myeloid leukemia (AML), myelodysplastic syndrome (MDS), myeloproliferative neoplasms (MPN), and myelodysplastic/myeloproliferative neoplasms (MDS/MPN). In general, sequencing was recommended if there was morphologic evidence of disease at diagnosis or first presentation, transformation, or relapse. Results were evaluated to determine fraction of positive tests and the number and type of mutations. Comparisons were made between tests that were concordant and discordant with algorithm recommendations.

Results: Sequencing was ordered on 673 bone marrows submitted for known or suspected myeloid malignancies. Of these 483 (72%) were positive for one or more mutations. Positive results were significantly more common (474/582; 81%) when test orders were concordant with algorithm recommendations than when they were discordant (9/91; 10%) ($P < 0.0001$). This is particularly true for morphologically negative bone marrows ordered to rule out MDS or MPN (4/64; 6%), as opposed to follow-up discordant testing from patients with a history of myeloid malignancy (5/27; 19%). In the 4 morphologically negative rule-out cases, all patients were older adults (52-88 years old) with mutations in a single gene at low variant allele fractions ($\leq 20\%$), suggestive of clonal hematopoiesis of indeterminate potential (CHIP). In contrast, concordant testing in MDS and MPN was positive for mutations in 77% and 74% of cases, with multiple genes mutated in 50% and 41% of cases, respectively.

Table 1: Fraction of Positive Cases by Diagnosis and Concordance

	AML	MDS	MPN	MDS/MPN	Total
Concordant	199/229 (87%)	140/183 (77%)	95/128 (74%)	40/42 (95%)	474/582 (81%)
Discordant	3/18 (17%)	4/42 (10%)	1/30 (3%)	1/1 (100%)	9/91 (10%)
Prior History	3/18 (17%)	1/3 (33%)	0/5 (0%)	1/1 (100%)	5/27 (19%)
Rule-out		3/39 (8%)	1/25 (4%)		4/64 (6%)

Conclusions: For bone marrow samples, NGS-based sequencing tests are usually negative in the absence of morphologic evidence of disease, and when positive, results are often of unclear clinical significance. Most morphologically positive cases have mutations, often more than one. These data suggest that morphology-based decision support algorithms are effective in identifying cases in which genomic testing is most likely to be clinically useful.

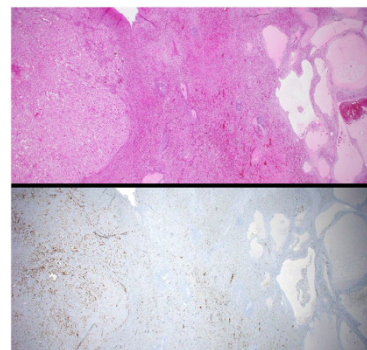
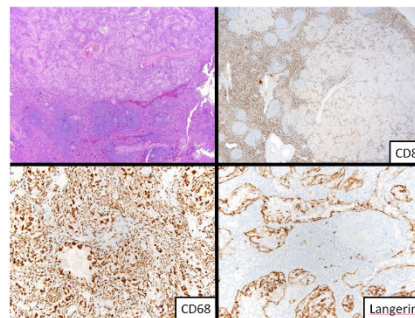
1549 Langerin Staining Identifies Most Littoral Cell Angiomas in the Absence of CD1a but not Most Other Splenic Angiomatous Lesions

William Selove¹, Jennifer Picarsic², Steven H Swerdlow³. ¹University of Pittsburgh Medical Center, Pittsburgh, PA, ²Children's Hospital of Pittsburgh of UPMC, Pittsburgh, PA, ³University of Pittsburgh School of Medicine, Pittsburgh, PA

Background: Although littoral cell angiomas (LCA) are phenotypically well-characterized, the individual positive antigens are found on many other cells in the spleen and most in other angiomatous lesions, complicating interpretation. Based on a Langerin/CD207+ LCA index case and anecdotal findings of Langerin staining in lymph node (LN) sinus lining cells (SLC), Langerin & other selected immunohistochemical (IHC) staining was performed on LCA, other splenic angiomatous lesions & reactive lymph nodes (LN) to better understand the role of Langerin as a diagnostic tool.

Design: 9 LCA and 20 other splenic angiomatous lesions (14 hemangiomas, 1 SANT, 1 hamartoma, 2 lymphangiomas and 2 not further classifiable) from 28 spleens with available tissue had IHC stains performed for Langerin (Cell Marque #392M-18, clone 12D6), CD34, & CD8. LCA were also stained for CD1a, S100, cyclin D1, and CD68. Electron microscopy of 1 LCA was attempted on formalin fixed paraffin embedded (FFPE) tissue. 7 reactive LN were also stained for Langerin and 4 for cyclin D1.

Results: 89% of LCA (8/9) were Langerin+ (33% extensive, 56% partial) with a distinctive sinus type staining pattern, while only 1/20 other vascular lesions was partially positive (5%) ($p < 0.00001$). All LCA were CD1a-, CD68+, CD34- & CD8- [Figure 1]. 22% were S100+, 78% at least partially CD21+ and 89% at least partially cyclin D1+. One case contained a Langerin negative lymphangioma in the same section as a Langerin+ LCA. [Figure 2]. Ultrastructural analysis in one LCA showed cytoplasmic Birbeck-type granules in a rare cell. 7/7 LN showed partial Langerin+ SLC with weaker positivity than on the Langerin+ cells present, & 4/4 showed partial SLC cyclin D1 positivity.



Conclusions: Langerin positivity is easy to interpret and a highly sensitive and specific (sens [0.89], spec[0.95]) IHC stain to help distinguish LCA from other vascular tumors of the spleen. Whether this represents an unusual cross-reactivity or true CD207 expression needs more investigation, as the other IHC studies, do not support a Langerhans cell origin. The staining pattern of Langerin is also distinct and different from that in Langerhans cells. The limited ultrastructural findings need further investigation. The cyclin D1 staining seen in most LCA could be consistent with their expression of other selected vascular and histiocytic markers. Whether the lining cells of the LCA have any relationship to those of lymph node sinuses is unknown.

1550 PREVIOUSLY PUBLISHED

1551 RAS/MAPK Pathway Activation Defines a Common Molecular Subtype of Histiocytic Sarcoma

Vignesh Shanmugam¹, Lynette Sholl¹, Christopher D Fletcher¹, Jason L Hornick¹. ¹Brigham and Women's Hospital, Boston, MA

Background: Histiocytic sarcoma is a rare malignant neoplasm of myeloid origin. It can be primary or secondary (i.e., clonally related to a synchronous or metachronous hematologic malignancy). Very little is known about the molecular genetics of histiocytic sarcoma. The purpose of this study was to identify somatic alterations in histiocytic sarcoma by next-generation sequencing.

Design: Cases of histiocytic sarcoma with available material were retrieved from institutional and consult archives; diagnoses were confirmed by retrospective review. DNA was isolated from formalin-fixed paraffin-embedded tissue from 18 cases. Targeted next-generation sequencing surveying all exonic and selected intronic regions of 447 cancer-associated genes was performed. All variant calls were manually reviewed and germline variants (SNPs) were excluded.

Results: Histiocytic sarcoma cases from 18 patients (14 female, 4 male; mean age: 51 years, range: 12-77; 16 primary, 2 secondary) from a variety of sites (14 extranodal - 4 skin, 2 colon, 1 each breast, heart, liver, omentum, retroperitoneum, spleen, and stomach; 4 nodal) were included. The mean mutational burden was 4.22 per megabase. Recurrent activating mutations in the RAS/MAPK pathway were identified in 8 (44%) cases in a mutually exclusive fashion, including hotspot activating missense mutations in *KRAS* (N=3; G13D, A146T) and *NRAS* (N=1; G12C), *MAP2K1* gain-of-function mutations (N=2; C121S, I103N), and activating mutations within the RING finger domain of *CBL* (N=2; T402_L405del, C396R); one of the latter cases also harbored a loss-of-function frameshift mutation in *NF1*. Of note, no *BRAF* V600E variants were identified. Copy number analysis showed recurrent deletions of 9p21 including the *CDKN2A* tumor suppressor gene in 10 (55%) cases with evidence of two-copy loss in 50%. Additional recurrent mutations were identified in genes involved in NF- κ B signaling (*MYD88*, *SOCS1*) and epigenetic regulation (*KMT2D*, *ARID1A*), which are also commonly mutated in B-cell lymphomas. In particular, missense and truncating mutations in

KMT2D were identified in 5 (28%) cases. A TPM3-NTRK1 fusion was identified in one case.

Conclusions: A large subset of histiocytic sarcomas harbors driver mutations in genes involved in the RAS/MAPK pathway. Some primary histiocytic sarcomas share mutational profiles with B-cell lymphomas. These findings provide insights into the genomic landscape and biology of these rare aggressive neoplasms.

1552 An integrated analysis of DNA methylation and transcriptome profiles identifies two distinct groups of pediatric ALK-positive anaplastic large cell lymphoma

Timothy Shaw¹, Stanley Pounds¹, Xueyuan Cao¹, Gustavo Palacios¹, Sherrie Perkins², Marsha C. Kinney³, Jacqueline M Kravaka⁴, Thomas Gross⁵, John Sandlund¹, Charles Mullighan⁶, Megan Lim⁷, Vasiliki Leventak⁸. ¹St. Jude Children's Research Hospital, ²ARUP Laboratories, Salt Lake City, UT, ³University of Texas Health Science Center at San Antonio, San Antonio, TX, ⁴Medical University of South Carolina, ⁵National Cancer Institute Center for Global Health, ⁶St. Jude Children's Research Hospital, Memphis, TN, ⁷Hospital/ University of Pennsylvania, Philadelphia, PA, ⁸Memphis, TN

Background: Anaplastic large cell lymphoma (ALCL) is a peripheral T-cell lymphoma accounting for 10–15% of all childhood lymphomas. Despite the observation that more than 90% of the cases show ALK rearrangement resulting in aberrant ALK kinase expression, there is significant clinical and morphologic heterogeneity. To identify molecular changes that could explain these heterogeneity, we profiled gene expression changes and methylation patterns in a large cohort of pediatric ALK-positive ALCL (ALK+ALCL).

Design: Fresh frozen ALK+ ALCL diagnostic samples obtained from three childhood cancer consortia (n=42) were analyzed by RNA sequencing (RNAseq) and/or DNA methylation array. The tumor purity of the cases ranged from 10 to 100% with >70% tumor content in 28 of 42 cases. Based on available material, 37 cases were analyzed by DNA methylation array and 32 cases by RNA-seq, including 27 cases with both RNA-seq and DNA methylation data.

Results: Unsupervised hierarchical clustering of DNA methylation and RNAseq each identified two sub-groups with 20 of 27 cases showing significant agreement in group assignment (p= 0.02199). Using the RNAseq clustering, the two groups were defined based on ALK expression levels as ALK-high (n=13) and ALK-low (n=19) that positively correlated with MYC levels in each group. Subsequently, DNA methylation and RNAseq data were integrated to identify epigenetically regulated genes and pathways that define each group. Using differentially methylated probes (DMPs) in gene promoters, 309 of 2142 differentially expressed genes showed DMPs. These overlapping genes were selected for pathway analysis. We found that ALK-high group genes were enriched for MYC targets, ribosomal components, and pyrimidine metabolism, while the ALK-low group displayed enrichment of PRC2 complex (EZH2 and SUZ12), H3K9m3 signature, and genes involved in interleukin (IL-2RG) and TCR signaling. Outcome data were available only for a subset of the cases (23/43). Interestingly, three out of the four patients who succumbed to the disease were classified as ALK-high group; however, small number of cases with available clinical data prevented correlation analyses between ALK expression status and clinical outcome.

Conclusions: Pediatric ALK+ALCL can be subclassified in two groups based on ALK expression, methylation, and gene expression signatures. Our findings provide new insights into the biology of pediatric ALCL, which may be utilized for better prognostic and therapeutic approaches.

1553 The SUVmax on FDG PET/CT Correlates with the Status of B-Cell Receptor Signaling in Diffuse Large B-Cell Lymphoma

Dong Sheng¹, Weige Wang², Ting Li¹, Xiaoqiu Li³. ¹Fudan University Shanghai Cancer Center, Fudan University Shanghai Medical College, ²Fudan University Shanghai Cancer Center, Shanghai, ³Fudan University Shanghai Cancer Center, Shanghai

Background: ¹⁸F-fluorodeoxyglucose (FDG) positron emission tomography with computed tomography (PET/CT) imaging has been widely used in lymphoma patients for staging, surveillance and assessment of response. And the maximum standardized uptake value (SUV_{max}) may quantitatively reflect the glucose accumulation of the tumor. Different subtypes of lymphomas exhibit varying degrees of FDG-avidity that correlate with the aggressiveness of the individual lymphoma. Diffuse large B-cell lymphoma (DLBCL), one of the most common subtypes of aggressive lymphomas, features a remarkable heterogeneity in morphology, immunophenotype, genetics, clinical behavior and functional radiology. Despite of being mostly FDG-avid tumors, DLBCL cases vary considerably in their degrees of FDG-avidity denoted by the SUV_{max}. And so far the biologic correlates of such a heterogeneity remain unknown.

Design: We immunohistochemically detected and compared the

expression levels of some key functional molecules involving in the B-cell receptor (BCR) signaling (pSYK) and glycolysis (GLUT1 and HK2) in 27 tumor samples from *de novo* DLBCL patients with high FDG-avidity and 13 ones with relatively low FDG-avidity. Then, DLBCL cell line-derived xenograft models were established and subjected to a small animal ¹⁸F-FDG PET/CT scan and immunohistochemical examination of pSYK, GLUT1 and HK2. The expression of GLUT1 and HK2 in DLBCLs was further detected by an immunoblotting assay.

Results: DLBCL patients with low FDG-avidity displayed relatively lower-level expression of pSYK, GLUT1 and HK2 compared with those with high FDG-avidity, suggestive of a possible inactivation of BCR signaling and glycolysis in these cases. Noticeably, the level of FDG-avidity correlates well with the levels of pSYK, GLUT1 and HK2 expression. In *in vivo* PET/CT experiment, tumors derived from BCR-deficient DLBCL cell lines tended to display lower SUV_{max} and lower-level immunohistochemical expression of pSYK, GLUT1 and HK2 contrasted with xenografts derived from BCR-dependent DLBCL cell lines. In *in vitro* Immunoblotting, the down-regulation of GLUT1 and HK2 expression by a chemical SYK inhibition was observed only in BCR-dependent DLBCLs whereas was lacking in those BCR-negative ones with low expression of GLUT1 and HK2.

Conclusions: The degrees of FDG-avidity denoted by SUV_{max} correlate with the key molecule of BCR signaling and thus SUV_{max} on PET/CT can be viewed as potential indicator for the BCR signaling status which assisting BCR signaling-inhibitory treatment.

1554 The Prognostic Impacts of CD3+ and CD8+ Tumor-infiltrating T-cell Densities and PD-L1 in Chinese Diffuse Large B-cell Lymphoma Patients

Yunfei Shi¹, Xianghong Li². ¹Peking University Cancer Hospital, Beijing, ²Peking University Cancer Hospital

Background: Diffuse large B cell lymphomas (DLBCL) is the most common subtype of aggressive and heterogeneous lymphoma. International prognostic index (IPI) and the cell of origin (COO) classification were widely used to predict its prognoses. Nowadays, standard chemotherapy with rituximab (R-CHOP) on DLBCL patients has generally improved the survival and obscured difference classified by COO. However, around 40% DLBCLs were still relapsed and refractory cases. So, it is eager to develop new predictive and therapeutic biomarkers. Besides double-expressor lymphoma (DEL) and programmed cell death ligand-1 (PD-L1), tumor microenvironment difference especially T-cells were prognostic in many cancers, and PD-L1 positivity correlated with CD3 and CD8 high density in hepatocellular carcinoma.

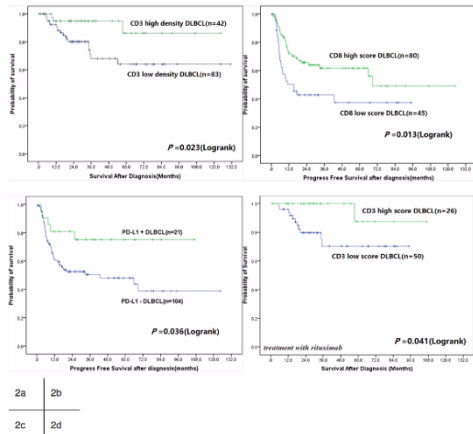
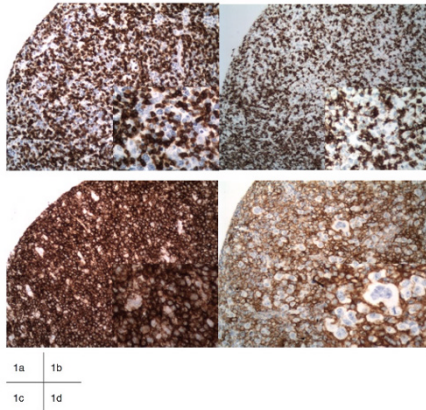
Design: Tumor paraffin blocks of 125 DLBCLs (Table 1) were subjected to the construction of tissue microarray (TMA). The TMA sections were applied to immunohistochemical staining (IHC) and EBER1/2 hybridization. CD3 and CD8 density (percentage to total cellularity) were reviewed and recorded, >25 % and >20 % for CD3 and CD8 high density. PD-L1 was positive if >30% tumor cells reacted, and microenvironmental PD-L1 (mPD-L1) was positive if ≥20% nonmalignant cells reacted. The relation between CD3, CD8, PD-L1 and clinicopathological parameters and the survival analysis were done with SPSS software (P < 0.05 are significant).

Results: 66.4% cases were CD3 high density (Fig. 1a), while 64.0% were CD8 high density (Fig. 1b). 16.8% cases showed PD-L1 positivity (Fig. 1c), and 29.8% cases were mPD-L1 positive (Fig. 1d) among PD-L1-negative cases. Both CD3 and CD8 high density were associated with mPD-L1 positivity (P=0.001 & P=0.0001). CD3 and CD8 high densities also related to IPI low score (score 0-2, P=0.029 & P=0.030), and they did not relate with COO or DEL (P > 0.05). In multivariate analysis, CD3 high density predicted better OS (P = 0.023, Fig. 2a), while CD8 high density and PD-L1 positivity were both associated with prolonged PFS (P=0.025 & P=0.041, Fig. 2b & 2c). In 76 cases treated with R, univariate analyses indicated CD3 high density and PD-L1 positivity with better OS (P=0.041, Fig. 2d) and PFS (P=0.033) respectively.

Table 1: Clinical characteristics and outcome dataset of the 125 DLBCL cases.

clinical characteristics		No. (Total N=125)	%
Age	Median	56.1(yrs)	
	range	23.6-84.3(yrs)	
	>60	43	34.4%
Gender	male	75	60.0%
Ann Arbor stage	I-II	63	50.4%
	III-IV	62	49.6%
B symptoms	present	47	37.6%
ECOG	>1	10	8.0%
Extranodal sites>1	present	28	22.4%
Elevated serum LDH	elevated	65	52.0%
Bulky mass	present	38	30.4%
IPI risk Group	high (3-5)	33	26.4%
Treatment (1 st chemotherapy)	R-CHOP/R-CHOP-like	76	60.8%
	Other chemotherapy	49	39.2%
Treatment response	CR	84	67.2%
	PR	16	12.8%
	PD	24	19.2%
	Not evaluable	1	0.8%
Follow-up (median in months, range)		25.7 (0.8- 131.1)	

CR, complete response; ECOG, Eastern Cooperative Oncology Group; LDH, lactate dehydrogenase; IPI, International Prognostic Index; No., number; PD, progressive disease; PR, partial response; R-CHOP: rituximab plus cyclophosphamide, doxorubicin, vincristine and prednisolone.



Conclusions: The infiltrating densities of CD3+, CD8+ T-cells and PD-L1 expression were variable in DLBCL patients. CD3 high density predict better OS, CD8 high density and PD-L1 positivity predict better PFS. CD3 and PD-L1 can be useful biomarkers even after treatment with rituximab.

1555 Bone Marrow Findings in Adult T-cell Leukemia/Lymphoma: A Single Medical Center Experience in the United States

Yang Shi¹, Murali Janakiram², Saed Sadeghi³, Beamon Agarwal⁴, Yanhua Wang⁵. ¹Montefiore Medical Center, Albert Einstein Collage

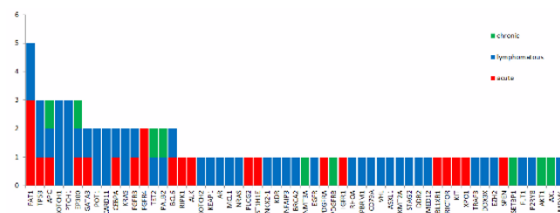
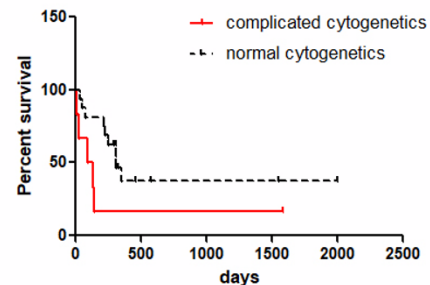
of Medicine, Tarrytown, NY, ²Montefiore Medical Center, ³Montefiore Medical Center, Albert Einstein Collage of Medicine, ⁴Secane, PA, ⁵Bronx, NY

Background: Adult T-cell leukemia/lymphoma (ATLL) is a human T-lymphotropic virus 1 (HTLV-1) –related peripheral T-cell leukemia/lymphoma that is endemic mostly in Japan and Caribbean regions. In the United States, it is a relatively rare disease with a prevalence of 0.2% in all registered lymphomas. ATLL are subclassified into four clinical variants: acute, lymphomatous, chronic and smoldering. Bone marrow involvement is common in all variants of ATLL. The diagnosis of ATLL in bone marrow sometimes can be challenging. Moreover, the morphologic features, distribution patterns, its accompanied reactions, immunophenotyping, cytogenetics and molecular mutations by next generation sequencing are not systemic studied.

Design: We retrospectively reviewed 47 cases in the past 14 years (from 1/1/2003 to 12/31/2016) of ATLL with bone marrow biopsies and studied their morphology, immunophenotyping, cytogenetics and next generation sequencing findings.

Results: Histologically, 24/29 (82.8%) cases of acute variant showed bone marrow involvement while 5/16 (31.3%) cases of lymphomatous variant showed bone marrow involvement (P<0.05). There are four distribution pattern of ATLL involvement in the bone marrow biopsy: interstitial, diffuse, nodular and paratrabeular. 7/47 (14.9%) of the cases showed concurrent granulocytic hyperplasia and 5/47 (10.6%) of the cases showed increased eosinophils. The most common immunophenotype is CD4+/CD25+/CD7-. 7/11 (63.6%) cases with ≥ 5% ATLL involvement showed complex cytogenetic changes (Table 1). The patients with complex cytogenetics showed worse overall survival compared with patients with normal cytogenetics (p<0.05) (Figure 1). Twenty patients had targeted gene sequencing, and five cases (25%) had the cadherin gene FAT1 mutation, while APC, TP53, NOTCH1, EP300, and PTCH1 mutations were detected in three cases (15%) each (Figure 2).

Case #	Age (yr)	sex	type	cytogenetics
19	54	F	Acute	84-85,XX,add(3)(q12)x2,+3,add(4)(q31),-4,del(5)(q15q33)x2,-7, add(9)(p13)x2,-10,-10,-11,add(11)(p15),-12,-13,-13,-13,add(13)(p10),-14,i(14)(q10),-15,add(15)(p10),-19,-19,-20, add(20)(q13.3)x2, i(21)(q10)x2,+10mar[cp5]/46,XX[15]
26	69	M	Acute	48-49,XY,+X,t(1;7)(q32;q36),add(9)(p24),t(11;19)(q13;p13.3),add(14)(p10),+14, add(20)(q11.2),del(20)(q11.2),+20[cp6]/46,XY[14]
28	42	M	Acute	44,X,-Y,-6,der(13)t(13;14)(q10;q10),+mar[24]/46,XY[2]
29	58	F	Acute	47,XX,t(1;13)(p36.3;q33),dup(2)(p11.2p14),t(4;9)(q34;q31.1),t(15;19)(p11.2;q13.2),+19,[cp6]/46,XX[14]
31	39	F	Acute	48-49,XX,+X,del(1)(p34),add(2)(p11.2),del(3)(q21),dic(3;3)(q21;p21), del(5)(q13q33),del(7)(p13),+8,del(9)(p13),dup(11)(q13q23),-12,-15,-16,-17,add(19)(p13.3),-20,+22[cp4]/46,XX[16]
40	53	M	Acute	47,XY+Y,add(2)(p21),der(9)t(9;11)(q34;q13),der(11)del(p12),del(11)(q13;q14), der(17)t(11;17)(q13;q24),add(13)(q34)[cp6]/46,XY[14]
43	36	F	Acute	47,XX,-2,-3,add(3)(q27),-8,add(9)(q34),add(11)(q23),-12,-13, add(14)(q24),-16,-16,-18,+8-12mar [cp16]/46,XX[4]



Conclusions: ATLL patients with acute variant had a much higher bone marrow involvement rate than those with lymphomatous variant. The complicated cytogenetics changes and the multiple gene mutations suggest that the tumorigenesis of ATLL might be a complicated multi-factorial process. Complex bone marrow cytogenetic changes is associated with worse prognosis in ATLL patients. The patients with complex cytogenetic changes might need more intensive chemotherapy.

1556 SLAMF7 (CD319/CS1) is Expressed on Plasmablastic Lymphomas and is a Potential Diagnostic Marker and Therapeutic Target

John Shi¹, Raj Bodo¹, Xiaoxian Zhao¹, Lisa Durkin¹, Tanu Goyal¹, Howard Myerson², Eric Hsi¹. ¹Cleveland Clinic, Cleveland, OH, ²Beachwood, OH, ³University Hospitals of Cleveland

Background: Plasmablastic lymphomas (PBL) are a heterogeneous group of aggressive lymphomas characterized by plasmablastic/immunoblastic morphology and an immunophenotype resembling plasma cells. SLAMF7 (CD319 or CS1) is a member of the Signaling Lymphocyte Activation Molecule (SLAM) family of receptors and is expressed on NK cells, a subset of CD8+ T lymphocytes, activated monocytes, mature dendritic cells, activated B-cells, and plasma cells. In late 2015, elotuzumab, a monoclonal antibody recognizing SLAMF7, was approved for the treatment of multiple myeloma. Expression of SLAMF7 in PBL has not been previously characterized. The aim of our study was to evaluate SLAMF7 expression in PBL and explore whether elotuzumab has *in vitro* activity against PBL.

Design: A computerized archival search identified 19 cases of PBL with sufficient material for this study and available clinical records. Immunohistochemical stains for CD20, CD138, PAX5, MUM1, HHV8, and ALK-1, as well as *in situ* hybridization for Epstein-Barr virus encoded RNA (EBV-EBER), were performed in a majority of cases. Expression for SLAMF7 was measured using a commercially available antibody (clone 3B3). SLAMF7 expression in ≥10% lymphoma cells was considered positive. The plasmablastic cell line BC2, derived from a case of primary effusion lymphoma (PEL), was used for antibody dependent cellular cytotoxicity (ADCC) studies using a granzyme B (GrB) ELISPOT assay and elotuzumab. This study was carried out with institutional review board approval.

Results: The diagnostic subtypes and immunophenotypic profiles of the 19 cases are shown in Table 1. SLAMF7 was expressed in 16/19 (84%) cases. No correlation between SLAMF7 expression and subtype or individual immunophenotypic marker was found. The cell line BC2 expressed surface marker SLAMF7 via flow cytometry and elotuzumab induced ADCC against BC2 target cells using the GrB ELISPOT assay. Compared to the IgG1 control antibody MSL109 (74 ± 9 GrB spots/well), elotuzumab elicited specific activity (131 ± 17 GrB spots/well, p < 0.01).

Table 1. Phenotypic Profile of PBL Subtypes

Diagnosis	# of cases	# positive for phenotypic marker (%)							
		SLAMF7	CD20	PAX5	MUM1	CD138	EBV-EBER	HHV8	ALK-1
PBL NOS	11	9/11 (82%)	1/10 (10%)	2/11 (18%)	11/11 (100%)	8/11 (73%)	5/10 (50%)	0/9 (0%)	0/9 (0%)
HIV+ PBL	5	5/5 (100%)	0/5 (0%)	0/2 (0%)	4/4 (100%)	4/5 (80%)	3/5 (60%)	0/4 (0%)	0/3 (0%)
ALK+ large B cell lymphoma	2	1/2 (50%)	0/2 (0%)	0/2 (0%)	2/2 (100%)	2/2 (100%)	0/2 (0%)	0/2 (0%)	2/2 (100%)
PEL	1	1/1 (100%)	0/1 (0%)	0/1 (0%)	1/1 (100%)	1/1 (100%)	1/1 (100%)	1/1 (100%)	0/1 (0%)
Total	19	16/19 (84%)	1/18 (6%)	2/16 (13%)	18/18 (100%)	15/19 (79%)	9/18 (50%)	1/16 (6%)	2/15 (13%)

Conclusions: SLAMF7/CD319 is expressed in the majority of PBL cases (84%), across a spectrum of entities, and is a promising addition to a diagnostic panel for PBL. Furthermore, our data show that SLAMF7 is a potential therapeutic target using elotuzumab, supporting further exploration of its use in this aggressive lymphoma.

1557 Lymphoid Variant of Hypereosinophilic syndrome in lymph node: A Phenotypic Study in Comparison with Angioimmunoblastic T-cell Lymphoma

Min Shi¹, Dragan Jevremovic¹, Andrew Feldman¹, Rong He¹, Matthew Howard¹, Dong Chen¹, Karen Rech¹. ¹Mayo Clinic, Rochester, MN

Background: Lymphoid variant of hypereosinophilic syndrome (LV-HES) is an expansion of clonal CD3-CD4+T-cells with a Th2 profile that produce IL-4, IL-5 and IL-13, causing peripheral eosinophilia with infiltration in various organs. LV-HES generally shows an indolent clinical course. Lymph node involvement by LV-HES is rare and can show overlapping morphologic features with angioimmunoblastic T-cell lymphoma (AITL). We sought to further investigate the Th2 phenotype of LV-HES in comparison with AITL.

Design: Mayo Clinic archives were searched for nodal LV-HES between 2010 and 2016, and chart review was performed. Immunohistochemical stains (IHC) included CD2, CD3, CD4, CD5, CD7, CD8, CD10, CD21, CD25, FOXP3, GATA3, PD-1, TCL-1A, and T-bet. Positive stain was defined as >20% of tumor cells. 23 AITL cases diagnosed by 2008 WHO criteria were also stained by GATA3.

Results: We identified 6 nodal LV-HES cases with median age at 55 years (25-78) and male to female ratio of 1:2. All patients had hypereosinophilia with median absolute eosinophil count at 5.1 (1.7-12), 2 had general pruritus, 1 had hepatosplenomegaly and 1 had splenomegaly. Histologic examination revealed preserved to slightly distorted nodal architecture with a monomorphic small to intermediate-sized lymphocyte infiltrate in the paracortex. Clonal T-cell receptor gene rearrangements were demonstrated by PCR in each case. The clonal populations showed sCD3-CD2+CD4+CD5+CD7(variable)CD8-CD10- by flow cytometry and were negative for CD25, FoxP3, PD-1, TCL-1A and T-bet. All cases had strong GATA3 expression, as predicted for Th2 cells. Despite the T follicular helper (TFH) cell phenotype of AITL, the vast majority of cases were positive for GATA3 (83%).

Conclusions: The lack of CD10 and PD-1 is useful to distinguish LV-HES from AITL. The distinct GATA3 expression, coupled with the Th2 cytokine profile, supports a Th2 origin of LV-HES. However, GATA3 expression does not appear specific for a Th2 profile in neoplastic T-cells, as expression was also seen in conjunction with TFH markers in the majority of AITL cases. It is important to note that patients with LV-HES show an indolent clinical course, indicating that overexpression of GATA3 is not always associated with an inferior prognosis as reported in patients with peripheral T-cell lymphoma, NOS.

1558 Primary Bone Diffuse Large B-Cell Lymphoma

Wen Shuai¹, Richard Wu², Yaohong Tan³, Nicholas Mackrides⁴, Juan Alderuccio⁵, Offiong F Ikpatt⁶, Francisco Vega⁶, Jennifer Chapman⁷. ¹University of Miami / Jackson Memorial Hospital, Miami, FL, ²U Health Pathology, Miami, FL, ³University of Miami/Sylvester Cancer Center, ⁴University of Miami/Sylvester Cancer Center, Hallandale Beach, FL, ⁵University of Miami / Jackson Memorial Hospital, ⁶University of Miami/Sylvester Cancer Center, Coral Gables, FL, ⁷University of Miami/Sylvester Cancer Center, Miami Shores, FL

Background: Lymphomas comprise 3% of primary bone tumors, the majority of which are primary bone diffuse large B-cell lymphomas (PB-DLBCL). Immunoblastic or pleomorphic morphology, non-GC phenotype, and BCL2 expression > 30% are poor prognostic factors.

Design: We identified 27 PB-DLBCL from our database, reviewed clinical and morphologic features and performed IHC to identify additional prognostic immunophenotypic markers (CD10, BCL6, MUM1, MYC, BCL2, LMO2 and p53).

Results: Patients included 15 men and 12 women, median age of 51 years (range, 14-85). Most patients presented with bone pain and without B symptoms or bone marrow involvement. Femur was most commonly involved, followed by pelvic bones and spine. 50% of patients presented at stage I, and 44% of patients presented at stage IV. Serum LDH was elevated in 20%, IPI was high in 7%. Most were treated with R-CHOP followed by radiation and achieved complete remission.

93% of cases showed centroblastic morphology with extensive sclerosis. 79% were GC phenotype and 21% were double expressors (DEL). All DELs were GC phenotype and 93% expressed p53 in >30% of tumor nuclei. The highest p53 expression rates were seen in the DELs. LMO2 expression was found in 64% and correlated with CD10 expression in all cases. However, there was no correlation between LMO2 expression and DELs. EBER was negative in all. FISH was performed in three non-DELs. One showed MYC rearrangement and absence of BCL2 and BCL6 rearrangements. The other two were negative for MYC, BCL2 or BCL6 rearrangements.

Only one patient had relapse (9 months after R-CHOP) and disease progression; this case was a DEL with the highest positivity for p53.

Conclusions: PB-DLBCL is most frequently GC phenotype and 21% were DELs (percentage similar or lower than nodal DLBCL). A significant positive association between p53 expression and double expression of MYC and BCL2 was found. Expression of p53 and double expression of MYC and BCL2 may serve as prognostic indicator in PB-DLBCLs where FISH assays are often not possible.

1559 Highly Multiplexed Analysis of the Tumor Microenvironment in Hodgkin Lymphomas by Imaging Mass Cytometry

Imran Siddiqi¹, Mohan Singh², Parvesh Chaudhry², Gerdtsen Erik², Wendy Cozen², James Hicks³, Peter Kuhn², Akil Merchant². ¹University of Southern California, Los Angeles, CA, ²University of Southern California, ³USC

Background: In classical Hodgkin lymphoma (CHL) and nodular lymphocyte predominant Hodgkin lymphoma (NLPHL), composition of the tumor microenvironment (TME) varies significantly across

and within histologic subtypes and affects disease prognosis. Characterization of the TME is currently hindered by the phenotypic complexity of T cell subsets, macrophage and other myeloid subtypes, and stromal/vascular components. Assessment of the spatial relationships of tumor cells and immune cell subsets is difficult using conventional techniques that either require tissue disruption (flow cytometry, gene expression profiling) or limit analysis to one to few markers per tissue section (immunohistochemistry, immunofluorescence). Using metal-tagged antibodies on FFPE tissue sections, the Fluidigm Hyperion imaging mass cytometry (IMC) combines a mass cytometer with a laser ablation system, enabling simultaneous immunophenotyping by >40 markers on a single slide with subcellular resolution. In this study, we demonstrate the feasibility of this approach to analyzing the TME of Hodgkin lymphomas.

Design: Metal-conjugated antibodies against epitopes relevant to B-cell/ Hodgkin lymphoma, T-cell subsets, macrophages, and stromal cells were obtained from Fluidigm or custom-conjugated as necessary. Antigen retrieval, blocking, and antibody staining concentrations were optimized for multiplexed analysis. A panel of markers was validated on FFPE sections from normal lymph node, CHL and NLPHL, using standard immunohistochemistry on serial sections for comparison. Stained slides were analyzed using the Fluidigm IMC instrument with a 1 µM laser ablation spot size and frequency of 100-200 Hz. Image analysis was performed with MCD viewer (Fluidigm).

Results: A panel of 25 markers was successfully applied on FFPE tissues from normal lymph node, CHL, and NLPHL, enabling visualization of normal lymph node compartments and neoplastic Reed-Sternberg (RS) and lymphocyte-predominant (LP) cells in different tumor foci. TME components, including T-cells subsets (CD4+, CD8+, TH1/TH2, T-regulatory, T-follicular helper, NK/T), macrophages, and tumor associated vessels were identifiable in relation to the tumor cells.

Conclusions: IMC enables highly multiplexed imaging of the tumor/TME interaction on standard FFPE sections and is particularly suitable for Hodgkin lymphomas given the scattered nature of the neoplastic cells and heterogeneity of the surrounding cell populations. Biological and clinical insights will be discussed.

1560 Persistence of Mutated Epigenetic Modifiers During Morphologic Remission of AML with Mutated NPM1

Craig Soderquist¹, Priya Velu², Dale Frank³. ¹Columbia University, New York, NY, ²University of Pennsylvania, Philadelphia, PA, ³Philadelphia, PA

Background: Acute myeloid leukemia (AML) is a genetic disease of hematopoietic precursors with altered proliferation and maturation. Clonal evolutionary models of AML describe the sequential acquisition of mutations in various gene classes, beginning with “early” initiating mutations in epigenetic modifiers, followed by “late” mutations in signaling pathway genes, among others. At the time of clinical presentation, AML is a heterogeneous neoplasm composed of distinct subclones. Each may have a different response to therapy and a critical effect on clinical outcome. We sought to characterize the clonal architecture of AML with mutated *NPM1* and describe its evolution in response to therapy.

Design: We studied patients with *NPM1*-mutated AML who underwent bone marrow mutational profiling 1) at initial diagnosis of AML and 2) during morphologic remission following induction chemotherapy. For each case, clinical, hematologic, and genetic data were analyzed. Using an NGS assay composed of 68 myeloid-associated genes, we characterized the response of leukemia-associated mutations to therapy. Genes were categorized into classes according to the gene's function or pathway involvement based on TCGA guidelines.

Results: Between 2013 and 2016, 17 patients fulfilled criteria. At initial diagnosis, 17 *NPM1* mutations (in 17 patients), 31 DNA methylator mutations (15 patients), 16 signaling pathway mutations (12 patients) and 4 “other” mutations (4 patients) were identified, with a median variant allele frequency (VAF) for each gene class as follows: *NPM1* 35%; DNA methylators 42%; signaling pathways 21%; “other” 31%. Following chemotherapy, no residual *NPM1* (0/17) or signaling pathway mutations (0/16) were detected at the level of sensitivity of the assay (1% VAF for insertions, 4% VAF for point mutations). Conversely, 17/31 DNA methylator and 1/4 “other” mutations persisted. Of 17 patients, 9 had at least one persistent mutation and 8 had no detectable mutations. In 22 months of follow-up 5/9 patients with persistent mutations relapsed, while 5/8 patients with no detectable mutations relapsed.

Conclusions: Mutations in *NPM1* and signaling pathway genes, thought to be late events in the evolution of AML, are cleared in response to induction chemotherapy. Conversely, mutations in DNA methylators, considered early events in hematopoietic neoplasia, frequently persist through therapy. We did not find a difference in relapse rate between patients whose mutations were persistent and those whose mutations were transient.

1561 PD-L1 expression in cases of breast implant-associated anaplastic large cell lymphoma reveals a new target for therapy

Jose L Solorzano¹, Alejandro Francisco-Cruz¹, L. Jeffrey Medeiros¹, Ken H. Young¹, Mark W Clemens¹, Ignacio Wistuba¹, Roberto Miranda¹. ¹The University of Texas MD Anderson Cancer Center, Houston, TX

Background: Breast implant-associated ALCL (BI-ALCL) is a provisional entity in the revised World Health Organization Classification. Patients most often present with effusion in which CD30+ anaplastic lymphoid cells of T-cell lineage are present in the peri-prosthetic fluid. In a subset of patients, the lymphoma invades through the fibrous capsule and forms a mass. Most patients with BI-ALCL have an overall indolent course; however, some cases may progress and fail to surgery or standard chemotherapy. Assessment of PD-L1 expression in BI-ALCL has not been explored, and its identification may be a promising strategy for patients with refractory or aggressive BI-ALCL. The aim of this study is to describe the immunohistochemical (IHC) pattern of PD-L1 expression in BI-ALCL cases.

Design: Automated immunohistochemistry for PD-L1 (Clone 22C3) was performed on formalin-fixed, paraffin-embedded (FFPE) of whole tumor sections from capsulectomy specimens of patients with a confirmed diagnosis of BI-ALCL. PD-L1 positivity was defined as complete circumferential or partially linear plasma membrane reactivity by the anaplastic cells. Evaluation of PD-L1 results was performed by two hematopathologists and positive cells on the whole slide were counted visually.

Results: 34 cases of BI-ALCL formed the study group. In all cases the lymphoma cells diffusely and uniformly expressed CD30. Thirty (88%) of cases were positive for PD-L1 with membranous expression pattern. Twenty one (70%) cases showed strong and complete membranous expression of PD-L1 and 9 (30%) cases showed strong-partial membranous expression of PD-L1.

Conclusions: We have shown for the first time that PD-L1 is expressed by the malignant cells of BI-ALCL. In this study, almost 90% of BI-ALCL cases were positive. These data suggest that PD-L1 is a biomarker that can identify patients who may benefit from immune checkpoint inhibitor therapy.

1562 Design of multiplex immunofluorescence panel with immune contexture markers of nodular sclerosis classical Hodgkin lymphoma

Jose L Solorzano¹, Alejandro Francisco-Cruz¹, Ana Martin-Moreno², Ruth Salazar Alejo¹, Edwin R Parra¹, Barbara Mino¹, Maria Dolores Lozano Escario³, Miguel Hernandez-Argüello⁴, Ignacio Wistuba¹, Sanam Loghavi¹, Joseph Khoury¹, Juan F Garcia². ¹The University of Texas MD Anderson Cancer Center, Houston, TX, ²MD Anderson, Madrid, Spain, ³Madrid, ⁴Navarra Clinic University

Background: Nodular sclerosis classical Hodgkin lymphoma (NSCHL) is the most frequent subtype of HL, characterized by a prominent interaction between Reed-Sternberg cells (RSCs) and tumor-infiltrating immune cells (TIC), including T-cells, tumor-associated macrophages (TAM) and eosinophils. Characterization of immune contexture (IC) involves assessment of quantity, topography, and immunophenotype of TIC. The interaction of TIC with RSC may correlate with clinical outcomes and response to immunotherapy. Multiplex immunofluorescence (mIF) immunophenotyping performed on a single slide in conjunction with automated multispectral image analysis allows simultaneous characterization of several TIC subpopulations. The aim of this study is to develop a mIF panel with emphasis on NSCHL-associated IC.

Design: We analyzed 70 annotated NSCHL cases in a tissue microarray. Single-antibody IHC was performed for CD3, CD4, CD8, FOXP3, granzyme-B, lysozyme, CD68, CD163 and STAT1 as well as 5 immune-checkpoint antigens (PD-1, PD-L1, PD-L2, CTL-4, and CD137). CD30 was used to highlight RSC. IHC-stained slides were scanned and the percentage of positive cells for each antigen was recorded. Markers shown to be associated with clinical outcome were selected to build a mIF panel using the Opal 7 kit and Vectra multispectral microscope.

Results: The study cohort included 37 men and 33 women with a median age of 45 years, all with treatment-naïve NSCHL. Ann Arbor stage was I/II in 26 patients and III/IV in 44. The percentage of TIC was as follows: CD3: 67%, CD4: 41%, PD-1 on T-cells: 18.4%; CD163: 25.5%, CD68: 14.3%. Expression of immune-checkpoint antigens on RSC was as follows: PD-L1: 12.6%, PD-L2: 10.5%, and CD137: 6%. Among patients with advanced-stage disease (III/IV) the following significant correlations between expressed antigens were identified: CD3 and PD-1, CD163 and CD68, CD163 and PD-L1, and CD68 and PD-L2 ($r > 0.5$, $p < 0.005$). The percentage of positive cells for these markers showed a tendency toward shorter progression-free survival without statistical significance. TAM was the most prevalent sub-population of TIC on NSCHL. Based on these findings, a mIF panel was designed to include CD30, CD137, CD68, CD3, PD-1 and PD-L1.

Conclusions: This model is useful in designing a statistically relevant panel for mIF. Further evaluation of these markers in NSCHL is needed in order to confirm their predictive and/or prognostic value.

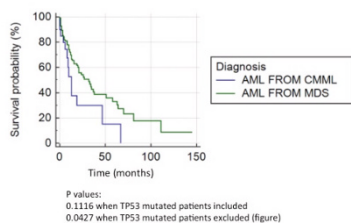
1563 Comparison of the Mutational Profiles of Acute Myeloid Leukemia Transformed from Myelodysplastic Syndrome and from Chronic Myelomonocytic Leukemia

Jinming Song¹, Mohammad Hussaini¹, Sallman David¹, Mary-Margaret Allen¹, Xiaohui Zhang¹, Ling Zhang², Lynn Moscinski¹, Hailing Zhang¹. ¹Moffitt Cancer Center, Tampa, FL, ²Tampa, FL

Background: Both myelodysplastic syndrome (MDS) and chronic myelomonocytic leukemia (CMML) have the potential to progress into acute myeloid leukemia with myelodysplasia-related changes (AML-MRC). Information about gene mutations has played increasing important roles in the stratification and treatment of AML. In this study, we compared the NextGen sequencing mutation profiles of patients who progressed into AML-MRC from MDS (AML-MRC-MDS) or from CMML (AML-MRC-CMML), to understand the genetic difference in these two groups of patients.

Design: NextGen sequencing for patients with myeloid neoplasms were performed in-house and in CAP/CLIA certified labs. Patients with NextGen sequencing results and AML-MRC, as well as previous history of MDS (179 patients) or CMML (20 patients) were selected for this study. The percentages of mutated patients for each group are calculated and compared for each gene.

Results: Patients with AML-MRC-CMML were found to have higher number of mutated genes on average than patients with AML-MRC-MDS (4 vs 2, p value 0.0046), and significantly higher mutation rates in the following genes: TET2 (60.00% vs 22.86%, p value 22.86%), ASXL1 (50.00% vs 25.14% p value 0.0318), SRSF2 (47.37% vs 20.36%, p value 0.0176), CBL (21.05% vs 5.39%, p value 0.031), CEBPA (20.00% vs 3.85%, p value 0.0335), and PHF6 (20.00% vs 3.43%, p value 0.0115). KRAS also appeared to be more frequent in AML-MRC-CMML (20.00%) than in AML-MRC-MDS (5.19%), but is not statistically significant (p value 0.0608). On the other hand, patients with AML-MRC-MDS showed significantly higher mutation rate in TP53 (22.81%) than patients with AML-MRC-CMML (0%, p value 0.0151). No significant differences in mutational frequencies were found in RUNX1, DNMT3A, EZH2, NPM1, FLT-3, IDH1, IDH2, SETBP1, SF3B1, ABL1, CSF3R, CUX1, ETV6, JAK2, KIT, KMT2A, NRAS, SH2B3, U2AF1, WT1, or ZRSR2. Patients with AML-MRC-CMML appeared to have worse prognosis, especially when TP53 mutated AML-MRC-MDS patients are excluded (figure 1).



Conclusions: Patients with AML-MRC-CMML were found to have higher frequencies of containing mutated TET2, ASXL1, SRSF2, CBL, CEBPA, and PHF6 genes, while TP53 is more frequently mutated in patients with AML-MRC-MDS. AML-MRC-CMML also appeared to show worse prognosis than AML-MRC-MDS, even though not statistically significant. These results indicate different mutation profiles of these two entities, and suggest different pathogenesis and potential different treatment strategies in the era of targeted therapy.

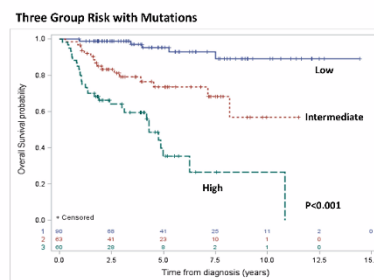
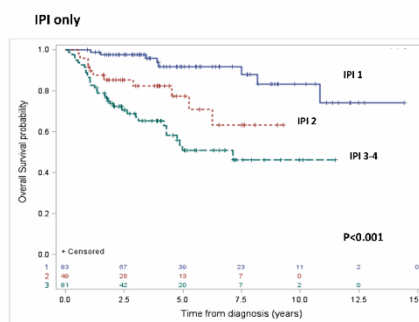
1564 Integration of mutation analysis as a risk predictor in patients with diffuse large B-cell lymphoma treated with R-CHOP

Joo Song¹, Anamarija Perry², Alex F Herrera³, Pamela Skrabek⁴, Michel Nasr⁴, Rebecca Ottesen³, Janet Nikowitz², Lu Chen³, Victoria Bedelf, Joyce Murata-Collins¹, yuanyuan chen¹, Yuping Li, Carlos Gomez Luna³, Christine McCarthy³, Raju Pillai, Jinhui Wang³, Xiwei Wu³, Jasmine Zain³, Auayporn P Nademane³, Joyce Niland³, Qiang Gong¹, Wing Chung Chan¹, Dennis D Weisenburger¹. ¹City of Hope National Medical Center, Duarte, CA, ²Winnipeg, MB, ³COH, ⁴University of Manitoba, ⁵City of Hope National Medical Center

Background: Diffuse large B-cell lymphoma (DLBCL) is a heterogeneous disease that is characterized by recurrent translocations and somatic mutations. Prognosis has been associated with clinical presentation, cell-of-origin, and genetic aberrations. The aim of this study was to determine whether somatic mutations are associated with OS in patients with DLBCL who have been treated with R-CHOP therapy and whether these mutations can be incorporated into a model to better predict survival.

Design: We identified 354 patients between 2000-2016 from two institutions with a diagnosis of *de novo* DLBCL and treated with R-CHOP therapy. A custom targeted panel with 334 genes which included the most frequently mutated genes in B-cell lymphoma was used and sequenced on an Illumina HiSeq 2500. Cases were evaluated by IHC (Hans algorithm, MYC, BCL2), and FISH analysis (BCL2, BCL6, and MYC). OS were estimated using K-M methods. Multivariable modeling of OS was performed which incorporated clinical characteristics, IHC, FISH, and mutation status of the most frequently mutated genes (>10%). LASSO regression was performed to select for significant variables and determine coefficients for these variables; a risk score was calculated based on the fitted model. Concordance C-index was used to assess the discriminatory ability of different models. Three risk groups were determined by stratifying the risk scores.

Results: 213 patients (median age 60 years, M:F ratio of 1.3:1) had complete clinical and sequencing data. GCB was more common (64%) compared to non-GCB (36%). The most frequently mutated genes were *KMT2D* (29%), *CREBBP* (20%), *TP53* (20%), and *B2M* (16%). Double/triple-hit lymphomas comprised of 10% of the cases and 15% were double-protein expressors (MYC and BCL2). Significant variables selected by LASSO include variables used in IPI, FISH analysis, and 5 mutated genes (*KMT2D*, *CREBBP*, *BCL2*, *PIM1*, and *EP300*). Three risk group model constructed based on these significant variables and their coefficients was superior in discriminating OS compared to IPI (C-index: 0.763 vs. 0.708). The hazard ratios (lowest group as reference) were 5.7 and 16.7 for the 3 risk group model compared to 3.3 and 6.3 using IPI alone.



Conclusions: In this study, we incorporated mutation analysis of select genes with clinical risk factors and developed an improved algorithm that could potentially prognosticate patients with DLBCL treated with first-line therapy. A validation cohort is required and is planned for future studies.

1565 SLAM Family Protein CD229 Identifies MLL Rearranged B-Lymphoblastic Leukemia/Lymphomas

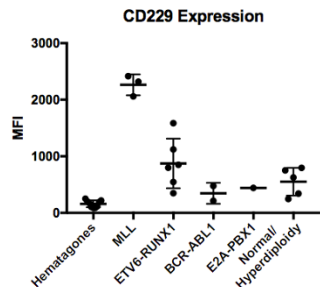
Jeffrey A SoRelle¹, Franklin Fuda², Kirithi Kumar³. ¹University of Texas Southwestern Medical Center, Dallas, TX, ²University of Texas Southwestern, Dallas, TX, ³University of Texas Southwestern, Coppell, TX

Background: The signaling lymphocytic activation molecule family (SLAMF) receptors play important roles in immune regulation but have barely been studied in the context of hematopoietic malignancy. One disease studied, multiple myeloma, was found to have high expression of SLAMF7, and now monoclonal immunotherapy targeting this receptor have finished phase III trials with positive results. There is no information on SLAMF expression in B-lymphoblastic leukemia/lymphoma (BLL), which has several cytogenetic abnormalities. Differential expression of SLAMF proteins could improve diagnostic immunophenotype or have implications as therapeutic targets.

Design: Residual clinical flow cytometry specimens (peripheral blood or bone marrow aspirates) were stained to detect SLAM family protein expression (SLAMF: CD48, CD150, CD84, CD224,

CD229 and CD352) in B cells, CD4+ / CD8+ T cells, granulocytes, and monocytes. Expression levels by mean fluorescence intensity (MFI) in B-lymphoblasts categorized by cytogenetic abnormalities were compared to hematogones.

Results: We performed SLAMF staining on 18 cases of B-LL with cytogenetic findings of hyperdiploidy/ normal (n=5), ETV6;RUNX1 (n=6), BCR; ABL (n=2), E2A (n=1), or MLL (n=3) rearrangements. Hematogones from samples with no evidence of malignancy served as controls. Compared to hematogones (MFI 160) and other B-LLs (MFI 346-875), those with MLL gene rearrangement showed significantly higher CD229 expression (MFI 2,264, $p < 0.0001$). Notably, CD229 was lower (MFI <1000) in background B cells, T cells and granulocytes in all specimens.



Conclusions: Our results identify CD229 as a surrogate marker for B-LL with MLL gene rearrangement. Importantly, the high level of CD229 expression is uniquely associated with the MLL+ lymphoblasts and not the background hematopoietic cells, such as neutrophils, monocytes, and T and B lymphocytes. Thus, CD229 could represent a novel immunotherapeutic target in MLL rearranged B-lymphoblastic leukemia, which carries a worse prognosis among childhood leukemias.

1566 Burkitt-like Lymphoma with 11q Aberration Is Not Uncommon in Children

Melissa Stalling¹, Aroop Kar², Madina Sukhanova³, Girish Venkataraman⁴, Katrin M Leuer², Lawrence J Jennings², Kristian Schaferna⁵, Nobuko Hijiyama⁵, Shunyou Gong². ¹McGaw Medical Center of Northwestern University, Chicago, IL, ²Ann & Robert H. Lurie Children's Hospital of Chicago, Chicago, IL ³University of Chicago Medicine, ⁴The University of Chicago Medical Center, Chicago, IL, ⁵Phoenix Children's Hospital

Background: Burkitt-like lymphoma with 11q aberration is a new provisional entity included in the 2016 revision of the World Health Organization classification (2016 WHO) with pathologic features closely resembling Burkitt lymphoma (BL), but lack *MYC* rearrangements. Instead, they show recurrent chromosome 11q alterations, particularly proximal gains and telomeric losses. Although the clinical course has been reported to be similar to BL, the number of cases reported is limited. Here we contribute to further characterize this entity and report its relatively high incidence in children, by identifying 4 new cases over a 5 year period in a single academic children's hospital.

Design: We searched our archive for all high grade B cell lymphoma (HGBL) cases and identified 38 cases of HGBL in the past 5 years; these included 20 classic BL, 13 diffuse large B-cell lymphomas (DLBCLs), and 5 other cases, which were all negative for *MYC* rearrangement. Clinica and pathologic data was collected. *MYC*, *BCL-2*, *BCL-6* FISH, and array comparative genomic hybridization (CGH) were performed in all 5 non-DLBCL, non-BL cases, aiming to identify them as HGBL, not otherwise specified (NOS), HGBCL with *MYC* and *BCL2* and/or *BCL6* rearrangements, or Burkitt-like lymphoma with 11q aberration based on 2016 WHO.

Results: Chromosome 11q aberration was identified in 4 out of 5 non-DLBCL, non-Burkitt HGBL cases by array CGH, which showed proximal gains in 11q13-q23 and telomeric losses in 11q24.1-qter. One case was classified as HGBCL, NOS. We did not find HGBCL with *MYC* and *BCL-2* and/or *BCL-6* rearrangements in our archive. Of these 4 Burkitt-like lymphoma with 11q aberration cases, 3 were male, and age at initial diagnosis ranged from 6-14 years old. All 4 cases occurred in the head & neck area (3 from cervical lymph node and 1 from tonsil). Morphologically, all 4 cases showed a diffuse proliferation of monotonous medium to large sized cells with mild nuclear pleomorphism and basophilic cytoplasm. By immunohistochemistry, all were CD10+, CD20+, BCL6+, and BCL2- with a very high Ki67 proliferation index.

FOR TABLE DATA, SEE PAGE 574, FIG. 1566

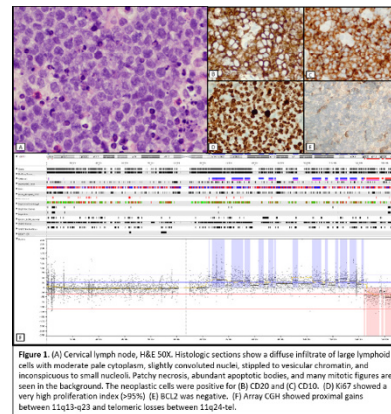


Figure 1. (A) Cervical lymph node, H&E 50X. Histologic sections show a diffuse infiltrate of large lymphoid cells with moderate pale cytoplasm, slightly convoluted nuclei, stippled to vesicular chromatin, and inconspicuous to small nuclei. Patchy necrosis, abundant apoptotic bodies, and many mitotic figures are seen in the background. The neoplastic cells were positive for (B) CD20 and (C) CD10. (D) Ki67 showed a very high proliferation index (>95%). (E) BCL2 was negative. (F) Array CGH showed proximal gains between 11q13-q23 and telomeric losses between 11q24-ter.

Conclusions: The 2016 WHO has added Burkitt-like lymphoma with 11q aberration as a new provisional entity. Our results suggest that in the pediatric setting, most non-DLBCL, non-Burkitt HGBL cases carry 11q aberrations. We propose that pediatric non-DLBCL, non-Burkitt HGBL cases are routinely tested for 11q alterations, to collect additional data and further investigate the pathology and clinics of this special form of lymphoma.

1567 Programmed Death-Ligand 1 status evaluation using Fluorescence in situ hybridization, RNAscope and Immunohistochemistry in Diffuse Large B-cell Lymphoma

Chenbo Sun¹, Yijun Jia¹, Tian Tian¹, Xiaoyan Zhou¹. ¹Fudan University Shanghai Cancer Center, Shanghai

Background: The expression of Programmed Death-Ligand 1 (PD-L1) plays a significant role in diffuse large B-cell lymphoma (DLBCL) and is associated with poor prognosis of DLBCL patients. Currently, PD-L1 amplification and expression levels were detected through Fluorescence in situ hybridization and immunohistochemistry (IHC) in DLBCL. However, little was known about the mRNA level and its clinical significance in DLBCL.

Design: RNAscope in situ hybridization is a novel technology to detect the mRNA expression level with a probe design strategy that allows both signal amplification and background suppression to achieve single-molecule visualization. Here we detected PD-L1 expression in three different levels through the combination of Fluorescence in situ hybridization, RNAscope and Immunohistochemistry in 287 DLBCL tissues.

Results: Our results showed that PD-L1 mRNA positive rate was 10.80% (31/287) and protein positive rate was 18.12% (52/287) in 287 patients respectively, while the PD-L1 amplification rate was 2.60% (5/192) in 192 patients with detectable PD-L1 expression. The protein expressions of PD-L1 were significantly higher in non-GCB than those in GCB-type ($P=0.037$). However, there was no significant difference in OS between different PD-L1 mRNA ($P=0.740$) or protein ($P=0.575$) expression in DLBCL.

Conclusions: This is the first research detecting the DNA, mRNA and protein levels of PD-L1 in DLBCL. So we draw a conclusion that PD-L1 is a potent biomarker and may indicate alternative therapeutic strategies in DLBCL.

1568 Cytogenetic Analysis of Adult T-Cell Leukemia/Lymphoma: Evaluation of a Cohort of Caribbean Patients

Yi Sun¹, Bachir Alobeid², Murty Vundavalli³, Govind Bhaga³. ¹Columbia University College of Physicians & Surgeons, New York, NY, ²New York, NY, ³Columbia University Medical Center, New York, NY

Background: Adult T-cell leukemia/lymphoma (ATLL) is a rare, highly aggressive malignancy linked to HTLV-1 infection. Only ~5% of HTLV-1 carriers develop ATLL and disease pathogenesis is poorly understood. ATLL is endemic in certain regions, including southwestern Japan and the Caribbean basin. The clinical course of ATLL from the Caribbean has been reported to differ from the Japanese cases. Numerous publications have described the cytogenetic profile of Japanese ATLL, however cytogenetic data of Caribbean ATLL are limited. In this study we sought to investigate whether cytogenetic changes differ between Japanese and Caribbean ATLL to explain the clinical differences by evaluating the karyotypes of Caribbean ATLL seen at our institution.

Design: ATLL cases diagnosed at our institution from 2003-2017 were retrieved. Clinical data, pathology and cytogenetic findings were reviewed. Chromosome analysis was performed by overnight and 72hr PHA-stimulated cultures. G-banding analysis was performed

and the karyotypes were described according to the International System for Human Cytogenetics Nomenclature (ISCN). Karyotypic abnormalities were classified as simple (up to 3 aberrations) or complex (≥ 4 aberrations).

Results: A total of 60 ATLL samples (32 PB, 22 BM, 5 LN, 1 lung) from 30 Caribbean patients (18 F /12 M, age 16-71 years, median 52) were analyzed. The cases comprised 23 acute, 5 lymphomatous and 2 smoldering variants. Abnormal karyotypes were detected in 39 samples (from 30 patients); 21 samples showed either normal karyotypes or were failures. The cytogenetic findings, including recurrent changes, are summarized in the table. Complex karyotypes with near diploidy, deletion 6q, and structural rearrangements involving 3q were the most common aberrations.

Karyotype	Number (%)
Complex	25 (83%)
Simple	5 (17%)
Sub-clones	11 (37%)
Near diploid	23 (77%)
Near tetraploid	7 (23%)
del (6q)	11 (37%)
Chromosome 14 loss	7 (23%)
Chromosome X loss	5 (17%)
Chromosome 13 loss	8 (27%)
Chromosome 5 loss	5 (17%)
Deletion 17p	6 (20%)
Marker chromosomes (range 1~17)	17 (57%)
Structural rearrangement breakpoints	
3q	13 (43%)
1q	9 (30%)
14q32	6 (20%)
2p	5 (17%)
Gene amplification HSR or DMs)	3 (10%)

Table: Cytogenetic features of Caribbean ATLL

Conclusions: The presence of highly complex chromosomal aberrations was a common feature in our Caribbean ATLL cohort, which included numerical abnormalities as well as structural chromosomal rearrangements. Many of our findings are similar to those reported for Japanese ATLL, however recurrent deletions on 17p (20%) and structural rearrangement at 2p (17%) have not been described before. Further studies, including higher resolution genomic analyses are warranted to determine whether the different clinical course of Caribbean ATLL is due to differences in the spectrum and frequency of genetic mutations, host and environmental factors, or delays in seeking clinical care.

1569 MYC Translocation Partner Matters in Diffuse Large B-Cell Lymphoma and Double/Triple-Hit High-Grade B-Cell Lymphoma

Nathan T Sweed¹, Rolando Garcia¹, Weina Chen¹, Prasad Koduru¹. ¹UT Southwestern Medical Center, Dallas, TX

Background: MYC is a global transcription factor that regulates 10-15% of the human genome. MYC rearrangement (MYC-R) is present in 5-15% of diffuse large B-cell lymphoma (DLBCL). MYC-R lymphomas with additional rearrangement(s) in BCL2 (BCL2-R) and/or BCL6 (BCL6-R) ("double/triple-hits") have been termed "high-grade B-cell lymphoma[s] (HGBL), with rearrangements of MYC and BCL2 and/or BCL6" (DTH-HGBL) by the 2016 revision of the WHO classification of lymphoid neoplasms. To better understand clinically aggressive DLBCL and DTH-HGBL, we explore the clinical significance of genetic rearrangement translocation partners.

Design: Cases were retrospectively selected on the criteria: 1) diagnosis of DLBCL (n=135), B-cell lymphoma, unclassifiable with features intermediate between DLBCL and Burkitt lymphoma (n=5), HGBL, not otherwise specified (n=2), DTH-HGBL (n=24); 2) FISH studies for MYC-IGH fusion, MYC breakapart (BA), BCL6 BA, and BCL2-IGH fusion. Cases were grouped as MYC negative (MYC-neg: -MYC-R, -BCL2-R, -BCL6-R), single-hit (SH: +MYC-R, -BCL2-R, -BCL6-R), and double/triple-hit (DTH: +MYC-R, +BCL2-R and/or +BCL6-R). Cases were further classified by MYC-R translocation partner as MYC-IGH (+MYC-IGH fusion) and MYC-non-IGH (-MYC-IGH fusion, +MYC BA). Overall survival (OS) data was compared using Kaplan-Meier analysis.

Results: One hundred sixty-six (166) cases (90 males, 76 females, median age 56, range 20 to 90 years) met the stated criteria: MYC-neg (n=118), SH-MYC-non-IGH (n=8), SH-MYC-IGH (n=16), DTH-MYC-non-IGH (n=14), and DTH-MYC-IGH (n=10).

Median OS for MYC-neg, MYC-non-IGH, and MYC-IGH was 83.72, 65.18, 42.36 months respectively ($\sigma=5.01, 9.96, 6.50$). MYC-R, MYC-IGH, SH-MYC-IGH, and DTH-MYC-IGH were significantly associated

with decreased OS compared with MYC-neg (log-rank p=0.028, 0.007, 0.038, 0.028). MYC-non-IGH, SH-MYC-non-IGH, and DTH-MYC-non-IGH were not significantly associated with decreased OS compared with MYC-neg (log-rank p=0.48, 0.27, 0.07).

Conclusions: Our study supports the hypothesis that survival in MYC-R DLBCL and DTH-HGBL may be affected by the MYC translocation partner. MYC-IGH, SH-MYC-IGH, and DTH-MYC-IGH demonstrated a significant association with decreased OS when compared to MYC-neg. This association was not demonstrated by MYC-non-IGH, SH-MYC-non-IGH, or DTH-MYC-non-IGH. Further investigation of additional translocation partners (eg. IGH, IGL) and genetic rearrangements is warranted to advance our understanding of these pathologic entities.

1570 TP53 Aberrations correlate with Immature Plasma Cell Morphology in Multiple Myeloma

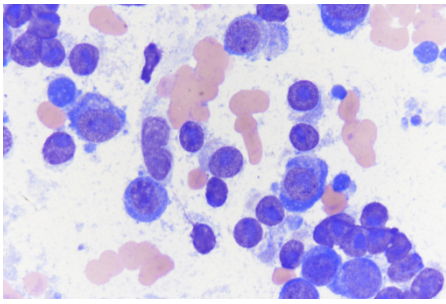
Sofia E Taboada¹, Shafinaz Hussein², Foxwell Emmons², Siraj El Jama³, Jane Houldsworth², Julie Teruya-Feldstein⁴. ¹Icahn School of Medicine at Mount Sinai, Plainview, NY, ²Icahn School of Medicine at Mount Sinai, ³Icahn School of Medicine at Mount Sinai, New York, NY, ⁴Mount Sinai Hospital Icahn School of Medicine, New York, NY

Background: Loss, gain or mutation of TP53 is seen in a small subset of multiple myeloma (MM) patients and are associated with poor prognosis. Plasmablastic/immature (P/IM) morphology distinguishes MM patients with poor prognosis, however identification of P/IM morphology is not integrated in daily clinical practice in a standard way. A modified quantitative Bartl grade is attempted and studied for an association with cytogenetic and molecular markers associated with known prognosis.

Design: We retrospectively analyzed MM cases collected at our institution from consented patients, from 11/2015 to 06/2017. Cases showing $\geq 20\%$ plasma cells (PC) on aspirate smears (n=31 cases) were reviewed by 3 independent reviewers with consensus agreement. Each reviewer counted 50 PC and enumerated the number showing P/IM features, strictly defined by the presence of both fine chromatin and prominent nucleoli. Cases were divided into 2 groups, showing $< 30\%$ versus $\geq 30\%$ P/IM morphology. Clinical, laboratory, pathologic, IHC (MIB1), cytogenetic, and molecular data were collected for the matched specimens. Cytogenetic abnormalities were scored based on plasma-enriched FISH and/or G-banded karyotype. The FISH panel included probes targeting TP53, IGH/CCND1, IGH/FGFR3, and MYC. NGS data was performed on total marrow aspirates (Foundation-Heme, Foundation Medicine) and risk categorization according to gene expression profiling through MyPRS.

Results: There were 9 cases with $\geq 30\%$ P/IM and 7 showed TP53 structural aberration (gains and losses). Of the 22 cases with $< 30\%$ P/IM, 4 were found with TP53 structural aberrations (Table 1). Statistical analysis was performed using univariate analysis and multivariate regression model. Cases with $\geq 30\%$ P/IM morphology showed a statistically significant association with gains/losses of TP53 (p<0.05). There was no significant difference between both groups in terms of complex karyotype; t(11;14), t(4;14), and MYC by FISH; High risk MyPRS categories; BRAF, KRAS, NRAS and TP53 mutations by NGS (Foundation Medicine).

Parameter	P/IM $\geq 30\%$ (n=9)	P/IM $< 30\%$ (n=22)	P Value by Univariate Analysis	P Value by Nominal Regression
TP53 (by FISH)	7 (Gain=3, Loss=4)	4 (Gain=1, Loss=3)	0.022	0.032
t(11;14)	0	8 (n=21)	0.301	0.114
t(4;14)	1	3 (n=21)	0.947	0.948
MYC	4 (n=6)	3 (n=10)	0.545	0.739
Complex karyotype	3	3	0.610	0.569
High Risk (MyPRS)	5 (n=8)	6	0.634	0.724
TP53 mutations	3 (n=8)	1	0.516	0.607
BRAF mutations	1 (n=8)	2	0.356	0.387
KRAS mutations	2 (n=8)	4	0.793	0.988
NRAS mutations	2 (n=8)	3	0.446	0.515



Conclusions: Plasmablastic/immature morphologic features in MM, defined as having both fine chromatin and prominent nucleoli, are significantly associated with *TP53* structural aberrations. Given the association of *TP53* aberrations with a poorer prognosis, we conclude that cases showing P/I/M morphologic features may be associated with more aggressive disease and identify patients for potential *TP53*-associated treatment.

1571 Expression of T-cell Receptor Signaling Pathway Components in Extranodal NK/T-cell Lymphoma

Tomoko Takata¹, Katsuyoshi Takata², Shih-Sung Chuang³, Yasuharu Sato⁴, Tadashi Yoshino⁵. ¹Okayama University Graduate School of Medicine, Dentistry and Pharmaceutical Sciences, Okayama, ²Okayama City, Japan, ³Chi Mei Medical Center, Tainan City, Taiwan, ⁴Okayama University Graduate School of Medicine, Okayama, Japan, ⁵Okayama University Medical School, Okayama

Background: Extranodal NK/T-cell lymphomas (ENKTL) may arise from NK- or T-cells. Although ENKTLs usually do not express T-cell markers, T-cell receptor (TCR) gene might be rearranged and TCR protein expressed in some cases. Downstream TCR pathway is important for the development of peripheral T-cell lymphoma (PTCL), but the expression of TCR pathway components is not well elucidated in ENKTL.

Design: Formalin fixed paraffin embedded tissues from 91 ENKTL patient samples were used to immunohistochemically characterize the expression of TCR pathway components (GRAP2, ITK, LCK, ZAP70, DOK2). Correlation with cellular lineage was also analyzed.

Results: The median age was 54 (range, 15-87) with a male to female ratio at 1.9: 1. 47 samples had nasal lesions alone, 31 had extranasal lesions alone, and 13 had both nasal and extranasal lesions. These tumors were classified as NK (45%; 41/91), T (16%; 15/91), or indeterminate (38%; 35/91) lineage. NK lineage was more frequent in cases with both nasal and extranasal lesions as compared to those with nasal lesion alone or extranasal lesion alone ($P = 0.02$ and 0.014 , respectively). The TCR pathway components were variably expressed: GRAP2 (68%; 60/88), ITK (10%; 9/90), LCK (35%; 31/88), ZAP70 (94%; 83/88), and DOK2 (42%; 38/90). GRAP2 expression rate was higher in T lineage tumors ($P = 0.0073$ vs. NK, $P = 0.00082$ vs. indeterminate). And GRAP2-positive NK lineage tumors more frequently expressed DOK2 ($P = 0.0073$) and were confined to nasal areas ($P = 0.014$). GRAP2-positive indeterminate lineage tumors were frequently confined to extranasal areas ($P = 0.042$). There was no difference of expression between TCR-silent and TCR-expressed cases in T lineage tumors. There was no apparent correlation with the site of origin. The number of expressed TCR pathway components was lower in NK than in T lineage tumors (average 2.58 vs. 3.4, $P = 0.015$), and the number in indeterminate tumors was in between the NK and T lineage tumors.

Conclusions: Although the expression rates of TCR pathway components in ENKTLs were lower than that in PTCLs, our study indicate that TCR pathway may be functioning in ENKTLs despite the defect in TCR gene rearrangement and protein expression.

1572 Mutational Profile of HIV-Related Diffuse Large B-Cell Lymphoma

Yaohong Tan¹, Nicholas Mackrides², Jo-Heon Kim³, Shuhua Yi⁴, Qiang Gong⁴, Kyle White⁵, Offiong F Ikpat⁶, Wing Chung Chan⁷, Jennifer Chapman⁸, Francisco Vega⁹. ¹Cutler Bay, FL, ²University of Miami/Sylvester Cancer Center, Hallandale Beach, FL, ³City of Hope Medical Center; Chonnam National University Hospital, Duarte, CA, ⁴City of Hope Medical Center, ⁵Miami, FL, ⁶University of Miami/Sylvester Cancer Center, ⁷City of Hope National Medical Center, Duarte, CA, ⁸University of Miami/Sylvester Cancer Center, Miami Shores, FL, ⁹University of Miami/Sylvester Cancer Center, Coral Gables, FL

Background: Diffuse large B cell lymphoma (DLBCL) constitutes ~50% of HIV-related lymphomas (HIV-DLBCL) and ~40% of these are EBV-associated (latency II) and usually associated with pronounced immunosuppression. HIV-DLBCL is characterized by frequent genetic alterations involving *MYC* and *BCL6*; however the genetic mutational profile of these neoplasm is largely unknown.

Design: We retrospectively identified 15 cases of HIV-DLBCL. Cases with features similar to Burkitt lymphoma (BL) were excluded. Tumor DNA was subjected to next generation sequencing (NGS) using a 334 gene custom panel, captured using the Agilent SureSelect platform, and the exons sequenced.

Results: Patients consisted of 13 (86.7%) men and 2 (13.3%) women with an average age of 48 (range 33 to 61 years). Morphologic features were similar to cases of non-HIV DLBCL. 10 cases (71%) were GC, 4 cases (29%) were non-GC, one was not determined. EBER was positive in 4 of 10 cases. IHC for *MYC* and *BCL2* was performed in 8 cases; 5 were double expressors (62.5%). FISH identified rearrangement of *MYC*, *BCL6* or *BCL2* in 7 of 10 cases (70%); 1 was double hit (*BCL6* and *MYC*), 5 had *MYC* rearrangement and 1 had *BCL6* rearrangement.

The most frequently mutated gene was *TP53* (31.3%) followed by *BIRC6*, *DDX3X*, *ITPKB*, *KMT2C*, *LRRN3* and *PAX5*. While some of the identified mutations are recurrent in HIV negative DLBCL (e.g. *LRRN3*, *HIST1H1C*, *SGK1*, *B2M*, *DOCK2*, *HIST1H1E*, *TNFAIP3* and *TRRAP*) we also found mutations rarely found in HIV-negative DLBCL, and more prevalent of BL (e.g. *PTEN*, *SBF1*, *TCF3* and *IF3*).

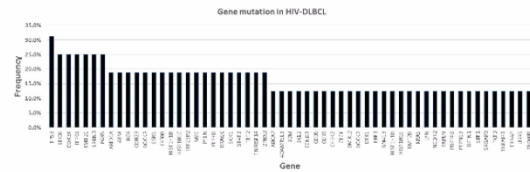


Figure 1. gene mutational profile of HIV-DLBCL.

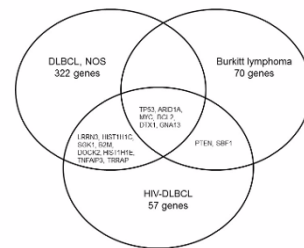


Figure 2. Frequently mutated genes in DLBCL, NOS, Burkitt lymphoma and HIV-DLBCL.

Conclusions: These findings suggest that HIV-DLBCLs have more frequent rearrangement of *MYC*, *BCL6* or *BCL2* and a mutational profile that seems to be distinct from HIV negative cases and include mutations in genes seen more frequently in BL.

1573 Clinicopathologic and Molecular Characteristics of Myeloid Neoplasms with Non-Canonical MPL Mutations

Beenu Thakral¹, Tariq Muzzafar¹, Ifra Badar¹, Sa Wang¹, Roberto Miranda¹, Pei Lin¹, Joseph Khoury¹, Mark Routbor², Rashmi Kanagal-Shamanna³, Sanam Loghavi⁴, Chi Young Ok¹, C. Cameron Yin¹, Zhuang Zuo¹, Srdan Verstovsek¹, Christopher Benton¹, Rajyalakshmi Luthra¹, Carlos Bueso-Ramos¹, L. Jeffrey Medeiros¹, Keyur Patel¹.

¹The University of Texas MD Anderson Cancer Center, Houston, TX, ²Bellaire, TX, ³The University of Texas MD Anderson Cancer Center, Bellaire, TX, ⁴Houston, TX, ¹¹The University of Texas MD Anderson Cancer Center, Sugar Land, TX

Background: Driver mutations in myeloproliferative neoplasms (MPN) typically involve limited hotspots in *JAK2* (codon 617, exon 12), *MPL* (codon 515), and *CALR* (exon 9). Widespread use of next generation sequencing (NGS) in routine clinical testing has identified recurring mutations outside of these hotspots, however, the significance of mutations occurring outside of codon 515, defined here as non-canonical mutations, is not well-studied. We describe the clinicopathologic characteristics of various myeloid neoplasms (MN) with non-canonical *MPL* mutations.

Design: Myeloid neoplasms were classified as per WHO 2008 classification for hematolymphoid neoplasms. Clinical and laboratory data were extracted from electronic medical records. DNA was extracted from bone marrow aspirate or peripheral blood samples and next generation sequencing (NGS) was performed using a 28-gene custom panel that included *JAK2*, *CALR* and *MPL* and a MiSeq sequencer (Illumina, San Diego, CA).

Results: The study group included 23 patients, 13 men and 10 women, with a median age of 68 years (range, 44-86). The diagnoses included MPN (n=11; 9 primary myelofibrosis [PMF] and 2 polycythemia vera), AML (n=8), CMML (n=2), MDS (n=1), and BPDCN (n=1). The most frequent non-canonical *MPL* mutation involved codon 591 in 20/23 (87%) cases. The substitutions involved were p.Y591D (n=13), p.Y591H (n=4), p.Y591N (n=3), p.S204P (n=2) and p.S493A (n=1) with a median variant allele frequency of 24.4 [range, 2.2-58.3]. Non-canonical *MPL*

mutation was seen as a sole molecular abnormality in 12 patients (52.2%) [p.Y591D/H/N (n=10), p.S204P (n=2)]. In 9 patients (39.1%), the *MPL* mutation was associated with one driver co-mutation [*JAK2* p.V617F (n=6), *MPL* p.W515L (n=3)]. Interestingly, 2 (8.7%) patients showed two co-mutations in MPN-associated genes. One patient with AML with myelodysplasia-related changes had a p.Y591D mutation (VAF: 44.8%) with additional *MPL* p.W515L (VAF: 9.4%) and *JAK2* p.V617F (VAF: 32.1%) mutations. A second patient with PMF had p.Y591D mutation (VAF:11.3%), *JAK2* p.F694S (VAF:5.3%) and type 1 *CALR* (VAF:11.3%) mutations. At last follow up (median: 24 months; range, 3-168), 17/23 (73.9%) patients were alive and 6 died of disease.

Conclusions: Non-canonical *MPL* mutations occur in a spectrum of MN including MPN, AML, MDS, and CMML. The presence of these mutations, in isolation and in association with driver mutations, suggests possible involvement in the pathogenesis and in clinical outcome.

1574 Early T-Precursor (ETP) Acute Lymphoblastic Leukemia/Lymphoma (ALL) versus Non-ETP ALL in Children and Young Adults: Clinicopathologic Differences

Cody A Thomas¹, Xiayuan Liang². ¹University of Colorado School of Medicine, ²Children's Hospital Colorado, Aurora, CO

Background: Early T-precursor (ETP) acute lymphoblastic leukemia/lymphoma (ALL) is a new provisional entity in the 2016 updated WHO Classification of Hematologic Malignancies. It is characterized by the absence of CD1a and CD8 expression, and expression of CD7 and one or more stem cell or myeloid antigens. ETP-ALL has been reported in 11-12% of childhood T-ALL and is associated with a more aggressive clinical behavior in children and young adults compared to Non-ETP ALL. Given that ETP-ALL is a recently described entity, certain clinicopathologic differences between ETP-ALL and non-ETP ALL have not been well studied. We performed retrospective data analysis to compare clinicopathologic differences between these two subtypes of T-ALL.

Design: Between 2011 and 2017, 45 cases of newly diagnosed T-ALL (17 ETP and 28 non-ETP) were identified at our institution. The data we analyzed were age at diagnosis, sex, cytogenetics of the tumor, presence of mediastinal mass, CSF involvement, hyperleukocytosis ($\geq 100k$), high S phase ($>10\%$), CD56 expression, *TCR* gene expression, and mortality. A p-value was calculated for each comparison with a value of less than 0.05 considered statistically significant.

Results: See the following table.

	ETP	Non-ETP	p value
Case #	17	28	
Age (mean)	3-22 y (11.5 y)	1-24 y (7.6 y)	0.0317
M:F	13:4	23:5	0.7109
Mediastinal mass	5/17 (29.4%)	19/28 (67.86%)	0.0161
CSF+	7/14 (50%)	11/27 (40.74%)	0.7652
Hyperleukocytosis ($\geq 100k$)	5/17 (29.4%)	13/28 (46.42%)	0.3513
High S phase ($\geq 10\%$)	3/16 (18.75%)	10/24 (41.67%)	0.1770
MLL+	4/17 (23.53%)	1/26 (3.85%)	0.0707
CD56+	5/17 (29.41%)	0/28 (0%)	0.0051
<i>TCR</i> gene rearrangement+	8/14 (57.14%)	23/23 (100%)	0.0013
Mortality	2/17 (11.76%)	6/28 (21.43%)	0.6900

Conclusions: Patients with ETP-ALL tend to be older than patients with non-ETP ALL.

- In T-ALL, *MLL* gene rearrangement seems to occur more often in ETP-ALL than non-ETP ALL (borderline p value) suggesting that, like B-ALL, *MLL* gene rearrangement is likely associated with a primitive stage of T-ALL; however, unlike B-ALL, *MLL* gene rearrangement in T-ALL is not associated with a specific age group or unfavorable outcome.
- CD56 appears to be expressed only in ETP-ALL, suggesting its association with a primitive stage of T-ALL and not suggesting an indication of NK cell lymphoblastic leukemia/lymphoma.
- ETP-ALL has a lower frequency of *TCR* gene rearrangement than non-ETP ALL, suggesting *TCR* gene rearrangement likely occurs post-ETP stage.

- Presence of a mediastinal mass occurs more frequently in non-ETP ALL and correlates with a higher incidence of hyperleukocytosis and high S-phase, suggesting that tumor cells in T-ALL may be more actively proliferating post-ETP stage.

1575 PREVIOUSLY PUBLISHED

1576 Identifying Bad Actors in DLBCL: Can We Tailor Gene Rearrangement FISH Studies Based on Immunohistochemistry?

Deirdre M Timlin, Dublin, Ireland

Background: The 2016 revised WHO lymphoma classification recommends that the cell of origin classification is reported in cases of DLBCL. Gene rearrangements involving MYC, Bcl-2 and Bcl-6 also need to be screened for, as lymphomas harbouring two ('double hit' / DH) or three (triple hit/ TH) rearrangements, behave aggressively and may require an alternate chemotherapeutic regimen to standard R-CHOP therapy. Some prior studies report no association between cell of origin and the presence of a DH or TH lymphoma and suggest that all DLBCL be tested by FISH, whereas other groups suggest that DH/TH lymphoma are more commonly seen in association with the germinal center (GCB) subtype. Equally there is as of yet no consensus opinion on the correlation between c-myc (defined as $>40\%$ lymphoma cells positive) and Bcl-2 protein (defined as $>50\%$ lymphoma cells positive) overexpression (double expressor status, DE) and gene rearrangement.

Design: We retrospectively analysed the cell of origin status (Hans classified) and FISH profiles of 367 cases of DLBCL, NOS.

Results: 78/367 (21%) cases had a MYC gene rearrangement of which 51/78 (65%) were of GCB subtype ($p<0.001$). 37/367 (10%) cases had DH/TH by FISH. 33/37 (89%) of these were of GCB subtype ($p<0.001$). 130/228 (57%) DLBCL cases were c-myc protein positive and of these, 46/130 (35%) had a MYC rearrangement ($p<0.0001$), 23/46 (50%) with an identified IgH translocation partner. Of 98/228 (43%) patients who were c-myc protein negative, 3/98 (3%) had a MYC rearrangement, none of these with a IgH translocation partner.

88/233 (38%) DLBCL cases were DE of which 47/88 (53%) were GCB subtype ($p=0.88$). 23/32 (72%) DE were also DH/TH ($p=0.001$).

Conclusions: To conclude, we show that the incidence of MYC rearrangement in our study is 21%, which is higher than the usual reported incidence of 8-14%. This likely reflects our position as the National Transplant Centre thus attracting a cohort of poor prognostic lymphomas for salvage transplantation. In our cohort MYC rearrangement and DH/TH groups are more often seen within the GCB subtype of DLBCL and they are also more likely to be DE. This may allow us to streamline our services by using IHC to select which patients will likely benefit from FISH testing. Although c-myc protein overexpression without gene rearrangement occurs, gene rearrangement without protein overexpression is rare.

1577 High EZH2 Protein Expression Is Associated with Inferior Survival in Patients with Multiple Myeloma

Rosemarie Tremblay-LeMay¹, Maryam Pourabdollah², Nasrin Rastgoo³, Hong Chang⁴. ¹University Health Network, Québec, PQ, ²University of Toronto, Toronto, ON, ³University Health Network, ⁴Toronto General Hospital, Toronto, ON

Background: Multiple myeloma (MM) is a malignancy characterized by highly heterogeneous genomic alterations. It has been shown that deregulation of epigenetic mechanisms like EZH2 plays an essential role in MM development. High *EZH2* mRNA expression in MM is correlated with increased proliferation, tumor cell aggressiveness and poor prognosis. However, EZH2 protein expression measured by immunohistochemical staining (IHC) has not been evaluated in MM.

Design: 67 cases diagnosed with MM at our institution were included in this study. All of them received the same treatment protocol; standard high dose chemotherapy followed by autologous stem cell transplant. The bone marrow specimens used for IHC studies were obtained prior to starting any treatment. CD138 and EZH2 IHC were performed on paraffin embedded bone marrow clot sections or biopsy tissue sections. We used the H-score method (0-300) based on percentage and intensity of nuclear EZH2 staining. The results were then correlated with patient's clinical and laboratory features and survival outcomes.

Results: There were 30 females and 37 males with median age of 54 (range 34-73) years. The median follow-up time after transplant was 58.3 (range: 2.8-196.6) months. The average H-score among our cohort was 142. High or low expressions were defined based on the H-score result being above or below the average H-score, respectively. 49% of cases showed low expression (H-score 50-135)

and 51% high expression (H-score 152-260). High expression of EZH2 was associated with higher beta 2 microglobulin levels (>3.5mg/L, p=0.0054). Furthermore, high expression was associated with shorter progression free survival (PFS) and overall survival (OS) compared to low expression (PFS: 10.22 vs 21.88 months, p=0.0024; OS: 36.93 vs. 87.95 months, p=0.0004, respectively). There was no correlation between EZH2 expression and other clinical and laboratory features: age, sex, creatinine, calcium, serum albumin, clinical stage, bony lytic lesion, and cytogenetics including t(4;14), t(11;14), 13q deletion, and 17p(P53) deletion.

Conclusions: High EZH2 protein expression predicted adverse outcome in MM patients. Assessment of EZH2 by IHC could be a useful tool for risk stratification as well as selecting candidates for EZH2 inhibition therapy in MM patients.

1578 PREVIOUSLY PUBLISHED

1579 N-Glycoproteomic Analysis Reveals Novel Biomarkers Including Killer Inhibitory Receptor (KIR) Family Members in Cutaneous T Cell Lymphoma

John S Van Arnam¹, Rui Wu¹, Delphine. C Rolland¹, Özlem Önder¹, Megan Lim², Kojo Elenitoba-Johnson³. ¹University of Pennsylvania, Philadelphia, PA, ²Hospital/ University of Pennsylvania, Philadelphia, PA, ³Perelman School of Medicine, Philadelphia, PA

Background: Cutaneous T cell lymphomas (CTCLs) are heterogeneous neoplasms with variable clinical outcomes; early stage disease would greatly benefit from novel biomarkers and late stage disease needs effective targeted therapies. While the mutational landscape of CTCLs is being defined, their proteomic signatures are largely unknown. Post-translational modification by N-glycosylation targets proteins to cell membranes or for secretion, making them excellent biomarkers and therapeutic targets. We sought to identify in an unbiased fashion novel proteins selectively expressed in Sézary syndrome (SS) that would facilitate early diagnosis and constitute precision targets.

Design: N-glycoproteomic analysis was performed on 40 human lymphoma-derived cell lines representing 14 distinct categories of lymphoma in technical and biological triplicates, including CTCL-derived cell lines representative of SS (HUT78), mycosis fungoides (HH), and ALK-negative anaplastic large cell lymphoma (ALCL) with *PCM1-JAK2* or *NPM1-TYK2* translocations (Mac1, Mac2a, and Myla). N-glycoproteins were enriched using solid phase extraction and hydrazide resin and analyzed with a LTQ OrbitrapXL mass spectrometer. Spectral counts were utilized for quantification. Flow cytometry and western blotting were performed using antibodies against KIR2DL1 (R&D Systems), KIR2DL5 (Lifespan Biosciences), and CD4 (BD Biosciences) on the cell lines and lysates.

Results: A total of 811 N-glycosylated proteins with 1215 assigned N-glycosites were identified in the T cell lymphoma cell lines, of which 99 were novel. Preferentially expressed N-glycoproteins in SS included known Killer-cell immunoglobulin-like receptor (KIR) biomarkers KIR3DL2 and KIR3DS1, but also novel KIR family members KIR2DS1, KIR2DL1, KIR2DL5A, and natural killer gene complex (NKG2C) members NKG2D, CD371, and KLRF2. Flow cytometry for KIR2DL5A and KIR2DL1 demonstrated preferential immunoreactivity on CTCL cell lines in comparison to ALCL cell lines. Western blotting for KIR2DL5A showed strong expression in CTCL cells but little expression in Mac1/2a. Overall, the proteomic data was corroborated by immunophenotypic analysis by flow cytometry and western blotting.

Conclusions: N-glycoproteomic analysis is a powerful approach for identification of novel proteins expressed in specific lymphoma subtypes. Selective expression of KIR and NKG2C family members in CTCL represent possible novel biomarkers and therapeutic targets.

1580 Cytogenomic Array Detects a High-Risk Subset of Myelodysplastic Syndrome Invisible to Conventional Karyotype

Steven B Van Norman¹, Sarah M Choi¹, Lina Shao¹. ¹University of Michigan, Ann Arbor, MI

Background: Prognostic classification of myelodysplastic syndrome (MDS) using cytogenetic anomalies is currently utilized to guide therapeutic decision making—including the potential use of aggressive therapies such as bone marrow transplantation. Single nucleotide polymorphism arrays (SNP-As) have emerged as a potential means of further categorizing prognostic risk beyond traditional karyotyping in many hematologic malignancies due to the assay's greater sensitivity in detecting unbalanced chromosomal defects and copy-neutral loss of heterozygosity. However, widespread adoption and incorporation into prognostic algorithms remains limited.

Design: To assess the prognostic potential of SNP-As in MDS, we retrospectively reviewed 108 consecutive patients who underwent karyotyping and SNP-A analysis for diagnosis/classification of a

suspected myeloid neoplasm (MDS or MDS/MPN). Overall survival was compared between patients with both low-risk karyotype (very good and good cytogenetic risk group) and consistent SNP-A, and patients with similar low-risk karyotype but abnormal SNP-A. These groups were compared to patients with abnormal karyotype stratified by the Revised International Prognostic Scoring System (IPSS-R) and to patients with abnormal karyotype stratified by known genetic risk factors (intermediate, poor, very poor cytogenetic risk groups). Mantel-Cox and Gehan-Breslow-Wilcoxon tests were used to compare overall survival between the groups.

Results: We found 45 patients with low-risk karyotype; SNP-A did not detect additional abnormalities beyond the karyotype in 23 patients and additional SNP-A abnormalities were detected in the remaining 22 patients. The additional SNP-A abnormalities were associated with significantly poor overall survival (p=0.0483). Patients with low-risk karyotype and additional abnormal SNP-A were found to group similarly to patients with poor – very poor risk karyotype and with high-very high IPSS-R, while patients with low-risk karyotype alone were found to group similarly to patients with very good-intermediate risk karyotype and with very low-intermediate IPSS-R (p=0.0117).

Conclusions: SNP-As, when used with traditional karyotyping methodology, can more accurately predict overall survival than karyotyping alone. This is especially cogent to patients with a normal karyotype who may harbor poor risk genetic alterations undetectable by traditional karyotyping. These patients would potentially benefit from therapeutic plans informed by more accurate prognosis.

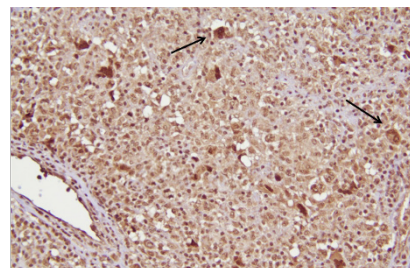
1581 BCL-W is Consistently Overexpressed and Amplified in Hodgkin and Reed-Sternberg Cells in Classical Hodgkin Lymphoma

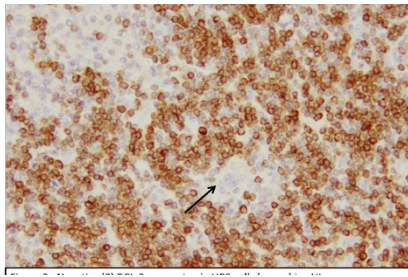
Ashley Vogel¹, Vandi Ly¹, Jinglan Liu¹, Guldeep Uppal², Clare M Adams¹, Christine Eischen¹, Jerald Gong¹. ¹Thomas Jefferson University, Philadelphia, PA, ²Glen Mills, PA

Background: BCL-W is an anti-apoptotic protein in the BCL-2 family with key regulatory functions. Recent studies by our group have uncovered a critical role for BCL-W in B cell survival and MYC-induced lymphomagenesis. Overexpression of BCL-W has been found in various types of hematologic malignancies. The purpose of this study is to further evaluate BCL-W protein expression and gene amplification and compare the differential expression of BCL-2 in classical Hodgkin lymphoma (cHL).

Design: BCL-W and BCL-2 expression was evaluated by immunohistochemistry on FFPE tissue sections. EBV status was evaluated by LMP-1 expression and EBER in situ hybridization. The intensity of BCL-W and BCL-2 expression was graded as 0-3+ and the percentage of positive cells graded in 10% increments. Reactive T cells were used as the normal standard to grade BCL-W expression: 0: no staining; 1+: weaker than T cells; 2+: same as T cells; 3+: stronger than T cells. FISH analysis using a probe encompassing the *BCL-W* region at 14q11.2 and chromosome 14 centromere (BAC clone RP11-81F9) was performed on 8 cases of cHL containing sufficient Hodgkin and Reed-Sternberg (HRS) cells. *BCL-W* signals were counted in 25 HRS cells and 25 small lymphocytes per case.

Results: 47 cases of cHL were studied, including 33 cases of nodular sclerosis type, 10 cases of mixed cellularity type, 2 cases of lymphocyte rich type, and 2 cases not further subtyped. BCL-W was overexpressed in HRS cells in the majority of cases (46/47) and with high intensity (2: 1+; 28: 2+; 16: 3+). In contrast, BCL-2 was expressed in fewer cases (14/47) and with lower intensity (9: 1+; 5: 2+; 0: 3+). FISH analysis detected increased signals in HRS cells in 8/8 cases compared to background reactive lymphocytes with the expected normal pattern. The average FISH signals in HRS cells for each case ranged from 7 to 20 with an overall mean of 13. There was no association of BCL-W expression with histologic subtype or EBV status.





Conclusions: We have shown that BCL-W, but not BCL-2, was consistently overexpressed in HRS cells in cHL. Furthermore, FISH analysis showed amplification of the *BCL-W* gene in HRS cells suggesting that upregulation of BCL-W was likely caused by gene amplification. Compromised apoptotic signaling as a result of increased BCL-W, and not BCL-2, may contribute to the survival of HRS cells in cHL and subsequent tumorigenesis. BCL-W expression in cHL may be used as a diagnostic marker and may serve as a potential target in therapeutic development.

1582 PD-L1 Over-expression is Driven by BCR Signaling in Diffuse Large B-cell Lymphoma

Weige Wang¹, Dong Sheng², Jimmy Lee³, Xiaoyan Zhou², Xiaojie Li⁴. ¹Fudan University Shanghai Cancer Center, Shanghai, ²Fudan University Shanghai Cancer Center, ³University of Chicago, Chicago, IL, ⁴Fudan University Shanghai Cancer Center, Shanghai

Background: Targeting the immune checkpoint programmed death 1 (PD-1)/programmed death ligand 1 (PD-L1) pathway represents the milestone of cancer therapy in recent years. PD-L1 over-expression has been reported in diffuse large B-cell lymphoma (DLBCL), and a variety of studies have been conducted to test anti-PD-L1/PD1 therapies as well as to develop companion diagnostic tools for PD-L1. However, the mechanism of PD-L1 expression in DLBCL remains unknown. In the present study we show that over-expression of PD-L1 in DLBCL can be mediated by the B-cell receptor (BCR) signal pathway.

Design: We first evaluated the correlation between BCR pathway activity (denoted by pSYK and pBTK expression level) and PD-L1 mRNA and protein levels with RNAscope *in situ* hybridization and immunohistochemistry in 108 cases of DLBCL, 25 of which featured loss of surface immunoglobulin (previously defined as BCR-, *Am J Surg Pathol.* 2015 39:902-11). We then investigated the effects of BCR signaling on PD-L1 mRNA and protein levels with qPCR, immunoblotting and flow cytometry in DLBCL cell lines. We also assessed PD-L1 gene amplification in the patient samples using fluorescent *in situ* hybridization. Finally, mice xenografts administered with ibrutinib were used to test the effect of BCR signaling on PD-L1 expression *in vivo*.

Results: PD-L1 gene amplification was seen in 2 (2%) patients, and PD-L1 positivity was found in 16 patients (19%), most of which were non-germinal center (non-GCB) subtype. BCR pathway activity correlated with both PD-L1 mRNA and protein levels. DLBCL without BCR (DLBCL, BCR-) featured a silent BCR signaling denoted by low level of pSYK and pBTK, and a significant lower level of both PD-L1 mRNA and protein compared with those in DLBCL, BCR+. In DLBCL, BCR+ cell lines, BCR stimulation increased the PD-L1 mRNA, total PD-L1 protein and surface PD-L1 expression. Inhibition of BCR signaling with SYK inhibitor (R406) and BTK inhibitor (ibrutinib) attenuated these effects. Neither BCR stimulation nor inhibition affected the PD-L1 status in DLBCL, BCR-. *In vivo* investigation demonstrated BCR inhibition with ibrutinib down-regulate PD-L1 mRNA and protein.

Conclusions: In DLBCL, the over-expression of PD-L1 may be driven by BCR signaling instead of PD-L1 genetic aberration. BCR inhibition and PD-L1 blockage may potentially synergize to targeting DLBCL, especially DLBCL, BCR+ and non-GCB DLBCL.

1583 IRTA1 and MNDA in Marginal Zone Lymphoma: Utility in Differential Diagnosis and Implications for Classification

Zhen Wang¹, James Cook¹. ¹Cleveland Clinic, Cleveland, OH

Background: The diagnosis of marginal zone lymphoma (MZL) is frequently challenging, due in part to a lack of specific phenotypic markers. MZL is also cytologically heterogeneous, with cases showing varying proportions of cells resembling normal monocytoid B-cells and/or marginal zone B-cells. In the current WHO classification, neoplasms resembling either monocytoid B-cells or marginal zone B-cells are each classified as MZL. Recently, IRTA-1, expressed in normal monocytoid B-cells, and MNDA, expressed by normal marginal zone B-cells, have been proposed as specific markers for MZL.

Design: We examined MNDA expression by immunohistochemistry (clone 188566, Abcam, Cambridge, MA) and IRTA-1 mRNA

expression by RNA in situ hybridization (IRTA1 probe, Advanced Cell Diagnostics, Newark, CA) using open probe software on a Benchmark XT (Ventana Medical Systems, Tucson, AZ) in 10 reactive lymph nodes, 80 MZL (including 23 nodal MZL, 32 MALT, and 25 SMZL) and 47 other small B-cell neoplasms (9 LPL, 14 FL, 15 CLL, and 9 MCL). Cases with >20% staining in neoplastic cells were classified as positive. In 36 lymph nodes involved by MZL, phenotypic results were correlated with the cytologic features and architectural growth pattern.

Results: In normal lymph nodes and tonsil controls, IRTA1 expression was found in monocytoid B-cells and in intraepithelial B-cells, but not in mantle/marginal zone areas. In contrast, MNDA expression was consistently seen in mantle/marginal zone areas while monocytoid B-cells and intraepithelial B-cells appeared negative. Results in 80 MZL and 47 other small B-cell lymphomas are summarized in the Table below. In lymph nodes involved by MZL, IRTA1 and MNDA expression was similar in cases with or without a predominance of monocytoid B-cells. IRTA1 expression was less frequent in cases with a predominantly diffuse growth pattern ($p=0.018$), while MNDA expression showed no association with growth pattern.

	IRTA1	MNDA	Either	Both
All MZL (n=80)	31/74 (42%)	51/79 (64%)	64/76 (84%)	22/73 (30%)
NMZL (n=23)	10/23 (43%)	12/22 (54%)	18/22 (82%)	7/22 (32%)
MALT (n=32)	17/32 (53%)	21/32 (65%)	27/32 (84%)	12/32 (37%)
SMZL (n=25)	4/19 (21%)	18/25 (72%)	19/22 (86%)	3/19 (16%)
LPL (n=9)	0/7 (0%)	3/8 (37%)	3/7(43%)	0/8 (0%)
p vs all MZL	p=0.040	p=0.25	p=0.02	p=0.10
FL (n=14)	1/14 (7%)	3/14 (21%)	3/14 (21%)	1/14 (7%)
p vs all MZL	p=0.015	p=0.003	p<0.001	p=0.10
CLL (n=15)	0/13 (0%)	8/15 (53%)	8/13 (61%)	0/14 (0%)
p vs all MZL	p=0.003	p=0.56	p=0.12	p=0.017
MCL (n=9)	0/9 (0%)	7/9 (78%)	7/9 (78%)	0/9 (0%)
p vs all MZL	p=0.023	p=0.72	p=0.64	p=0.10

Conclusions: IRTA1 expression as detected by RNA in situ hybridization is a specific marker for MZL. MNDA is broadly expressed across small B-cell neoplasms except for FL, providing utility in distinguishing MZL from FL. The expression of IRTA1 and MNDA is similar in MZL with or without predominantly monocytoid cytology, supporting the current WHO approach of classifying lymphomas resembling either normal monocytoid B-cells or marginal zone B-cells as MZL. IRTA1 and MNDA can assist in the differential diagnosis of small B-cell neoplasms.

1584 CD5-Negative and CD10-Positive Mantle Cell Lymphoma: A Clinicopathologic Study of 10 Cases

Lifu Wang¹, Pei Lin¹, Jie Xu¹, Zenggang Pan², C. Cameron Yin¹, Sanam Loghavi³, Joseph Khoury¹, L. Jeffrey Medeiros¹, Shaoying Li¹.

¹The University of Texas MD Anderson Cancer Center, Houston, TX, ²Aurora, CO, ³Houston, TX

Background: Mantle cell lymphoma (MCL) is a distinct type of B-cell lymphoma with a typical CD5+, CD10- immunophenotype and *CCND1/IGH*. While a small subset of MCL cases may be CD5- or CD10+, CD5-/CD10+ MCL cases are exceedingly rare but might pose significant diagnostic challenges.

Design: We analyzed 10 cases of CD5-/CD10+ MCL identified over the course of 8 years. CD5 and CD10 expression were assessed by flow cytometry (FC) or immunohistochemistry (IHC). *CCND1/IGH* was detected by Fluorescence in situ hybridization (FISH). Clinicopathologic features and outcomes were extracted from electronic medical records.

Results: There were 6 men and 4 women with a median age of 66 years (range, 46-74). Three cases were diagnosed in lymph nodes and the other 7 in extranodal sites, including bone marrow (n=2), GI tract (n=2), skin (n=1), nasal cavity (n=1), and tonsil (n=1). 8 of 9 (89%) patients presented with high stage (III/IV) disease with frequent extranodal (7/9, 78%) involvement. Eight cases were blastoid and 2 were classical MCL. All cases were positive for cyclin D1 and harbored *CCND1/IGH*. All cases were positive for CD10 detected by IHC (n=3), FC (n=2) and by both methods (n=5). All cases were negative for CD5 by IHC (n=3), FC (n=1), or both methods (n=6). 4 of 7 (57%) were positive for SOX11, and Ki-67 proliferation rate was high ($\geq 30\%$) in 7/9 (78%). All 4 cases tested were negative for *BCL2/IGH*. Clinical follow-up and therapeutic data was available in 9 patients; all received rituximab-based immunochemotherapy. After induction, 7 patients achieved complete remission (CR) (7/9, 78%), 1 partial remission, and 1 had progressive disease. Five patients who originally achieved CR relapsed later. After a median follow up of 31 months (range 1-162 months), 2 patients died and 7 were alive at last follow up. The median

overall survival was not reached.

Conclusions: CD5-/CD10+ MCL cases frequently have blastoid morphology, a high proliferation rate and extranodal involvement. The unusual immunophenotype makes it critical to distinguish these tumors from follicular lymphoma and high-grade B-cell lymphoma. A complete workup, especially immunohistochemistry for cyclin D1 and FISH for *CCND1/IGH*, is important for the differential diagnosis. Although extremely rare, pathologists need to be aware of these tumors to avoid misdiagnosis and inappropriate treatment.

1585 Characterization of Chronic Myelomonocytic Leukemia with TP53 mutations

Wei Wang¹, Mark Roubort², Sanam Loghavi³, Zhenya Tang¹, L. Jeffrey Medeiros¹, Sa Wang¹. ¹The University of Texas MD Anderson Cancer Center, Houston, TX, ²Bellaire, TX, ³Houston, TX

Background: *TP53* mutations occur in approximately 10% of patients with myelodysplastic syndrome (MDS) or acute myeloid leukemia (AML), and are associated with a complex karyotype and a poor prognosis. In contrast, *TP53* mutations in chronic myelomonocytic leukemia (CMML) are much rarer with a reported rate of 1%. The clinicopathological features of CMML cases with *TP53* mutations are not well studied.

Design: We identified 9 cases of CMML with *TP53* mutations. Clinicopathological features, treatment regimens, response and follow-up data were analyzed.

Results: There were 6 men and 3 women with a median age of 72 years (range, 63-86). Based on the 2016 WHO classification, they were classified as: CMML-0 (n=6) and CMML-1 (n=3). Based on the WBC count, 5 cases were "proliferative type" and 4 cases were "dysplastic type". Monocyte counts ranged from 22% to 51% (median 31%) and the absolute monocyte count ranged from 1.4x10⁹/L to 14.3 x10⁹/L (median 3.8 x10⁹/L).

In total, 10 *TP53* mutations were identified in 9 cases, of which 8 (89%) had one *TP53* mutation and 1 (11%) had two *TP53* mutations. All *TP53* mutations were present at the time of initial CMML diagnosis. Most *TP53* mutations (8/10, 80%) occurred in the DNA binding domain (exons 5-8). The median mutant allele frequency was 47% (range, 1.2%-80%). Conventional karyotyping analysis showed that 5 (56%) had a normal karyotype, 2 (22%) had 1 cytogenetic abnormality and 2 (22%) cases had a complex karyotype. Six cases also underwent targeted molecular testing for *ASXL1* and *TET2*; 1 (17%) case had *ASXL1* mutation and 1 (17%) case had *TET2* mutation. *KRAS* and *NRAS* mutations were detected in 1 case each and both were "proliferative type" CMML.

Six patients received hypomethylating agent based therapy and 3 were observed due to stable disease. During a median follow-up of 17.2 months (range, 11.5 to 37.1), 3 patients showed disease progression. Five patients have died and 4 were alive at the last follow-up.

Conclusions: *TP53* mutations in CMML are rare and commonly occur in DNA binding domain with 1 mutation predominant. Different from MDS and AML in which over 80% of cases showed complex karyotypes in *TP53* mutated cases, only 22% of CMML cases with *TP53* mutations had a complex karyotype. *ASXL2* and *TET2* mutations, the most common mutations reportedly seen in 40-60% of CMML cases, appear to have a lower frequency (17%) in cases with *TP53* mutations. CMML patients with *TP53* mutations showed a variable prognosis with a subset showing a rapid disease progression.

1586 Identification of CCR4 Mutations in Adult T-cell Leukemia/Lymphoma by Immunohistochemistry

Hao-Wei Wang¹, Maryknoll Palisoc², Winnifred Navarro³, Liqiang Xi⁴, Elaine Jaffe⁴, Mark Raffeld⁵, Stefania Pittaluga⁶. ¹NIH, Bethesda, MD, ²Penn State College of Medicine, ³NCI, NIH, ⁴National Cancer Institute/NIH, Bethesda, MD, ⁵NCI/NIH Lab of Pathology, Bethesda, MD, ⁶National Cancer Institute, Bethesda, MD

Background: Adult T-cell Leukemia/Lymphoma (ATLL) is an aggressive mature T-cell neoplasm associated with human T-cell leukemia virus type-1. Despite decades of advances in treatment modalities, the prognosis remains poor, with a median survival of less than one year in the acute and lymphoma subtypes. Recent next-generation sequencing studies identified recurrent nonsense or frameshift mutations in the carboxy-terminal domain (CTD) of CC chemokine receptor 4 (CCR4) in approximately 25% of ATLL cases, which lead to impaired internalization of the CTD-truncated receptors and a phenotype favorable for cancer cell survival and proliferation. These findings suggested the therapeutic potential of CCR4 inhibition in this aggressive malignancy. As such, a simple and reliable clinical assay would be useful to identify ATLL cases that harbor CCR4 mutations.

Design: Immunohistochemical stain (IHC) for CCR4 was performed in 34 ATLL patient samples using an antibody (HPA031613, Sigma) that targets CCR4-CTD which is truncated and deleted in the mutant CCR4. A pyrosequencing primer set encompassing codons 329 to 348

was designed to cover known CCR4-CTD mutation hotspots. DNA was extracted from formalin-fixed paraffin-embedded samples, and analyzed for CCR4 mutations by pyrosequencing. The pyrosequencing results were validated using targeted next-generation sequencing (Ion Torrent) in 4 samples.

Results: Nonsynonymous CCR4-CTD mutations were detected in 10 cases (29.4%), including 9 nonsense and 1 missense mutations (Table 1). In cases with wild-type CCR4, IHC consistently showed strong and diffuse membranous expression of CCR4 (22/24, 91.7%). In contrast, IHC demonstrated either weak cytoplasmic/Golgi (n=4) or variable staining (n=4) patterns of CCR4-CTD in cases with nonsense CCR4 mutations (Table 1 and Figure 1).

Table 1. Summary of CCR4-CTD IHC in ATLL cases with nonsynonymous CCR4 mutations

Case #	Nucleotide change	Amino acid change	Mutation type	CCR4-CTD IHC*
1	c.988C>T	p.Gln330*	Nonsense	weak, g
2	c.993C>A	p.Tyr331*	Nonsense	weak, c
3	c.993C>A	p.Tyr331*	Nonsense	variable
4	c.993C>A	p.Tyr331*	Nonsense	moderate, m
5	c.993C>G	p.Tyr331*	Nonsense	variable, g
6	c.993C>G	p.Tyr331*	Nonsense	weak, c
7	c.1006C>T	p.Gln336*	Nonsense	weak, c
8	c.1006C>T	p.Gln336*	Nonsense	variable
9	c.1027C>T	p.Pro343Ser	Missense	strong, m
10	c.1041C>A	p.Tyr347*	Nonsense	variable

*IHC patterns: c, cytoplasmic; g, Golgi; m, membranous

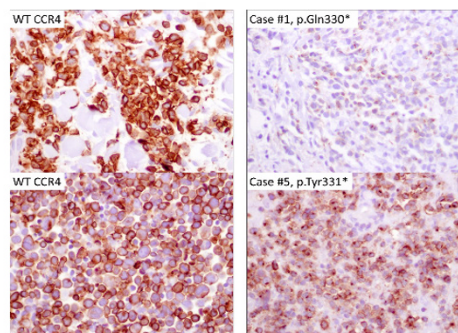


Figure 1. Representative CCR4-CTD IHC in ATLL cases with wild-type (WT) CCR4 (left panel) or nonsense CCR4 mutations (right panel).

Conclusions: Our data showed that in ATLL with CCR4-CTD mutations, although the mutant CCR4 is known to be overexpressed on the cell surface, the remnant wild-type CCR4 protein is often down-regulated and internalized, suggesting a feedback regulation. The distinct expression pattern may allow CCR4-CTD IHC to be a useful tool to identify ATLL cases with CCR4 mutations for further confirmation by sequencing methods.

1587 Ex vivo Trabecular Bone Fraction Measurements in Bone Marrow Core Biopsy Samples using High Resolution Bed Side X-ray Imaging Tool

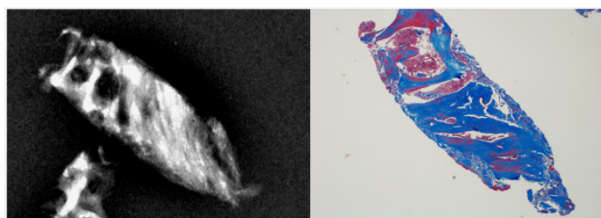
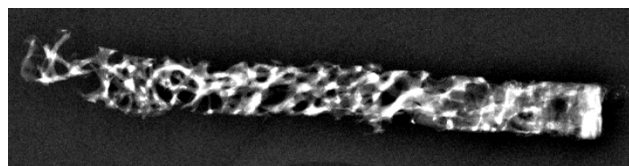
Milad Webb¹, Srikanth Ragothaman², Rajan Dewar². ¹Ann Arbor, MI, ²University of Michigan, Ann Arbor, MI

Background: Bone marrow core biopsies have a significant proportion of trabecular bone. Routine histopathological examination enables identification of trabecular bone pathology, such as thickened bony trabeculae in osteopetrosis, primary myelofibrosis or thin trabeculae in osteopenia or renal osteodystrophy. Trabecular bone and the region immediately adjoining it (paratrabecular space or osteoblastic niche) is also affected in various pathologies including preferentially involved by lymphoma, such as follicular lymphoma, and stem cell development processes (instance PGE2 stimulated marrow; Frisch et al., Blood 2009). We have developed an automated image analytic method for accurately quantifying trabecular bone fraction (TBF) from freshly biopsied bone marrow cores, by x-ray analysis. We propose that this bedside method could gain clinical utility in patients with BM pathology.

Design: 10 consecutively collected bone marrow specimen were utilized in this study. Soon after the core biopsy was obtained, the specimen was placed in a cabinet model x-ray analysis instrument, that is routinely used for breast specimen radiography (Faxitron). Bone marrow images were obtained at a high resolution. An image analytic algorithm was developed that could segment the bony trabeculae

based on density and calculate the trabecular bone fraction (TBF) from the input dimensions of the marrow (constant width). In addition, we also identified collagen fibrosis in the marrow bx and matched this with the grey density, with an attempt to automatically identify fibrotic areas in bone marrow biopsies.

Results: Results of TBF is given as a percentage fraction of bone volume to the total biopsied area. The estimates in the 10 specimens range from 44-56% (mean 50.1%). Histological correlates were performed by routine microscopy and lower than the TBF estimation. This discrepancy is thought to be due to the three dimensional images obtained by X-ray techniques, compared to 2D images of routine microscopy.



Conclusions: The clinical utility of measuring bone marrow trabecular fraction in routine hematopathology is not yet explored. We feel that the x-ray based image analysis enables immediate results, 3D reconstruction of bone marrow biopsy and accurate estimation of trabecular bone fraction and fibrosis than conventional H&E/trichrome and Reticulin stains. Further refinement of these techniques and correlation with a larger clinical cohort of myelofibrotic patients and other patients with bone marrow pathology, is warranted.

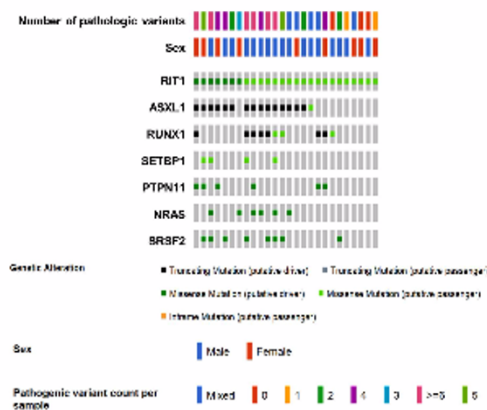
1588 *RIT1* Variants Are Uncommon In Myeloid Neoplasms But Associated With High Risk Features

Olga Weinberg¹, Sanjay S Patel¹, Bradford J Siegel², Annette Kim¹.
¹Brigham and Women's Hospital, Boston, MA, ²Massachusetts General Hospital

Background: Activating somatic mutations in RAS genes in myeloid neoplasms occur both as recurrent progression mutations and may be found characteristically in certain characteristic entities such as chronic myelomonocytic leukemia. *RIT1* is a less common member of this family of GTPases and is highly homologous to both *NRAS* and *KRAS* at the genetic level. Although little is known about pathogenic variants in *RIT1*, we hypothesized that pathogenic *RIT1* variants might similarly be found as a subclonal progression events and might be associated with specific morphologic features.

Design: We queried the Dana Farber Cancer Institute's instance of cBioPortal and identified 33 cases from 26 patients with variants in *RIT1* identified by targeted next-generation sequencing of blood or bone marrow. Presumed pathogenicity in *RIT1* was determined through germline pathogenicity in Noonan's syndrome as well as through homology to *NRAS*. Individual types of dysplastic features of 12 *RIT1*-mutated cases were scored as the percentage of each lineage affected by three blinded reviewers. In addition, 20 cases from a comparable set of diseases without a *RIT1* variant were also scored.

Results: *RIT1* variants were identified in 0.49% of 6798 samples, with pathogenic variants co-occurring significantly with *ASXL1*, *PTPN11*, *SETBP1*, *RUNX1*, *NRAS*, and *SRSF2*. The male:female ratio was 1.9 with an average age of 64.7 (range 28-86). The *RIT1* cases evaluated for dysplasia included 6 cases of de novo AML (2 with background dysplasia, 1 with a history of XLP) and 6 cases of chronic myeloid neoplasms with progression (increased blasts, dysplasia, monocytosis, or fibrosis). The cases were associated with a mean of greater than 4 total variants, significantly more than the overall cohort ($p = 5.83E-08$) and similar to cases with other RAS pathway mutations. When comparing *RIT1*-mutated cases with a *RIT1* variant allele fraction of >15% with control cases lacking any RAS pathway mutation, there was a statistically significant increase in the number of small megakaryocytes with widely spaced nuclear lobes ($p = 0.019$).



Conclusions: Although rare in myeloid malignancies, *RIT1* mutations are associated with small megakaryocytes with widely spaced nuclei and aggressive features such as increased blasts, a high number of pathogenic variants and significant co-occurrence with the poor prognosis gene *ASXL1* and progression variants such as *SETBP1* and *RUNX1*.

1589 Myeloid Sarcomas and Concurrent Bone Marrow Biopsies Frequently Demonstrate Molecular Discordance by Massively Parallel Sequencing

Brian Werstein¹, Jennifer Dunlap², Michael Cascio³, Robert Ohgami⁴, Guang Fan⁵, Richard Press³, Philipp Raess³.
¹Oregon Health & Science University, Portland, Oregon, ²Portland, OR, ³Oregon Health & Science University, Portland, OR, ⁴Stanford University, Stanford, CA, ⁵Lake Oswego, OR

Background: Myeloid sarcoma (MS) is a rare architecture-effacing proliferation of myeloid blasts at an extramedullary site. Although the mutational spectrum of acute myeloid leukemia is well-characterized, relatively few studies have compared the mutational profile of MS and concurrent bone marrow biopsy (BMBx) specimens by massively parallel sequencing.

Design: Fourteen cases of MS with concurrent bone marrow biopsies were retrospectively identified. All BMBx and thirteen of the MS specimens were evaluated by targeted massively parallel sequencing to identify mutations frequent in myeloid neoplasms. Sanger sequencing was used to evaluate one case of MS.

Results: Thirteen of 14 MS demonstrated pathogenic mutations. *NPM1* and *FLT3* were the most commonly mutated genes (6/14 each) followed by *NRAS* (5/14). *NPM1* mutations were present in 5 of 7 cutaneous MS cases, while present in only one of 7 cases of non-cutaneous MS. Twelve of 15 BMBx demonstrated pathogenic mutations. *NPM1*, *FLT3*, and *NRAS* were the most commonly mutated genes in BMBx, with each gene mutated in four BMBx. Patients with a morphologically uninvolved BMBx showed a trend toward increased overall survival versus those with a morphologically involved marrow ($p = 0.09$; median survival not met in uninvolved BMBx group versus 27.8 weeks in involved BMBx group, median follow-up 38.6 weeks).

Interestingly, 57% of cases (8/14) demonstrated discordant molecular findings in the MS or the BMBx. Five cases demonstrated different mutational profiles between the MS and BMBx. Of these cases, the discordance was present in up to four genes per case. Two of 5 cases showed discordance in *NPM1* mutational status; no other discordant mutation was present more than once. Three cases demonstrated morphologically unremarkable BMBx with pathogenic mutations that were also seen in the concurrent MS. These mutations were present in the *FLT3*, *NRAS*, *RUNX1*, *CREBBP*, and *GATA2* genes with a mutant allele fraction ranging from 0.6% to 49%.

Conclusions: Myeloid sarcomas frequently demonstrate pathogenic mutations. Approximately half of MS and concurrent BMBx show discordant molecular findings. Discordance occurs both in the spectrum of mutations identified (5/14 cases) and as pathogenic mutations that co-occur in both the MS and the morphologically unremarkable BMBx (3/14). Further investigation into molecular discordance between MS and BMBx may help understand clonal evolution of myeloid neoplasms and mechanisms controlling extramedullary blast localization.

1590 Immunophenotypic Variation Is Common in IGH-CCND1-Positive Mantle Cell Lymphoma and is not Associated with Variant Cytogenetic or Morphologic Findings: Retrospective Review of 107 Consecutive Cases

Todd Williams¹, Philipp Raess¹, Katy Lawson², Susan B Olson¹, Stephen

Background: Mantle cell lymphoma (MCL) is a mature B-cell lymphoma that classically shows a CD5+, bright CD20+, bright surface light chain+, and CD23- immunophenotype (IP), harbors the IGH-CCND1 gene fusion and expresses cyclin D1 and SOX11 proteins. Variation in antigen expression has been reported in up to 40% of MCL, making separation from diagnostic mimics challenging and necessitating immunohistochemical or cytogenetic studies to achieve accurate diagnosis for therapeutic and prognostic purposes. In this study, we retrospectively evaluated 107 cases of cytogenetically-confirmed MCL to assess the frequency of IP variation and to assess the relationship of IP variation with other clinicopathologic features.

Design: 107 consecutive cases of IGH-CCND1+ MCL with available flow cytometry data were identified. For each case, the IP and all available morphologic, cytogenetic, and clinical findings were recorded. IP variation was defined as >1 antigen expression pattern deviating from the classic IP. Cytogenetic findings were deemed classic (isolated IGH-CCND1) and variant (harboring additional abnormalities). Morphologically, MCL was separated into classic/small or pleomorphic/blastoid categories. Chi-square analysis was performed to evaluate the relationship of IP variation with other clinicopathologic features.

Results: 49.5% of cases (53/107) showed a variant IP, consistent with previous studies. Variations included abnormal expression of CD5 (12%, 13/107), CD10 (4%, 4/104), CD19 (1%, 1/107), CD22 (10%, 10/100), CD23 (30%, 32/106), and surface light chain (5%, 5/107). Variation in CD20 was noted in 8 cases (complete absence, n=3; dim n=5). Rituximab therapy as a confounder could not be assessed as complete treatment history was unavailable. Pleomorphic/blastoid morphology was noted in 12% (10/83) of cases with adequate material for analysis. 37% of MCL showed variant cytogenetic findings (40/107). Variant IP is independent of morphology, cytogenetic status, and extranodal sites of disease (p=0.437).

Conclusions: This is the largest study assessing immunophenotypic variation in IGH-CCND1-confirmed mantle cell lymphoma. Our results indicate that IP variation is common in MCL and appears to be unrelated to morphology or cytogenetic features. As accurate diagnosis is critical for therapy and prognosis, the generous use of ancillary studies is warranted when considering other B-cell leukemias/lymphomas with overlapping morphologic or IP characteristics.

1591 Post-transplant Engraftment Chimerism Analysis by Next Generation Sequencing of Informative Germline Polymorphisms

Xuemei Wu¹, Richard Press². ¹Hillsboro, OR, ²Oregon Health & Science University, Portland, OR

Background: Next-generation sequencing (NGS) is increasingly being used to monitor disease burden in patients with hematopoietic malignancies being treated with allogeneic hematopoietic stem cell transplant (HSCT). In addition to detecting tumor-associated mutations to directly monitor leukemic burden, NGS also detects germline single nucleotide polymorphisms (SNPs) that are specific to either the host and/or donor. We hypothesize that NGS-based-identification of informative host- and/or donor-specific SNPs will enable the quantitative evaluation of the chimerism status of post-HSCT patients, providing critical information on engraftment status and possible early relapse.

Design: Among 94 transplant patients from our institution who underwent simultaneous 42-gene "myeloid targeted" NGS and short tandem repeat (STR)-based post-transplant chimerism tests between early 2013 and early 2017, 33 samples from 23 patients (20-78 yrs old) were confirmed as being "chimeric" (5-95% host cells) by our standard quantitative STR multiplex PCR assay. The criteria for defining NGS-based host-specific SNPs were: reported germline with reference SNP (rs) numbers; located in intronic regions of somatic chromosomes; minimal 20-read variant coverage; minimal 100 total sequence coverage; heterozygosity (35-65%) in the pre-transplant (host-only) sample; and absence in fully engrafted post-HSCT (donor-only) samples. The average allele percentage of these selected host SNPs were calculated in each sample, and compared with the host percentage derived from quantitative STR-based PCR.

Results: 52 host-specific SNPs in 18 post-HSCT samples (from 15 patients) met the above criteria. Using these selected host-specific alleles, we found no statistically significant quantitative difference in the percent host cell chimerism detected by NGS (mean 24.9%) vs STR multiplex PCR (mean 24.7%; P=0.97). The two detection methods were linear and highly correlated (R=0.97, slope =1.02, P<0.001).

Conclusions: We confirm the feasibility of using informative germline SNPs detected by NGS in lieu of routine STR-based multiplex PCR to evaluate post-transplant chimerism status. Our longer-term goal is to generate an automated computational algorithm for choosing and quantitating informative SNP's for routine post-transplant NGS-based clinical monitoring.

1592 Ordering Patterns of NGS Testing and Impact of Results on Clinical Management in Patients with Hematological Disorders

Yan Xie¹, Bhumika Patel², James Cook³, Hetty Carrway², Eric Hs². ¹Galveston, TX, ²Cleveland Clinic, ³Cleveland Clinic, Cleveland, OH

Background: Next generation sequencing (NGS)-based mutation testing may provide information on diagnosis, prognostic risk stratification, and therapy, the ordering patterns and implications for clinical care are not well-established. The objective of this study is to evaluate the NGS ordering patterns and impact on patients (pts) with hematological disorders (HD) at a large academic medical center.

Design: All clinical NGS test results associated with bone marrow biopsy from Jan 1, 2016 to July 12, 2017 were included for pts with suspected or known HD. The NGS panel employed was a PCR based, amplicon enrichment assay targeting mutational hot spots of 37 genes recurrently mutated in myeloid neoplasms. Clinicopathologic information was obtained in collaboration with hematologists.

Results: Of the 250 pts annotated to date, the mean age is 60 yrs (range 5-90), with 54% males. The average turnaround time was 14 days. Distribution of working diagnoses prior to NGS were: idiopathic cytopenia of undetermined significance (ICUS) 23%, myelodysplastic syndrome (MDS) 16%, myeloproliferative neoplasms (MPN) 26%, acute leukemia (AL) 29%, bone marrow failure syndromes (BMF) 4%, and other 2%. At least one mutation was detected in 74% of samples. Distribution of diagnoses after NGS were: ICUS(N=10)/Clonal cytopenias of undetermined significance (CCUS;N=4) 6%, MDS 20%, MPN 22%, AL 44%, BMF 6%, and other 3%. NGS results changed pts diagnosis 5% of the time, impacted therapy in 21% (53 pts), and in 74% of pts there was no impact on their diagnosis or treatment based on NGS testing. Of the 53 pts, 31 (58%) went on a clinical trial (10 pts on targeted and 21 non-targeted), and 22 (42%) received targeted therapy outside of a trial. NGS impacted future therapy in 76 pts (30%), the bulk of which were offered and received BMT. Most common mutations were *TET2* (18%), *DNMT3A*(15%), *ASXL1* (13%), *TP53*(11%), *SRSF2*(10%), *FLT3*(10%), and *RUNX1*(9%). NGS results provided prognostic information considered additive to standard cytogenetic and clinical factors in 68% of pts based on current literature. Of note, the most frequent genes impacting the recommendation for BMT were *TP53* (22%), *FLT3* (22%), *ASXL1* (21%), and *RUNX1* (13%). NGS was reassuring for 26% of pts (i.e. no mutation detected).

Conclusions: These results show that NGS results assist in arriving at an accurate diagnosis, help determine therapy, and refine prognosis. These data document the utility of NGS testing in routine clinical practice.

1593 Myeloid Neoplasms with t(11;16)(q23;p13): A Study of 11 Cases

Wei Xie¹, Jing Wang², Zi Chen¹, Guilin Tang¹, Sa Wang¹, Sanam Loghavi³, L. Jeffrey Medeiros³, Shimin Hu¹. ¹The University of Texas MD Anderson Cancer Center, Houston, TX, ²Baylor College of Medicine, ³Houston, TX

Background: Fusion partners of the 11q23/*KMT2A* (*MLL*) gene rearrangement affect disease phenotype and classification. In the current WHO classification, t(11;16)(q23;p13)/*KMT2A-CREBBP* is considered presumptive evidence of myelodysplastic syndrome (MDS) in the absence of morphologic dysplasia in the setting of cytopenia, and is also considered a MDS-related cytogenetic abnormality in the classification of acute myeloid leukemia (AML) with myelodysplasia-related changes. We investigated the clinicopathologic features and patient outcome of myeloid neoplasms with t(11;16)(q23;p13).

Design: Patients with myeloid/lymphoid neoplasms and t(11;16)(q23;p13) diagnosed over 20 years were reviewed retrospectively. Clinicopathological, genetic and follow-up data were analyzed.

Results: The study group included 11 patients with myeloid neoplasms and t(11;16)(q23;p13): 6 patients had MDS, one had chronic myelomonocytic leukemia (CMML) and 4 had AML. No lymphoid neoplasms with t(11;16) were identified. There were 5 men and 6 women with a median age of 62 years at initial diagnosis. Ten patients had t(11;16) at initial diagnosis and 1 patient acquired t(11;16) 67.9 months after initial diagnosis. Nine patients had a history of chemotherapy and/or radiation for hematologic or non-hematologic malignancies a median of 16.5 months prior to the diagnosis of myeloid neoplasms with t(11;16). Six of them were treated with topoisomerase II inhibitors. In 5 patients, t(11;16) was observed as a sole chromosomal abnormality. Fluorescence *in situ* hybridization analysis was performed in 5 patients and all were positive for *KMT2A* rearrangement. A variable degree of dysplasia was observed in 10 of 11 patients at initial diagnosis. Of 7 patients with an initial diagnosis of MDS/CMML, 4 developed AML after a follow-up time of 7.2 months. Of the 8 patients who had AML initially or later, all had blasts with monocytic differentiation. After the diagnosis of myeloid neoplasm with t(11;16), 8 patients were treated with chemotherapy and the treatment was unknown in the other 3 patients. Eight patients died at last follow-up with a median survival of 12.6 months.

Conclusions: t(11;16)(q23;p13) is rare and is commonly associated with previous chemotherapy, particularly topoisomerase inhibitors. t(11;16) is associated exclusively with myeloid neoplasms that frequently are associated with dysplasia and/or monocytic blast morphology. The overall prognosis of these patients is extremely poor.

1594 Mutational Analysis of Splicing Factor Genes SF3B1, U2AF1, ZRSR2, SRSF2, and U2AF2 in Chinese Patients With Acute Myeloid Leukemia

Fei Xing¹, Qi Sun², Ya n Lin², Li Qin², Yu j Jia², Kun Ru², Dong I Zhang².
¹Tianjin Sino-us Diagnostics Inc, Jinghai, Tianjin, ²Chinese Academy of Medical Sciences & Peking Union Medical College (CAMS & PUMC)

Background: Over the past few years, a growing number of studies have demonstrated the important role of splicing factor genes mutations in patients with myeloid malignancies.

Design: Here we aimed to detect the mutation frequency of splicing factor genes and explored the potential association of these genes with risk stratification, blood parameters, karyotypes and other clinical features in patients with acute myeloid leukemia (AML). In the current study, next-generation sequencing was performed to screen the mutation spectrum of U2AF1, ZRSR2, SRSF2, SF3B1 and U2AF2 in 183 Chinese patients with AML.

Results: Our results showed that 22.4% of AML patients harbored at least 1 target gene mutation, and the mutational frequencies of SF3B1, U2AF1, U2AF2, ZRSR2 and SRSF2 were 10.9%, 8.7%, 3.3%, 2.7% and 1.1%, respectively. Subsequently, we found that the frequency of splicing factor gene mutations in AML-RGA and AML-NOS was 28.2% and 25.0% respectively, and SF3B1, U2AF2, SRSF2 gene mutations were the most frequent in AML-RGA and U2AF1 gene mutations in AML-NOS. Meanwhile, we identified that U2AF1 gene mutation was more frequently observed in favorable and intermediate risk group, and ZRSR2 gene mutation in intermediate and adverse risk group, but SRSF2 only in adverse risk group. Furthermore, the amount of red blood cell (RBC) and hemoglobin (HGB) were significantly lower in patients with SF3B1 mutations than patients without such mutations, and U2AF1-mutated patients showed more higher blood platelet count (BPC) than those without U2AF1 mutations. However, the clinical differences between mutated U2AF2, ZRSR2 and SRSF2 with unmutated genes were not statistically significant.

Conclusions: Taken together, this study highlights that splicing factor gene especial U2AF1 and SF3B1 are more common mutated splicing factor genes in Chinese patients with AML, and may play an important role in oncogenesis and progression of AML.

1595 Characterization of SOX11-Negative Mantle Cell Lymphoma: Clinicopathologic and Prognostic Features of 53 Patients

Jie Xu¹, Annapurna Saksena², Lifu Wang¹, C. Cameron Yin¹, Sa Wang¹, Zhihong Hu³, Pei Lin¹, Guilin Tang¹, L. Jeffrey Medeiros¹, Shaoying Li¹.
¹The University of Texas MD Anderson Cancer Center, Houston, TX, ²UTHSCSA, San Antonio, TX, ³The University of Texas Health Science Center at Houston, Houston, TX

Background: SOX11, a neuronal transcription factor, has been identified as a useful diagnostic marker of mantle cell lymphoma (MCL). Although some recent studies suggested that SOX11 expression might be a predictor of outcome in MCL patients, results have been conflicting and the prognostic utility of SOX11 is controversial. Furthermore, no studies have investigated the prognostic factors in SOX11-negative MCL patients.

Design: We studied 166 patients with MCL in whom SOX11 expression was detected by immunohistochemical method at time of diagnosis. The clinicopathologic features and outcome of patients with SOX11-negative MCL were compared to patients with SOX11+ MCL. Fisher's exact test was used to compare the SOX11-negative and SOX11+ groups. Overall survival (OS) was analyzed using the Kaplan-Meier method and compared using the log-rank test.

Results: In this cohort, 53 of 166 (32%) cases were negative for nuclear expression of SOX11. Compared to patients with SOX11+ MCL, SOX11-negative MCL patients were less often older than 60 years (32% vs 74%, p = 0.0001), more frequently had leukemic non-nodal disease (17% vs 6%, p = 0.04), and had a higher mean WBC count (20.7 vs 10.1 K/ul; p = 0.039). Pathologically, SOX11-negative MCL more often had classic morphology (76% vs 61%, p = 0.04), and a lower mean Ki67 index (30% vs 53%, p < 0.0001). Other clinicopathologic features of patients with SOX11-negative MCL were very similar to their SOX11+ counterparts. Overall survival (OS) was not significantly different between patients with SOX11-negative versus SOX11+ MCL (p = 0.81). High Ki67 index ($\geq 30\%$ or $\geq 60\%$), high MCL International Prognostic Index (MIPI), and blastoid/pleomorphic morphology were associated with shorter OS in both the SOX11-negative (p < 0.05) and SOX11+ MCL groups (p < 0.05). In addition, nodal involvement and advanced stage (stage III-IV) were associated with worse outcome in SOX11+ MCL (p = 0.02 and p = 0.04, respectively), but not in SOX11-

negative MCL (p = 0.92 and p = 0.76, respectively).

Conclusions: SOX11-negative MCL is characterized by younger patient age, leukemic non-nodal disease, leukocytosis, classic morphology, and lower Ki67 index. SOX11 was not associated with OS in this MCL cohort. High Ki67 index, high MIPI score, and blastoid/pleomorphic morphology are associated with worse OS in both SOX11-negative and SOX11+ MCL groups. Nodal involvement and advanced stage were not associated with shorter OS in patients with SOX11-negative MCL.

1596 Double Staining for PD-1 and PAX5 is a Useful Adjunct in the Pathological Diagnosis of Angioimmunoblastic T-cell Lymphoma

Shuo Amanda Xu¹, Kevin Yi Mi Ren, Jillann Jaynes², David LeBrun³.
¹Queen's University, Kingston, ON, ²Queen's University, ³Queen's University, Kingston, ON, Canada

Background: The pathological diagnosis of angioimmunoblastic T-cell lymphoma (AITL) is challenging. Although AITL cells have immunophenotypic features of follicular T-helper (TFH) cells, their immunophenotype is difficult to ascertain in part due to their intimate physical juxtaposition with B-cells. We developed a double stain (DS) for PD-1, a cell surface marker of TFH cells, and PAX5, a sensitive and specific nuclear marker of B-cells. We hypothesized that the DS will aid in the pathological distinction between AITL and its mimics, including peripheral T-cell lymphoma not otherwise specified (PTCL), anaplastic large cell lymphoma (ALCL), classical Hodgkin lymphoma (cHL), nodular lymphocyte predominant Hodgkin lymphoma (NLPHL), Castleman disease (CD) and follicular lymphoid hyperplasia (FH).

Design: The DS was carried out on a Bond III automated immunostainer using the Cell Marque PD-1 NAT105 (surface/cytoplasmic red signal) and the Leica PAX5 1EW (nuclear brown signal) mouse monoclonal antibodies. Representative slides from cases of AITL (n=16), PTCL (9), ALCL (8), NLPHL (11), cHL (12), CD (4), and FH (6) were stained and evaluated.

Results: The DS permitted confident assessment of the relative distributions of B-cells and PD-1-expressing T-cells. No PD-1 expression was evident among B-cells. The DS demonstrated distinctive staining patterns in AITL compared to cHL, NLPHL, ALCL, FH and CD. In AITL, the neoplastic paracortical T-cells generally expressed abundant PD-1 whereas any residual lymphoid follicles were depleted of PD-1-positive TFH cells relative to FH-associated follicles. In contrast, the vast majority of (non-neoplastic) paracortical T-cells in cHL, NLPHL, FH and CD, and neoplastic T-cells in ALCL, were PD-1-negative. The (PAX5-positive) neoplastic cells in cHL and NLPHL were consistently PD-1-negative. NLPHL was distinctive in showing concentration of PD-1-expressing cells within the B-cell-rich nodules, depletion of PD-1-expressing cells in the inter-nodular areas and rosetting of PD-1-positive cells around PAX5-positive LP cells. In FH, the PD-1-positive cells were largely restricted to follicle centers. In CD, PD-1-positive cells were notably rare in both the paracortex and regressed follicle centers. The number and distribution of PD-1-expressing cells in AITL and PTCL was similar.

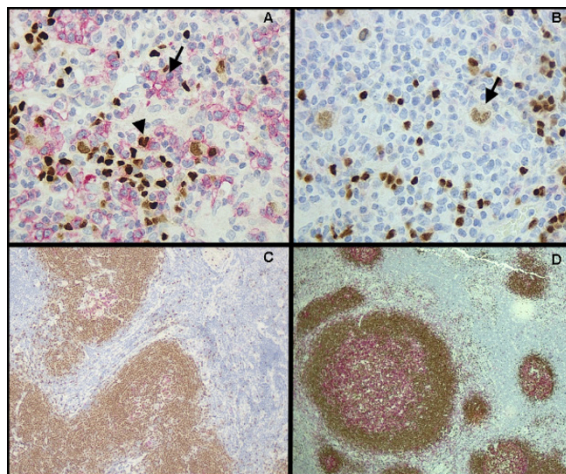


Figure 1. PAX5/PD-1 DS demonstrated distinctive staining patterns in AITL and its mimics. A, The neoplastic paracortical cells in AITL intensely expressed PD-1 (arrow) and were intimately admixed with PAX5-positive B cells (arrowheads). B, Depletion of PD-1-expressing cells was noted in cHL while PAX5 highlighted the Hodgkin/Reed-Sternberg cells (arrow). C, In cHL, there was significant depletion of PD-1-positive cells in the follicle center and paracortex; D, FH showed restriction of PD-1-positive cells to the follicle centers (PAX5 nuclear, PD-1 cytoplasmic. Fast Red stain, hematoxylin counterstain, original magnifications x400 [A and B], x100 [C], and x40 [D]).

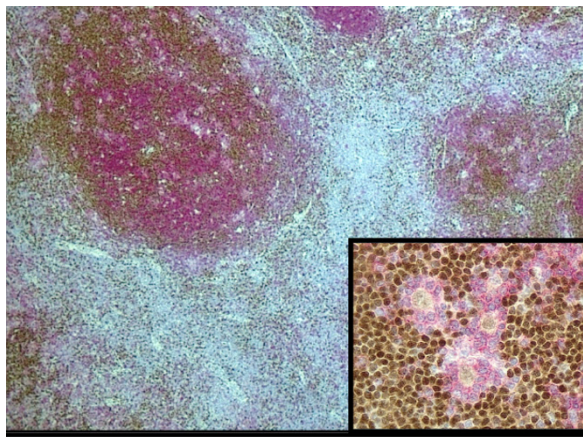


Figure 2. NLPHL showed significant intensification of PD-1 expression in the nodular areas with PD-1 depletion in the inter-nodular areas. The LP cells (PAX5-positive) are resorted by PD-1-positive T cells (inset). (PAX5 nuclear brown signal, PD-1 cytoplasmic red signal, hematoxylin counterstain, original magnifications x40 and x400[inset]).

Conclusions: Although of little use in distinguishing AITL from PTCL, the PD-1/PAX5 DS is a useful adjunct in distinguishing AITL or PTCL from other common mimics, including cHL, NLPHL, ALCL, FH and CD.

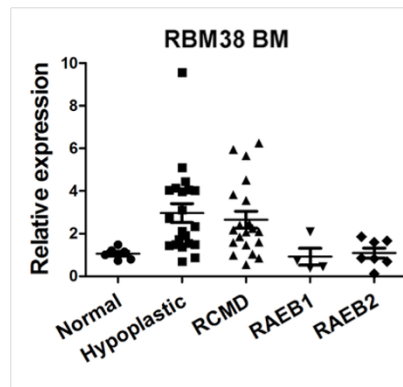
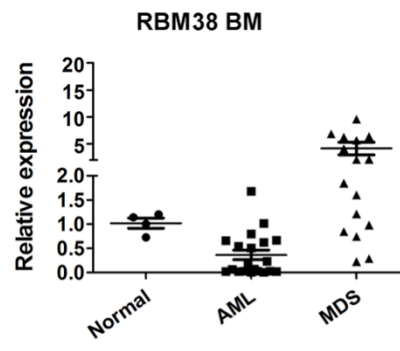
1597 Dysregulation of RNA Binding Protein RBM38/RNPC1 in the Pathogenesis of High Grade Hematolymphoid Malignancy

Xiang Xu¹, Xianbin Chen², Kun Ru³, Mingyi Chen⁴, Jin Zhang⁵. ¹UT Southwestern Medical Center, Southlake, Texas, ²UC Davis, ³Chinese Academy of Medical Sciences, ⁴UT Southwestern Medical Center, ⁵UC Davis, Davis, CA

Background: The p53 tumor suppressor is the most commonly mutated gene in human cancers and aberrations in the p53 pathway are associated with hematologic malignancies. Loss of p53 promotes leukemia and lymphoma development, while increased p53 activity inhibits hematopoietic stem cells (HSCs) function and results in HSC quiescence and myelodysplasia. The RNA binding protein RBM38, is a target of the p53 family and modulates p53 expression via mRNA translation. Altered expression level of RBM38 is found to be associated with survival rate in patients with cancer. Overexpression of RBM38 in canine lymphoma is correlated with decreased expression of p53. However, the mechanism by which RBM38 is involved in the pathogenesis of hematopoietic malignancies is not clear.

Design: In order to investigate the essential role of RBM38 in the function of HSCs quiescence, self-renewal, differentiation and lineage development, we have generated and characterized RBM38-deficient mice. We performed gross necropsies on WT and *Rbm38*^{-/-} mice to measure the size and weight of various organs. Histological analysis was used to find hematopoietic changes. We used in vitro cell culture system to determine the potential role RBM38 in HSCs biology. Meanwhile, the expression of RBM38 in bone marrow and peripheral blood cells of cases with myelodysplastic syndromes (MDS), acute myeloid leukemia (AML), and normal control groups were measured by real-time polymerase chain reaction and were analyzed for clinical significance.

Results: We found that these RBM-null mice, like p53 mutant mice, display accelerated aging phenotypes and are prone to hematopoietic defects and tumors. The hematological disorders of mice lacking RBM38 include anemia, megakaryocytic and myeloid hyperplasia as well as splenomegaly with extramedullary hematopoiesis. Through analyze the RBM gene expression in human myelodysplasia and lymphoma/leukemia, we found that RBM38 gene was repressed in acute myeloid leukemia (AML) while highly expressed in MDS patients, and was increased as MDS progressed. Moreover, the expression of RBM38 mRNA was positively correlated with the proportion of the bone marrow blasts, which suggested a higher malignant clone burden of MDS.



Conclusions: Our results suggest the importance of p53-RBM38 loop in regulating balance of HSC self-renewal, differentiation and hematopoiesis, and dysregulation of RBM38 may cause human hematolymphoid diseases. Therefore detection of RBM38 is a potential biomarker for risk stratification of MDS.

1598 Accelerated Phase and Richter Transformation of Chronic lymphocytic leukemia/Small lymphocytic lymphoma: Pathological and Molecular Genetic Features of 21 Cases (A Single Institution Experience)

Wei Xue¹, Jacqueline Barrientos², John F Katsetos², Kanti Ra², Sujata Sajjan², Silvat Sheikh-Fayyaz², Xinmin Zhang², Judith Brody³, Peihong Hsu⁴, Kalpana Reddy⁵. ¹Donald and Barbara Zucker School of Medicine at Hofstra/Northwell, New Hyde Park, NY, ²Donald and Barbara Zucker School of Medicine at Hofstra/Northwell, ³Northwell Health, New Hyde Park, NY, ⁴North Shore-LIJ Health System, New Hyde Park, NY, ⁵Northwell Health, Mineola, NY

Background: Chronic lymphocytic leukemia/small lymphocytic lymphoma (CLL/SLL) is a low grade B-cell hematologic malignancy with high global prevalence. Richter transformation (RT) including diffuse large B-cell lymphoma (DLBCL 2-8%) and classical Hodgkin lymphoma (CHL <1%) can occur. However, aggressive clinical behavior has also been noted in 'accelerated phase' (AP) of CLL.

Design: Retrospective assessment of our departmental archives from 2011-present, consisting of biopsies (lymph node and bone marrow) from CLL patients, specifically those flagged clinically to rule out transformation. Criteria for acceleration assessment included expanded and/or confluent proliferation centers and Ki-67 >30%. Positivity for cyclin D1, c-myc, p53, MUM1, and EBER were noted. Cytogenetic, FISH, *IGVH* mutational and molecular studies were available for most cases.

Results: 21 patients were identified with ages ranging from 42-94 years, 15 males and 6 females, 11 with RT (8 to DLBCL and 3 to CHL). Also 10 AP cases were observed including 1 with HRS like cells. All patients had received prior therapy for CLL, except for 2 RT cases. The proliferation index Ki-67 ranged from 30-90%. MUM1 was noted in all 7 RT and 2 of 3 AP cases tested while EBER was positive in 2 of 6 RT cases tested. Variable staining patterns were noted for c-myc and p53. Cytogenetic/FISH studies done in 19 cases (10 RT, 9 AP) displayed complex karyotypic abnormalities in 6 RT and 7 AP cases. FISH data showed del 13 (6 RT, 5 AP), del TP53 (4 RT, 4 AP), del ATM (3 RT, 3 AP) and *MYC* rearrangement (2 RT, 1 AP) were noted. *IGVH* mutational analysis in 13 cases done showed unmutated *IGVH* in 4 RT and 5 AP. Molecular analysis data was available in 6 cases showing *NOTCH1* (3 RT, 1 AP), *TP53* (2 RT), *SF3B1* (1 RT, 1 AP), and *ATM* (VUS in 1 AP) mutations.

FOR TABLE DATA, SEE PAGE 574, FIG. 1598

Conclusions: In our study all cases suspected clinically of transformation showed either confirmed RT or AP, indicating that a high index of suspicion is an important first step to identifying these cases. Complex cytogenetic abnormalities and unmutated *IGVH* were noted in over 60% of cases occurring about equally in both RT and AP. *NOTCH1* and *TP53* high risk mutations were more common in RT as was *MYC* rearrangement, while *SF3B1* appeared to occur equally in both RT and AP in this relatively small sample size tested.

1599 Dissection of ERG Aberrant Expression and its Related Pathway in a Subset of Diffuse Large B-Cell Lymphoma through Genome-Wide miRNA Profiling and Whole Exome Sequencing

Shanxiang Zhang, Indianapolis, IN

Background: ETS-related gene (*ERG*), a member of the E-26 transformation-specific (ETS) family of transcription factors has been shown to be involved in vasculogenesis, angiogenesis, hematopoiesis and bone development. Aberrant *ERG* expression is oncogenic in prostate carcinoma, Ewing's sarcoma and is associated with poor prognosis in patients with acute myeloid leukemia and T lymphoblastic leukemia. However, little is known about its expression and underlying mechanism in lymphomas.

Design: *ERG* expression in diffuse large B-cell lymphoma (DLBCL) was studied by immunohistochemical stain of tissue microarrays of *de novo* DLBCL diagnosed in our institute during 2000-2014. Genome-wide miRNA library array expression profiling was performed in 20 *ERG*-positive (*ERG*+) and 20 *ERG*-negative (*ERG*-) DLBCLs. Selected miRNAs showing differential expression in *ERG*+ vs *ERG*- DLBCLs were further studied by real-time reverse transcriptase PCR (RT-PCR) assays. Whole exome sequencing was performed in five *ERG*+ and 13 *ERG*- DLBCLs. StrandNGS software and Wikipathways database were used for mutation analysis and pathway prediction.

Results: Approximately 30% of DLBCL cases were *ERG*+ (37/118). Forty-three out of the entire 1881 miRNAs annotated in Sanger miRBase Release 21 showed significantly different expression levels in *ERG*+ vs *ERG*- DLBCLs. miR-4638-5p was the only one with hybridization signal > 500 and was decreased by more than two folds in *ERG*+ vs *ERG*- DLBCLs. Downregulation of miR-4638-5p was confirmed by real-time RT-PCR study of the same DLBCL group. Whole exome sequencing revealed mutations in *ERG* in approximately 20% of DLBCLs with no difference ($p=0.888$) between *ERG*+ and *ERG*- DLBCLs. However, multiple genes including *POLA1*, *E2F1*, *PSMD8*, *AXIN1*, *GAB2* and *GNB2L1* showed significantly higher mutation rate in *ERG*+ DLBCLs.

Conclusions: *ERG* aberrant expression in a subset of DLBCL is associated with down-regulation of miR-4638-5p, which represses *Kidins220* expression and *PI3K/AKT* in castration-resistant prostate cancer, indicating a potential similar mechanism in *ERG*+ DLBCLs. In addition, *ERG* expression is significantly associated with mutations in genes important in cell cycle control, B-cell receptor-mediated signaling and degradation of beta-catenin. Further clinicopathological correlation and functional studies of *ERG*-related miRNAs and pathways may provide new insight into the pathogenesis of DLBCL and reveal novel targets for better prognosis stratification and treatment for patients with DLBCL.

1600 Immunophenotypic Features of 141 cases of Syncytial Variant Nodular Sclerosis Classical Hodgkin lymphoma

Qingling Zhang¹, Wei Wang¹, L. Jeffrey Medeiros¹. ¹The University of Texas MD Anderson Cancer Center, Houston, TX

Background: The syncytial variant (SV) of nodular sclerosis classical Hodgkin lymphoma (NSHL) is uncommon and has not been well studied. In a few earlier studies, mostly based on small case series, others suggested that SV-NSHL is associated with advanced stage disease and an aggressive clinical course. In this study, our aim was to characterize the immunophenotypic features of a large cohort of SV-NSHL cases.

Design: The inclusion criteria included: 1) sheets of neoplastic cells; 2) foci of necrosis; and 3) an appropriate immunophenotype by immunohistochemistry. The clinicopathologic features of SV were analyzed. Immunohistochemical studies were performed variably using standard methods over the study interval and the following markers were assessed: CD3, CD15, CD20, CD30, CD45/LCA, CD79a, PAX5, OCT2, BOB-1, MUM1/IRF4, BCL-2, and BCL-6. Epstein-Barr virus (EBV) infection status was detected by *in situ* hybridization EBV encoded RNA (EBER). The overall survival was calculated by using the Kaplan-Meier method analysis.

Results: The study cohort was composed of 75 men and 66 women. The median age at the time of diagnosis was 28 years old (range, 12-82 years old). All patients were treated with chemotherapy, most often with the ABVD regimen. The median clinical follow-up time was 35.4 months (range, 0.3 to 203.4 months). At last follow-up, 31 had died and 109 were alive. For patients who died of disease, the median survival time was 29 months. Immunohistochemical analysis

showed that the lymphoma cells were positive for CD30 (100%); PAX5 in 112/116 (97%), MUM1/IRF4 in 102/106 (96%), CD15 in 87/104 (84%), CD20 in 32/137 (25%), and EBER in 17 of 95 (18%). Other markers were assessed in smaller subsets of cases and showed: OCT2 35%, BOB-1 26%, CD79a 24%, BCL-2 82%, and BCL-6 57%. All cases were negative for CD3 and CD45.

Conclusions: In this study, in addition to PAX5, about 25-50% of cases of SV-NSHL expressed one of more additional B-cell markers including CD20, CD79a, OCT-2, BOB-1, and BCL-6. BCL-2 is also commonly expressed in SV-NSHL. Upregulation of the B-cell program in SV-NSHL may explain the more aggressive behavior of these neoplasms.

1601 Acute Epstein-Barr virus infections mimicking T/NK cell lymphoma in lymph node: are there infectious mononucleosis, T/NK cell type

Yanlin Zhang¹, Jianlan Xie², Yuanyuan Zheng², Ping Wei³, Yu-Hua Huang⁴, Xiao-Ge Zhou². ¹Beijing Friendship Hospital Capital Medical University, Beijing, ²Beijing Friendship Hospital Capital Medical University, ³San Diego, CA, ⁴State Key Laboratory of Oncology in South China, Guangzhou, Guangdong, China

Background: Infectious mononucleosis (IM) is a benign self-limited disease with Epstein-Barr virus (EBV) primary infection that results in a polyclonal B cell proliferation and T and natural killer (T/NK) cell cellular immune response. It is not clear whether there is IM with EBV infection in predominantly T and NK cells. The aim of our study is to display IM-like cases of acute EBV infection of T/NK cells, and to analyze their clinicopathological features.

Design: 7 cases of children and young people from China with acute EBV infections of T/NK cells was retrospectively analyzed using HE stain for morphology, immunohistochemistry for phenotype, EBV encoded small RNA (EBER) *in situ* hybridization for EBV status and TCR, coupled with clinical data study and follow-up.

Results: (1) Five patients were male and two were female. The age of the patients ranged from 10 months to 19 years with a median age of 5.9 years. They were healthy as ordinary people before sick. Sudden onset was seen in all the patients with high fever as first symptoms followed by lymphadenopathy and hepatosplenomegaly. The course of the diseases before diagnosis ranged from 22 days to 1.5 months. All patients received conservative treatment but not chemotherapy. Only one child died of serious complications after diagnosis in 3 months. Other patients achieved long-term clinical observation and follow-up did not relapse. (2) All the samples were lymph nodes which architecture were destructed. There were numerous infiltrating lymphocytes with medium and large in size in the lesion, with focal to extensive coagulative necrosis obviously. Mitotic figures were easily found, most of cells showed highly atypia. (3) The majority of lymphocytes in the lesion expressed CD3 and Granzyme B or TIA-1, but not CD5 in all cases. CD56 was expressed in numerous cells in 5 cases. EBER was detected in medium to large-sized cells (50 to over 100 cells per high power field) in all cases. TCR gene rearrangement was performed in 6 cases, in which monoclonal rearrangement was found in 4 cases.

FOR TABLE DATA, SEE PAGE 575, FIG. 1601

Conclusions: Acute EBV infection of T/NK cell could express malignant features mimicking T/NK cell lymphoma pathologically as well as benign features mimicking IM clinically. The findings indicated that there may be infectious mononucleosis, T/NK cell type in China. Special clinical information (such as children and young people, sudden onset, short disease course, systemic symptoms, acute EBV infection, etc.) are the main clues for diagnosis and evaluation of prognosis.

1602 Correlative Study of P53 Immunohistochemical Stain (IHC) and TP53 Mutational Status in Myeloid Neoplasms (MN)

Fang Zhao¹, Dong Chen¹, Min Shi¹, David Viswanatha¹, Rong He¹. ¹Mayo Clinic, Rochester, MN

Background: Somatic mutations in tumor suppressor gene *TP53* is a well-established marker for tumor aggressiveness and poor survival in both solid tumor and hematologic malignancies. P53 IHC which detects p53 nuclear accumulation is used as a surrogate marker for mutational analysis in solid tumors, with strong/diffuse and total lack of staining recognized as indicative of a missense (MS) or null mutations, respectively. The aim of this study was to evaluate the utility of p53 IHC in *TP53* mutation analysis in MN.

Design: We retrospectively identified 103 cases underwent *TP53* exons 4-9 next generation sequencing (7/2015-5/2017), including 30 AML, 37 MDS, 15 MDS/MPN, 9 MPN and 12 undiagnostic of MN. 5 normal BM were included in the study. *TP53* antibody (DO-7, Ventana, Tucson, AZ) was used following manufacturer's instructions. Slides were stained on Ventana Benchmark XT. IHC Staining was

scored by intensity as weak (1/3) or strong (2-3/3). Percent of positive cells of total BM cellularity was recorded.

Results: TP53 mutations were identified in 48 cases, including 45 harboring pathogenic (P) mutations and 3 with variants of unknown significance (VUS). They encompassed 37 MS (34 MS-P, 3 MS-VUS), 8 nonsense/frameshift (NS/FS), 2 MS and NS/FS, and 1 FS and splicing variant (SV). 25/34 (73.5%) and 9/34 (26.5%) MS-P cases showed strong staining in 20-95% and 5-10% of cells, respectively. 1/8 NS/FS exhibited 95% strong stain and the 2 MS+FS showed 10% and 40% strong stain, respectively. 7/8 of NS/FS, 1 FS with SV, and 3 MS-VUS showed none to rare (<5%) strong stain. In the 55 TP53-wild type (WT) cases, 47(85.5%) showed none to rare (<5%) strong stain, and 8 (14.5%) showed 5-10% strong stain with half (4/8) exhibiting a high background of weak staining (1+) in 30-60% of cells. The 5 normal cases showed none to rare (<5%) strong stain. Using a cut-off value of 20% strong stain, the sensitivity and specificity for detecting a MS-P were 73.5% (25/34) and (55/55) 100%, respectively. NS/FS could not be reliably distinguished from the TP53-WT and normal cases on BM.

Conclusions: P53 IHC is useful for identifying TP53 MS-P mutations but of limited value in detecting NS/FS mutations in MNs, likely due to the topographically heterogeneous nature of the BM architecture reflected on the core biopsy and the genetically heterogeneous nature of MN. It may serve as a useful screening tool for TP53 mutation evaluation to identify the IHC-equivocal to negative cases (<20% strong stain) for further molecular testing.

1603 Isolated Anemia in Patients with T-cell large granular lymphocytic leukemia (T-LGLL)

Fang Zhao¹, Jennifer L. Oliveira¹, Dragan Jevremovic¹, Ronald S Go², William Morice³, Min Shi¹. ¹Mayo Clinic, Rochester, MN, ²Mayo Clinic, ³Rochester, MN

Background: T-LGLL is a clonal expansion of mature cytotoxic T lymphocytes. Patients with T-LGLL frequently present with neutropenia, splenomegaly and autoimmune diseases. Although anemia is common in T-LGLL, it is usually accompanied by neutropenia and/or thrombocytopenia, and isolated anemia in T-LGLL is rarely reported. We characterized the clinicopathologic and immunophenotypic features of T-LGLL presenting with isolated anemia, and further compared these features between patients with and without pure red cell aplasia (PRCA).

Design: We identified Mayo Clinic Rochester T-LGLL cases between 1/1/2007 and 4/30/2016 and performed clinical and pathological data review. T-LGLL diagnosis utilized WHO criteria. Isolated anemia was defined as hemoglobin <13g/dL for males or <12g/dL for females, absolute neutrophil count >1.5x10⁹/L and platelet count >150x10⁹/L. The diagnosis of PRCA was based on: 1) Reticulocyte count <0.5%; 2) Absence of erythroid precursors in the bone marrow; 3) Normal granulopoiesis and megakaryopoiesis; 4) No other known causes of PRCA. Statistical analyses were performed using JMP® Pro 10.0.0. P<0.05 was considered statistically significant.

Results: Among 153 identified T-LGLL patients, 25 (16%) presented with isolated anemia at diagnosis: 11 (7%) with PRCA, and 14 (9%) with non-PRCA. The 25 patients had median age at 68 years (32-85), male to female ratio of 4:1 and median follow-up duration at 31 months (4-155). 8 of 25 (32%) patients had other hematologic disorders, 4 (16%) had splenomegaly and 3 (12%) had autoimmune disorders. All 25 patients had a clonal T-cell population, 24% had killer immunoglobulin-like receptor restriction and 95% had intrasinusoidal distribution of cytotoxic T-cells. Among the 25 T-LGLL patients with isolated anemia, patients with PRCA were more transfusion dependent (P=0.01), more commonly treated for T-LGLL (P=0.02), and less likely to have TIA-1 expression (P=0.02), in comparison to non-PRCA patients. The treatment response rate was similar (67% for PRCA, 86% for non-PRCA; P=0.58) and other features were shared between these two groups.

Conclusions: Anemia can be the sole clinical presentation at initial diagnosis of T-LGLL, with PRCA seen in 44% of patients. Compared with T-LGLL patients with non-PRCA, patients with PRCA are more likely to be treated for T-LGLL and demonstrate similar therapeutic responses. The two groups largely share other clinicopathologic features, suggesting other mechanisms contributing to the range of anemia in T-LGLL.

1604 The clinical utility of somatic mutation sequencing in discriminating etiologies of cytopenias

Gang Zheng¹, Hua Ling², Aparna Pallavajjala³, Lisa Haley⁴, Kimberly F Doheny⁵, Ming-Tseh Lin⁶, Amy Dezern⁴, Christopher Gocke⁷. ¹Johns Hopkins Hospital, Ellicott City, MD, ²Johns Hopkins University, Baltimore, MD, ³Johns Hopkins University, Baltimore, MD, ⁴Johns Hopkins University, ⁵Johns Hopkins University School of Medicine, Baltimore, MD, ⁶Clarksville, MD, ⁷Johns Hopkins Medical Institutions, Baltimore, MD

Background: The clinical utility of somatic mutation sequencing in discriminating etiologies of cytopenias is uncertain: some of the causes of cytopenias such as myelodysplastic syndrome (MDS) are clonal, but clonal hematopoiesis can be found in healthy individuals and patients with aplastic anemia (AA), and patients with cytopenia can have clonal cytopenia of undetermined significance (CCUS). We examined a large cohort of well-studied patients with cytopenias with a next-generation sequencing (NGS) panel to determine its utility in the diagnosis of MDS.

Design: This cohort study comprised 123 patients with cytopenias and a specimen (blood or marrow) submitted to a molecular pathology laboratory for 640-gene NGS from 07/2015 to 06/2017. These patients had additional workup including marrow biopsies and cytogenetic studies. Patients with diagnoses of acute leukemia, lymphoma or with a history of cytotoxic therapy were excluded. Using a combination of marrow morphology and cytogenetics as a diagnostic "gold standard" for MDS, we assessed the diagnostic value of somatic mutations detected by the 640 gene NGS panel.

Results: Based on marrow morphology and cytogenetics, 72 of the 123 patients were diagnosed with MDS, 24 with AA, while the remaining 27 with no evidence of a primary marrow disorder. 13 of 24 AA patients showed somatic mutations with a VAF as high as 20%; 7 patients showed somatic mutations but no evidence of a primary marrow disorder, meeting the criteria for CCUS (Figure 1). The sensitivity of the NGS panel for MDS reached 97%, and when there were no variants present, the negative predictive value (NPV) in excluding a diagnosis of MDS was 94%. Conversely, when the VAF was set at 20%, the positive predictive value (PPV) for MDS was 95% with a specificity of 94%. Presence of two or more somatic mutations at any VAF in a specimen predicts MDS with a PPV of 82%, which increases to 98% as VAF increases to 10%. Interestingly, mutation analysis may also predict high vs. low-grade MDS: mutations in TP53, SRSF2, STAG2, or NF1 are enriched in high-grade MDS.

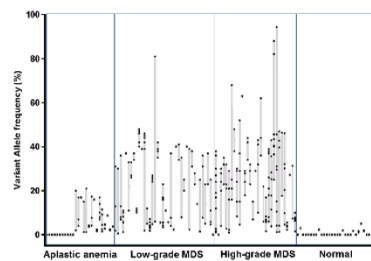


Figure 1. Range plots of variant allele frequencies (VAFs) of all cases. All variants are shown as dots; a dot at VAF=0 indicates that the case shows no somatic mutations. Boundaries of the boxes indicate the min and max VAFs of the cases.

Conclusions: The large NGS panel has high predictive value and accuracy in excluding MDS. Although a significant subset of patients with AA or CCUS show somatic mutations with significant clone size, the presence of mutations with a VAF ≥ 20%, or two or more mutations with a VAF ≥ 10%, is highly predictive of MDS. Such mutation analysis has the potential to improve the diagnostic approach and accuracy for unexplained cytopenia.

Table 1. Clinico-pathologic features of the SF3B1 mutated cases.

Case #	Age, years	Sex	Diagnosis	Duration of MPN, years	JAK2/ CALR/ MPL; VAF %	SF3B1; VAF%	Fibrosis	Cytogenetics	WBC (10 ⁹ /L)	Hgb (g/dL)	MCV (fL)	Platelet (10 ⁹ /L)	Marrow RS %	FU
1	60	M	PMF	8	JAK2; 49	K666Q; 22	MF-3	Normal	3.09	8.5	88.9	114	n/a	Alive
2	69	F	PMF	4	JAK2; 75	K700E; 41	MF-3	46,XX,add(4)(p175)[2] / 46,XX[18]	12.09	8.3	85.5	154	0	Dead
3	53	M	PMF	5	TN	T663I; 3	MF-2	46,XY,del(11)(q22.1q24.3)[12]	1.76	8.7	95.4	116	n/a	Dead
4	66	M	PMF	2	JAK2; 73	K700E; 37	MF-3	Normal	7.88	7.5	93.2	328	25	Alive
5	79	F	post-ET MF	33	CALR; 40	H662D; 3	MF-3	Normal	3.57	9.5	91.1	133	0	Alive
6	47	F	PV	7	JAK2; 44	K666N; 23	MF-1	Normal	14.2	15.7	84.5	618	0	Alive
7	74	F	post-PV MF	15	JAK2; 56	K666N; 5	MF-2	48XX,+8,+9	7.38	9.8	102	77	n/a	Alive
8	76	F	post-ET MF	8	JAK2; 99	K666N; 43	MF-2	n/a	191	7.6	103.5	352	n/a	Dead
9	66	F	post-ET MF	13	JAK2; 97	H662Q; 44	MF-3	Normal	78.96	7	89.4	454	n/a	Alive
10	65	M	early PMF	0	JAK2; 43	K666N; 46	MF-1	Normal	11.5	12.7	81.0	925	30	Alive
11	74	M	early PMF	5	JAK2; 5	K666N; 47	MF-1	Normal	39.4	11.2	95.4	1294	0	Alive
12	85	M	PMF	6	JAK2; 48	K666T; 40	MF-3	n/a	4.7	9.6	97.0	470	13	Alive
13	71	M	PMF	7	JAK2; 79	K666N; 46	MF-2	46,XY,del(20)(q11.2)[cp19]	17.3	14.8	99.0	76	0	Alive
14	53	F	post-ET MF	34	JAK2; 80	K666T; 37	MF-3	Normal	14.0	8.9	84.0	400	8	Alive
15	75	M	early PMF	0	JAK2; 59	K666N; 47	MF-1	Normal	39.9	12.2	86.4	807	0	Alive
Mean	67.5	-	-	10	-	-	-	-	29.8	10.1	91.8	421	7.6	-

Abbreviations. MPN: myeloproliferative neoplasms; VAF: variant allele frequency; WBC: white blood cell count; Hgb: hemoglobin; MCV: mean corpuscular volume; RS: ring sideroblasts; M: male; F: female; TN: triple negative.

Flow Cytometric Findings on Diagnostic Specimens and Staging Marrows in Patients with T-Cell Histiocyte Rich Large B-Cell Lymphoma1					
	Site	CD4/CD8 Ratio	T-Cell/B-Cell Ratio	Percentage of Lymphocytes CD19+	Other Clinical Findings
59 y/o M	Inguinal LN	1.9	76	1.3	•Marrow involvement by THRLBCL •Previous history of CLL/SLL, in remission •IgG <200 mg/dL
	Staging BM Biopsy	1.4	32.7	2.5	
34 y/o M	Cervical LN	1	8.1	10.9	•No evidence of marrow involvement
	Staging BM Biopsy	2.2	5.3	12.4	
49 y/o M	Axillary LN	ND	ND	13.3	•Marrow involvement by THRLBCL
	Staging BM Biopsy	3.1	61.5	1.5	
56 y/o F	Liver Biopsy	ND	ND	ND	•Marrow involvement by THRLBCL •Lymphopenia: 0.30 K/uL •Peripheral blood flow cytometric analysis revealed 0.3% CD19+ lymphocytes
	Staging BM Biopsy	0.7	449.5	0.2	
64 y/o M	Axillary LN	3.8	6.7	12.8	•No evidence of marrow involvement •Previous history of Small Mature B-cell Lymphoma
	Staging BM Biopsy	2.3	118.7	0.7	
77 y/o F	Supraclavicular LN	N/A	N/A	2.0	•No evidence of marrow involvement
	Staging BM Biopsy	N/A	N/A	3.4	
76 y/o F	Cervical LN	6.1	10.0	9.0	•No evidence of marrow involvement •Lymphopenia: 0.24 K/uL
	Staging BM Biopsy	3.3	9.4	7.3	
78 y/o F	Cervical LN	2.6	4.8	16	•No evidence of marrow involvement
	Staging BM Biopsy	2.6	6.5	2	
53 y/o F	Supraclavicular LN	12.8	3.75	20	•No evidence of marrow involvement
	Staging BM Biopsy	4.3	13.0	2	
70 y/o M	Cervical LN	18.8	31.67	3	•No evidence of marrow involvement
	Staging BM Biopsy	7.0	12.6	0.5	
51 y/o M	Liver	0.6	N/A	N/A	•No evidence of marrow involvement, per clinical report •Lymphopenia: 0.09 K/uL •Peripheral blood flow cytometric analysis revealed <1% CD19+ lymphocytes
	Peripheral blood	4.5	N/A	<1	
63 y/o F	Mesenteric LN	n/a	0.09	5	•No evidence of marrow involvement
	Staging BM Biopsy	4.4	0.13	1	
32 y/o M	Distal Femur Biopsy	0.9	43	2	•History of sickle cell disease •Second biopsy is recurrent disease, one year later
	Distal Femur Biopsy	0.5	116.4	0.5	
82 y/o M	Inguinal LN 2	7.4	3	22	•Original biopsy was unavailable •Psoas muscle T-cell and B-cell percentages are estimated by immunohistochemistry.
	Psoas Muscle 2	N/A	2.33	30	
	Staging BM Biopsy	4.0	7.5	2	
48 y/o F	BM Biopsy 3	2.4	8.8	8.8	•Discrete cluster of CD4+/CD8+ T-Cells comprising 4.8% of the lymphocytes
25 y/o M	Inguinal LN	0.7	70	1	•No staging BM biopsy was performed
31 y/o M	Spleen Biopsy	1.7	6.4	5	•No staging BM biopsy is available •Lymphopenia: 0.45 K/uL •Peripheral blood flow cytometric analysis revealed <1% CD19+ lymphocytes
	Peripheral Blood	1.0	undefined	<1	
	Left rib 2	N/A	N/A	<1	
38 y/o M	Axillary LN	1.4	4.9	12	•No staging BM biopsy is available •24% of lymphocytes by flow cytometry were kappa light chain restricted and were negative for CD5 and CD10
65 y/o M	Retroperitoneal LN	0.9	7.6	10	•No staging BM biopsy is available
66 y/o F	T4 bone lesion 2	1.4	70	<1	•Flow cytometric analysis also revealed 5% kappa clonal plasma cells
64 y/o M	Inguinal LN	5.8	94	<1	•No staging BM biopsy is available
56 y/o M	Pelvic LN	11.0	96.5	0.85	•No staging BM biopsy is available

BM, bone marrow; LN, lymph node; N/A, no data available

- 1.All flow cytometric analyses, unless otherwise stated, were negative for B-cell light chain restriction.
- 2.These biopsies represent disease recurrences.
- 3.The bone marrow biopsy is the diagnostic specimen.

FIG. 1493

Diagnosis	Age/ Sex	Peripheral Counts	BM Dysplasia	FC Abnormalities	Molecular (NGS Panel)	FISH Abnormalities	Karyotype
Atypical CML	60/M	leukocytosis, anemia, thrombocytosis	dyserythropoiesis, dysgranulopoiesis, small/hypolobate megs, sep nuclear lobes	blasts, granulocytes	TP53 p.V272L	5q-, 7q-, 13q-	complex
Atypical CML	69/M	leukocytosis, anemia, thrombocytopenia	dysgranulopoiesis, small/hypolobate megs, sep nuclear lobes	blasts	GATA2 p.L386fs*2 SETBP1 p.G870S SRSF2 p.P95L ZRSR2 p.Q273fs*13	none	normal
AMML, later converted to CMML	62/M	leukopenia, anemia	dysgranulopoiesis	granulocytes, monocytes	ASXL1 p.C789fs*2 ZRSR2 p.L71fs*3	AMML: t(1;19) CMML: none	normal
CMML	55/M	leukocytosis, anemia, thrombocytopenia	dyserythropoiesis, dysgranulopoiesis, large hyperlobulated megs	blasts, granulocytes, monocytes	ETV6 p.L201P KRAS p.Q61H	none	47,XY,+6
CMML	70/F	leukocytosis, anemia, thrombocytopenia	dyserythropoiesis, small/hypolobate megs, sep nuclear lobes	blasts, granulocytes, monocytes	ASXL1 p.I980fs*4 CSF3R p.T618I SETBP1 p.G870S	none	normal
CMML	69/F	leukocytosis, anemia, thrombocytopenia	dyserythropoiesis, dysgranulopoiesis, megs with sep nuclear lobes	blasts, granulocytes	CBL p.Y371C RUNX1 p.D99fs*15 SRSF2 p.P95L TET2 p.R1516* TET2 p.C1289F	none	normal
CMML	78/M	anemia, thrombocytopenia	dyserythropoiesis, dysgranulopoiesis, small/hypolobate megs	monocytes	SRSF2 p.P95H TET2 splice site (c.4045-1G>A)	13q-	46,XY, del(13) (q12q14)
CMML	66/M	leukocytosis, anemia, thrombocytopenia	dyserythropoiesis, dysgranulopoiesis, megs with sep nuclear lobes	blasts, granulocytes, monocytes	CBL p.C419S SETBP1 p.D868N SRSF2 p.P95H	none	normal
MDS/MPN-RS-T	70/M	anemia, thrombocytosis	dyserythropoiesis, large/hyperlobulated megs	blasts, granulocytes	DNMT3A p.R882H JAK2 p.V617F SF3B1 p.K700E	none	normal
MDS/MPN-RS-T	77/F	anemia, thrombocytosis	dyserythropoiesis, small/hypolobate, sep nuclear lobes, and large atypical megs	granulocytes	DNMT3A p.Y436* SF3B1 p.K700E TET2 p.R1359C	none	normal
MDS/MPN-U	75/F	leukocytosis, anemia	dyserythropoiesis, dysgranulopoiesis, small megs, sep nuclear lobes	blasts, granulocytes, monocytes	IDH2 p.R140Q JAK2 p.V617F SRSF2 p.P95R	none	normal
MDS/MPN-U	85/M	leukocytosis, anemia, thrombocytosis	dyserythropoiesis, dysgranulopoiesis, large hyperlobulated, clustered megs	granulocytes	JAK2 p.V617F IDH1 p.R132H SRSF2 p.P95R102del	none	45,X,-Y
MDS/MPN-U	21/M	anemia	dyserythropoiesis, dysgranulopoiesis, hypolobate megs, sep nuclear lobes	blasts, granulocytes	JAK2 p.V617F ZRSR2 splice site (c.827+1G>A)	+8, gain of 16q22	complex
MDS/MPN-U	71/M	leukocytosis, anemia, thrombocytosis	dyserythropoiesis, dysgranulopoiesis, small/hypolobate megs	blasts, granulocytes	TP53 p.G245S TP53 p.V274A	5q-, 7q-, +8, 13q-, +RUNX1	complex
MDS/MPN-U	62/F	anemia	dyserythropoiesis, clustered, pleomorphic megs	none	Negative	none	47,XX,+14
MDS/MPN-U	76/M	leukocytosis, anemia, thrombocytosis	clustered, small/hypolobate megs, sep nuclear lobes	blasts	ASXL1 p.E635fs*15 SETBP1 p.G870S SRSF2 p.P95R NRAS p.G12S	none	47,XY,+18
MDS/MPN-U	82/M	leukocytosis, anemia, thrombocytopenia	dysgranulopoiesis	blasts	NPM1 p.W288fs*12 SRSF2 p.P95R	none	normal
MDS/MPN-U	70/M	anemia	dyserythropoiesis, dysgranulopoiesis, small/hypolobate megs, sep nuclear lobes	blasts, granulocytes	JAK2 p.V617F	5q-, 7-, gain of 3q21	complex

FIG. 1530

= Acute myeloid leukemia; MDS/MPN = Myelodysplastic syndrome/myeloproliferative neoplasm. Commonly mutated genes within each MDS entity are highlighted in grey.

Pt	Previous History	Current Diagnosis	Probable Somatic Mutation				Probable Germline Polymorphism			
			Nucleotide Change	Protein Change	Predicted Effect	VAF	Nucleotide Change	Protein Change	Predicted Effect	VAF
2		AML	c.1574G>A	p.R525H	MS	4.5	c.3G>A	p.?	SCL	49.1
4		AML	c.1574G>A	p.R525H	MS	4.7	c.572-1G>A	Splice	?	43.7
5		AML in remission					c.415_418dup-GATG	p.D140fs	FS	49.1
15		AML	c.1574G>A	p.R525H	MS	1.7	c.415_418dup-GATG	p.D140fs	FS	48.2
1	MDS	AML	c.1574G>A	p.R525H	MS	15	c.3G>A	p.?	SCL	47.9
			c.1036G>A	p.A346T	MS	9.6				
8	MDS	AML	c.1574G>A	p.R525H	MS	2.8	c.3G>A	p.?	SCL	47.6
9	MDS	AML	c.1574G>A	p.R525H	MS	3.8	c.3G>A	p.?	SCL	48.4
10	MDS	AML	c.1574G>A	p.R525H	MS	1.4	c.3G>A	p.?	SCL	54.9
13	MDS	AML	c.1574G>A	p.R525H	MS	19.2	c.142C>T	p.Q48*	NS	49.3
21	MDS	AML	c.1105C>T	p.G530C	MS	1.2	c.1105C>T	p.R369*	NS	61.4
23	MDS	AML	c.1574G>A	p.R525H	MS	11.4	c.475C>T	p.R159*	NS	51.8
17	MDS/ CMML	AML					c.25A>G	p.K9E	MS	50.9
16		MDS					c.59G>A	p.G20E	MS	55.4
18		MDS	c.1574G>A	p.R525H	MS	1.4	c.3G>A	p.?	SCL	48
22		MDS	c.1222G>T	p.V408F	MS	3.2	c.121C>T	p.Q41*	NS	53.2
11		Suspicion of MDS	c.962C>T	p.P321L	MS	25	c.1046T>A	p.M349K	MS	49.2
14		CMML					c.1766G>A	p.G589D	MS	41.1
19		MPN					c.821A>G	p.H274R	MS	45
6		Post PV-MF					c.38C>T	p.T13I	MS	49.2

FIG. 1542

Table 1. Summary of cases per diagnosis, number of mutations per case, and the ten most commonly mutated genes in MDS

2016 WHO Entities	# Cases	Mean	# mutations		Number of mutations										Commonly mutated gene(s)
			Per Case	Median (Range)	TP53	SF3B1	ASXL1	TET2	DNMT3A	SRSF2	U2AF1	RUNX1	SETBP1	STAG2	
SLD	1	NA	NA	NA	0	0	0	0	1	0	0	0	1	0	NA
RS	2	1.5	2 (1-2)	3	6	0	3	0	2	0	0	0	0	0	SF3B1
RS, SLD	4	2.3	3 (1-3)	0	3	0	1	2	0	0	0	0	0	0	SF3B1
RS, MLD	12	3.3	3 (1-5)	1	15	2	5	2	1	1	1	3	0	0	SF3B1
MLD	14	3.5	3 (1-9)	6	0	5	4	2	3	6	1	2	1	0	TP53, U2AF1
EB	28	3.3	3 (1-9)	11	4	5	5	4	4	2	6	0	6	0	TP53, RUNX1, STAG2
5q	1	NA	NA	NA	0	1	0	0	0	0	0	0	0	0	NA
Unc	1	NA	NA	NA	0	0	0	0	0	1	0	0	0	0	NA
TR	16	3.6	3 (0-7)	12	2	7	1	4	2	0	1	1	0	0	TP53, ASXL1
AML arising from MDS	12	4.3	3 (1-8)	6	0	6	2	1	1	4	2	1	2	0	TP53, ASXL1
MDS/MPN	3	1.7	0 (0-5)	0	0	1	0	0	0	1	0	1	0	0	NA
Negative	20	9	0 (0-2)	0	0	0	1	0	0	0	0	0	0	0	NA
Total	114	323		39	31	26	22	16	14	14	11	9	9		

SLD = MDS with single lineage dysplasia; RS = MDS with ring sideroblasts (MDS-RS); RS, SLD = MDS-RS and single lineage dysplasia; RS, MLD = MDS-RS and multilineage dysplasia; MLD = MDS with multilineage dysplasia; EB = MDS with excess blasts; 5q = MDS with isolated del(5q); Unc = Unclassifiable; TR = Therapy related MDS; AML

FIG. 1566

Case	Age	Gender	Site	CD10	CD20	BCL2	BCL6	Ki67	Cytogenetics/FISH/CGH array
Case 1	14	Male	Nasopharynx, Cervical node	+	+	-	+	100%	FISH: MYC and MLL translocations negative, but revealed MLL gene duplication suggestive of 11q13-q23 gain (confirmed by array). Karyotype: 48,XY,+add(8)(p11.2),dup(11)(q23q21),+12,+19
Case 2	13	Male	Cervical node, tonsils	+	+	-	+	Close to 100%	FISH negative for MYC, BCL2, BCL6 translocations. Karyotype: 46,der(11)dup(11)(q13q22)dup(11)(q22q23) suggestive of 11q13-q23 gain (confirmed by array)
Case 3	13	Male	Left tonsil	+	+	-	+	Close to 100%	FISH negative for MYC, BCL2, BCL6 translocations. Array positive for 11q13-q23 gain, 11q23-tel loss. Karyotype not available
Case 4	6	Female	Cervical node	+	+	-	+	90-95%	FISH negative for MYC, BCL2, BCL6 translocations. Array demonstrated 11q13-q23 gain, 11q24-tel loss. No karyotyping.
Case 5	8	Female	Kidney	+	+	-	+	Close to 100%	FISH negative for MYC, BCL2, BCL6 translocations. Array negative for 11q aberration. No karyotyping.

FIG. 1598

Age	Diagnosis	Myc	Ki67	Cyclin D1	CD30/ MUM-1	FISH	Cytogenetic	IgVH mutation	Molecular
60/M	Accelerated	< 40%	60-70%	Neg	Neg/Pos	del ATM	Complex	Unmutated	Notch 1 mutation
91/F	Accelerated	>40%	30%	Neg	Pos / Neg	del ATM; del D13S319	Complex	Unmutated	ATM gene, VUS
69/M	Accelerated	>40%	40-50%	Neg	Neg / NA	IGH rearrangement	Complex	Unmutated	SF3B1 mutation
77/M	Accelerated	NA	30%	Dim	Neg/NA	del ATM; del D13S319	Normal	Unmutated	No mutation
68/M	Accelerated	NA	50%	NA	NA / NA	NA	NA	NA	NA
60/M	Accelerated	NA	10-40%	Neg	NA / NA	del TP53; del 13q	Complex	NA	NA
64/M	Accelerated	NA	50%	Neg	NA / NA	del TP53; del 13q	Complex	NA	SF3B1 , TP53 mutation
42/M	Accelerated	NA	30%	Neg	NA / NA	del TP53; del of MYB; del 13q	Complex	Unmutated	No mutation
64/F	Accelerated	NA	70%	Neg	NA / NA	del TP53; MYC rearrangement	Complex	NA	NA
78/F	Accelerated HL-like	<40%	70-80%	Neg	Pos / Pos	Trisomy 12, deletion of 17p	Trisomy 12	Mutated	NA
53/M	Transformation	40%	95%	Neg	Neg/Pos	del ATM, CMYC rearrangement	Add(8)(q24)	Mutated	No mutation
79/M	Transformation	<40%	90%	Some Pos	Neg/Pos	NA	NA	NA	NA
84/M	Transformation	<40%	90%	Neg	Neg/Pos	Neg	Normal	NA	NA
94/M	Transformation	NA	60-80%	NA	NA / NA	del TP53; del D13S319; MYC and IGH rearrangement	Complex	Mutated	No mutation
84/M	Transformation	NA	60-80%	Neg	NA / NA	del TP53; del 13q	Complex	Unmutated	TP53, Notch 1 mutated
76/M	Transformation	NA	90%	Neg	NA / NA	del TP53; del MYB; del 13S319 ; monosomy 13	Complex	Unmutated	NA
65/F	Transformation	NA	50-70%	Neg	NA / NA	del ATM	Del(11)(q13q23)	NA	NA
73/F	Transformation	NA	NA	Neg	NA / NA	del TP53 ; TRISOMY 12; del 13q	Complex	NA	NA
80/F	Transformation to HL	NA	30%	NA	Pos / Pos	del D13S319	Normal	Mutated	TP53
64/M	Transformation to HL	NA	30-40%	NA	Pos / Pos	del ATM; del D13S319; del RB1	Complex	Unmutated	Notch 1 mutation
56/M	Transformation to HL	NA	30%	Neg	Pos / Pos	IGH rearrangement	Complex	Unmutated	NA

FIG. 1601

Case no	sex / Age	course of disease	Clinical symptoms	blood test	EBV detected in blood	Follow-up (month)								
1	F/10y	1m	fever, hepatosplenomegaly, lymphadenopathy	WBC 2.5x10 ⁹ /L, HB 80g/L, PLT 57x10 ⁹ /L, CRP 97.2mg/L	EBV-CV-IgM- EBV-CV-IgG+ EB-DNA2.2x10 ⁶ copy/ml, EBV-PCR+	3,Alleviation,but the fourth month dead for MOF suddenly								
2	M/2y	1m	fever, hepatosplenomegaly, lymphadenopathy	WBC0.7x10 ⁹ /L,HB71g/L,PLT17x-10 ⁹ /L, CRP133mg/L,LDH893U/L,-FERR 10440ug/L, ALT 103U/L, AST 223U/L	EBV-CV-IgM+ EBV-CV-IgG+	20,Alleviation								
3	M/19y	1.5m	fever, hepatosplenomegaly, lymphadenopathy pleural effusion, ascites,pneumonia	WBC 2.7 x10 ⁹ /L, HG 112 g/L, PLT119 x10 ⁹ /L	EBV- CV-IgM- EBV- CV-IgG+	18,Alleviation								
4	M/3y	1m	fever, hepatosplenomegaly, lymphadenopathy Pleural effusion,pneumonia	WBC2x10 ⁹ /L, HG 98 g/L, PLT 140x10 ⁹ /L CRP 111mg/L,FERR1179ng/ml, LDH695U/L, AST 51.8U/L	EB-DNA2.01x10 ⁶ copy/ml	12,Alleviation								
5	M/10m	1m	fever, hepatosplenomegaly, lymphadenopathy	WBC3.2x10 ⁹ /L,HB-106g/L,PLT256.4x10 ⁹ /L CRP 3mg/L, LDH 754U/L,AST61.6 U/L	NA	39, Alleviation, grow fatter and higher								
6	F/1y	22d	fever, hepatosplenomegaly, lymphadenopathy	WBC1.99x10 ⁹ /L,HB102g/L,PLT63x-10 ⁹ /L, ALT 206U/L, AST 286U/L, LDH 1670 U/L, CRP1.43mg/L	EBV- CV-IgM- EBV- CV-IgG+ EB-DNA1.09x10 ⁶ copy/ml	19, Alleviation, grow fatter and higher								
7	M/5y	1.5m	fever, hepatosplenomegaly, lymphadenopathy	WBC2.32x10 ⁹ /L,HB94g/L,PLT75x-10 ⁹ /L, ALT 370U/L, AST 2392U/L, FERR 1495.3ug/L, CRP 21mg/L	EBV- CV-IgG+ EBV-PCR+	6, Alleviation								
Case no	struc-ture destruc-tion	compo-nents of cells	atypia	Coagulative necrosis	CD3	CD5	CD56	TIA-1	Gran-zyme B	CD30	CD4	CD8	EBNA2	EBER(/HPF)
1	Yes	L	H	Yes	+++	+	+	+	+	+	+++	-/+	+	50 □ 100
2	Yes	M	M	No	+++	-	-	+	NA	-	-/+	-/+	+	>100
3	Yes	L	H	Yes	+++	+	+	NA	+	-/+	-/+	++	-	50 □ 100
4	Yes	L	H	Yes	++	-	+	+	NA	-	-	++	+	>100
5	Yes	L	H	Yes	+++	+	-	NA	+	-	-/+	+++	NA	>100
6	Yes	L	H	Yes	+++	-	+	+	+	-	-	+++	NA	>100
7	Yes	L	H	No	+++	+	+	+	+	+	-	-/+	NA	>100